HAMBURG UNIVERSITY OF TECHNOLOGY

INSTITUTE OF WASTEWATER MANAGEMENT AND WATER PROTECTION

CONDITIONING, STARTING AND NITRIFICATION STUDY IN AERATED FIXED BED REACTORS FOR THE TREATMENT OF SLUDGE WATER

JAIRO D. MELO P.

Submitted to

Prof. Dr.-Ing. Ralf Otterpohl

&

Prof. Dr.-Ing. Wilfried Schneider

December 2017

Statutory Declaration

I declare that I have developed and written the enclosed Master Thesis completely by myself, and have not used sources or means without declaration in the text. Any thoughts from others or literal quotations are clearly marked. The Master Thesis was not used in the same or in a similar version to achieve an academic grading or is being published elsewhere.

Hamburg, 05.12.2017

Jairo D. Melo P.

DOI: https://doi.org/10.15480/882.3725

ORCID: Jairo D. Melo P.; https://orcid.org/0000-0001-8388-9017

TABLE OF CONTENTS

LIST OF FIGURES

LIST OF TABLES

LIST OF ABBREVIATIONS, & UNITS

List of Abbreviations

Add.	Added
AC	Ammonium-nitrogen consumed
ACR	Ammonium-nitrogen consumption rate
ALR	Ammonium loading rate
Anammox	Anaerobic ammonium oxidation
AO	Ammonium oxidation
AOB	Ammonia oxidizing bacteria
Aver.	Average
BAF	Biological aerated filter
bf	Biofilter
BOD	Biological oxygen demand
BOD_5	Biological oxygen demand, 5 day test
C	Carbon
CAFR	Chemische ammonium fällung und rezyklierung
Cal.	Calibration
Calc.	Calculated
COD	Chemical oxygen demand
Conc.	Concentration
Cons.	Consumption
Conv.	Converted
DAF	Dissolved air flotation
DEV	Deutsche Einheitsverfahren
df	Dilution factor
DO	Dissolved oxygen
EEC	European economic community
EPA	Environmental protection agency
EPS	Extracellular polymeric substances
EU	European Union
EUR	Currency code for Euros
FA	Free ammonia
FBBR	Fluidized bed bioreactors
FNA	Free nitrous acid
Gener.	Generated
HLR	Hydraulic loading rate
HRT	Hydraulic retention time
ISWA	International solid waste association

Liq.	Liquid
m	Mass
MAP	Magnesium ammonium phosphate
Max.	Maximum
MBBR	Moving bed biofilm reactor
MW	Molecular weight
n	moles
N	Nitrogen
NB	Nitrobacter
No.	Number
NOB	Nitrite oxidizing bacteria
NS	Nitrosomonas
PE	Population equivalent
RBC	Rotating biological contactor
Re	Reynolds number
SAF	Submerged aerated filter
SBBR	Sequencing batch biofilm reactor
SBR	Sequencing batch reactor
Sc	Schmidt number
SD	Sample standard deviation
SEM	Standard error of the sample
SFBBR	Submerged fixed bed biofilm reactor
Sh	Sherwood number
SHARON	Single reactor system for high activity ammonium removal over nitrite
Sltn.	Solution
SLV	Surface loading value
SRB	Sulfate reducing bacteria
SRT	Solid retention time
SSA	Specific surface area
Std.	Standard
SW	Sludge water
T	Temperature
t	time
t_g	time of generation
TAN	Total ammonia nitrogen
TC	Top column
TCMP	2-chloro-6-(trichloromethyl) pyridine
Theo.	Theoretical
TIN	Total inorganic nitrogen
TK	Tank

TKN	Total Kjeldahl Nitrogen
Tot.	Total
TP	Total phosphorous
TSS	Total suspended solids
UWWT	Urban wastewater treatment
UWWTP	Urban wastewater treatment plant
V	Volume
Vol.	Volume
VS	Volatile solids
w	weight
WEF	Water Environment Federation
WWTP	Wastewater treatment plant

List of Units

atm	Atmosphere
°C	Degree Celsius
cm	centimeter
d	day
g	gram
h	hour
Kg	Kilogram
L	Liters
M	Molar
mg	milligram
mL	milliliter
mm	millimeter
mmol	millimole
min	minute
N	Normal
rpm	revolutions per minute
s	second
tds	tons of dry solids
y	year
µm	micrometer
W	Watts

1. INTRODUCTION

Nitrogen is an essential nutrient required for life on earth, without it the growth and survival of living organisms would not be possible. However, human induced activities have altered the natural proportions of this nutrient in the environment. For instance, in Europe the uncontrolled used of fertilizers and chemical products had led to an excessive increase of nitrates within surface and ground waters which have led to problems related to human health. Moreover, the relatively high concentrations of nitrogen found in the effluents of treated wastewater have led to severe eutrophication and deterioration of many aquatic areas.

In wastewater treatment plants, due to their high ammonium concentrations the sludge digester liquor may constitute approximately 20% of their total nitrogen load. However, this high nitrogen concentrations and in combination with the typical sludge water conditions can be beneficial for the application of separate biological treatments that can reduce in a cost effective way the negative impacts that this side stream may have in a WWTP.

In this thesis, the ammonium consumption rates of aerated fix bed reactors at pilot plant scale under different operation conditions were studied. High-strength ammonium sludge water collected from a local WWTP with a concentration of about 833,2 mg NH_4^+-N/L and COD of 385,0 mg O_2/L was treated. A first bioreactor with a media depth of 0,8 m was operated in batch and semi-bath modes at HLRs ranging from 4,5 m/h to 14,0 m/h and at air flowrates of 1,5 L/h and approximately 10,0 L/h. A second bioreactor with a media depth of 1,8 m was started by using plastic biofilm carriers with a specific surface area of 660 m^3/m^2. Sludge from the already running bioreactor was used to inoculate the starting bioreactor and the high-strength ammonium sludge water was used during the starting process. Once stable nitrification was observed a batch process was performed with a HLR and air flowrate of 3,0 m/h and 9,0 L/h respectively. The highest ammonium consumption rate with a value of 5524,3 mg NH_4^+-N/m^2.d was obtained during the batch process performed in the first bioreactor operating at a HLR and air flow rate of 13,8 m/h and 10,1 L/h respectively. Furthermore, during the starting of the second bioreactor stable ammonium oxidation was observed after 20 days of treatment and reaching an ammonium consumption rate of 962,8 mg NH_4^+-N/m^2.d.

2. LITERATURE REVIEW

2.1. NITROGEN

Elemental nitrogen is found in municipal wastewater generally in organic nitrogen compounds (e.g. Urea), ammonium (NH_4^+)/ammonia (NH_3), nitrate (NO_3^-) and nitrite (NO_2^-). The nitrogen in domestic wastewater is composed primarily of organic and ammonium nitrogen in which 60 to 70 percent is related to ammonium nitrogen and 30 to 40 percent to organic nitrogen. One of the reasons is that these kinds of nitrogen are more related to plants and animals compared to the other forms. In average, the total nitrogen concentration in domestic low to high strength wastewater can range in between 20 to 70 mg N/L, but these values can vary depending on the collection system, industrial activities, season and rainfall events (USA-EPA, 2009).

In aqueous solution ammonium ion (NH_4^+) and ammonia (NH_3) can co-exist in equilibrium depending on the pH and temperature conditions. Figure 1, illustrates their distribution in water as a function of pH and temperature.

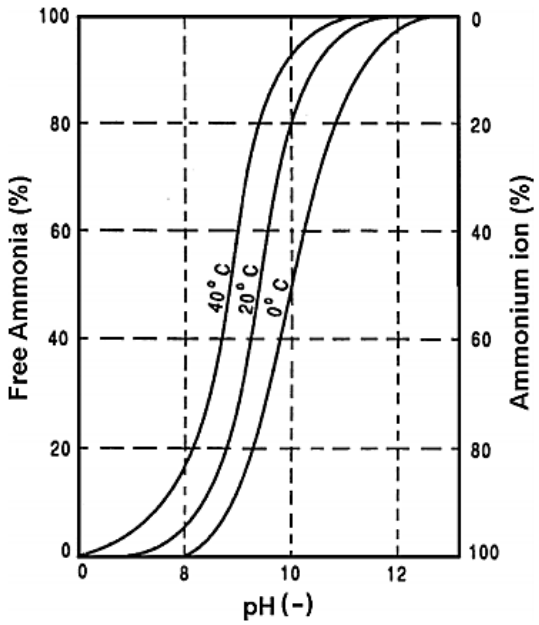

Figure 1. Ammonia and ammonium equilibrium in water (Capodaglio, et al., 2015)

The different kind of nitrogen forms commonly use in wastewater treatment are illustrated in table 1.

Table 1. Nitrogen species (Metcalf & Eddy, Inc., 2003)

Nitrogen form	Abbreviation	Definition
Ammonia gas	NH_3	NH_3
Ammonium	NH_4^+	NH_4^+
Total ammonia nitrogen[1]	TAN	$NH_3 + NH_4^+$
Nitrite	NO_2^-	NO_2^-
Nitrate	NO_3^-	NO_3^-
Total inorganic nitrogen[1]	TIN	$NH_3 + NH_4^+ + NO_2^- + NO_3^-$
Total Kjeldahl nitrogen[1]	TKN	Organic N + NH_3 + NH_4^+
Organic nitrogen[1]	Organic N	TKN – (NH_3 + NH_4^+)
Total nitrogen[1]	TN	Organic N + NH_3 + NH_4^+ + NO_2^- + NO_3^-

1. The concentration is based on elemental N

Moreover, different nitrogen conversion process can take place within a WWTP. The most important ones are listed below (Gustavsson, 2010). The numbers in parenthesis correspond to the steps of their simplified relationships given in figure 2.

- Nitrogen fixation (1)
- Ammonification or degradation of nitrogen bound organic material (2)
- Assimilation (3)
- Aerobic ammonium oxidation or nitritation (4 + 5)
- Nitrite oxidation (6)
- Denitrification (7 – 10)
- Denitritation (8 – 10)
- Anaerobic ammonium oxidation (ANAMMOX) (11)

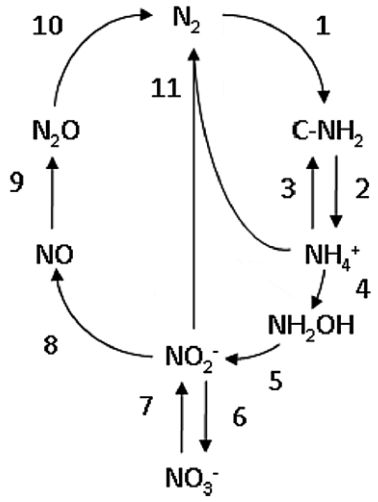

Figure 2. Nitrogen conversion processes in WWTP (Gustavsson, 2010)

2.1.1. Problematic

Even though, nitrogen is essential for microbial growth its presence in effluents from wastewater treatment facilities and drinking water sources threatens not only the quality of the environment but also human health. For example, one of the main problems associated with nitrate is related to a blood disorder that affects mainly children under the age of 4 months known as the blue baby syndrome. In the blood, nitrates will react with hemoglobin inhibiting its bonding capacity with oxygen and leading to suffocation and potential dead (WEF, 2008). Furthermore, a high concentration of nitrate in receiving waters can lead to eutrophication due to an excess growth of aquatic plants and algae which puts the aquatic biodiversity at risk (WRIG, 2007). Additionally, the presence of ammonium in receiving waters is of great interest due to the ammonia toxicity to fresh water organisms. At certain temperature and pH conditions ammonia is favor in the ammonium/ammonia equilibrium thus leading to an increase in ammonia concentration affecting the aquatic life (Dombrowski & In Su Choi, 2007). Nitrite problems are more related to treatment plants where water disinfection is performed by chlorination where a high a concentration of nitrite may interfere with this step making the process inefficient and increasing the probabilities of pathogenic diseases (Maine Lagoon Systems, 2003).

2.1.2. Legislation

There has been a concern in European countries related to the increase of nitrate concentration in ground and surface waters from agricultural sources trough fertilizers and inadequate farming practices. This led to the European Union (EU) Nitrates Directive of 1991 with title “concerning the protection of waters against pollution caused by nitrates from agricultural sources”. The EU in the council directive of 1991 with title “concerning urban waste water treatment” has stablished a total nitrogen limit discharge to sensitive areas vulnerable to eutrophication from UWWTPs with capacities in between 10000 to 100000 PE of 15 mg N/L and for UWWTPs with capacities of more than 100000 PE of 10 mg N/L. The concentration of nitrate and nitrite in drinking water is stipulated in the EU council directive of 1998 with title “on the quality of water intended for human consumption”. The limit values are 50 mg/L and 0.50 mg/L for nitrate and nitrite respectively (European Commision, 2017).

2.2. OVERVIEW OF SLUDGE TREATMENT

Sludge is a term that encompasses the by-products in the form of a semi-solid liquid generated in wastewater treatment process. The sludge may contain in between 0,25 to 12 percent solids by weight and tends to accumulate nutrients, heavy metals, poor biodegrable trace organics and pathogenic organisms. In the case of a biological treatment process, the term biosolids is frequently used to describe the sludge generated considering that part of the organic matter present in the treated wastewater stream is degraded by microorganisms and converted into biomass. Normally, the term sludge is used in combination with the process description such as primary sludge, waste-activated sludge and secondary sludge (Metcalf & Eddy, Inc., 2003). The management of the sludge generated becomes important considering that it represents about 20 to 60% of the total operational cost of the treatment plant (Andreoli, et al., 2007).

In general, the objectives of the sludge treatment include stabilization, volume reduction, disinfection and further operations for safe use or disposal.

- Thickening

As the word implies, thickening refers to the sludge enrichment of its solid content by removing a portion of its liquid. There are several physical methods used for sludge thickening, these include gravity settling, flotation, centrifugation, gravity belt and rotatory drum. The volume reduction of sludge is important especially in large wastewater treatment plants where the sludge may have to be transported over large distances. The reduction of its volume helps to decrease the operational and investment costs in subsequent unit operations such as pumps, piping system, tanks, dewatering units and energy and chemicals consumption, among others (Metcalf & Eddy, Inc., 2003). In general, a volume reduction ranging from 30 to 80% can be achieved through sludge thickening (LENNTECH, 2017).

- Stabilization

A stabilization process can be described as one that can effectively reduce pathogens, odors and putrefaction from sludge. In other words, sludge stabilization is directly related to its volatile or organic content since microorganisms benefit from this organic fraction in order to growth but generating undesirable odors and increasing the pathogenic characteristics of the sludge. The main processes used for sludge

stabilization are alkaline stabilization, anaerobic and aerobic digestion and composting (Metcalf & Eddy, Inc., 2003). Indicators of a stable sludge include the volatile to total solid ratio, the percentage of volatile solid reduction and the oxygen uptake rates with values of below 0,6, above 40% and less than 2 mg/g VS·h at 18°C respectively (ISWA, 1998).

- Dewatering

As in the thickening case, the further removal of moisture from the sludge helps subsequent processes become more efficient. For instance, the further volume reduction improves the sludge handle and transportation characteristics making it easier to be moved around by shovels and tractors, hence saving costs in trucking transportation to the final disposal sites. Furthermore, dewatering improves sludge qualities depending on the subsequent process such as the calorific value prior to incineration, reduction of leachate in landfill sites and enhances its properties when blended with bulking agents and amendments in composting. The more common units used for dewatering are centrifuges, belt-filter presses, recessed-plate filter press, drying beds, etc. (Metcalf & Eddy, Inc., 2003).

The final usages or disposal of the treated sludge are agricultural, incineration and landfilling. Figure 3 depicts the cost for some treatment and disposal options. These values may vary depending on the local conditions for investment and operational costs as well as changes in current regulations.

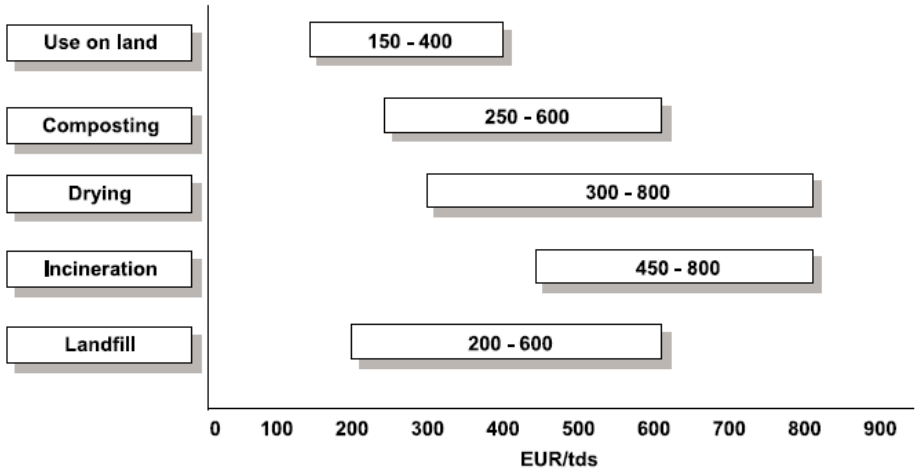

Figure 3. Cost of sludge treatment and disposal comparison (Langenkamp & Marmo, 2000)

As illustrated by figure 3, the agricultural use of sludge is relatively the most cost effective used of treated sludge. The Sewage Sludge Directive 86/278/EEC of June 12, 1986 on the protection of the environment, and in particular of the soil, when sewage sludge is used, promotes through regulation the use of treated sludge in agriculture by reducing the negative impacts that it may have in the environment (European Commission, 2016).

In Europe the implementation of the council Directive 91/271/EEC of May 21, 1991 concerning Urban Wastewater Treatment has led to an increased in the amount of sewage sludge needed to be treated and disposed. This is due to the increase of the number of households connected to sewage treatment facilities across the European member states and the expansion of treatment facilities by upgrading their plants with tertiary treatment process for the removal of nutrients. It was estimated that by the end of the year 2005 approximately 9 million of tons per year in dry weight of sewage sludge would have been generated (European Commission, 2016). Figure 4 compares the amount of sludge produced among the European member states before and after the Urban Wastewater Directive 91/271/EEC.

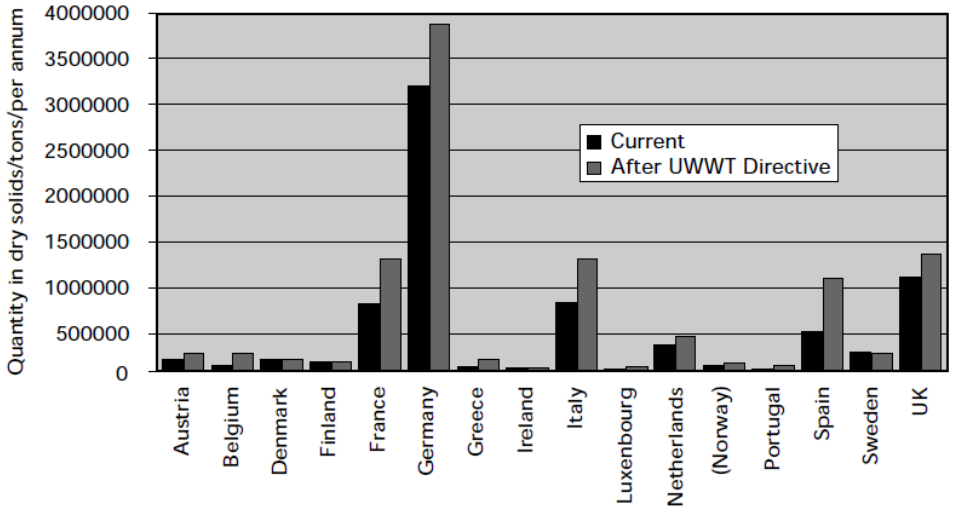

Figure 4. Sludge generated in European member states before and after Directive 91/271/EEC (ISWA, 1998)

The increase of sludge in WWTPs has also increased the side streams volumes generated across the sludge treatment process. One example, is the dewatering of stabilized sludge from anaerobic digesters by decanter centrifuges where the effluent liquid also known as centrate or sludge water is returned back to the head of the process and consequently affecting the performance and/or design of the treatment plant.

2.3. SIDE STREAMS

In general, the side streams of a WWTP include the flows generated inside the plant originated from liquid and sludge treatment. Depending on the unit operation, some side streams include supernatants from thickeners, backwash wastewater from absorbers or centrate from centrifuges among others. In most cases side streams are recycle to the head of the process but they can also be fed to secondary treatment steps. Even though, their volumes only represent about 5 to 10% compare to the influent stream their impact on the plant performance may become important considering that their characteristics such as BOD, TSS and Nutrient content may differ considerable from those associated with the input stream and thus affecting the overall performance of the treatment plant (EPA, 1985). Figure 5 depicts some of the different side streams that can be found in a WWTP.

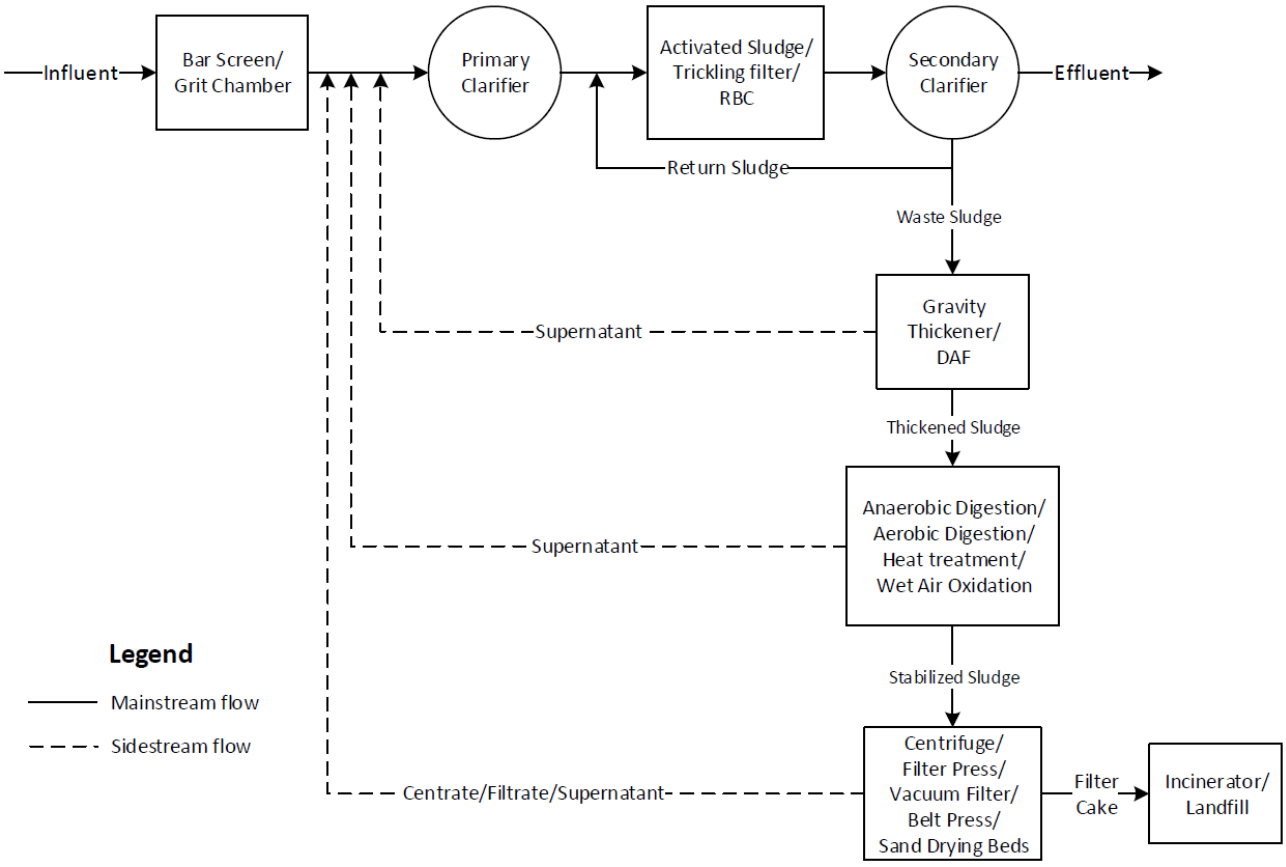

Figure 5. Different side streams in a WWTP (EPA, 1985)

The characteristics of each side stream varies based on the input stream entering the wastewater treatment unit since its composition changes along the process. Also, the wastewater source, chemicals used and the equipment specification directly influences each side stream composition. For that reason, the composition of side

streams can differ largely specially when they are compared among different WWTPs (EPA, 1987).

The BOD_5 and TSS composition of some side streams generated in different unit operations commonly use in WWTPs for liquid and sludge treatment are shown in table 2.

Table 2. Side streams and composition (EPA, 1987)

	Treatment Step	Treatment process	Side stream	Composition Range	
				BOD_5 (mg/L)	TSS (mg/L)
Sludge Treatment	Thickening	Gravity thickener	Supernatant	100 – 1200	200 - 2500
		Dissolve air flotation	Subnatant	50 – 1200	100 - 2500
	Dewatering	Centrifuge	Centrate	100 – 2000	200 - 20000
		Belt filter press	Filtrate	50 – 500	100 - 2000
	Stabilization	Anaerobic digestion	Supernatant	100 – 2000	100 – 10000
		Incineration	Scrubber water	30 – 80	600 - 8000
Liquid treatment	Cleaning	Carbon absorption	Washwater	50 – 400	100 - 1000
		Dual and multimedia filters	Washwater	50 – 500	100 – 1000

Depending on the effect that the recycle side streams may have in the treatment process, separate biological or chemical treatments for side streams may be required to mitigate their negative effects and decreased their possible high loads of BOD, suspended solids, pollutants, ammonia, and phosphorus concentration across the treatment process (EPA, 1987).

2.4. SLUDGE WATER

The sludge digester liquor also known as centrate, sludge water or reject water generated after the dewatering of the digested sludge produced in anaerobic digestion systems is normally recycle to the head of the treatment. This side stream represents around 1% of the total plant influent flow (Pugh & AECOM, 2010). In the anaerobic digesting process the biological degradation of proteins or urea leads to the formation of high concentrations of ammonia. This fact explains the high concentration of

nitrogen mainly in the form of ammonium/ammonia contain within this side stream which typically constitutes about 20% of the plant's nitrogen load (Pedros, et al., 2006). In sludge water the ammonium concentration can range in between 500 to 2000 mg NH_4^+-N/L (Wang, et al., 2017). The sludge water side stream from an anaerobic digestion system is illustrated in figure 6.

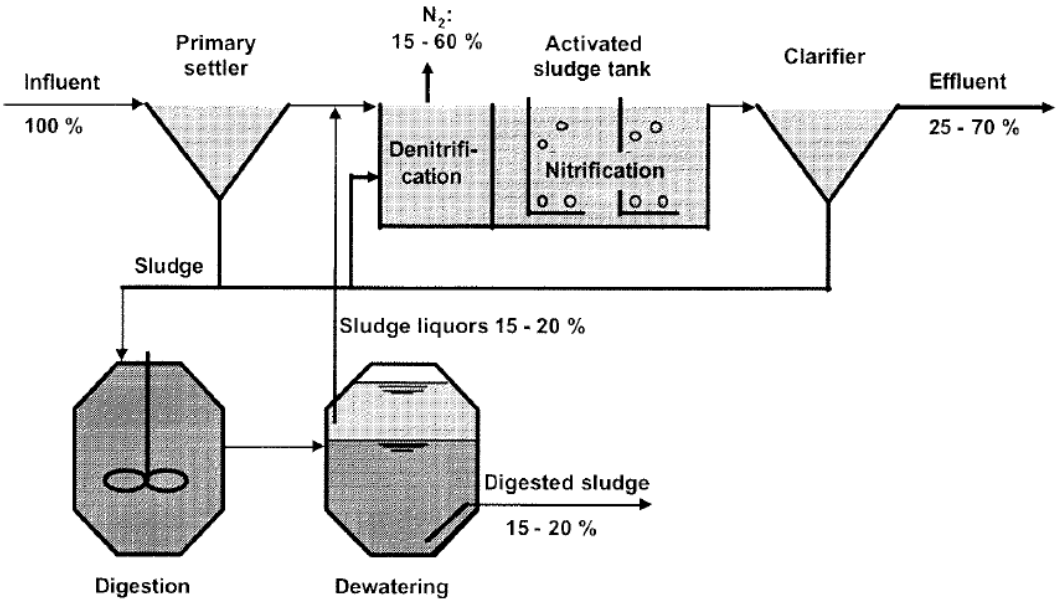

Figure 6. Sludge water side stream (Fux, 2003)

As observed in figure 6 the sludge water is recycle to the wastewater treatment plant input and it represents about 15 to 20% of the nitrogen inlet load. Moreover, the characteristics of the sludge water are a function of the wastewater source, the equipment specifications and chemicals used during the anaerobic digestion process and/or prior to it. Typical compositions of sludge water from different sources are given in table 3.

Table 3. Sludge water composition

Composition	Values
$N\text{-}NH_4^+$ / $N\text{-}NH_3$ (mg/L):	1029 – 1400[a] ; 800 – 2500[b] ; 900[c] ; 890[d] ; 943 – 1513[e]
TN (mg/L):	1025[d]
TP (mg/L):	200[c] ; 26,7[d]
pH:	11,9 – 12,8[a] ; 7,6[d] ; 7,18 – 8,42[e]
T (°C):	30 – 35[a] ; 30 – 38[b] ; 35[c]
TSS (mg/L):	1500[c] ; 150 – 1350[e]
COD (mg/L):	700 – 1000[a] ; 690[d] ; 390 – 2720[e]
Alkalinity (mmol/L):	100 – 150[a] ; 76,6 – 107,1[e]

a. **(Wett, et al., 1998)**; b. **(Pugh & AECOM, 2010)**; c. **(Constantine, 2006)**; d. **(Thorndahl, 1994)**
e. **(Marsalek, et al., 2005)**

In Germany the ammonium-nitrogen (NH_4^+-N) load of treatment plants as a result of sludge treatment represents in between 10 to 15% of the input stream nitrogen load (Jardin, et al., 2006).

Figure 7 illustrates the ammonium nitrogen load in Germany from sludge treatment as function of the WWTP capacity in PE.

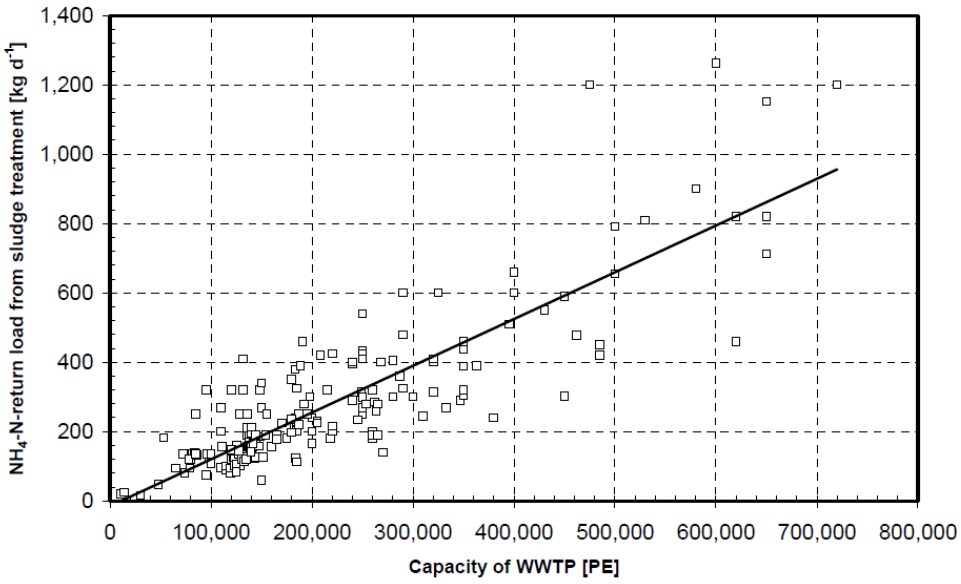

Figure 7. Ammonium-nitrogen load from sludge treatment in Germany (Jardin, et al., 2006)

In general, the ammonium-nitrogen concentration of sludge water is very high when compared to the total nitrogen concentration found in domestic low to high strength wastewater which can be in between 20 to 70 mg N/L (USA-EPA, 2009). However, this high nitrogen concentration in combination with the typical sludge water temperature, pH, and its relatively low flow rate can be beneficial for the application of separate treatments that can reduce in a cost effective way the negative effects that this high ammonium concentration may have in a WWTP (Constantine, 2006).

2.5. NITROGEN REMOVAL AND RECOVERY TECHNOLOGIES

The application of treatment technologies that help to reduce or recover the nitrogen load caused by sludge water returns become important for the optimization of WWTPs. In general the treatment technologies can be divided as biological and physico-chemical. Figure 8 describes different alternatives for the treatment of sludge water.

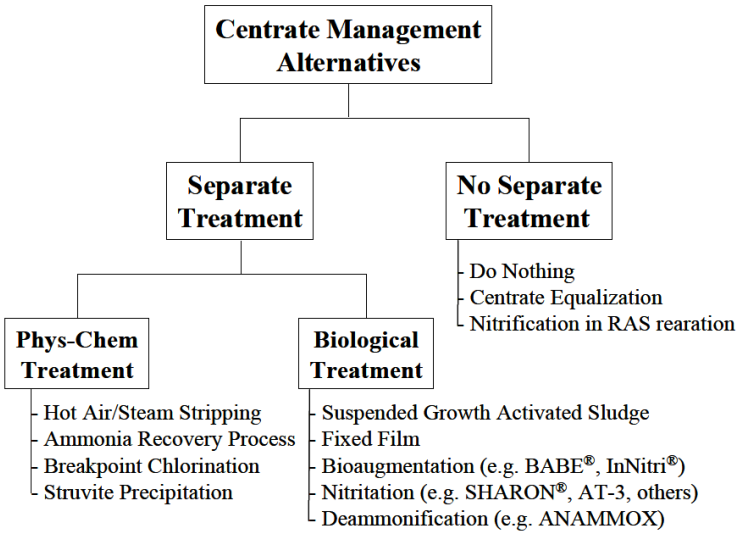

Figure 8. Alternatives for the treatment of sludge water (Constantine, 2006)

In Germany several separate treatment technologies have already been implemented at full scale capacity for the management of sludge water. Some example of WWTPs and their apply technologies are given in table 4.

Table 4. Nitrogen treatment technologies for sludge water in Germany (Jardin, et al., 2006)

WWTP	Capacity (PE)	Technology
Hamburg	2100000	Nitrification only
München I	2000000	Nitrification only
Köln-Stammheim	1450000	SBR
Hanau	270000	SBR
Ingolstadt	235000	SBR
Cuxhaven	400000	Air stripping
Göttingen	220000	Air stripping
Dormagen	80000	Membrane system
Hattingen	100000	Deammonification/Moving bed
Landshut	260000	Moving bed

A review of the different separate treatment technologies being apply by WWTPs in Germany for nitrogen removal showed that the sequencing batch reactor (SBR) process configuration is the most common technology used for the management of sludge water (Jardin, et al., 2006).

A comparison between the different nitrogen removals technologies of both biological and physico-chemical are given in table 5.

Table 5. Comparison between N- removal technologies (Kempen, et al., 2001)

N-removal Technology	Sludge production		Dosage Chemicals	Energy requirements	Operation	Cost Estimate (EUR/Kg-N)
	Chemical	Biological				
Air stripping	yes	no	yes	average	average	6,0
Steam stripping	yes	no	yes	high	complex	8,0
CAFR process	yes	no	yes	low	complex	6,0
Biofilm airlift reactor	no	low	yes	average	average	5,7
SHARON process	no	low	yes	average	simple	1,5

As seen in table 5, among the biological treatment technology the SHARON process has the lowest cost estimate with a value of 1,5 EUR/Kg-N and within the physico-chemical treatment options air stripping and CAFR processes share the same cost estimate value of 6,0 EUR/Kg-N.

2.5.1. Biological Process

The processes involve in the different technologies used for the biological removal of nitrogen generally includes either Nitrification/Denitrification, Nitritation/Denitritation or Deammonification. The main steps of the mentioned processes and some of their characteristics are given in figure 9.

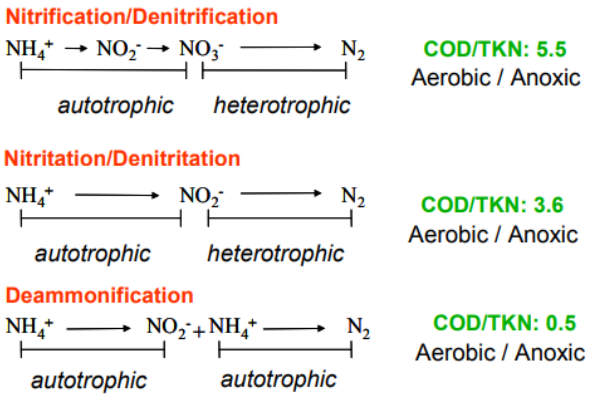

Figure 9. Processes involve in the biological removal of nitrogen (Jardin, et al., 2006)

The oxygen and organic demand varies from process to process. For instance, the Nitrification/Denitrification process is characterized by being the one with the highest demand for oxygen and organic substrate. A comparison between these processes is given in figure 10.

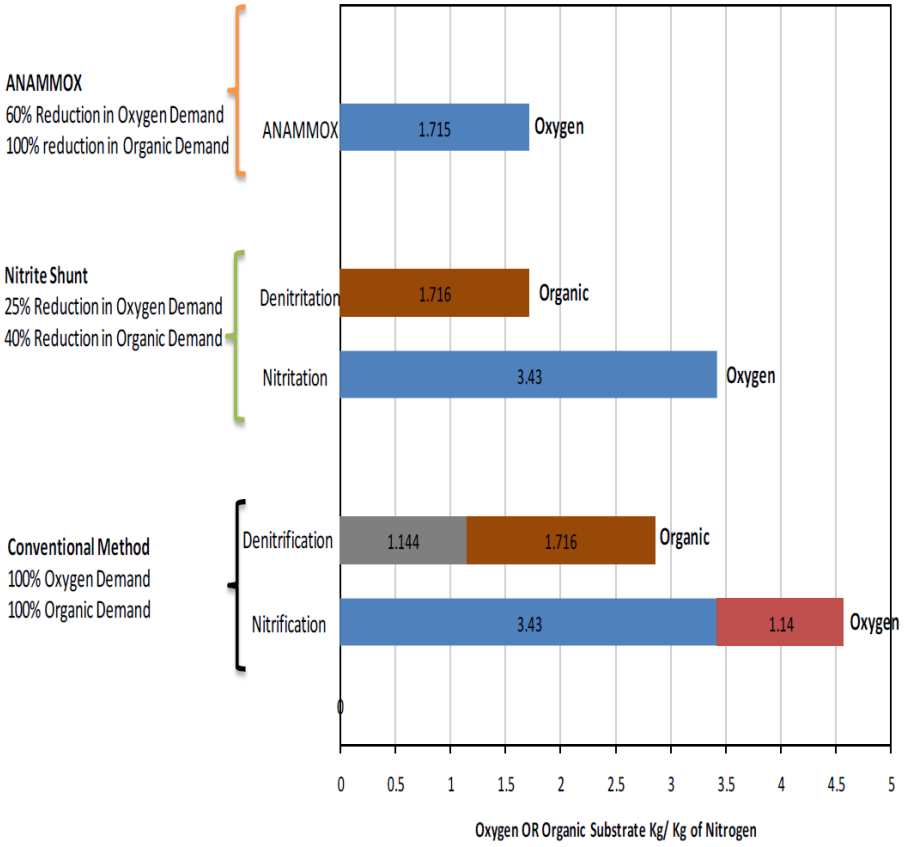

Figure 10. Oxygen and organic demand for biological nitrogen removal processes (Magdum & Kalyanraman , 2017)

2.5.1.1. Nitrification/Denitrification

Nitrification/Denitrification is regard as the conventional method for the removal of nitrogen. The conventional pathways follow by nitrogen in biological treatment process are shown in figure 11. It can be seen that the main forms of nitrogen with respect to their oxidation state are ammonia (NH_3) and ammonium (NH_4^+) with an oxidation number of minus three (-3), nitrogen gas (N_2) with an oxidation number of zero (0) and nitrite (NO_2^-) and nitrate (NO_3^-) with oxidation numbers of plus three (+3) and plus five (+5) respectively.

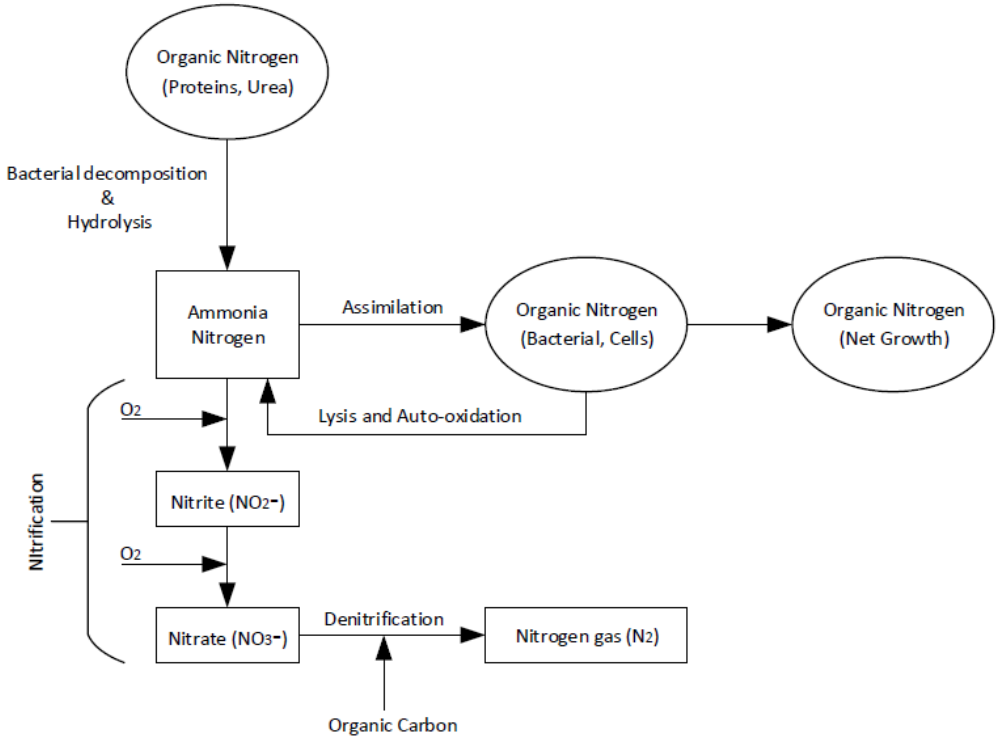

Figure 11. Conventional nitrogen transformation in biological treatment process (Sedlak, 1991)

As depicted in figure 11, biochemical decomposition and hydrolysis of organic nitrogen compounds like urea leads to the formation of ammonia. The ammonia nitrogen will eventually be assimilated by microorganisms for the formation of new cells where approximately 12 to 13 % of the cell dry mass corresponds to nitrogen. Some of the assimilated nitrogen will return to the system due to lysis caused by the process conditions or other biological factors. Furthermore, ammonia nitrogen in the presence of oxygen can be further oxidized to nitrate in a process known as nitrification by two groups of microorganism commonly known as nitrifiers. Finally, nitrate in the absence of oxygen but with the presence of carbon source can be transformed to nitrogen gas through a process known as denitrification (Sedlak, 1991) .

A common operational mode use in WWTP for the removal of nitrogen from side streams by the application of the nitrification/denitrification processes is the sequencing batch reactor (SBR). Figure 12 illustrates the SBR operating work principles.

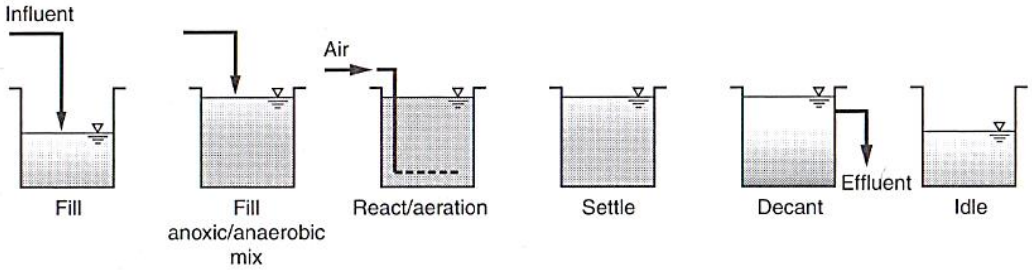

Figure 12. SBR Operational mode principles (Metcalf & Eddy, Inc., 2003)

Depending on the wastewater strength, BOD concentration and operation condition almost of the nitrate present in the mixed liquor from the idle step is removed in the SBR system. The removal of nitrate also takes place during the non-aerated settle and decant steps. During the filling step the removal of nitrogen is enhance by mixing without aeration which increases the contact between the mixed liquor and the incoming wastewater. The NO_3^--N concentration has been reported to be less than 5 mg/L in SBR wastewater treatment facilities (Metcalf & Eddy, Inc., 2003).

2.5.1.1.1. Nitrification

Nitrification can be described as a two-step process in which aerobic, autotrophic nitrifying bacteria oxidizes ammonia to nitrate. In activated sludge processes the main genera of nitrifying bacteria are the *Nitrosomonas* and *Nitrobacter*. In the first step, the *Nitrosomonas* or ammonia oxidizing bacteria (AOB) oxidizes ammonium to nitrite and in the second step the *Nitrobacter* or nitrite oxidizing bacteria (NOB) oxidizes the nitrite produced by the AOB to nitrate. The reactions for AOB, NOB and the total oxidation reaction are shown in equations 1, 2 and 3 respectively (Dombrowski & In Su Choi, 2007).

$$NH_4^+ + 1.5O_2 \xrightarrow{Nitrosomonas} NO_2^- + H_2O + 2H^+ \qquad (Eq.1)$$

$$NO_2^- + 0.5O_2 \xrightarrow{Nitrobacter} NO_3^- \qquad (Eq.2)$$

$$NH_4^+ + 2O_2 \rightarrow NO_3^- + H_2O + 2H^+ \qquad (Eq.3)$$

Furthermore, the overall reaction that includes both oxidation and synthesis is given by equation 4, where the bacteria cells are represented by the formula $C_5H_7NO_2$ (Sudarno, 2011).

$$NH_4^+ + 1{,}863O_2 + 0{,}098CO_2 \rightarrow 0{,}0196C_5H_7NO_2 + 0{,}98NO_3^- + 0{,}0941H_2O + 1{,}98H^+ \quad (Eq.4)$$

As described by equations 3 and 4, the main characteristics of nitrifiers can be described as high demanders for oxygen, they generate small amount of biomass when compared to the oxygen they take and they affect the alkalinity of the system by their generation of hydrogen ions (H^+) and depletion of CO_2. For example, for each gram of ammonia nitrogen (NH_3·N) they convert to nitrate, approximately 4.57 grams of oxygen are consumed, 0.16 grams of new biomass is formed, 7.14 grams of alkalinity are lost and 0.08 grams of carbon dioxide are used for the formation of new biomass. Another important characteristic is that they are slow growers compare to heterotrophic bacteria whose maximum specific growth rate is approximately 10 to 20 times larger compared to nitrifying bacteria. During the process, nitrification can be affected by depletion of DO below 3.0 mg/L and when the pH becomes acidic. Nitrification processes are commonly design to have solid retention times (SRT) ranging from 10 to 20 days at 10° C and 4 to 7 days at 20° C (USA-EPA, 2009).

The slow growth of nitrifiers is explained by the low amount of energy obtained by the oxidation of inorganic matter and the high energy that is required to assimilate the inorganic carbon as the carbon source. The exponential growth time for nitrifiers at 20°C is in between 24 to 48 h while the doubling time for heterotrophic bacteria is approximately in between 20 to 30 min (AQUAFIX, 2016). A comparison between the auto-chemolithotrophic process corresponding to nitrifiers and a hetero-chemoorganotrophic process is shown in figure 13.

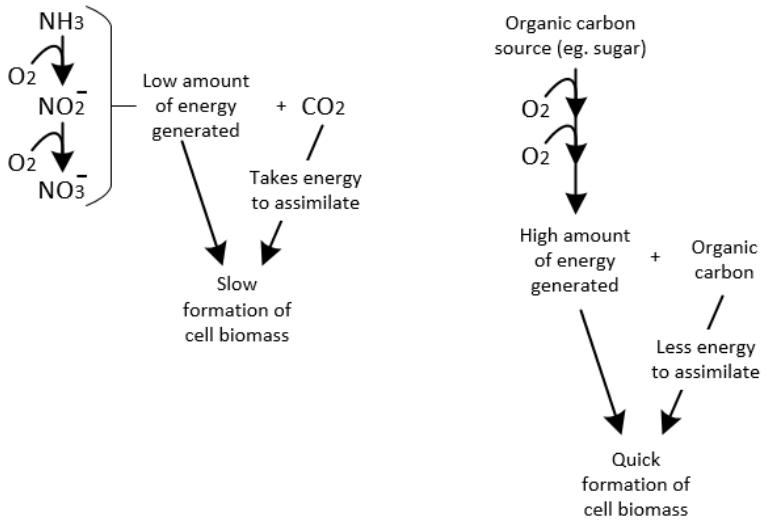

Figure 13. Auto-chemolithotrophic vs. hetero-chemoorganotrophic process (AQUAFIX, 2016)

2.5.1.1.2. Denitrification

Denitrification is known as the reduction of nitrate or nitrite to different reduced forms such as nitrous oxide (N_2O), nitrogen monoxide (NO) and Nitrogen (N_2). The biological reduction is performed by a diverse group of facultative heterotrophic microorganisms that are able to used nitrate or nitrite as the final electron acceptor instead of molecular oxygen (O_2). As illustrated in equation 5, the reduction of nitrate or nitrite-nitrogen in the denitrification process is a chain of different intermediate products owed to the activity of specific reductase enzymes which are promoted by the lack of molecular oxygen (O_2) in the system. The term anoxic is used to distinguish a denitrifying system from other metabolic process.

$$NO_3^- \rightarrow NO_2^- \rightarrow NO \rightarrow N_2O \rightarrow N_2 \qquad (Eq.5)$$

If the organic substrate present within wastewater is represented by the molecular formula $C_{10}H_{19}O_3N$ then its oxidation reaction can be simplify as shown in equation 6.

$$C_{10}H_{19}O_3N + 10NO_3^- \rightarrow 5N_2 + 10CO_2 + 3H_2O + NH_3 + 10OH^- \qquad (Eq.6)$$

The increase of alkalinity given by equation 6 is equivalent to the ratio of 3,57 mg of alkalinity generated as $CaCO_3$ per milligram of nitrate-nitrogen reduced (USA-EPA, 2009).

A comparison between nitrifying and denitrifying bacteria is given in table 5.

Table 6. Nitrifying vs. denitrifying bacteria (Dombrowski & In Su Choi, 2007)

Characteristic	Nitrifiers		Denitrifiers
	Nitrosomonas	***Nitrobacter***	
Carbon source	Inorganic carbon (CO_2)	Inorganic carbon (CO_2)	Organic carbon
Cell shape	Coccus (spherical)	Bacillus (rod shape)	-
Cell size (µm)	1.0 – 1.5	0.5 – 1.0	-
O_2 requirements	Obligate aerobic	Obligate aerobic	Facultative anaerobic
pH range	5.8 – 8.5	6.5 – 8.5	6.5 – 8.5
t_g (h)	8 - 36	12 - 60	0.25 – 0.5
T, growth range (°C)	5 – 30	5 - 40	

2.5.1.2. Nitritation/Denitritation

The most common Nitritation/Denitritation process is known as single reactor for high activity ammonia removal over nitrite or SHARON process which was developed to remove the nitrogen from high strength ammonia side streams. In general, as illustrated in figure 9, the Nitritation/Denitritation mechanism involves the oxidation of ammonium-nitrogen to nitrite-nitrogen and then the reduction of nitrite-nitrogen to nitrogen gas by heterotrophic bacteria under anoxic conditions. The SHARON process is made up of a single reactor where the oxidation of nitrite is inhibit by the temperature conditions and the manipulation of the hydraulic retention time (HRT) and/or solid retention time (SRT). The process takes advantage of the relative high temperatures of sludge digester liquor which are generally in between 25 to 30°C (EPA, 2007). At this temperature conditions the growth rate of AOB is higher than the NOB. The minimum doubling time for AOB has been reported to be in between 7 to 8 hours while for NOB is in between 10 to 13 h. Thus, for this process the SRT is usually set higher than the AOB doubling time but shorter than the NOB doubling time. (Sanchez, et al., 2014). In this process, the HRT equals the SRT with values ranging in between 1 to 2 days (EPA, 2007). A common SHARON process scheme is illustrated in figure 14.

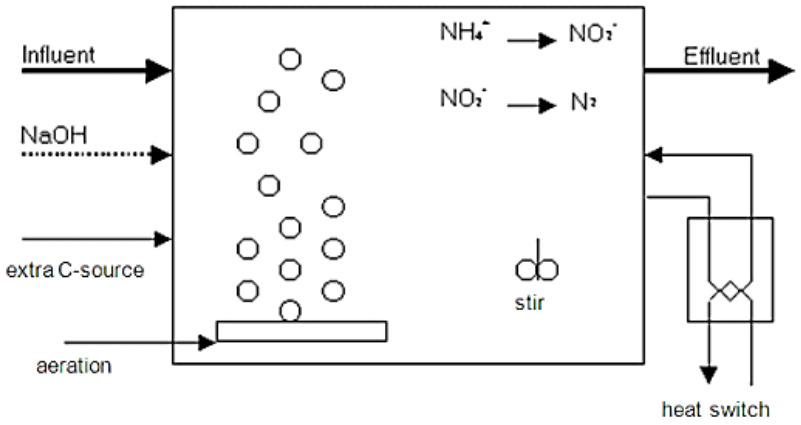

Figure 14. SHARON process (emis, 2015)

2.5.1.3. Deammonification

Deammonification is a two-step process that involves the conversion of half of the ammonium to nitrite and then the oxidation of ammonium to nitrogen gas by using nitrite as the electron acceptor and carbon dioxide as the carbon source. The first step in the deammonification process can be achieved by the implementation of the

SHARON process while the second step is the anaerobic ammonium oxidation or ANAMMOX process (Jenkins & Wanner, 2014).

The anammox process is a relative new anoxic process that uses bacteria which is able to produce nitrogen gas by the oxidation of ammonium with nitrite instead of oxygen. Anammox organisms belong to the *Planctomycetes phylum*. They are autotrophic bacteria, characterized by having slow growth with generation times of about 2 weeks. The general reaction is illustrated in equation 7 (Ward, 2013).

$$NO_2^- + NH_4^+ \rightarrow N_2 + 2H_2O \qquad (Eq.7)$$

During the deammonification process the production of sludge is slow due to the fact that both SHARON and ANAMMOX processes are autotrophic and it can be performed by the used of the SBR configuration (Jenkins & Wanner, 2014). The working principle of the deammonification process is given in figure 15.

Figure 15. Deammonification process principle (Schmidt, et al., 2003)

Other common deammonification technologies exist under different trade names. Amon them are DEMON®, CANON® and ANITA®. Table 6 compares the different deammonification technologies in terms of their number of facilities being either in operation or under construction.

Table 7. Deammonification technologies and facilities in operation (Capodaglio, et al., 2016)

Technology Trade Name	Number in operation or construction	Facility Size (Kg N/d)		First installed (y)
		Smallest	Largest	
ANAMMOX®	22	50	12100	2002
ANITA™Mox	6	110	350	2010
DeAmmon®	3	130	2455	2001
DEMON®	37	50	13500	2004
Terra-N®	5	90	750	2008

2.5.2. Physico-Chemical Process

Contrary to biological process whose end result is the removal of nitrogen from side streams, the physico-chemical process provide the opportunity to not only remove but

also recover nutrients. Some of the most commonly used physico-chemical process include ammonia stripping and precipitation of struvite.

2.5.2.1. Ammonia Stripping

The desorption process or stripping is a physical process that allows the removal of nitrogen from side streams by adjusting the alkalinity of the liquid medium. The increase in pH switches the equilibrium between ammonium and ammonia towards ammonia gas. Usually the ammonia gas is stripped from the liquid phase by using either ammonia free air or steam. Generally, the stripping process takes place in a packed column that is design to operate in countercurrent flow mode where the ammonia-laden liquid enters at the top of the column and the air or steam enters at the bottom section. The treated liquid and the ammonia-laden gases leave the column at the bottom and top sections respectively. For the case of air stripping, one way of recovering the ammonia is through the use of the scrubbing process with sulfuric acid. During the absorbing process the ammonia gas enters the liquid phase and reacts with sulfuric acid to form ammonia sulfate as the end product. The ammonia sulfate solution is usually used as a fertilizer (TASK , 2017). The general ammonia stripping process is depicted in Figure 16.

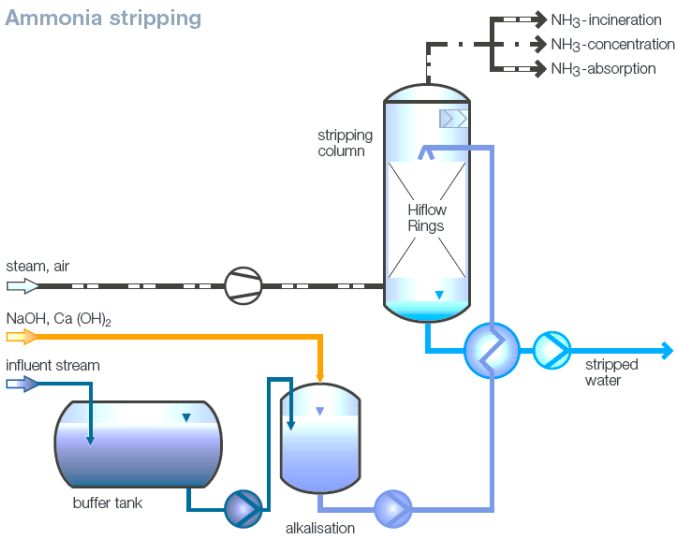

Figure 16. Ammonia stripping process (RVT, 2015)

2.5.2.2. Precipitation of Struvite

Under pH control conditions ammonium, magnesium and phosphate react to form the Magnesium Ammonium Phosphate complex known as struvite. The struvite reaction formation is described in equation 8 (Lens, et al., 2002).

$$NH_4^+ + PO_4^{3-} + Mg^{2+} + 6H_2O \rightarrow NH_4MgPO_4 \,.\, 6H_2O \qquad (Eq.8)$$

The precipitation of struvite depends strongly on the pH conditions having an optimal around 10. Figure 17 shows the solubility of struvite as a function of pH at 25°C.

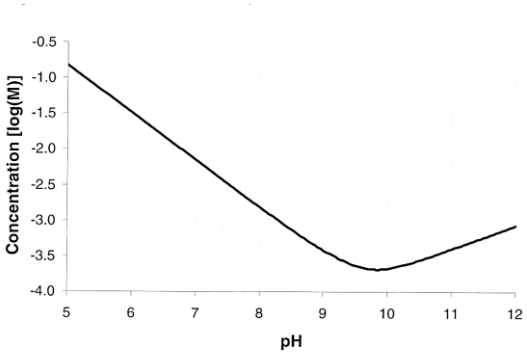

Figure 17. Struvite solubility as a function of pH at 25°C (Lens, et al., 2002)

The CAFR (Chemische Ammonium Fällung und Rezyklierung) process applies the precipitation of struvite for the removal and recovery of nitrogen. The basic steps of this technology are pretreatment of the ammonium-laden liquid to remove solids follow by the formation, separation and thermal treatment of struvite. The process diagram is illustrated in figure 18.

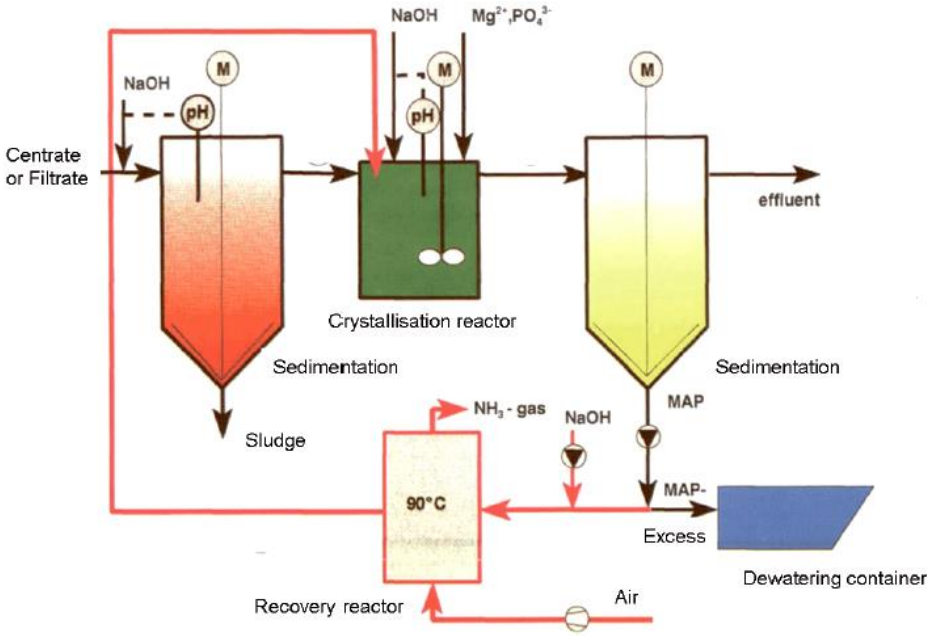

Figure 18. CAFR process diagram (stowa, 2012)

The thermal decomposition of struvite takes place within temperatures ranging from 80 to 90°C and at pH greater than 12,7 (stowa, 2012). At this condition struvite decomposes to magnesium sodium phosphate as described by equation 9 (Lens, et al., 2002).

$$NH_4MgPO_4 + NaOH \rightarrow MgNaPO_4 + NH_3 + H_2O \qquad (Eq. 9)$$

The ammonia formed during the thermal decomposition step is strip out by air from the system and later it can be processed into a concentrated ammonia solution. And, the formed $MgNaPO_4$ can be recycle and reuse in the precipitation step.

2.6. BIOFILMS

The term biofilm describes the non-uniform growth of microorganisms held together and attached to a solid support by the action of extracellular polymeric substances (EPS) (Sudarno, 2011). The EPS are produced by the cells and can contain polysaccharides, proteins, free nucleic acids and water (Henze, et al., 2008). In general, a biofilm system is composed by a support material, biofilm zone and bulk fluid. The biofilm zone is divided in two zones known as the base film and surface film. The base film is characterized by having defined boundaries contrary to the surface film whose shape is irregular. The surface film is the transition zone between the biofilm and the bulk fluid. A visualization of a biofilm system is shown in figure 19.

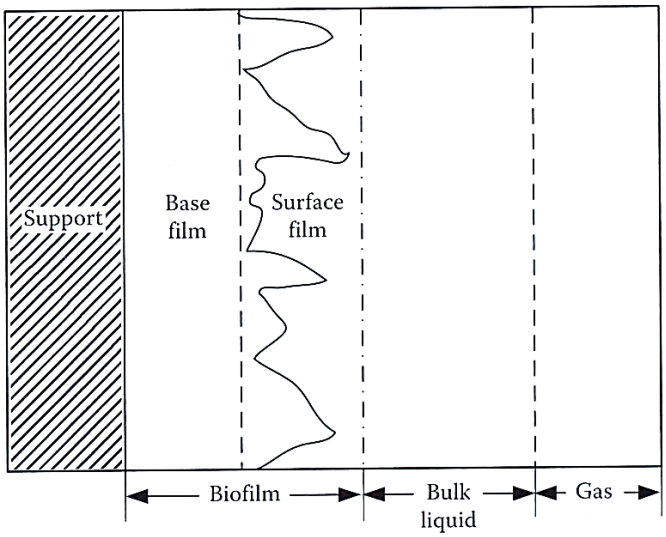

Figure 19. Biofilm system (Daigger, et al., 2011)

Furthermore, substrates and oxygen are transported from the bulk fluid to the biofilm by convection and diffusion mechanisms. Depending on the biofilm development stage and thickness the available substrates may diffuse into the biofilm and be partially or

entirely consumed by the microorganisms. This characteristic leads to the distinction between a completely penetrated or shallow biofilm and incompletely penetrated or deep biofilm (Logan, 2012). The available substrates within a biofilm either by transport from the bulk fluid or by production through the different metabolic process taking place within the biofilm causes the generation of different metabolic zones. These zones are aerobic, anoxic and anaerobic. For the case of a shallow biofilms, oxygen may be only available for the biofilm outer zone, promoting the growth of aerobic microorganism such as nitrifying bacteria and protozoa. The metabolites produced by the aerobic microorganism such as nitrate and nitrite may diffused to the middle or anoxic layer where anoxic processes can take place. Furthermore, cell lysis and the anaerobic conditions within the biofilm inner layer results in the reduction of acetic acid and sulfates (Dombrowski & In Su Choi, 2007). The representation of the different biofilm zones are illustrated in figure 20.

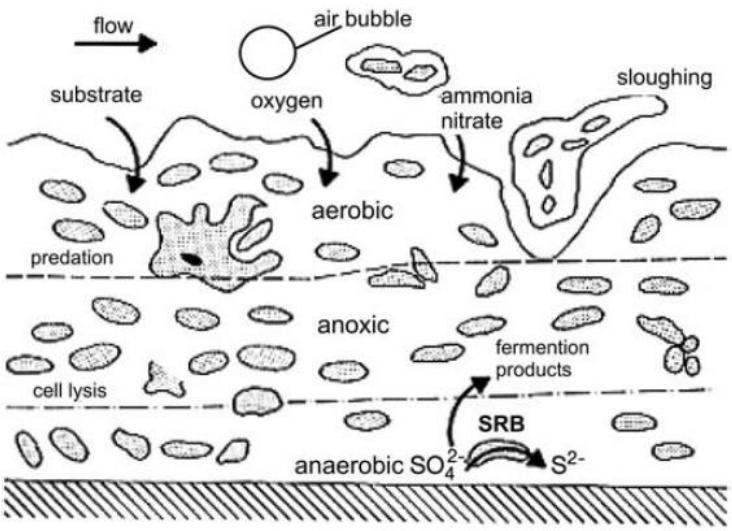

Figure 20. Biofilm metabolic zones (Dombrowski & In Su Choi, 2007)

2.6.1. Biofilm development steps

The formation of biofilms can be attributed to basically three mechanisms, these include the redistribution of the already attached cells through surface motility, the spread of the attached cells through binary division and the retention of cells from the bulk fluid into the developing biofilm. The last mechanism may be promoted by the adsorption of substances such as proteins and polysaccharides contained within the

bulk fluid into the clean solid surface. These adsorbed substances may serve as a bridge allowing the easier transport and eventual adherence of microorganisms from the bulk fluid to the solid surface. The degree of contribution from each of these mechanisms depends on the nature and all of the physical, chemical and biological characteristics of the system such as the type of bulk fluid, microorganisms and solid material (Stoodley, et al., 2002).

The development of biofilms can be summarized in five steps. These steps are reversible attachment, irreversible attachment, maturation, detachment and return of the cells to planktonic life where the sessile cycle is repeated again (Sudarno, 2011). The general steps involve in biofilm development are illustrated in figure 21.

Figure 21. Biofilm development steps (Sudarno, 2011)

The earliest stage of biofilm formation or reversible attachment step is characterized by a deficiency of EPS surrounding the individual cells. The lack of EPS leads to a weak interaction between the already attached cell and the available surface or substratum. The weak interaction allows for cell motility which is characteristic for each cell species and possible migration out of the substratum. The increase of EPS is essential for the transition from the reversible to the irreversible attachment step. The second step indicates a permanent bonding between the cell and the solid surface which allows for further interaction between cells resulting in a stronger attachment to the substratum. At this stage micro colonies within the biofilm have been developed leading to the maturation stage. The third stage in biofilm development is characterized by spread of the biofilm away from the solid surface and the presence of diverse microorganisms along with their complex actives involving adaptation,

protection and changes in their metabolic process. Once maturation has been stablished in the biofilm, detachment of cells or group of cell start to take place in the biofilm. The detachment process of cells away from the biofilm allows them to enter the planktonic state where growth takes place and eventual biofilm development can be repeated by following the five steps cycle (Sudarno, 2011).

2.6.2. Factors affecting biofilm formation

As stated before biofilm formation is influenced by the physical, chemical and biological characteristics of the system. Basically, the main factors affecting the biofilm formation are the substratum characteristics, kind of microorganisms present in the system, hydrodynamic conditions and availability of nutrients in the bulk and biofilm phases.

Substratum characteristics such as geometry, reactivity, corrosivity, roughness, hydrophobicity among others directly impact the development of biofilms. For example, it has been observed that a rough material facilitates biofilm formation and provides protection against shear forces.

The hydrodynamic conditions and the availability of nutrients in the system are determinant factors that affect the biofilm formation and its density. For instance, for the case of constant nutrients supply the mass transfer of nutrients and products between the bulk and biofilm phases is greater at high flow velocities leading to a faster biofilm development and increase in biofilm density. Furthermore, the high shear forces generated in turbulent systems may alter the biofilm stability leading to an increase in the biofilm detachment rate. The detachment of cells from the biofilm or substratum occurs at places where the mechanical stress due to the flowing fluid overcomes the biofilm mechanical strength (Sudarno, 2011). In general there are three detachment mechanisms known as erosion or shear removal, abrasion and sloughing. Erosion is the continuous removal of bacterial surface layers caused by the action of shear forces exerted by the moving fluid in contact with the biofilm surface. On the other hand, Sloughing is a random event resulting in the detachment of large portions of the biofilm all the way down to the substratum. Biofilm sloughing may be promoted by nutrients and oxygen deficiencies in the biofilm deeper layers leading to an increase of anoxic and anaerobic zones where the production of volatiles fatty acids and insoluble gases may interfere with the biofilm stability. Others factors involving drastic

changes in the biofilm surroundings may result in biofilm sloughing. Additionally, collision between the biofilm support particles during operation or backwashing processes result in the loss of cells from the biofilm surface layers being denser biofilms more resistant to abrasion (Costerton & Lappin-Scott, 2003). The different detachment mechanisms are illustrated in figure 22.

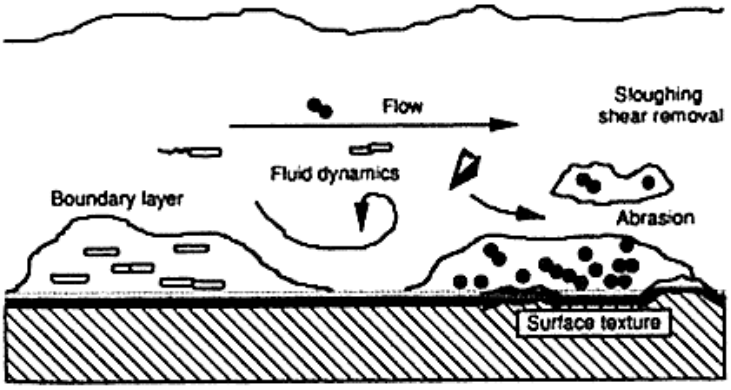

Figure 22. Biofilm detachment mechanisms (Costerton & Lappin-Scott, 2003)

The biological factor is elemental in biofilm formation considering that by nature different species of microorganisms experience different growth rates and have different responses and adaptation mechanisms under different system conditions. Hence, the structure and characteristics of the biofilm is a reflection of the kind of microorganisms present in the system (Sudarno, 2011).

2.6.3. Biofilm mass transfer mechanisms

The concept of a stagnant film and boundary layer theory has been used repeatedly to model the external mass transfer mechanisms in biofilm systems while microbial uptake kinetics usually follow the Michaelis-Menten model (Logan, 2012). Basically, the stagnant film model is a one dimensional approach that represent the biofilm and bulk fluid as planes parallel to the substratum and with the existence of a hypothetical mass transfer boundary layer above the biofilm which is assume to be constant over the entire biofilm (Henze, et al., 2008). In this idealization model the substrate concentration in the whole bulk fluid is assume to be constant and the resistance to mass transfer from the bulk fluid to the biofilm is assume to take place in the stagnant film (Daigger, et al., 2011). The representation of the stagnant film model is shown in figure 23.

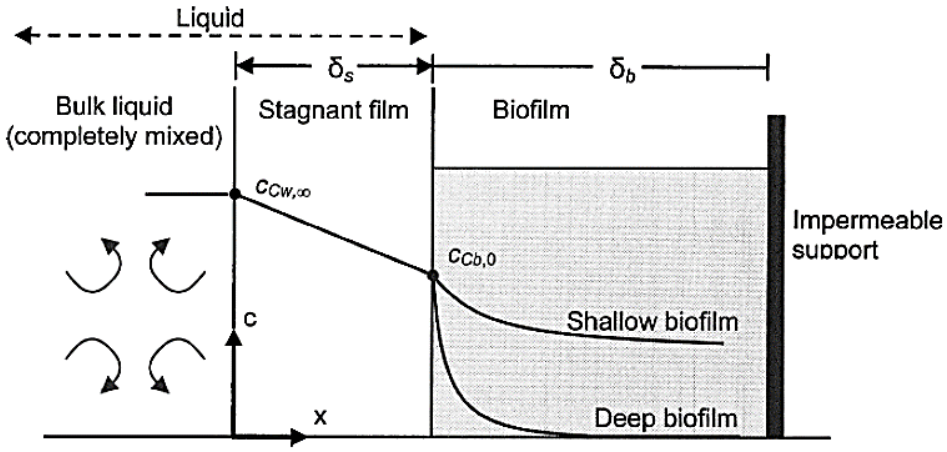

Figure 23. Stagnant film model (Logan, 2012)

In figure 23, $C_{Cw,\infty}$ represents the substrate concentration in the bulk liquid and the bulk liquid-stagnant film interface, $C_{cb,0}$ is the substrate concentration at the biofilm surface or biofilm-stagnant film interface and δ_s and δ_b are the stagnant film and biofilm thickness respectively.

The mass transport boundary layer approach is one way of modeling the external mass transfer from the bulk fluid to the biofilm with the use of the mass transfer coefficient which accounts for the diffusive and convective mass transfer effects. This approach is described by equation 10 (Logan, 2012).

$$J_{C,x} = k_w \left(C_{Cw,\infty} - C_{Cb,0}\right) \qquad (Eq.10)$$

Wilson and Geankoplis developed a mass transfer correlation for the case of biofilms on spherical particles in packed beds. This correlation and its application limits are given by equations 11 (Logan, 2012).

$$Sh = \frac{1{,}09}{\theta} Re^{\frac{1}{3}} Sc^{\frac{1}{3}} \qquad \begin{matrix} 0{,}0016 \leq Re \leq 55 \\ 0{,}35 < \varepsilon < 0{,}75 \end{matrix} \qquad (Eq.11)$$

Where,

Sh = Sherwood number
Re = Reynolds number
Sc = Schmidt number
$J_{C,x}$ = Substrate flux
k_w = Mass transfer coefficient
$C_{Cw,\infty}$ = Substrate concentration in the bulk liquid
$C_{cb,0}$ = Substrate concentration at the biofilm surface
d_c = Dimension characterizing the media
D_{Cw} = Diffusivity of the substrate in water
ε = Bed porosity

Sherwood, Reynolds and Schmidt numbers can be calculated by using equations 12, 13 and 14 respectively (Logan, 2012).

$$Sh = \frac{k_w d_c}{D_{C_w}} \qquad (Eq. 12)$$

$$Re = \frac{v \rho_w d_c}{\mu_w} \qquad (Eq. 13)$$

$$Sc = \frac{\mu_w}{\rho_w D_{C_w}} \qquad (Eq. 14)$$

Where,

v = Bulk fluid velocity passing the biofilm
ρ_w = Fluid density
d_c = Dimension characterizing the media
μ_w = Fluid viscosity
D_{Cw} = Diffusivity of the substrate in water

The stagnant film concept is the other approach use to model the external mass transfer. In this case the mass transfer across the stagnant film with thickness "δ_s" is assume to take place only by molecular diffusion (Logan, 2012). This approach is described by equation 15.

$$J_{C,x} = \frac{D_{C_w}}{\delta_s} \left(C_{Cw,\infty} - C_{Cb,0} \right) \qquad (Eq. 15)$$

A comparison between equations 10 and 15 results in the relation between the mass transfer coefficient and the stagnant fluid film thickness. This relation is given by equation 16.

$$k_w = \frac{D_{C_w}}{\delta_s} \qquad (Eq. 16)$$

Furthermore, the stagnant liquid film thickness can be estimated for the case of biofilms on spherical particles in packed beds by solving equations 11, 12 and 16. The resulting expression is given by equation 17 (Logan, 2012).

$$\delta_s = \frac{d_c \varepsilon}{1{,}09} Re^{-\frac{1}{3}} Sc^{-\frac{1}{3}} \qquad (Eq. 17)$$

As described by equation 17, the mass transfer coefficient and stagnant film thickness values are functions of the bulk fluid properties such as its viscosity and density, the diffusivity of the substrate in the fluid and the turbulence conditions of the system which

is strongly influenced by the bulk fluid velocity passing the biofilm (Daigger, et al., 2011). The influence of the bulk fluid velocity on the thickness of the boundary layer is illustrated in figure 24.

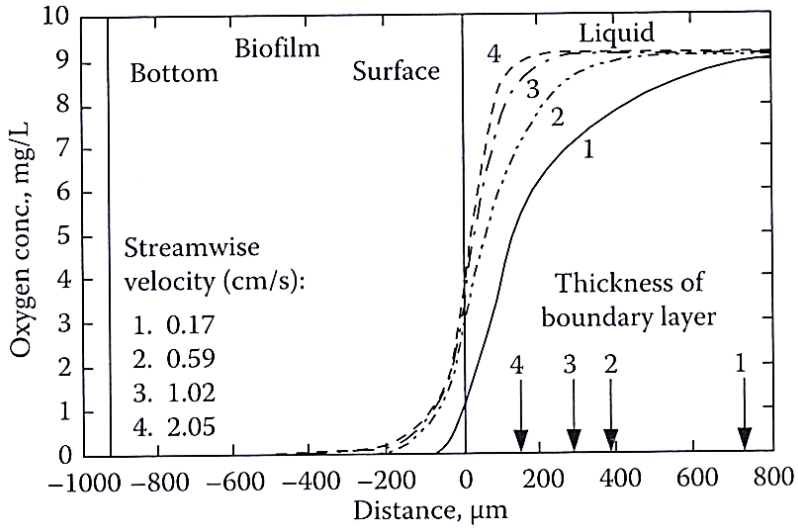

Figure 24. Effect of fluid velocity on boundary layer (Daigger, et al., 2011)

In figure 24, it can be observed how the increase in the bulk stream velocity decreases the thickness of the boundary layer and thus increasing the oxygen mass transfer coefficient value or the external mass transfer of the substrate from the bulk fluid to the biofilm surface.

2.7. BIOFILM REACTORS

Biofilm reactors are used as an alternative option other than suspended growth systems for the treatment of wastewaters. In both treatment options the same kind of microorganisms are involved in the removal of pollutants. For that reason, the same optimal operation conditions apply in order to achieve an effective treatment process such as temperature, pH and availability of the electron donor and acceptor (Henze, et al., 2008).

The advantages and disadvantages of biofilm reactors may be particular for a specific case depending on factors such as organic and nutrients load. In general, some of main advantages of biofilm reactors when compared to suspended growth systems include the reduction of reactor volume leading to lower demand for land, high biomass concentration, operation simplicity and their implementation can lead to a reduction in operating and energy costs (WEF, 2010). For instance, biofilm reactors may minimized or eliminate the settling capacity needs and with that all of the equipment required for

the operation of settling tank systems such as pumps, piping and control units (Lewandowski & Beyenal, 2014).

One of the biggest drawbacks of biofilm reactors involves the mass transport limitation inherent to its nature. In biofilm reactors substrates dissolved in the bulk fluid are mostly available to the microorganisms present at the biofilm surface through diffusion mechanisms. On the other hand, in theory all of the cells comprising the biological flocs in suspended systems have access to the dissolve substrates in the bulk fluid. Other problems may arise during the operation of biofilm reactors such as clogging of the media system either by external materials or by excessive overgrowth (WEF, 2010).

Based on their design configuration, biofilm reactors can be divided in four groups. The first group is the non-submerged biofilm reactors which include the trickling filters and rotating biological contactors (RBCs). The second group is the submerged fix bed biofilm reactor (SFBBR) which can be operated as up or down flow. The third group is fluidized bed biofilm reactors which include different configurations such as air lift, fluidized bed and moving bed biofilm reactors (MBBR). And, the last group is the membrane attached biofilm reactors (Henze, et al., 2008). The representation of the different types of biofilm reactors are illustrated in figure 25.

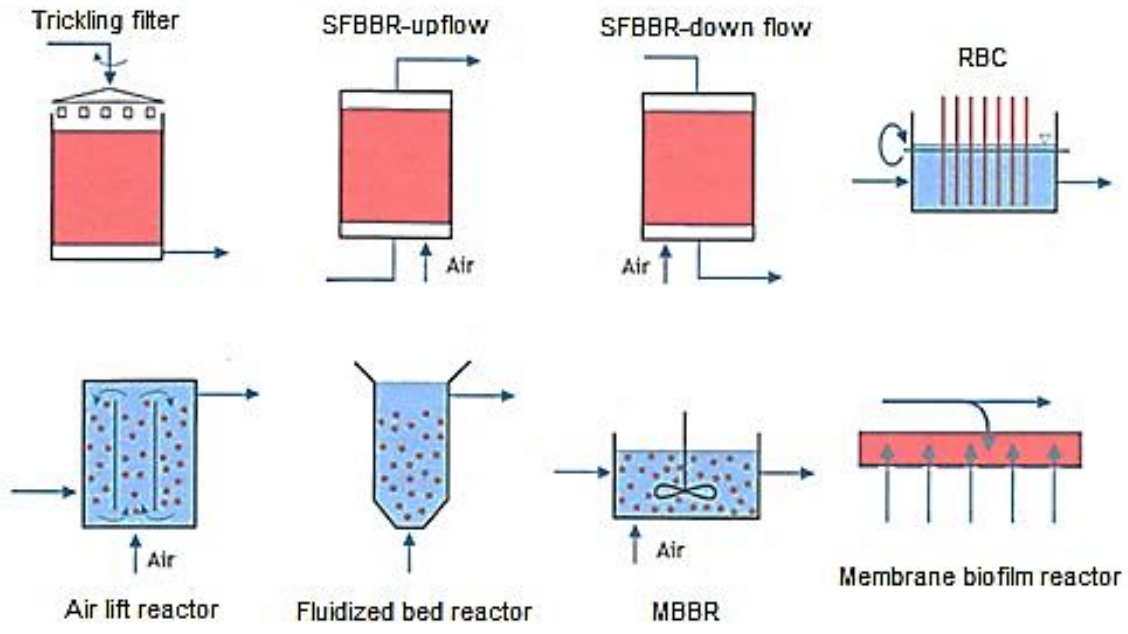

Figure 25. Different types of biofilm reactors (Henze, et al., 2008)

Independently of the biofilm reactor design, they all have to fulfill four general requirements. The first one is related to the nature of biofilm formation which is performed by the retention and growth of microorganisms on the surface of a carrier medium or substratum. This allows for the separation of the HRT from the SRT by biomass immobilization rather than the use of settling tanks like in the case of activated sludge processes. The second requirement is the dependency of the pollutants mass transfer efficiency to the biofilm on the hydrodynamic conditions of the system represented by the bulk flow velocity and mixing and turbulence conditions within the system. The third one, involves the balance between the growth and detachment of microorganisms at the biofilm that can lead to the prevention of reactor clogging while maintaining a stable and active biofilm for maximum substrate removal. The last requirement is the need of biofilm reactors for the addition of external substances that can help the system to achieve the desire operation conditions through the feeding of electron donors and/or acceptors, nutrients, alkalinity control agents, oxygen etc. (Henze, et al., 2008).

2.7.1. Carrier material

The ideal carrier material should have affinity for the attachment of microorganisms, mechanical strength against shear forces and collisions, low cost and easy accessibility. One of the most important features related to biofilm carrier media involves the surface characteristics since properties such as surface charge, hydrophobicity, porosity, roughness, density, shape, dimensions and material influence at some degree the attachment and grow of the microorganisms.

In general, the different carrier materials use in biofilm reactors can be divided as inorganic and organic, some of them can be found naturally others are synthetic and they are produced in different shapes and sizes. Inorganic carrier materials include ceramic, glass, sand and clay minerals and organic carrier materials are dominated by artificial polymeric materials. Furthermore, unlike inorganic carrier material, plastic biofilm carriers can be molded and design according to the specific needs of the process (Muffler & Ulber, 2014). Table 8 describes some common plastic biofilm carriers used in biofilm reactors.

Table 8. Plastic biofilm carriers (WEF, 2010)

Manufacturer	Name	Bulk specific surface area	Nominal carrier dimensions (depth; diameter)	Carrier photo
Veolia Inc.	AnoxKaldnes™ K1	500 m^2/m^3	7,2 mm; 9,1 mm	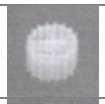
	AnoxKaldnes™ K3	500 m^2/m^3	10 mm; 25 mm	
	AnoxKaldnes™ Biofilm Chip (M)	1200 m^2/m^3	2,2 mm; 45 mm	
	AnoxKaldnes™ Biofilm Chip (P)	900 m^2/m^3	3 mm; 45 mm	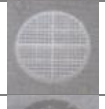
Infilco Degremont Inc.	ActiveCell™ 450	450 m^2/m^3	15 mm; 22 mm	
	ActiveCell™ 515	515 m^2/m^3	15 mm; 22 mm	
Siemens Water Technologies Corp.	ABC4™	600 m^2/m^3	14 mm; 14 mm	
	ABC5™	660 m^2/m^3	12 mm; 12 mm	
Entex Technologies Inc.	Bioportz™	598 m^2/m^3	14 mm; 18 mm	

2.7.2. Trickling filters

Trickling filters are non-submerged fixed-film biological rectors being used in WWTPs for more than 100 years. Its operation can be described as an even distribution of the wastewater over the top of the packing material and a continuous flow of the liquid over the attached biofilm where treatment takes place. Originally, rocks were used as support material for biofilm development however many treatment facilities have been replacing the inorganic material for plastic packings allowing them to increase their treatment capacity (Metcalf & Eddy, Inc., 2003).

A conventional trickling filter with rock media and four-arm rotatory distributor is illustrated in figure 26.

Figure 26. Conventional trickling filter (Greenion, 2014)

The design considerations for trickling filters depends on the packing material being used. For instance, trickling filters using rocks as packed bed material usually are built in circular shapes and with a depth ranging in between 0,9 to 2,5 m. On the other hand, trickling filters using plastic bed material are built in different shapes such as circular or square with depths ranging from 4 to 12 m. Furthermore, tricking filters can be classified as low, intermediate and high rate and roughing filters based on the packed bed material, hydraulic and organic loading rates (Metcalf & Eddy, Inc., 2003).

A comparison between the different trickling filters with some of the design parameters are given in table 9.

Table 9. Classification of trickling filters and characteristics (Metcalf & Eddy, Inc., 2003).

Design Characteristics	**Low rate**	**Intermediate rate**	**High rate**		**Roughing**
Packing material	Rock	Rock	Rock	Plastic	Rock/ Plastic
Specific surface area (m^2/m^3)	45 – 60	45 – 60	45 – 60	90 – 150	-
Hydraulic loading ($m^3/m^2 \cdot d$)	1 – 4	4 – 10	10 – 40	10 – 75	40 – 200
Organic loading (Kg $BOD/m^3 \cdot d$)	0,07 – 0,22	0,24 – 0,48	0,4 – 2,4	0,6 – 3,2	>1,5
Depth (m)	1,8 – 2,4	1,8 – 2,4	1,8 – 2,4	3,0 – 12,2	0,9 – 6
BOD removal efficiency (%)	80 – 90	50 – 80	50 – 90	60 – 90	40 – 70
Effluent quality	Well nitrified	Some nitrification	No nitrification	No nitrification	No nitrification
Recirculation ratio	0	0 – 1	1 – 2	1 – 2	0 – 2

A proper performance of trickling filters can be achieved during operation by guaranteeing an input stream with low solids concentrations. This is usually done by passing the influent through a primary clarifier before entering the biological treatment step. Additionally, the trickling filter design must ensure optimal contact between the downward liquid, the upward or downward air and the biofilm.

The air within trickling filters is usually supply either by natural or forced aeration. In natural aeration normally two air flow conditions can take place depending on the season. In winter time the cold air outside the biofilm is denser than the warmer air inside the trickling filter hence the air flows upwards and in the opposite way the air would flow downwards in summer time. In natural aeration, the efficiency of trickling filters can be affected when the temperature of the liquid and the air are almost the same which results in no airflow. For that reason, the use of ventilators located at the top of the trickling filter may be used in order to maintain a more reliable airflow (Dombrowski & In Su Choi, 2007).

2.7.3. Rotating biological contactor

Compare to trickling filters, RBCs are a relative newer technology considering that they were first introduce around the 1960s. Basically, RBCs are composed of biofilm developed in light plastic disks attached to a rotating shaft and partially submerged in the liquid. The rotation of the plastic disk allows the biofilm to pass from an aeration to a submerged cycle. The biofilm exposure to the atmosphere provides them with aeration while the motion of the biofilm through the liquid provides shear which in turn helps to control biofilm growth. Additionally, the input streams is previously pass through a primary clarifier for the removal of solids (Metcalf & Eddy, Inc., 2003). A RBC system is illustrated in figure 27.

Figure 27. RBC system (Balteau, 2012)

A standard unit in a RBC system is conformed by cylindrical disks attached to the horizontal shaft and they are designed to have diameters and lengths of approximately 3,5 and 7,5 m respectively. A standard unit may have a surface area of about 9300 m^2 however units up to 13900 m^2 can be found. In general, RBC processes are composed by a series of units operating in series mode. The amount of units in the RBS process depends on the desire effluent quality and about 40% of the unit is submerged in the tank containing the wastewater rotating at speeds ranging from 1,0 to 1,6 rpm. The main advantages related to RBCs process are operational simplicity and relative low energy cost (Metcalf & Eddy, Inc., 2003).

Table 10 provides some of the typical RBCs design parameters.

Table 10. Typical RBCs design parameters (Metcalf & Eddy, Inc., 2003)

Parameter	Treatment level		
	BOD removal	**BOD removal and nitrification**	**Separate nitrification**
Hydraulic loading ($m^3/m^2 \cdot d$)	0,08 – 0,16	0,03 – 0,08	0,04 – 0,1
Organic loading (g BOD/$m^2 \cdot d$)	8 – 20	5 – 16	1 – 2
NH_3 loading (g N/$m^2 \cdot d$)		0,75 – 1,5	
HRT (h)	0,7 – 1,5	1,5 – 4	1,2 – 3
Effluent BOD (mg/L)	15 – 30	7 – 15	7 – 15
Effluent NH_4^+-N (mg/L)		<2	1 – 2

2.7.4. Fluidized and expanded bed biofilm bioreactors

In fluidized bed bioreactors (FBBRs) the carrier material is maintained in suspension by the action of the up flowing air or liquid. Depending on the fluid upflow velocity the bed material can be fluidized or expanded. An expanded biofilm reactors is characterized by incomplete fluidization of the packing material (Henze, et al., 2008). The operational upflow velocity is independent of the input flow and it is normally achieved by effluent recirculation. Normally, the FBBR upflow velocities are in between 30 to 36 m/h with HRT ranging from 5 to 20 min and bed depths of about 3 to 4 m (Metcalf & Eddy, Inc., 2003). A general FBR system is illustrated in figure 28.

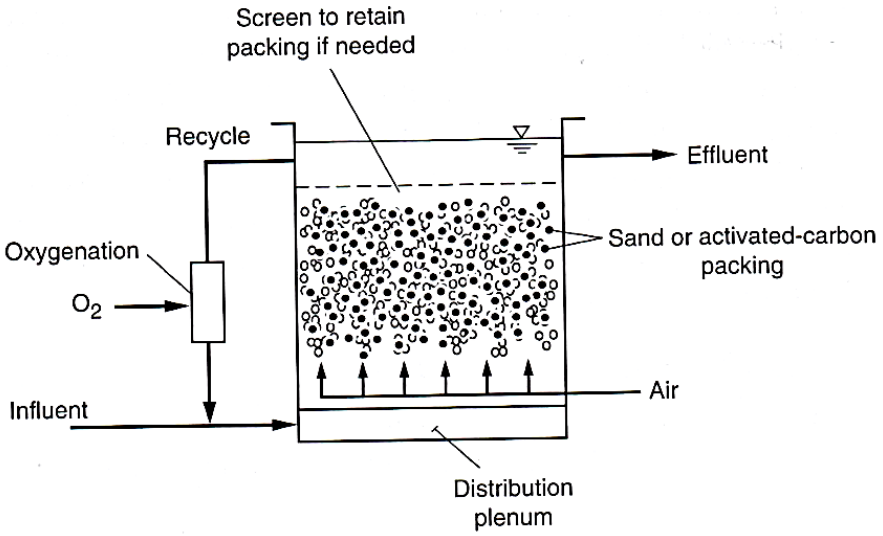

Figure 28. FBBR system (Metcalf & Eddy, Inc., 2003)

One common application of FBBRs is the treatment of groundwater for the removal of hazardous substances. This application uses activated carbon as support material which allows for the adsorption and biotreatment of the toxic organic compounds. Furthermore, several configurations have been developed for fluidized or partially fluidized biofilm bed reactors and have been designed to achieve BOD removal, nitrification and denitrification. One example is the moving bed biofilm reactor (MBBR) developed by Kaldnes® (Metcalf & Eddy, Inc., 2003)

2.7.5. Submerged and aerated fix bed reactors

Submerged fix bed biofilm reactors (SFBBRs) are characterized by having the biofilm support material completely submerged in the liquid. The substrates are removed from the liquid while it moves through the fix bed biofilm either in up or down flow configuration. The sizes of the carrier material are usually small and can be in between 2 to 8 mm with specific surface areas ranging in between 1000 to 3000 m^2/m^3. The use of small media provides the SFBBRs with the capability of performing biodegradation and solid separation in one step. This characteristic also generates the need for the installation of backwashing systems needed for the removal of biomass and entrapped particles and hence avoiding clogging problems (Henze, et al., 2008).

The most common operation mode for SFBBRs is continuous but they can also be operated as sequencing batch biofilm reactors (SBBRs). In SBBR mode the wastewater is fed to the bioreactor, then it is recirculated for a period of time depending

on the desire treatment quality and at the end of the treatment cycle the treated water is discharged (Henze, et al., 2008).

In aerated SFBBRs, the air is normally introduced at the bottom of the bioreactor where the oxygen is transferred to the biofilm as the air bubbles travel thought out the fix bed. Another way of aeration is by predissolving the air into the influent liquid (Metcalf & Eddy, Inc., 2003).

Based on their design, aerated SFBBR can be classified as biological aerated filters (BAFs) or submerged aerated filters (SAFs). In BAFs, both solid retention and biodegradation can be achieved while SAFs make use of coarser carrier material and are designed to only achieve biodegradation. Usually SAFs do not require backwashing systems but the implementation of a post-clarification or filtration step is required for the separation of solids (Henze, et al., 2008).

The SFBBRs have several advantages such as relative low space requirements, ability to treat dilute wastewaters and elimination of sludge settling tanks. However, when compared to activated sludge treatment a major disadvantage is related to a higher capital cost such as the need for complex instrumentation and control systems resulting in potential economic limitations for applications in larger treatment facilities (Metcalf & Eddy, Inc., 2003).

Some of the most known SFBBR processes include the downflow Biocarbone® process and the upflow Biofor® and Biostyr® processes illustrated in figure 29, 30 and 31 respectively.

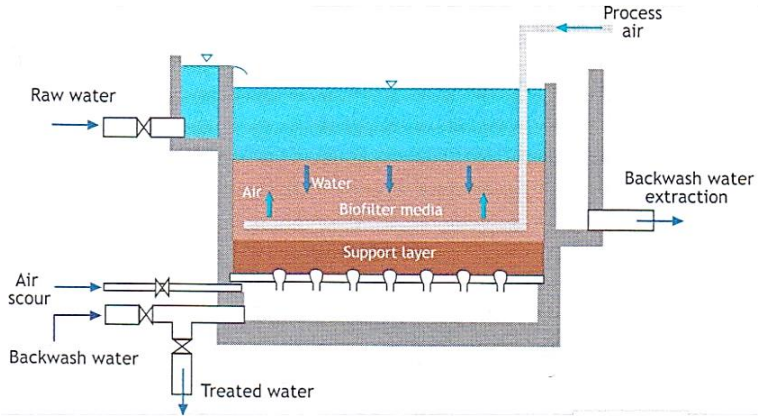

Figure 29. Downflow Biocarbone® process (Henze, et al., 2008)

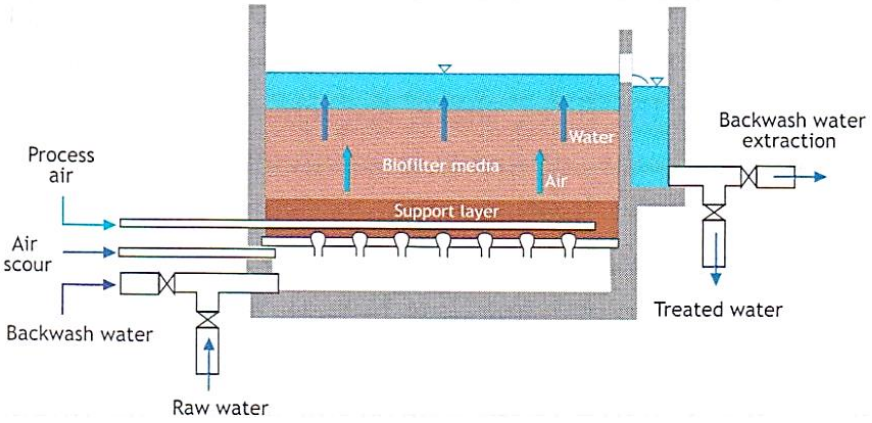

Figure 30. Upflow Biofor® process (Henze, et al., 2008)

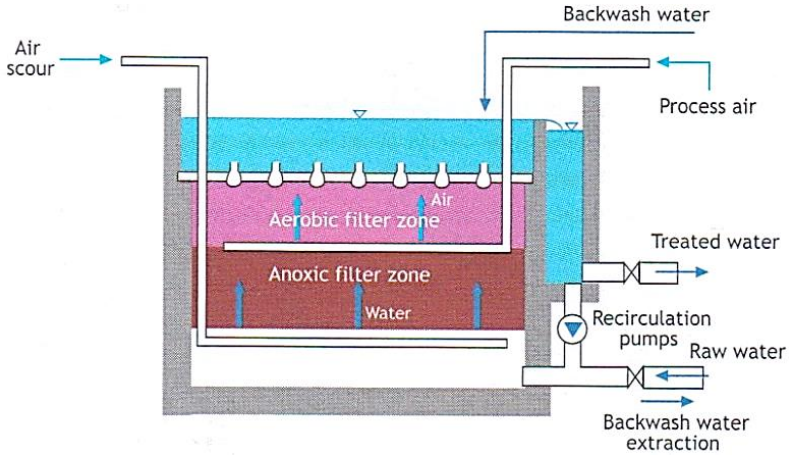

Figure 31. Upflow Biostyr® process (Henze, et al., 2008)

Moreover, the typical design parameters between the Biocarbone®, the Biofor® and the Biostyr® processes are compared in table 11.

Table 11. Comparison between the Biocarbone®, the Biofor® and the Biostyr® processes (Metcalf & Eddy, Inc., 2003)

Parameters	Biocarbone®	Biofor®	Biostyr®
Liquid flow configuration	Downflow	Upflow	Upflow
Carrier material Size (mm) SSA (m^2/m^3)	Fired clay 3 – 5 -	Clay 2 – 4 -	Polystyrene beads 2 – 4 1000
Bed depth (m)	-	2 – 4	1,5 – 3
Backwashing frequency Water flush rate (m/h)	Once per day -	Once per day 10 – 30	- -
Hydraulic loading ($m^3/m^2 \cdot h$)	2,4 – 4,8	5 – 6[d] 10 – 12[b]	-
Organic loading	2,0 – 2,75[a] (Kg BOD/$m^3 \cdot d$) 3,5 – 4,5[d] (Kg BOD/$m^3 \cdot d$)	10 – 12[d] (Kg COD/$m^3 \cdot d$)	4 – 5[a] (Kg COD/$m^3 \cdot d$) 8 – 10[d] (Kg COD/$m^3 \cdot d$)

Nitrogen loading[b] (Kg N/ m^3·d)	1,2 – 1,5	1,5 – 1,8	1,0 – 1,7
Effluent BOD (mg/L)	<10	-	7
Effluent NH_4^+-N (mg/L)	1 – 4	-	1,8
Nitrification rate[a] (Kg/m^3·d) or (%)	0,45	-	80 – 90 % nitrogen oxidation
Recommended DO[c] (mg/L)	3 – 5	-	-

a. For BOD removal and nitrification application; b. For tertiary nitrification application;
c. For efficient nitrification; d. For BOD removal application

2.7.6. Nitrification application for biofilm reactors

As already stated, biofilm reactors have been used in wastewater treatment applications as an alternative to the conventional suspended activated sludge processes, but economic limitations challenge the use of biofilm reactors mainly for large scale applications. However, some biofilm reactors such as trickling filters, RBCs, BAFs and fluidized bed reactors have proved to be efficient and economically feasible in many wastewater treatment applications especially in municipal WWTPs for the removal of organic substances and nitrification (Sudarno, 2011).

The performance of biofilm reactors may be superior to suspended activated sludge processes in nitrification applications especially for the treatment of low strength carbon streams like in the case of side streams from WWTPs. For instance, in activated sludge systems nitrifying microorganisms can be easily wash out of the system due to their low specific growth rate and low capability for flocs formation while biofilm reactors provides the opportunity for nitrifying bacteria to be adsorbed ad further developed in the biofilm system (Dombrowski & In Su Choi, 2007).

The removal of organic matter and ammonia in biofilm reactor systems depend strongly on the organic strength of the wastewater. The main reason is due to the slow biomass formation of the auto-chemolithotrophic microorganisms compare to the faster biomass formation of the hetero-chemoorganotrophs present in the biofilm system. Therefore, for this application the efficiency of a biofilm system will be affected by the wastewater COD concentration, since a competition for the available oxygen will take place between the two groups of microorganisms resulting in the outperformance of heterotrophic organisms over the slow growing nitrifiers. In general,

the configuration for a biofilm reactor system needs to be done in a way that best balances BOD and ammonia removal (Sudarno, 2011).

The most common configurations used for the removal of organic substances and ammonia include a single biofilm reactor, two separate biofilm reactors with a clarification step and two separate biofilm reactors with two clarification steps. In the first configuration BOD and ammonia removal takes place in a single biofilm reactor where a clarification step may be included depending on the biofilm reactor being used. In the second configuration, BOD removal takes place in one biofilm reactor follow by another biofilm reactor where nitrification takes place and the effluent passes to a clarification step for biomass separation. The third configuration is similar to the second one with the exception that it includes another clarification step in between the two biofilm reactors (Sudarno, 2011).

The main parameters that influence nitrifying biofilm performance are divided in biofilm specific and reactor specific. The biofilm specific parameters are more related to the microscopic level of the system which include transport and reaction processes at and in the biofilm. On the other hand, the reactor specific parameters are more related to the macroscopic level of the system which basically includes the surrounding biofilm conditions such as reactor configuration and hydraulic and temperature conditions, etc. (Sudarno, 2011).

Some of the main biofilm and reactor specific parameters that affect the performance of nitrifying biofilms are described in Table 12.

Table 12. Main parameters affecting nitrifying biofilm performance (Sudarno, 2011)

Biofilm specific parameters	Reactor specific parameters
• Concentration of dissolved nutrients at and in the biofilm: COD, NH_4^+, NO_2^-, NO_3^-, O_2 • Concentration of HCO_3^- and pH • Diffusion coefficients for: COD, NH_4^+, NO_2^-, NO_3^-, HCO_3^-, O_2 • Saturation coefficients for COD, NH_4^+, NO_2^-, NO_3^-, HCO_3^-, O_2 • Maximum growth rate of microbial species; e.g. from genus *Nitrosomonas*, *Nitrobacter* • Biomass density and biofilm thickness	• Bioreactor design; e.g.: Completely stir, plug flow • Hydraulic flow: laminar or turbulent • Oxygen transfer • Temperature • Biofilm detachment rate

2.7.7. Design parameters

Each biofilm reactor system has its own series of specific design characteristics which depend on the selected biofilm reactor, carrier media, mixing conditions, aeration and hydraulic, organic and nutrient loads, etc. However, some general parameters for biofilm reactors may include hydraulic loading (HLR), hydraulic retention time (HRT), surface and volumetric loading rates and specific surface area (SSA). (Henze, et al., 2008). The expressions corresponding to each of the mentioned general parameters are given below.

- Surface loading rate (Henze, et al., 2008):

$$B_A = \frac{Q * C_{in}}{A_F} \qquad (Eq. 18)$$

Where,

B_A (mg/m^2·d) = Surface loading rate
Q (L/d) = Volumetric flow rate
C_{in} (mg/L) = Influent substrate concentration
A_F (m^2) = Effective surface area of the biofilm

- Volumetric loading rate (Henze, et al., 2008):

$$B_V = \frac{Q * C_{in}}{V_R} \qquad (Eq. 19)$$

Where,

B_V (mg/L·d) = Volumetric loading rate
Q (L/d) = Volumetric flow rate
C_{in} (mg/L) = Influent substrate concentration
V_R (L) = Volume of biofilm reactor containing the filter media

- Hydraulic loading rate (Henze, et al., 2008):

$$HLR = \frac{Q_{in} + Q_R}{A_R} \qquad (Eq. 20)$$

Where,

HLR (m/h) = hydraulic loading rate
Q_{in} (m^3/h) = Wastewater flowrate influent to the treatment plant
Q_R (m^3/h) = Recirculation flow
A_R (m^2) = Cross sectional area of the biofilm reactor in the flow direction

For a cylindrical SFBBR with radius r, the cross sectional area can be calculated as:

$$A_R = \pi r^2 \qquad (Eq. 21)$$

Where,

A_R = Cross sectional area of the biofilm reactor in the flow direction
π = 3,1416
r = Cross sectional area radius

- Hydraulic retention time (Sudarno, 2011):

$$HRT = \frac{V_R}{Q} \qquad (Eq. 22)$$

Where,

HRT (d) = Hydraulic retention time
V_R (L) = Liquid volume of the reactor
Q (L/d) = Volumetric flow rate

- Specific surface area (Henze, et al., 2008):

$$SSA = \frac{A_F}{V} \qquad (Eq. 23)$$

Where,

SSA (m^2/m^3) = Specific surface are
A_F (m^2) = Effective surface area of the biofilm
V (m^3) = Volume of the biofilm reactor containing the filter media

- Porosity (Ebeling, 2006):

$$\varepsilon = \frac{V_{void}}{V_{T_B}} = \frac{V_{void}}{(V_{void} + V_{bf})} \qquad (Eq. 24)$$

Where,

ε = Porosity
V_{void} (L) = Volume not occupied by biofilter media
V_{TB} (L) = Total biofilter volume
V_{bf} (L) = Volume of biofilter media

For a cylindrical SFBBR with radius r, the total biofilter volume can be calculated as:

$$V_{T_B} = \pi r^2 h \qquad (Eq. 25)$$

Where,

V_{TB} (L) = Total biofilter volume
π = 3,1416

r = Biofilter radius
h = Biofilter height

2.8. ENVIRONMENTAL FACTORS AFFECTING NITRIFICATION

In general, nitrifiers are more sensitive to changes in environmental conditions than heterotrophic microorganisms. The main environmental factors affecting nitrification processes are substrate availability, pH, temperature and the presence of toxic substances (Wang, et al., 2009).

2.8.1. Substrate availability & DO concentration

The effects of substrate concentration on the kinetics of the nitrification process can be describes by Monod equation. In its standard form, the Monod equation describes the growth rate of bacteria as a function of the dissolve limiting substrate concentration available for the microorganisms. The standard Monod equation is given by equation 26 (Sudarno, 2011).

$$\mu = \mu_{max} \frac{S}{K_s + S} \qquad (Eq. 26)$$

Where,

μ (mg new cells/mg cells·h^{-1}) = Specific growth rate
μ_{max} (h^{-1}) = Maximum specific growth rate
S (mg/L) = Concentration of limiting substrate
K_s (mg/L) = Saturation coefficient or Monod constant

The specific growth rate can be defined as the ration between the rate of biomass produced and the original biomass present in the system and the saturation coefficient is the substrate concentration corresponding to one half the maximum specific growth rate (Metcalf & Eddy, Inc., 2003). Figure 32 describes the relation between specific growth rate and substrate concentration given by the Monod equation.

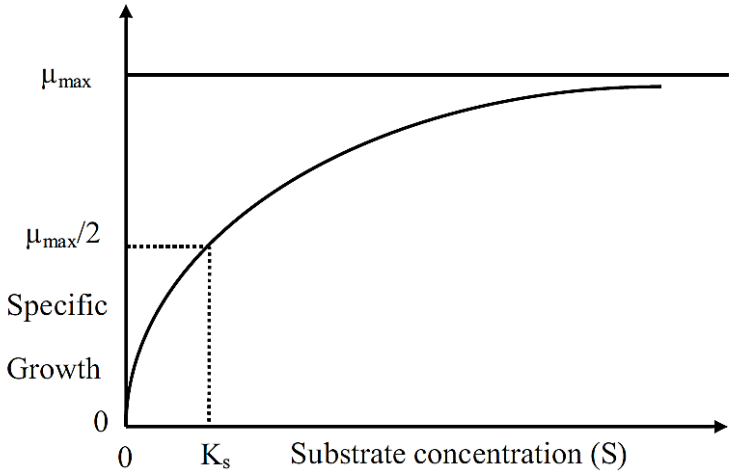

Figure 32. Monod model (Sudarno, 2011)

As seen in the Monod model, the bacteria grows at its maximum rate when the substrate concentration is high. Furthermore, for the case of the aerobic nitrifying bacteria, substrate and oxygen limitation needs to be considered. Thus, the standard Monod equation can be expanded to include the oxygen concentration effect on bacteria growth as shown in equation 27 (Dombrowski & In Su Choi, 2007)

$$\mu = \mu_{max} \frac{S}{K_s + S} \frac{c'}{K' + c'} \qquad (Eq. 27)$$

Where,

c' (mg/L) = Oxygen concentration
K' (mg/L) = Oxygen saturation coefficient

The first substrate factor in equation 27 can be approached to 1 when the substrate concentration (S) is so much greater than its saturation coefficient (K_s). This assumption leads to a simplified relation described by equation 28 (Dombrowski & In Su Choi, 2007).

$$\mu = \mu_{max} \frac{c'}{K' + c'} \qquad (Eq. 28)$$

The oxygen limitation in a nitrification process can be estimated by assuming that the specific growth rate value is equal to 90% of the maximum specific growth rate as shown by equation 29.

$$\frac{\mu}{\mu_{max}} = 0{,}9 = \frac{c'}{K' + c'} \qquad (Eq. 29)$$

Then, solving for oxygen concentration (c') in equation 29 yields the following expression.

$$c' = \frac{0{,}9\,K'}{(1-0{,}9)} \qquad (Eq.30)$$

The oxygen saturation coefficient values given by Wiesmann (1994) at 20°C are 0,3 and 1,1 mg O_2/L for AOB and NOB respectively. These values can be replaced in equation 30 to estimate the oxygen concentration values required to reach the specific growth rates equal to 90% the maximum specific growth rates corresponding to the nitrifying microorganisms. (Dombrowski & In Su Choi, 2007).

Furthermore, the dissolved oxygen concentration saturation in wastewater at 20°C is approximately equal to 9,09 mg O_2/L. This value can be estimated by using Henry's Law which is given in equation 31 (Metcalf & Eddy, Inc., 2003).

$$P_{gas} = Hx_{gas} \qquad (Eq.31)$$

Where,

P_{gas} (atm) = Partial pressure of gas
H = Henry's constant
x_{gas} = mole fraction of gas in water

For the case of suspended systems, it has been reported that optimal nitrification takes place at values above 1 mg/L and 2 mg/L for nitritation and nitratation respectively. However, for the case of biofilm systems due to their mass transfer limitations, higher DO concentration values are suggested for optimal nitrification with values above 5 mg/L (Sudarno, 2011). For that reason, the oxygen concentration in nitrification processes should be monitored and control in order to maintained a relative constant ammonium, nitrite and nitrate concentration values in the effluent stream (Dombrowski & In Su Choi, 2007).

The un-ionized forms of ammonium (NH_4^+) and nitrite (NO_2^-) are ammonia (NH_3) and nitrous acid (HNO_2) respectively. The transport of the un-ionized forms into the cells requires less energy than their ionized counterparts which provides them with a greater probability to be the real electron donors in the nitrification process. Their equilibrium relation are described by equations 32 and 33 (Sudarno, 2011).

$$NH_4^+ \underset{k_2}{\overset{k_1}{\rightleftarrows}} NH_3 + H^+ \qquad (Eq.32)$$

$$NO_2^- + H^+ \underset{k_4}{\overset{k_3}{\rightleftarrows}} HNO_2 \qquad (Eq.33)$$

However, free ammonia (FA) and free nitrous acid (FNA) are known to inhibit nitrification. In general, FA can affect both AOB and NOB where NOB are more sensitive than AOB to FA concentration. Free ammonia can start to inhibit AOB and NOB at concentrations around 10 to 150 mg/L and 0,1 to 4,0 mg/L respectively. The FA inhibition may lead to accumulation of nitrite in the system which may promote the formation of nitrous acid. Hence, further affecting the NOB whose nitrous acid inhibition can take place at concentrations starting from 0,2 – 2,8 mg/L (Wang, et al., 2009).

A typical non-inhibition and nitrite oxidation inhibition graphs during nitrification are illustrated in figures 33 and 34 respectively.

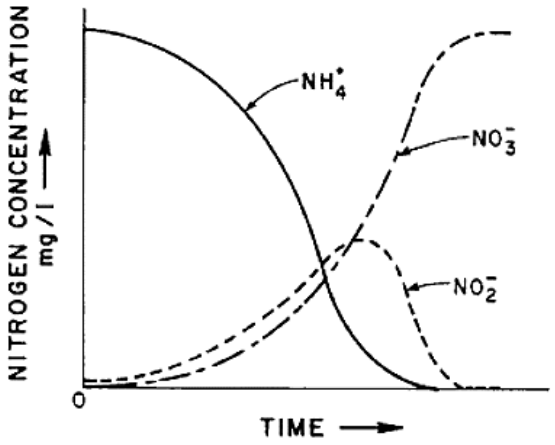

Figure 33. Schematic of a typical non-inhibited nitrification process (Anthonisen, et al., 1976)

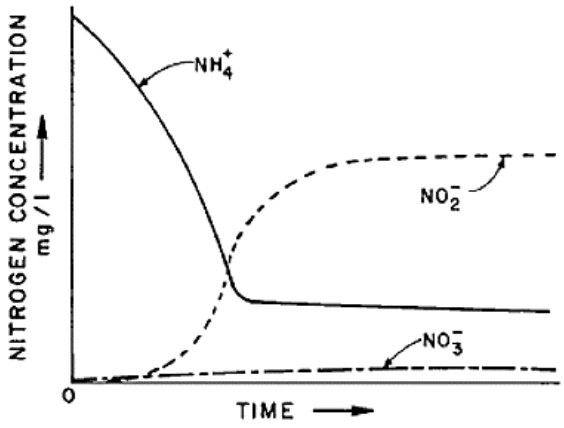

Figure 34. Schematic of typical nitrification process with inhibition of nitrite oxidation (Anthonisen, et al., 1976)

Additionally, the free ammonia and nitrous acid concentrations can be estimated by the used of the following expressions (Anthonisen, et al., 1976).

$$FA\ as\ NH_3\ \left(\frac{mg}{L}\right) = \frac{17}{14} * \frac{total\ ammonia\ as\ N\ \left(\frac{mg}{L}\right) * 10^{pH}}{e^{\left(\frac{6344}{273+°C}\right)} + 10^{pH}} \qquad (Eq.34)$$

$$FNA\ as\ HNO_2 \left(\frac{mg}{L}\right) = \frac{46}{14} * \frac{[NO_2^-.N]\ \left(\frac{mg}{L}\right)}{e^{\left(\frac{-2300}{273+°C}\right)} * 10^{pH}} \qquad (Eq.35)$$

In equation 34, the total ammonia is defined as the sum of NH_3 and NH_4^+.

2.8.2. pH and Alkalinity

The nitrification process is very sensitive to pH changes in the system. The two main reasons are related to inhibitory effects and the consumption of the medium's alkalinity which can potentially lead to the pH drop if not controlled. As already depicted in figure 1, an increase of pH switches the equilibrium between free ammonia and ammonium towards free ammonia which in turn can result in inhibitory problems in the nitrification system. Furthermore, a decreased of pH switches the equilibrium between nitrite and nitrous acid towards nitrous acid which affects mainly NOB like those from the genus *nitrobacter* who are responsible for nitrite oxidation to nitrate (Orhon & Artan, 1994).

Therefore, based on the pH value a nitrification system can be divided into inhibitory and non-inhibitory zones. The different zones as a function of pH are illustrated in figure 35.

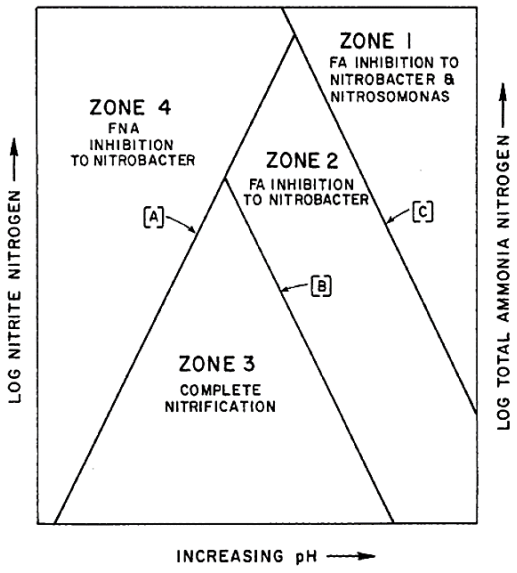

Figure 35. Nitrification inhibitory and non-inhibitory zones as a function of pH (Anthonisen, et al., 1976)

The concentration values for the boundary lines corresponding to the different zones and represented the by letters A, B and C may represent ranges rather that specific values considering that the nitrification process is influenced by many biofilm and environmental factors. (Anthonisen, et al., 1976).

Moreover, the pH range where the maximum rate of nitrification occurs has been reported to be in between 7,5 to 8,5 (Orhon & Artan, 1994). The effect of the pH value on the maximum rate of nitrification is illustrated in figure 36.

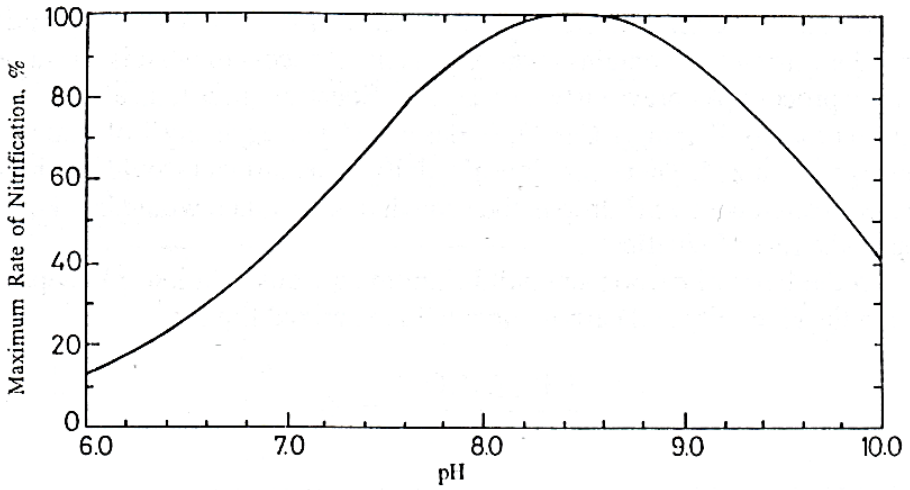

Figure 36. Maximum rate of nitrification vs pH (Orhon & Artan, 1994)

As already described by equations 3 and 4, the alkalinity of the system is affected due to the formation of hydrogen ions and the consumption of inorganic carbon. Thus, alkalinity becomes important in nitrification processes since it provides to the system not only with its buffer capacity but also with the carbon source required by the autotropic microorganisms.

The buffer capacity in nitrification processes which helps to prevent pH changes in the system is mainly own to the carbonate (CO_3^{2-}) and bicarbonate (HCO_3^-) ions. However, the equilibrium of these species involves two other inorganic carbon substances which are carbon dioxide (CO_2) and carbonic acid (H_2CO_3) (Sudarno, 2011).

The concentration of each of the mentioned species is a function of pH as illustrated in figure 37. Carbonic acid (H_2CO_3) is not shown in the figure since it is a very unstable substance.

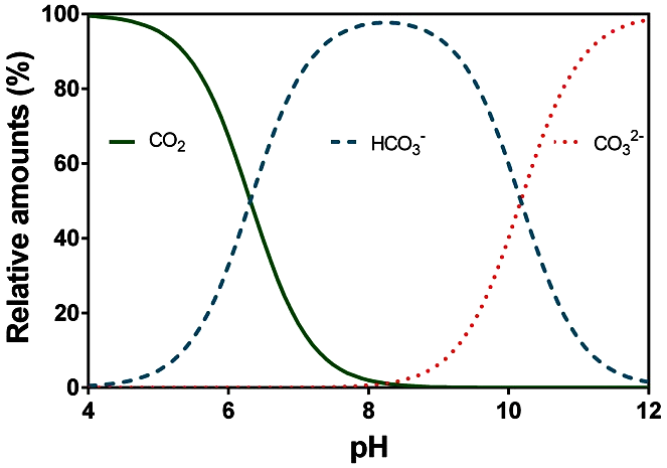

Figure 37. Relative amounts of inorganic carbon vs. pH (Pedersen, et al., 2013)

The equilibrium reactions between the different inorganic carbon species and the corresponding overall reaction are described in equations 36 and 37 respectively (Lee, 2016).

$$CO_{2(aq)} + H_2O \leftrightarrow H_2CO_3 \leftrightarrow HCO_3^- + H^+ \leftrightarrow CO_3^{2-} + 2H^+ \qquad (Eq.36)$$

$$CO_{2(aq)} + H_2O \leftrightarrow CO_3^{2-} + 2H^+ \qquad (Eq.37)$$

One common way of expressing alkalinity is in terms of calcium carbonate ($CaCO_3$). In general, 7,01 mg of alkalinity as $CaCO_3$ are required to oxidized 1 mg of NH_4^+-N (Sudarno, 2011). A representation of the inorganic carbon balance in terms of calcium carbonate during sludge water treatment is illustrated in figure 38.

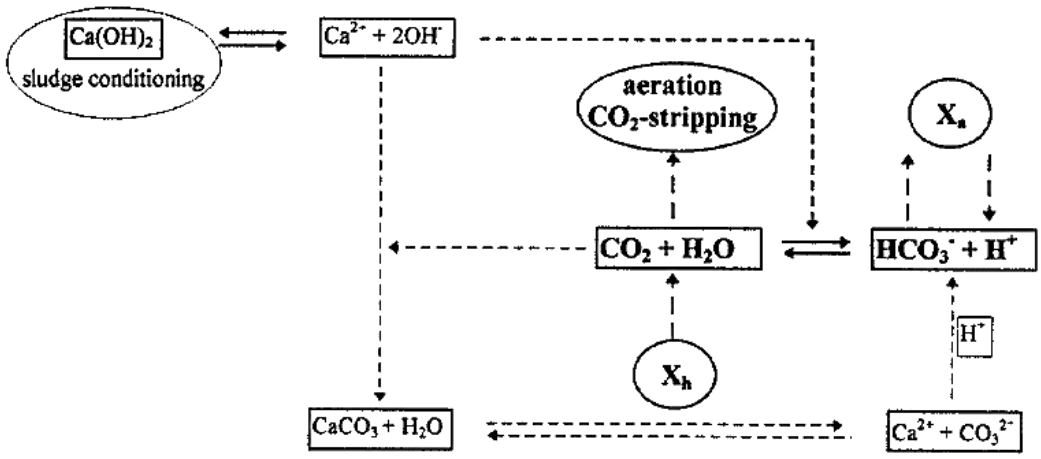

Xh ... CO2-production due to aerobic degradation by heterotrophic biomass
Xa ... bicarbonate-consumption and hydronium ions production by autotrophic organisms (nitrification)

Figure 38. Inorganic carbon balance during treatment of sludge water (Wett, et al., 1998)

2.8.3. Temperature

The effect of temperature in nitrification systems is mainly reflected in the growth rate of the microorganisms. This effect can be quantified by using the Arrhenius equation which describes the dependency of the reaction rate on temperature. The Arrhenius equation is given in equation 38 (Dombrowski & In Su Choi, 2007).

$$k = k_0 \, exp\left(-\frac{E_A}{RT}\right) \qquad (Eq. 38)$$

Where,

k = Reaction rate coefficient
k_0 = A constant that represents the theoretical maximum value for $T \rightarrow \infty$
E_A (KJ/mol) = Activation energy
R (KJ/mol·K) = The general gas constant ($8{,}314*10^{-3}$ KJ/mol·K)
T (K) = Temperature

Expressions describing the specific growth rate constant (μ) of *nitrosomonas* and *nitrobacter* in suspension systems as a function of temperature have already been published and are given in equations 39 and 40 for *nitrosomonas* (NS) and *nitrobacter* (NB) respectively (Knowles, et al., 1965).

$$log_{10}\mu_{NS}(d^{-1}) = 0{,}0413T(°C) - 0{,}944 \qquad (Eq. 39)$$

$$log_{10}\mu_{NB}(d^{-1}) = 0{,}0255T(°C) - 0{,}492 \qquad (Eq. 40)$$

The application range of the given expression is approximately in between 8 to 30°C. These expressions suggest an increase in the *nitrosomonas* and *nitrobacter* growth constant of approximately 10 and 6 % per increase in degree Celsius respectively and for a given temperature the growth rate of *nitrobacter* is almost 50% greater than the one from *nitrosomonas* (Knowles, et al., 1965). However, for the case of biofilm systems the effect of temperature on nitrification growth rates is more complex to quantify than in suspended systems considering the effects of other external factors such as limitations of oxygen and mass transfer (Sudarno, 2011).

The specific growth rate of *nitrosomonas* and *nitrobacter* as a function of temperature and pH and some given conditions is illustrated in figure 39.

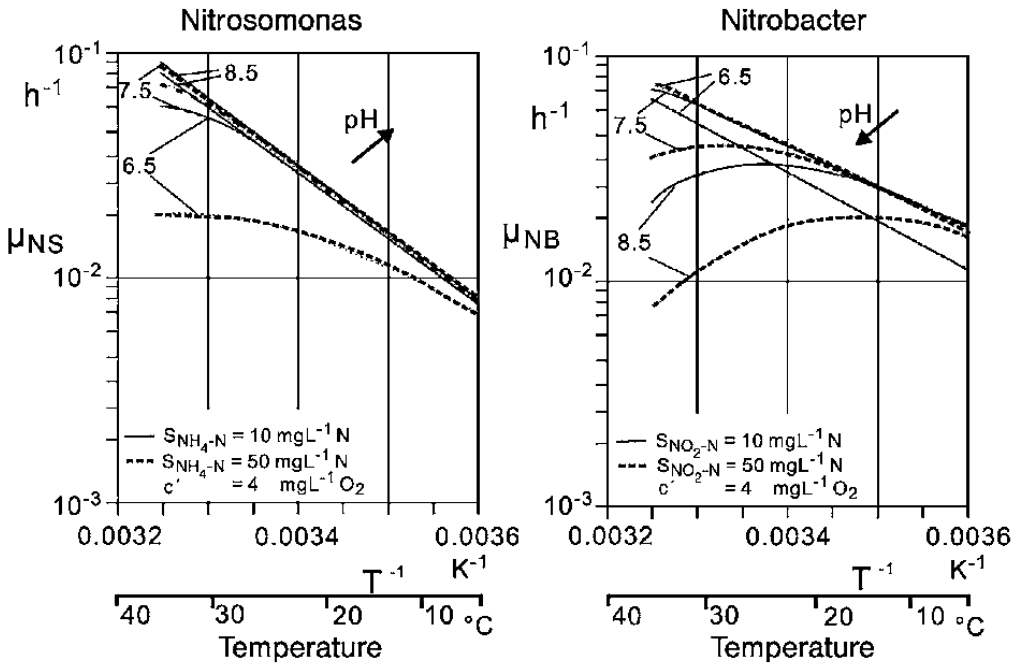

Figure 39. Nitrosomonas and nitrobacter specific growth rate as a function of T & pH (Dombrowski & In Su Choi, 2007)

As seen in figure 39, AOB and NOB behave differently under the same temperature and set of conditions. In general, nitrification critical temperatures are found to be below 5°C and over 40°C and at a pH value of 7,5 the optimal nitrification temperature ranges in between 30 to 37,5 °C (Dombrowski & In Su Choi, 2007).

2.8.4. Toxic compound

Besides the inhibitory effects caused by FA and FNA, other organic and inorganic compounds have been reported to inhibit nitrification rates at concentration levels so much lower compared to the ones that normally affect aerobic heterotrophic microorganisms. Many organic compounds include amines, proteins, tannins, phenolic compounds, alcohols, cyanates, ethers, carbamates and benzene. For that reason, in wastewater treatment plants it is difficult to find the source of nitrification toxicity considering the complexity of wastewater composition and the large amount or organic substance that may interfere with the nitrification process (Metcalf & Eddy, Inc., 2003). Some example of organic compounds include thiourea and 2-chloro-6-(trichloromethyl) pyridine (TCMP) which have been used to inhibit nitrification during BOD tests (Orhon & Artan, 1994). Furthermore, some metals such as nickel (Ni), chromium (Cr) and copper (Cu) have been reported to inhibit ammonia oxidation at concentrations levels of 0,25, 0,25 and 0,10 mg/L respectively (Metcalf & Eddy, Inc.,

2003). Other metals include cadmium (Cd), zinc (Zn) and lead (Pb). Their general inhibitory strength in nitrification systems is given in the following order Cd > Cu > Zn and Pb> Cr (Wang, et al., 2009).

3. MATERIALS AND METHODS

3.1. EQUIPMENT

The main equipment used during the experimental procedures are listed below.

- Diaphragm pump GA-170 from Milton Roy

Table 13. Diaphragm pump GA-170 - Milton Roy (MILTON ROY, 2007)

Main technical characteristics	
✓ Max. flow = 170 L/h ✓ Max. pressure = 3,5 bar ✓ Max. pumped liq. T = 40°C ✓ Motor power = 180 W	

Figure 40. Diaphragm pump GA-170 - Milton Roy

- Overhead and magnetic stirrers from Heidolph

Table 14. Overhead and magnetic stirrers

Main technical characteristics	
▪ Overhead stirrer: ✓ Max. rpm = 700 ✓ Motor power = 50 W ▪ Magnetic stirrers: ✓ Max. rpm = 1250 ✓ Motor power = 30 W	 

Figure 41. Overhead and magnetic stirrers - Heidolph

- Spectrophotometer with software, V-550 from JASCO & RQflex 10 - Reflectoquant® from MERCK

Figure 42. Spectrophotometer V-550 from JASCO

Figure 43. RQflex 10 – Reflectoquant® - MERCK

- pH controller from Bluelab and DO sensor – Portavo® 907 MULTI from Knick

Figure 44. pH controller from bluelab®

Figure 45. DO sensor – Portavo® 907 MULTI from Knick (Knick, 2017)

- Aquarium heater from Jäger and laboratory hot plate from Schott

Figure 46. Aquarium heater from Jäger

Figure 47. Hot plate from Schott

3.2. ANALYTICAL AND MEASUREMENT METHODS

3.2.1. Ammonium

Ammonium concentration was determined by following the procedures describe in the German standard method (DEV) DEV E5; DIN 38406-5:1983-10. The reagents solutions, and procedures given by the standard for the photometric determination of ammonium-nitrogen are described below.

- Salicylate-reagents solution: For 1 L solution, dissolve 130 g of sodium salicylate ($C_7H_5NaO_3$) and 130 g of trisodium citrate dihydrate ($Na_3C_6H_5O_7 \cdot 2H_2O$) in approximately 800 mL of distilled water contained in a 1 L volumetric flask. Then, add 0,970 g of sodium pentacyanonitrosylferrate(III) dihydrate ($Na_2Fe(CN)_5NO \cdot 2H_2O$) and after complete mixing add distilled water up to the 1 L mark. The solution should be stored under dark conditions and not to be used longer than 2 week.
- Hypochlorite-reagents solution: For a 100 mL solution, dissolve 3,2 g of sodium hydroxide (NaOH) in approximately 50 mL of distilled water contained in a 100 mL volumetric flask. After complete mixing, allow the solution to reach room temperature, then add 0,2 g of sodium dichloroisocyanurate ($C_3Cl_2N_3NaO_3$) and after complete mixing fill with distilled water up to the 100 mL mark. The solution should be prepared in a daily basis.
- Ammonium - Stock solution (0,1 g NH_4^+-N/L): For 1 L of stock solution, dissolve 0,4717 g of ammonium sulfate ($(NH_4)_2SO_4$) previously dry at 105°C with distilled water contained in a 1L volumetric flask. The stock solution should be stored in a glass bottle and used within 1 week.
- Ammonium - Standard solution (1 mg NH_4^+-N/L): For 1 L of standard solution, pipet 10 mL of previously made ammonium stock solution into a 1 L volumetric flask containing distilled water and fill up to the mark. After careful mixing, the standard solution should be used immediately after preparation.

In general, the analysis relies on the interactions of the reagents under alkaline conditions at pH values of about 12,6 where the ammonium ions contained in the sample react with hypochlorite ions and salicylate ions and in the presence of sodium pentacyanonitrosylferrate a solution with blue appearance is formed. The hypochlorite

ions are generated after hydrolysis of the dichloroisocyanuric acid in the alkaline medium.

Several substances such as chloride, phosphates, cyanide, calcium, copper, lead and aniline may interfere with the described ammonium analysis but above all the presence of amines can lead to the highest deviations in the results.

A short description of the ammonium analysis procedure given by the standard is illustrated in figure 48.

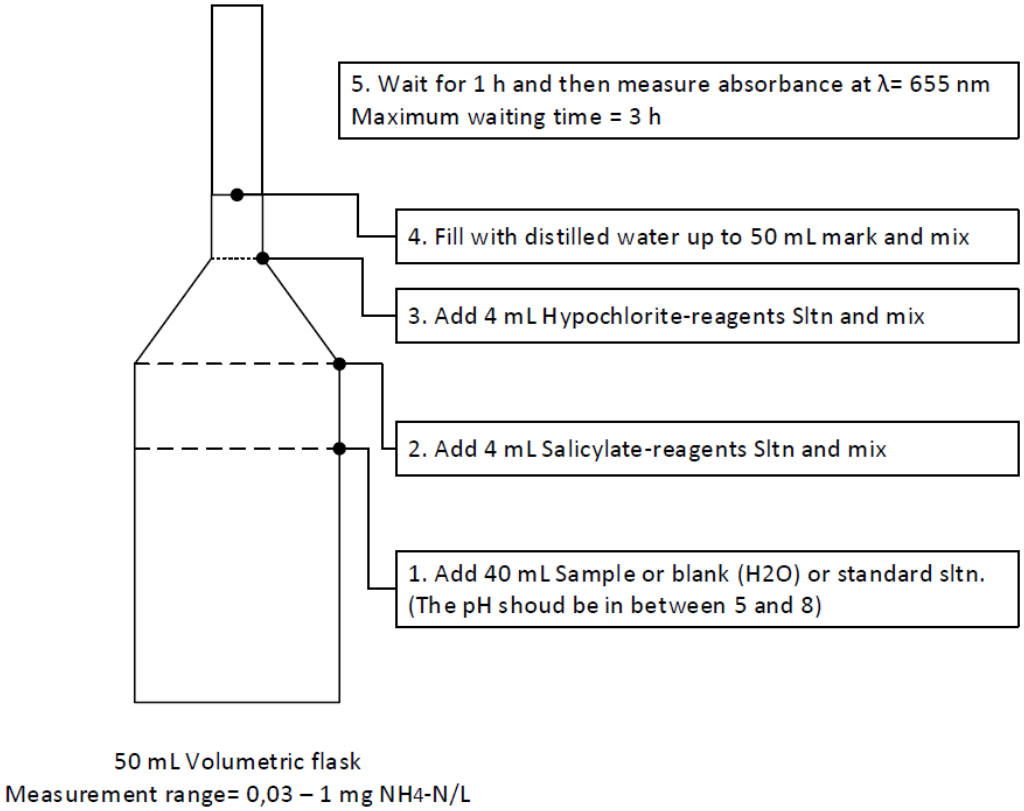

Figure 48. Ammonium analysis procedure (DEV) DIN 38406-E5:1983-10

For the development of the calibration curved, 10 standard calibration curved solutions at concentrations ranging from 0,1 to 1 mg NH_4^+-N/L and a blank solution containing distilled water plus the reagent solutions were prepared. Their absorbances were measured with the help of the spectrophotometer against distilled water and by using 1 cm cuvettes at a wavelength of 655 nm.

Table 16 indicates the volumes and concentrations of the standard solutions and the blank solution used for the preparation of the calibration curved.

Table 15. Ammonium-N, Calibration curved preparation

No.	Cal. curved Std. Sltns Conc. (mg NH_4^+-N/L)	Add. Volume Ammonium - Std. Solution (mL)	Add. Volume distilled water (mL)
Blank	0	0	40,0
1	0,1	4,0	36,0
2	0,2	8,0	32,0
3	0,3	12,0	28,0
4	0,4	16,0	24,0
5	0,5	20,0	20,0
6	0,6	24,0	16,0
7	0,7	28,0	12,0
8	0,8	32,0	8,0
9	0,9	36,0	4,0
10	1,0	40,0	0

3.2.2. Nitrate

Nitrate concentration was determined by following the procedures described in the DEV D9; DIN 38405-9:2011-09. The reagents solutions, and procedures given by the standard for the photometric determination of nitrate-nitrogen are described below.

- Dimethylphenol solution: For 1 L solution, dissolve 1,2 g of 2,6-dimethylphenol in anhydrous acetic acid. The suggested maximum storage time is 1 week.
- Mixed-Acid reagent solution: Mix equal volume amount of sulfuric acid (H_2SO_4 – 96%) and phosphoric acid (H_3PO_4 – 85%). The suggested maximum storage time at temperatures in between 15 to 25°C is 1 year.
- Sulfamic acid (15 w/w%): For 100 mL solution, dissolve 17,6 g of sulfamic acid (H_3NSO_3) in 100 mL of distilled water.
- Nitrate - Stock solution (0,05 g NO_3^--N/L): For 1 L stock solution, dissolve 0,3609 g of potassium nitrate (KNO_3) previously dry at 105°C with distilled water contained in a 1L volumetric flask. The stock solution should be stored under dark conditions at temperatures ranging from 15 to 25°C and used within 30 days.

In this method, the quantification of nitrate is determined by its reaction with 2,6-dimethylphenol under acidic conditions with a reaction time of approximately 5 min.

The reaction between the two reagents is given by equation 41.

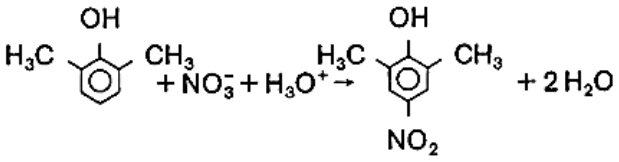

$(Eq. 41)$

One of the major interferences is due to the presence of nitrite ions in the sample at concentrations equal to 0,2 mg NO_2^--N/L or greater . Thus, it is recommended to add approximately 50 mg of sulfamic acid to the analyzed sample.

A short description of the nitrate analysis procedure given by the standard is illustrated in figure 49.

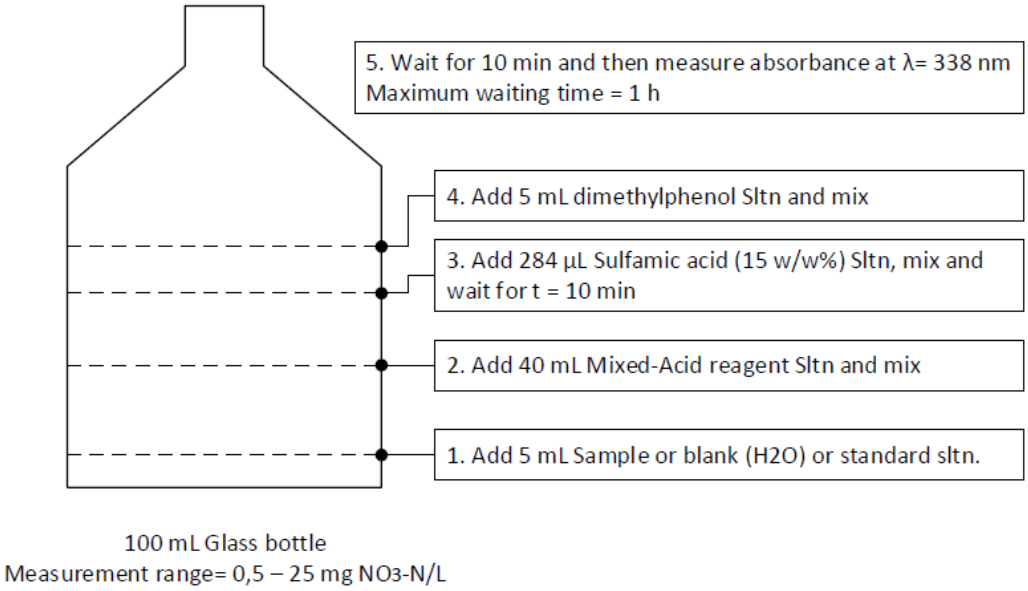

Figure 49. Nitrate analysis procedure (DEV) DIN 38405-D9:2011-09

For the development of the calibration curved, 7 standard calibration curved solutions at concentrations ranging from 1 to 25 mg NO_3^--N/L and a blank solution containing distilled water plus the reagent solutions were prepared. Their absorbances were measured with the help of the spectrophotometer against distilled water and by using 1 cm cuvettes at a wavelength of 338 nm.

Table 17 indicates the volumes and concentrations of the standard solutions and the blank solution used for the preparation of the calibration curved.

Table 16. Nitrate-N, Calibration curved preparation

No.	Cal. curved Std. Sltns Conc. (mg NO_3^--N/L)	Add. Volume Nitrate - Stock Solution (mL)	Add. Volume distilled water (mL)
Blank	0,0	0	50,0
1	1,0	1,0	49,0
2	2,0	2,0	48,0
3	5,0	5,0	45,0
4	10,0	10,0	40,0
5	15,0	15,0	35,0
6	20,0	20,0	30,0
7	25,0	25,0	25,0

3.2.3. Nitrite

Nitrite concentration was estimated by using the Reflectoquant® Nitrite test which have a reaction time of 15 s and a measuring range of 0,5 to 25,0 mg NO_2^-/L. The sample should have a temperature ranging from 15 to 30°C with pH values in between 1 to 13. The steps for the measurement procedure are described below.

1. Take one of the test strips, then press the start button while immersing for 2 s the reaction zone of the test strip inside the sample.
2. Carefully remove any excess of liquid by placing the edge of the test strip over a paper towel allowing the excess liquid to drain off.
3. Properly insert the strip inside the reflectoquant strip chamber before the reaction time has been concluded, usually 5 s before.
4. After the reaction time has been concluded read the nitrite concentration from the device in mg NO_2^-/L.

During the analysis, nitrite ions react with an aromatic amine forming diazonium salt under acidic conditions. Then, the diazonium salt reacts with N-(1-naphthyl)-ethylene-diamine forming a red-violet azo dye which is determined reflectometrically. The test strips should be stored at cool temperatures from 2 to 8°C.

3.2.4. Alkalinity

The alkalinity was determined according to the DEV H7; DIN 38409-7:2005-12. The sample was titrated to a pH value of 4,3 by using a hydrochloric acid solution with a

concentration of 0,1 mol HCL/L. The steps followed during the analysis are described below.

1. 100 mL of the sample volume were pipetted into an Erlenmeyer flask and a magnetic stirring rod was added to it.
2. The volumetric flask was placed on a magnetic stirrer and the pH electrode was immersed into the liquid.
3. A burette was filled with the 0,1 M hydrochloric acid solution.
4. The magnetic stirrer was turned on and the volume sample was titrated until reaching the pH value of 4,3. The volume of the acid consumed during the titration was recorded.
5. The alkalinity was calculated based on the expression given in the standard:

$$K_{s4,3} = \frac{c_{HCl} * V_1 * 1000}{V_2} \qquad (Eq. 42)$$

Where,

$K_{s4,3}$ (mmol H^+/L) = Acid capacity to the pH value of 4,3
c_{HCl} (mol/L) = Concentration of hydrochloric acid solution
V_1 (mL) = Volume of acid consumed to pH value of 4,3
V_2 (mL) = Sample volume

In order to get a titration curve, the acid was added at small volume intervals and the pH was recorded for each interval. The stirrer was turned on during addition of the acid and after further stirring the pH was recorded under static conditions by turning the stirrer off.

The results are recommended to be reported either in mmol/L or mol/m^3 up to three significant figures.

3.2.5. COD

The COD was determined by using the LCK 114 cuvette test from HACH. The analysis concentration range is in between 150 to 1000 mg O_2/L and it is based on the dichromate method. In this method the oxidizable substances present in the sample react with a sulphuric acid – potassium dichromate solution which contains silver sulphate as catalyst. The green coloration of Cr^{3+} is evaluated by photometric means (HACH, 2017).

3.2.6. pH, Temperature and DO

The pH and DO were measured by using their corresponding probes connected to the pH controller from bluelab® and the Portavo® 907 Multimeter from Knick respectively. And, both devices provided temperature measurements.

The pH probe was located in the collection tank corresponding to each biofilm reactor system. The potassium carbonate (K_2CO_3), sodium carbonate (Na_2CO_3), and sulfuric acid (H_2SO_4) solutions were used to adjust the pH and were prepared by mixing and dissolving the respective reagents in distilled water to a total volume of 1 L. The prepared solutions were fed to the collection tank based on the needs of each treatment process and with the help of the dosing pump belonging to the pH controller. The preparation of the solutions and the characteristics of each reagent are indicated in table 18.

Table 17. pH adjust solutions

Reagent	Reagent Used mass or Vol.	Vol. Sltn. (L)	MW[a] (g/mol)	ρ[a] (g/mL)	Sltn. Conc.
K_2CO_3	100,0 g	1,0	138,21	2,43	0,7 M
Na_2CO_3	100,0 g	1,0	105,99	2,53	0,9 M
H_2SO_4	27,1 mL 96% H_2SO_4 Sltn.	1,0	98,08	1,84	1 N

a. **(SIGMA-ALDRICH, 2017)**

For each experimental practice, the prepared solutions were added to a 1,0 L graduated cylinder and their consumption was monitored throughout each treatment process.

The DO probe was located at the top of the packed bed biofilm and the DO device was set to record DO and T values every 2 h throughout each treatment process. The DO in the collection tank was also measured for most of the experimental practices.

The pH sensor was calibrated by applying the three point calibration with their respective pH solutions of 7, 4 and 10. The DO sensor was calibrated by applying the 100% water saturated air calibration as illustrated in figure 50.

Figure 50. DO Sensor, 100% water saturated air calibration

3.2.7. Liquid and air flows

The recirculation liquid flow rate was estimated by measuring the time required for the liquid to fill a particular volume within a 1000 mL graduated cylinder. It was measured at the output line coming from the top of the column section corresponding to each bioreactor. Furthermore, a bubble flowmeter set up consisting of a 50 mL graduated cylinder, a rubber bulb and a soap solution, was used to determine the air flow rate by measuring the time taken for the air stream to move a soap bubble from one specific volume mark to another. The bubble flowmeter set up used during the experimental practices is shown in figure 51.

Figure 51. Bubble flowmeter set up

3.2.8. Carrier material density, porosity and bioreactors liquid volume

- **Density of the carrier material:**

The density of the carrier material was determined by using a laboratory balance and a 250 mL graduated cylinder. The volume of water displaced by 20 carrier material

selected randomly was determined and their masses were measured by using the laboratory balance. A glass stopper was used to maintain the packing material completely submerged inside the graduated cylinder. Then, the carrier material density was determined by application of the density equation relating mass and volume given in equation 43.

$$\rho_c = \frac{m_{20}}{V_{20}} \qquad (Eq.43)$$

Where,

ρ_c (g/mL) = Density of carrier material
m_{20} (g) = Mass of 20 carrier materials
V_{20} (mL) = Volume of 20 carrier materials

- **Porosity:**

Porosity was defined as the ratio of the volume not occupied by the carrier material to the total packed bed volume. The total packed bed volume was estimated by measuring the packed bed heights corresponding to each biofilm reactor and using equation 25.

For the SFBBR-1 system, the biofilm carrier volume was estimated by first calculating a theoretical volume based on a reference point, a top column point and by using the dimensions of the bioreactor. Then the total volume occupied by the liquid from the reference point to the column output point was measured by using a 1000 mL graduated cylinder. The water measured in the graduated cylinder was added inside the column through the top open column area. Then, the difference between the theoretical and measured volumes corresponded to the biofilm carrier volume. And, equation 24 was used to determine the porosity of this biofilm reactor.

For the SFBBR-2 system, the volume of the carrier material was estimated by weighting the total amount of carrier material packed into the bioreactor column and then by solving for volume in the density equation with the already estimated carrier material density value. Then, equation 24 was used to determine the porosity of the bioreactor by assuming an increment of 30% in the carrier volume due to biofilm formation.

- **Bioreactors liquid volume:**

Due to the column design corresponding to the SFBBR-1 system, the liquid volume for this bioreactor was estimated by first emptying completely the column and then measuring the liquid volume required to fill the column up to the output point located at the top of the column. The liquid volume corresponding to the SFBBR-2 was estimated based on the column dimensions and the packed bed volume.

Furthermore, the volume of the treated sludge water in the collection tank was observed to change during operation. This was mainly due to samples taken from the tank, the volumes of the added pH adjustment solutions and possible losses due to evaporation. For that reason, in order to determine the change in volume and sludge water loss rate mainly due to evaporation the volume of the treated sludge water was measured in the collection tank corresponding to each bioreactor during two different treatment processes at different flow rate conditions where the volume of sludge water in the collection tank was measured at the initial and final days with the help of 1 and 3 L graduated cylinders.

3.2.9. Data analysis

The data was treated by using any of the following equations.

- Average (StatsDirect, 2000):

$$\bar{x} = \frac{\sum_{i=1}^{n} x_i}{n} \qquad (Eq. 44)$$

Where,

$\bar{x}$ = Sample arithmetic mean
x_i = observed value
n = sample size

- Sample standard deviation (StatsDirect, 2000):

$$s = \sqrt{\frac{\sum_{i=1}^{n}(x_i - \bar{x})^2}{n-1}} \qquad (Eq. 45)$$

Where,

s = Sample standard deviation
x_i = observed value
$\bar{x}$ = Sample arithmetic mean
n = sample size

- Standard error of the sample mean (StatsDirect, 2000):

$$SEM = \frac{s}{\sqrt{n}} \qquad (Eq. 46)$$

Where,
SEM = standard error of the sample
s = Sample standard deviation
n = sample size

- Linear relation (Wolfram, 1999):

$$\frac{a}{b} = \frac{c}{d} \rightarrow d = \frac{b * c}{a} \qquad (Eq. 47)$$

Where, a, b, and c are known values.

3.3. EXPERIMENTAL SET-UP

The pilot scale set-up consisted of two submerged fix bed biofilm reactors (SFBBR) systems labeled SFBBR-1 and SFBBR-2 operated in upflow mode. The experimental set-up picture and the schematics for each bioreactor are illustrated in figures 52.

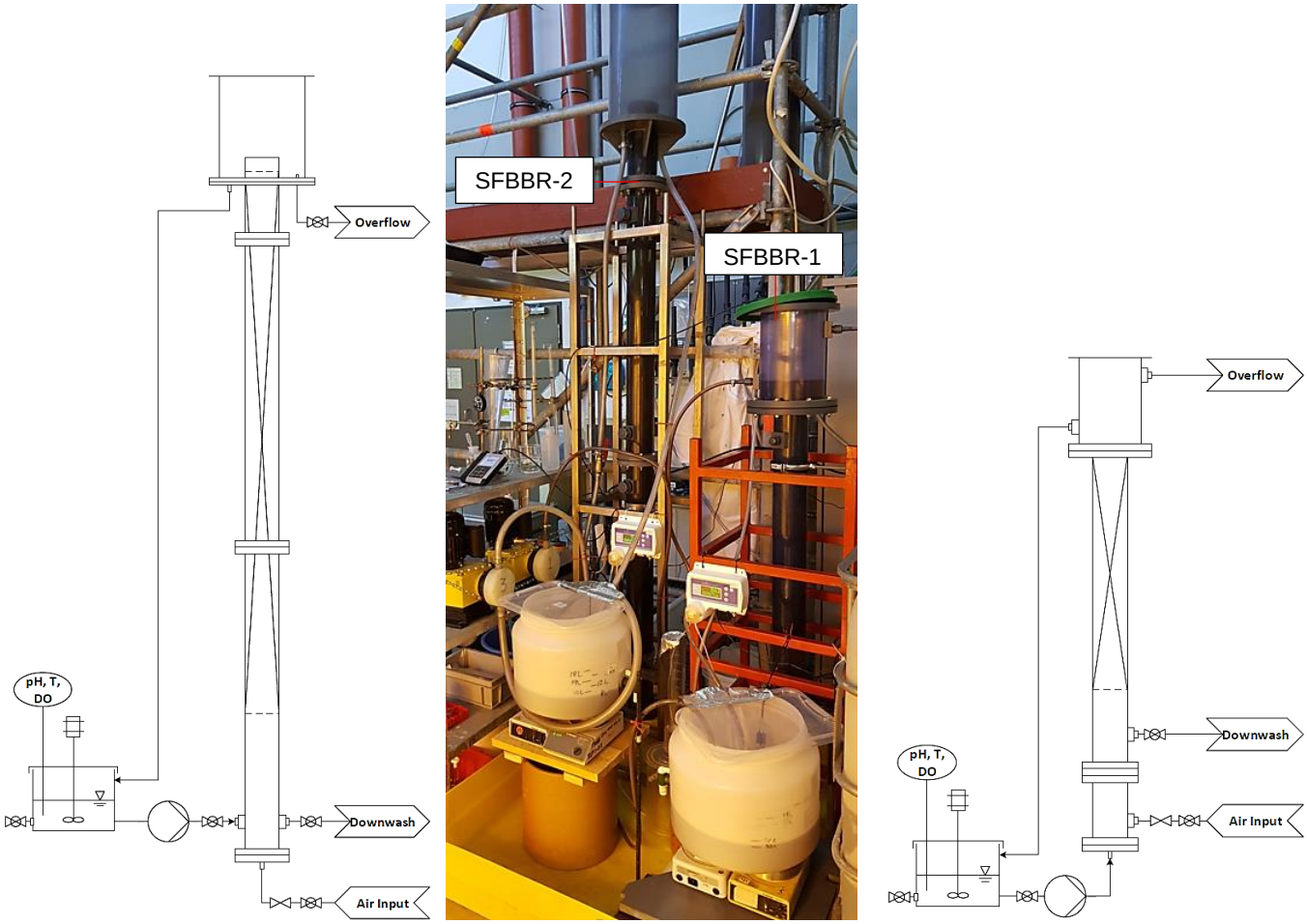

Figure 52. Experimental set-up. Left: Schematic SFBBR-2; Center: Set-up picture; Right: Schematic SFBBR-1

The SFBBR columns were made out of clear PVC having both an inside diameter of 10,0 cm and packed bed heights of 77,0 and 180,0 cm for the SFBBR-1 and the SFBBR-2 respectively. The packed bed material in each bioreactor consisted of plastic biofilm carriers with a SSA of approximately 660 m^2/m^3 and with similar characteristics as the ABC5^{TM} described in table 8. The packed bed areas were approximately 1,0 and 2,0 m^2 for bioreactors SFBBR-1 and SFBBR-2 respectively. Figure 53 shows different views of the carrier material.

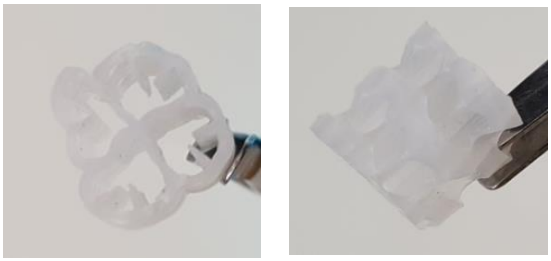

Figure 53. Different views of the carrier material used in SFBBR 1 and 2

In general, the pre-treated sludge water was fed at the bottom section of each bioreactor by the action of their corresponding diaphragm pumps GA-170 from Milton Roy. The liquid flow was set by manipulating the pump struck adjustment knobs which have a percentage graduated scale ranging from 0 to 100% for stop and maximum flow operating modes respectively.

The air was also fed at the bottom section of each bioreactor in parallel to the liquid flow. The air flow rate was set by manipulating the valves corresponding to each bioreactor piping system. Additionally, the air bubbles were dispersed through each bioreactor by the action of their corresponding bubble diffusers.

The sludge water used during experimentation was collected from Seevetal WWTP located in Glüsingen. After collection, the sludge water was stored under refrigeration at temperatures within 5 to 10° C. Moreover, solid particles were removed from the sludge water prior to every treatment process by sieving it through a 300 and 200 µm mesh system, hence minimizing operational problems related to clogging. And, if required the sludge water temperature was also adjusted to approximately 22°C prior and/or during every treatment processes with the help of the aquatic heater from Jäger and/or the hot plate from Schott, hence minimizing environmental shocks that may result in the reduction of biological activity due to drastic temperature changes.

The sludge water in the collection tank was mechanically mixed during each biological treatment process by using the overhead and magnetic stirrers from Heidolph which were set at velocities ranging from 200 to 250 rpms. The mixing in the collection tank allowed to maintain relatively pH, T and DO constant condition during each of the biological treatment processes.

In between each of the experimental practices, the packed bed biofilms from both SFBBR systems were downwashed several times with tap water. The manual downwashing was performed until an effluent with a relative clear appearance was observed. Moreover, fouling in the hose system was treated by recirculating in the pump hose system approximately 5 L of a 1 N sulfuric acid (H_2SO_4) solution for about 3 h at 28° C.

Figure 54 shows a piece of the hose system before and after the sulfuric acid treatment.

Figure 54. Hose system fouling treatment with a 1 N H_2SO_4 Sltn. Left: Before treatment; Right : After treatment

3.4. SUBMERGED FIX BED BIOFILM REACTOR – 1

3.4.1. Bioreactor conditioning and testing

Before the experimental practices took place, the bioreactor system labeled SFBBR-1 was already running during some period with sludge water, thus biofilm was already formed on the carrier material. However, due to the different activities done with bioreactor system, it presented an extremely fouling pipe system and a lack of appropriate mixing conditions was observed in the collection tank. Furthermore, the working station and equipment were under unhygienic conditions making it difficult to work with. For that reason, the bioreactor system was conditioned before the experimental runs took place. The main activities performed during the conditioning and testing stages are listed below:

- Cleaning of the working area including the bioreactor column, collection tank and equipment.
- Replacement of pump's hose system and rubber gaskets.
- Testing of pump at different flow rates and checking for possible leakages.
- Setting up of the overhead or magnetic stirrer in the collection tank for proper mixing conditions.
- Installation of protecting mesh against large particles at the head of the hose line leading to the pump and column input.
- Several manual downwashing of the bioreactor with tap water for removal of undesirable suspended material within the packed bed biofilm.
- Calibration of pH and DO sensors.

3.4.2. Batch operation

A total of 6 batch treatment processes were performed during the experimental practices with the biofilm reactor labeled SFBBR-1. For most of the processes, approximately 20,0 L of high-strength ammonium sludge water were treated at different liquid recirculation and air flow rates and they were maintained relatively constant during each batch process. The treatment period for each batch varied in between 6 to 14 days depending on the flow rate conditions and each batch treatment was stopped when the estimated concentration of nitrite was smaller than 2,0 mg NO_2^--N/L.

In order to determine the ammonium consumption rate and nitrogen conversion, liquid samples of approximately 80,0 mL were taken from the collection tank during the treatment period. Before the chemical analysis, the collected samples were vacuum filtrated through a 2,5 µm paper filter from Whatman™. For each batch, the DO probe was located closed to the top of the packed bed biofilm and the DO was recorded for most of the running process. The DO in the collection tank was also measured during the last three batches numbered 4, 5 and 6.

The pH was kept at 7,5 by using a 0,7 M solution of potassium carbonate (K_2CO_3) which was added into the collection tank with the help of the dosing pump belonging to the pH controller from Bluelab. For the first three batches, the liquid in the collection tank was mix by using the overhead stirrer from Heidolph at a fix velocity of 250 rpm, but due to malfunctioning problems it was later replaced for the magnetic stirrer from

Heidolph at a fix velocity of 200 rpm. The temperature of the liquid in the collection tank varied in between 20,0 to 24,0°C and was maintained at approximately 22,0°C with the help of the aquatic heater from Jäger. The operational conditions for each batch are specify in table 18.

Table 18. Operational conditions for each batch treatment process in the SFBBR-1 system

Batch No.	1	2	3	4	5	6
Total Operation (d)	10	10	6	14	11	10
Air flow rate (L/h)	10,1	10,1	10,1	1,5	1,5	1,5
HLR (m/h)	4,6	9,9	13,8	4,9	10,1	11,6
NH_4^+-N initial conc. (mg/L)	936,20	915,07	845,33	852,84	808,28	791,6
Vol. SW treated (L)	24,0	20,0	20,0	20,0	20,0	20,0
set - pH	7,5	7,5	7,5	7,5	7,5	7,5
pH control	0,7 M K_2CO_3	0,7 M K_2CO_3	0,7 M K_2CO_3	0,7 M K_2CO_3	0,7 M K_2CO_3	0,7 M K_2CO_3
Average, TK-T (°C)	22,0	22,6	21,6	22,4	22,9	22,3

3.4.3. Semi-batch operation

The SFBBR-1 was operated in semi-batch mode with a HLR and air flow rate of 12,5 m/h and 1,5 L/h respectively. These flow rate conditions were kept constant during the treatment process and the recycle flow rate was measured once a week. The biofilm reactor system with approximately 20,0 L of high strength ammonium sludge water was initially operated in batch mode for 7 days until the ammonium-nitrogen concentration was smaller than 0,5 mg NH_4^+-N/L. In order to estimate the ammonium consumption rate at the operation conditions, liquid samples were taken during the batch stage and based on this value the bioreactor system was switch to semi-batch mode.

The bioreactor system was operated in semi-batch for 18 days where 3,0 L of the high strength ammonium sludge water were added daily to the collection tank while removing 3,0 L of the treated sludge water from the treatment system. Samples were taken daily to determine the ammonium removal capacity of the biofilm system at the working conditions.

The pH controller was set at 7,5 and adjusted during the treatment process by using a 0,9 M solution of sodium carbonate (Na_2CO_3). The temperature of the high strength ammonium SW was brought up to approximately 22,0°C by using the hot plate from Schott and it was maintained in the collection tank at an average temperature of 22,0°C by the used of the aquarium heater from Jäger. DO measurements were made at the top of the packed bed biofilm and the collection tank before and after renewal of the sludge water.

The operational conditions for the semi-batch treatment process are specify in table 19.

Table 19. Operational conditions for the semi-batch treatment process in the SFBBR-1 system

Batch operation (d)	7
Semi-batch operation (d)	18
Air flow rate (L/h)	1,5
HLR (m/h)	12,5
NH_4^+-N initial conc. range (mg/L)	802,32 – 829,56
Initial Vol. SW treated (L)	20,0
Vol. SW renewed (L/d)	3,0
set – pH	7,5
pH control	0,9 M Na_2CO_3
Average, TK-T (°C)	22,1 °C

3.5. SUBMERGED FIX BED BIOFILM REACTOR – 2

3.5.1. Bioreactor conditioning and testing

The state of the SFBBR-2 system was under deplorable conditions before the experimental practices took place. The bioreactor column presented an already degraded rusty nozzle plate at the top of the column, the valve corresponding to the downwash line was old and out of service, leakage at the bottom of the column was observed, the pump needed to be installed and it was very probable that the stability and activity of the biofilm was greatly affected by the septic conditions to the liquid long static period and metal contamination caused by the deterioration of the nozzle plate. After evaluation of the bioreactor system it was concluded that a series of conditioning and testing activities need to be done before any experimental run could take place. The main activities are listed below with some of their corresponding pictures.

- Cleaning the bioreactor column. These included emptying out the old liquid and carrier material that was inside the column and washing the inside of the column and the carrier material. After washing several times the carrier material, it was left drying to be used for later activities.

Figure 55. Conditioning of SFBBR-2. Left: Empty column; Right: Carrier material left drying

- Installation of the pump system and pump testing at different flow rates.

Figure 56. Conditioning of SFBBR-2. Installation of pump system

- Sealing of leakage with PVC cleaner & glue Tangit and replacement of downwash line valve.

Figure 57. Conditioning of SFBBR-2. Left: Sealing of leakage with glue Tangit & PVC cleaner; Right: Replacement of downwash line valve

- Loading of carrier material inside the column.

Figure 58. Conditioning of SFBBR-2. Loading of carrier material inside the column

- Installation of a plastic nozzle plate at the top of the column allowing the packed bed to be completely submerged.

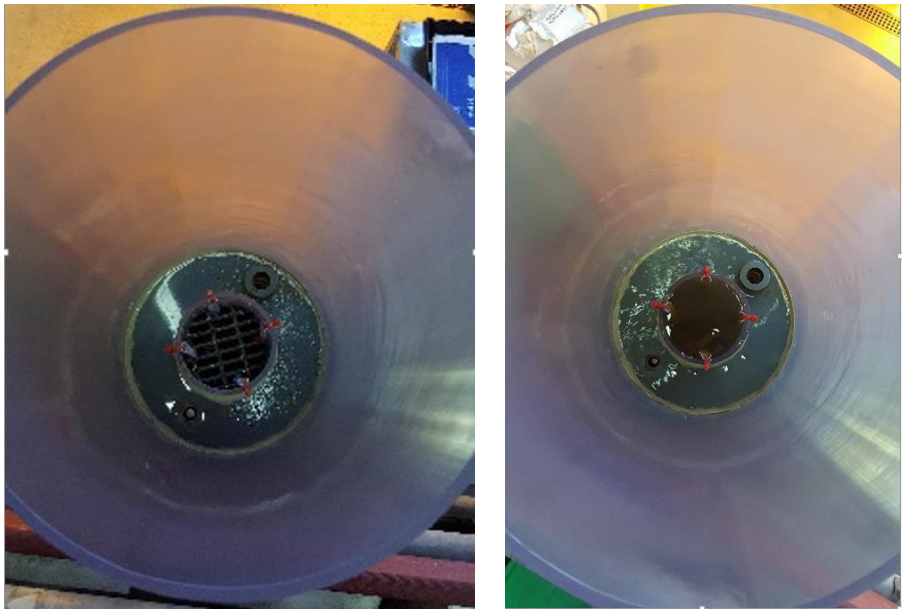

Figure 59. Conditioning of SFBBR-2. Left: Installation of plastic nozzle plate; Right: Packed bed completely submerged in the liquid

- Installation of protecting mesh against large particles at the head of the hose line leading to the pump and column input.

Figure 60. Conditioning of SFBBR-2. Installation of protecting mesh at input line

- Calibration of pH and DO sensors.

3.5.2. Starting of Bioreactor

The starting of bioreactor period lasted for 31 days until stable nitrification was observed. First, the bioreactor was filled up with high strength ammonium sludge water by using a total volume of 25,0 L. Then, the bioreactor system was inoculated by

adding approximately 35,0 mL of sludge collected from the already running SFBBR-1 system and on day 10 another 50 mL of sludge were added to the system. The high strength ammonium SW was renewed on days 10, 14, 19, 21, 24, 26 and 28 by addition of 5,0, 3,5, 5,0, 5,0, 5,0, 5,0 and 7,5 L respectively of the high strength ammonium SW while removing from the bioreactor system equivalent amounts of the already treated SW. Furthermore, during the starting period 80 mL samples were taken out from the system for chemical analysis.

Figure 61 shows the some of the sludge used during inoculation of the SFBBR-2 system.

Figure 61. Sludge collected from SFBBR-1 used for inoculation of SFBBR-2

After inoculation the bioreactor was operated for 10 days at a HLR of approximately 6,0 m/h and for the remaining 21 days it was operated at approximately 2,7 m/h. The air flow rate was kept constant along the bioreactor starting period at approximately 9,0 L/h. Additionally, the liquid recirculation flow rate was measured every week.

A pH effect during the starting period wanted to be evaluated thus during the first 7 days there was no pH control. At day 7 the pH controller was set at 7,8 and then at day 10 it was set at 7,5. In between days 7 and 12 the pH was controlled only by using a 1 N sulfuric acid solution and in between days 12 and 24 the pH was controlled by using the 1 N sulfuric acid solution and a 0,9 M sodium carbonate solution. After day 24 only the 0,9 M sodium carbonate solution was used to control the pH in the bioreactor system.

The DO and T were monitored at the top of the packed bed biofilm and in the collection tank. The temperature in the collection tank varied in between 20,0 to 24,0°C and was maintained at an average temperature of 21,9°C by the used of the aquarium heater from Jäger. The temperature of the renewed high strength ammonium SW was heated up before added to the collection tank to about 22,0°C by using the Hot plate from Schott.

The operational conditions during the columns starting period are specify in table 18.

Table 20. Operational conditions during the bioreactor starting period in the SFBBR-2 system

Operation period (d)	**0-10**	**10-14**	**14-19**	**19-21**	**21-24**	**24-26**	**26-28**	**28-31**
Air flow rate (L/h)	9,0	9,0	9,0	9,0	9,0	9,0	9,0	9,0
HLR (m/h)	6,0	2,7	2,7	2,7	2,7	2,7	2,7	2,7
NH_4^+-N Initial conc. (mg/L)	842,38	812,15	821,34	819,8	818,35	829,56	810,12	817,60
Vol. SW renewed (L)	-	5,0	3,5	5,0	5,0	5,0	5,0	7,5
set - pH	7,8	7,5	7,5	7,5	7,5	7,5	7,5	7,5
pH[a,b,c,d] control	1 N H_2SO_4	1 N H_2SO_4 & 0,9 M Na_2CO_3	1 N H_2SO_4 & 0,9 M Na_2CO_3	1 N H_2SO_4 & 0,9 M Na_2CO_3	1 N H_2SO_4 & 0,9 M Na_2CO_3	0,9 M Na_2CO_3	0,9 M Na_2CO_3	0,9 M Na_2CO_3
Average, TK-T (°C)	21,8	23,2	22,3	21,5	21,5	21,3	21,0	21,5

a. No pH control from day 0 to day 7.
b. Between days 7 and 12, the pH was controlled only by using 1 N H_2SO_4 sltn.
c. Between days 12 and 24, the pH was controlled by using 1 N H_2SO_4 sltn and 0,9 M Na_2CO_3 sltn.
d. After day 24, the pH was controlled only by using 0,9 M Na_2CO_3 sltn.

3.5.3. Batch operation

After stable nitrification was observed in the SFBBR-2 system a batch treatment was performed containing approximately 30,0 L of the high strength ammonium SW.

The SFBBR-2 system was operated in batch mode for 11 days until the concentration of ammonium-nitrogen was low and with HLR and air flow rate of about 2,9 m/h and 9,0 L/h respectively. The recirculation liquid flow rate was measured four times during the treatment period. The pH controller was set at 8,3 during the first 4 days and

adjusted by the used of the 1 N H_2SO_4 solution. After day 4 the pH controller was set at 7,5 and was adjusted by using the 0,9 M Na_2CO_3 solution. The temperature of the liquid in the collection tank varied in between 21,0 to 22,0°C and was maintained within this range temperature by the used of the aquatic heater from Jäger. Furthermore, the DO was measured daily at the top of the packed bed biofilm and in the collection tank and 80 mL samples were taken out periodically from the collection tank for chemical analyses. The batch operational conditions are specify in table 21.

Table 21. Operational conditions during the batch treatment process in the SFBBR-2 system

Batch operation (d)	11
Air flow rate (L/h)	9,0
HLR (m/h)	2,9
NH_4^+-N initial conc. (mg/L)	813,97
Initial Vol. SW treated (L)	30,0
set – pH	7,5
pH control	1 N H_2SO_4 & 0,9 M Na_2CO_3
Average, TK-T (°C)	21,5 °C

4. RESULTS AND DISCUSSION

4.1. CARRIER MATERIAL DENSITY, POROSITY AND BIOREACTORS LIQUID VOLUME

- **Density of the carrier material:**

The masses of the 20 randomly selected carrier materials are shown in table 22. The mass average value was calculated with application of equation 44.

Table 22. Mass value for 20 carrier materials

No.	No. Packing	m_{20} (g)
1	20	6,794
2	20	6,767
3	20	6,761
	Aver.	6,774

The results obtained for the determination of the volume corresponding to each of the 20 carrier materials are given in table 23. The glass stopper volume was estimated as

12,0 mL. The calculations done on data No. 1 to estimate the volume of the 20 carrier materials are shown below. The average value was calculated by using equation 44.

$$V_{20} = 172{,}0\ mL - 150{,}0 - 12{,}0 = 10{,}0$$

Table 23. Volume value for 20 carrier materials

No.	No. Packing	Volume (mL)		
		Water	Total	V_{20}
1	20	150,0	172,0	10,0
2	20	190,0	212,0	10,0
3	20	150,0	172,0	10,0
			Aver. =	10,0

Then, the density of the carrier material was determined by using equation 43 with the mass and volume average values.

$$\rho_c = \frac{6{,}774\ g}{10{,}0\ mL} = 0{,}7\ g/mL$$

- **Porosity:**

The packed bed heights corresponding to the SFBBR-1 and the SFBBR-2 were measured as 77,0 and 180,0 cm respectively. The total biofilter volume corresponding to each bioreactor was calculated by using equation 25.

$$V_{Tot._{B-1}} = \pi\left(\frac{10{,}0\ cm}{2}\right)^2 * 77{,}0\ cm\ \left|\frac{1\ L}{1000\ cm^3}\right| = 6{,}0\ L$$

$$V_{Tot._{B-2}} = \pi\left(\frac{10{,}0\ cm}{2}\right)^2 * 180{,}0\ cm\ \left|\frac{1\ L}{1000\ cm^3}\right| = 14{,}1\ L$$

The dimensions for the SFBBR-1 column including the reference point and the top column point used for the estimation of the packed bed volume are illustrated in table 24.

Table 24. SFBBR-1 column dimensions

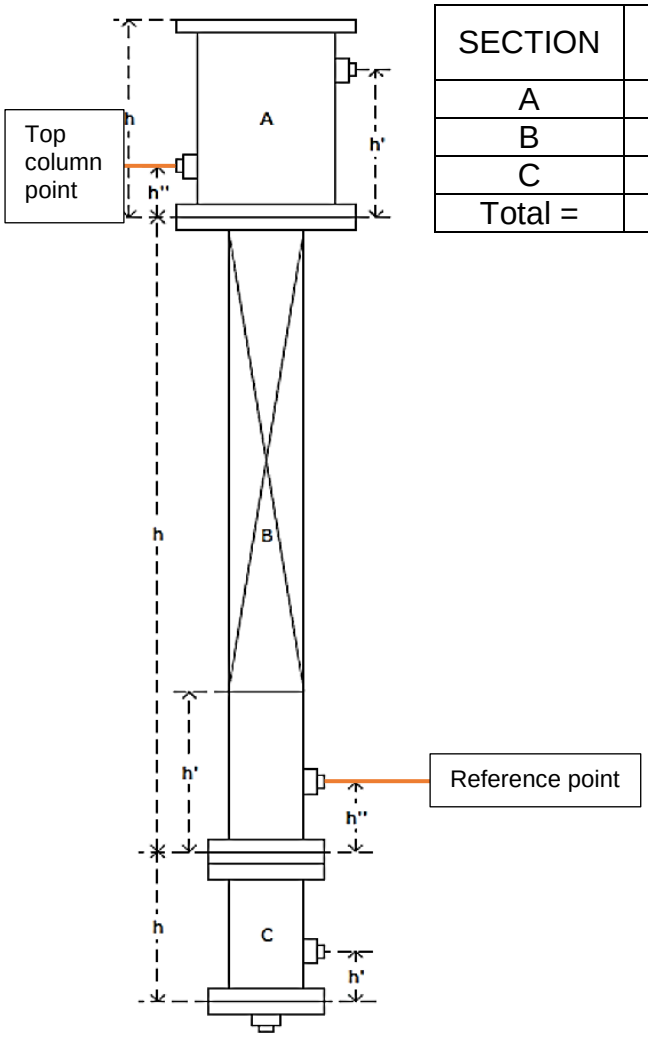

SECTION	h (cm)	h' (cm)	h'' (cm)	ID (cm)
A	31,5	23,5	8,0	19,0
B	101,5	25,5	11,0	10,0
C	24,0	8,0	-	10,0
Total =	157,0			

The theoretical volume from the reference point to the top column point was calculated based on the column dimensions and by using equation 25 for the general cylindrical case. The calculations done for the section B of the column are shown below.

- Height from reference point to top section B point:

$$h_B = 101{,}5\ cm - 11{,}0\ cm = 90{,}5\ cm$$

- Volume from reference point to top section B:

$$V_B = \pi \left(\frac{10{,}0\ cm}{2}\right)^2 90{,}5\ cm \left|\frac{1\ L}{1000\ cm^3}\right| = 7{,}1\ L$$

The same calculation was done for section A having a volume of 2,3 L. Then, the theoretical volume was calculated as:

$$V_{Theo.} = 2{,}3\ L + 7{,}1\ L = 9{,}4\ L$$

The volume of water required to fill the column from the reference point to the top column point is given in table 25. The total volume was estimated as 7,2 L

Table 25. Volume of water required to fill the SFBBR-1 column based on reference points

No.	Vol. (L)
1	1.0
2	1,0
3	1,0
4	1,0
5	1,0
6	1,0
7	1,0
8	0,2
Sum =	7,2

Then, the volume of the biofilm carrier material corresponding to the SFBBR-1 system was calculated as:

$$V_{bf-1} = 9{,}4\ L - 7{,}2\ L = 2{,}2\ L$$

The total biofilter volume and the biofilter volume were used in equation 24 to estimate the void volume and the porosity in the SFBBR-1 system as indicated below.

$$V_{void} = 6{,}0\ L - 2{,}2\ L = 3{,}8\ L$$

$$\varepsilon_{B-1} = \frac{3{,}8\ L}{6{,}0\ L} = 0{,}63 * 100\% = 63{,}0\%$$

Furthermore, the carrier material SSA of 660 m^2/m^3 and the biofilter volume were replaced in equation 23 to solve for the effective surface area of the biofilm. The approximate packed bed area of the SFBBR-1 was calculated as described below. A 30% decreased in the biofilter volume was considered due to the already formed biofilm.

$$SA_{B-1} = 2{,}2\ L * (1 - 0{,}3) \left| \frac{1\ m^3}{1000\ L} \right| * 660\ \frac{m^2}{m^3} = 1{,}0\ m^2$$

The total mass of the packing material fed into the SFBBR-2 column was measured twice. The average value was calculated by using equation 44. The results are given in table 26.

Table 26. Mass of the carrier material fed into the SFBBR-2 column

No.	Mass (g)	
1	557,42	493,45
2	568,75	540,25
3	508,21	950,90
4	546,72	196,67
Sum =	2181,10	2181,27
Aver. =	2181,19	

The average mass value and the already calculated density value were replaced in equation 43 for the general density case and solved for the carrier material volume. A 30% increment in the volume was considered due to biofilm formation. The calculation is given below.

$$V_{bf-2} = \frac{2181{,}19\ g}{0{,}7\ \frac{g}{mL}} * (1 + 0{,}3)\ \left|\frac{L}{1000\ mL}\right| = 4{,}0\ L$$

Finally, solving for void volume and porosity in equation 24:

$$V_{void} = \ 14{,}1\ L - 4{,}0\ L = 10{,}1\ L$$

$$\varepsilon_{B-2} = \ \frac{10{,}1\ L}{14{,}1\ L} = 0{,}71 * 100\% = 71{,}0\ \%$$

The packed bed area of the SFBBR-2 was calculated by using equation 23. The 30% increase in volume due to biofilm formation was not considered in the calculation, hence the value of 3,1 L was used instead of 4,0 L as the filter media volume.

$$SA_{B-2} = \ 3{,}1\ L\left|\frac{1\ m^3}{1000\ L}\right| * 660\ \frac{m^2}{m^3} = 2{,}0\ m^2$$

- **Bioreactor liquid volume:**

The liquid volume corresponding to the SFBBR-1 column was calculated as described in the methodology section. The final measured volume was subtracted from the initial measured volume. The results are given in table 27.

Table 27. Liquid volume in bioreactor column 1

	Volume (L)
Initial =	12,0
Final =	2,5
Vol. Liq. =	9,5

The calculations done to estimate the liquid volume corresponding to the SFBBR-2 column are shown below. Equation 25 was used for the general cylindrical case.

Column $h_{Tot.}$ = 220,0 cm

ID = 10,0 cm

$$V_{Tot} = \pi \left(\frac{10{,}0\ cm}{2}\right)^2 220{,}0\ cm \left|\frac{1\ L}{1000\ cm^3}\right| = 17{,}3\ L$$

$$V_{Liq.B-2} = 17{,}3\ L - 4{,}0\ L = 13{,}3\ L$$

The results obtained during the characterization of the SFBBR-1 and SFBBR-2 columns are given in table 28.

Table 28. Characterization of the SFBBR-1 and SFBBR-2 columns

Plastic carrier material: 12 mm * 12 mm; SSA= 660 m^2/m^3; ρ = 0,7 g/mL			
		SFBBR-1	**SFBBR-2**
Biofilter	Height (m)	0,77	1,8
	Total Vol. (L)	6,0	14,1
	Vol. (L)	2,2	4,0
	ε (%)	63,0	71,0
Packed bed	SA (m^2)	1,0	2,0
Bioreactor Liq.	Vol. (L)	9,5	13,3
Main column	Height (m)	1,3	2,2
	ID (cm)	10,0	10,0

The carrier material used in each bioreactor system consisted of a depth and diameter size of 12 mm each. As indicated in table 11, these dimensions are relatively larger when compared to the polystyrene beads used in the Biostyr® process with sizes ranging in between 2 to 4 mm. On the other hand, the SSA of 660 m^2/m^3 is smaller compared to SSA value of 1000 m^2/m^3 given for the polystyrene beads. However, as seen in table 9 the used carrier material SSA is considerably larger than the one from the rock material used in trickling filters which have values in between 45 to 60 m^2/m^3. Moreover, the reported bed depth range for the SFBBR with upflow configuration is given as 1,5 to 4 m. The bed depth for the SFBBR-2 is found to be within this range but the bed depth for the SFBBR-1 is much smaller.

Furthermore, the results obtained during the determination of the sludge water loss rate possibly mainly due to evaporation are given in table 29-

Table 29. Sludge water loss rate

No.	HLR (m/h)	Air flow rate (L/h)	Initial Vol. (L)	Final Vol. (L)	Loss Vol. (mL)	Loss rate (mL/d)
1	12,5	1,5	day 0: 10,3	day 2: 10,0	300,0	150,0
2	2,7	9,0	day 0: 7,5	day 3: 7,4	100,0	33,3

Furthermore, by using the linear relation described in equation 47 similar values were encounter at the HLR conditions. The calculation is described below.

$$Loss\ rate_{HLR-1} = \frac{150{,}0\frac{mL}{d} * 2{,}7\frac{m}{h}}{12{,}5\frac{m}{h}} = \ 32{,}4\ mL/d$$

$$Loss\ rate_{HLR-2} = \frac{33{,}3\frac{mL}{d} * 12{,}5\frac{m}{h}}{2{,}7\frac{m}{h}} = \ 154{,}2\ mL/d$$

The loss rate of 154,2 mL/d obtained in the linear relation corresponding to the second case (HLR-2) was a little higher than the measured value of 150,0 mL/d. The slightly increase can be related to the higher air flow rate used in the second case. The opposite occurred in the first case were the air flow rate was lower than the second case. Thus, based on the results and within the measured values, the HLR seems to have a higher impact in the sludge water loss than the air flow rate. Thus, the sludge water loss is expected to be higher for those experimental processes operating at larger HLR values with a slightly increase at higher air flow rates.

4.2. COLLECTED SLUDGE WATER ALKALINITY AND COD

The raw data obtained during the sludge water titration is given in appendix A.

The titration curved for the sludge water sample obtained from the experimental values is illustrated in figure 62

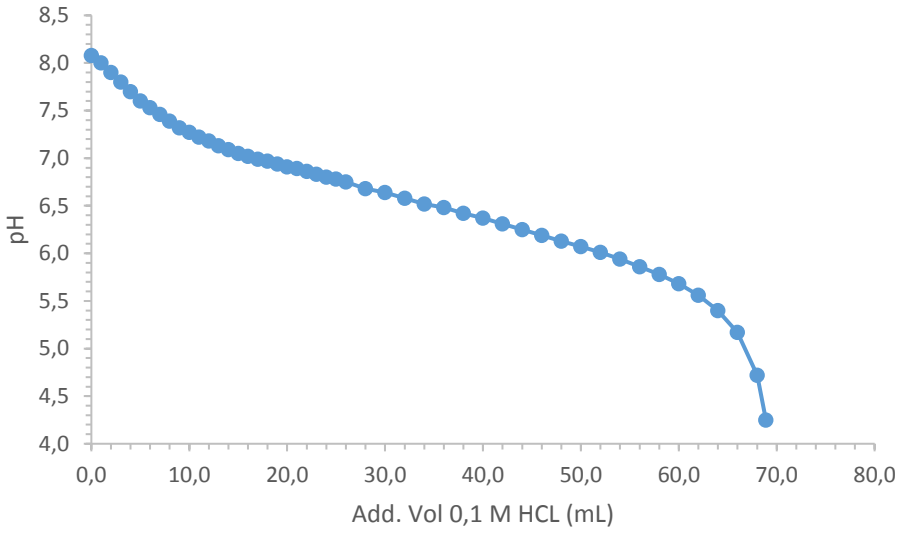

Figure 62. Titration curve for the sludge water sample

The volume of the acid consumed until pH 4,3 was equal to 68,9 mL. Then, the alkalinity was determined by using equation 42 as indicated below.

$$K_{s4,3} = \frac{0{,}1\ M * 68{,}9\ mL * 1000}{100{,}0\ mL} = 68{,}9\ mmol\ H^{+}/L$$

The estimated alkalinity value of 68,9 mmol/L corresponding to the collected sludge water was almost equal to the lower value reported for other sludge digester liquors whose range is in between 76,6 and 107,1 mmoL/L as indicated in table 3.

Moreover, the COD value of 385,0 mg O_2/L corresponding to the collected sludge water was determined as indicated in the methodology section. As indicated in table 3, the estimated COD value is very close to the lower value of 390 mg/L reported for other sludge digester liquors ranging in between 390 to 2720 mg/L.

4.3. LIQUID AND AIR FLOW RATES

The raw data collected during the experimental practices for the determination of the liquid and air flow rates are given in appendix B.

The recirculation liquid flow rates for batches 1, 2, 3, 4, 5 and 6 performed in the SFBBR-1 were calculated based on the individual recirculation rates corresponding to each collected data and then an average value was estimated by using equation 44. The average recirculation rate was used to estimate the HLR corresponding to each

batch treatment by using equations 20 and 21. For the batch case, the flow rate influent (Q_{in}) in equation 20 was equal to zero. The calculations done for Batch No.1 performed in the SFBBR-1 system is shown below.

- Cross sectional area of the column corresponding to each bioreactor:

$$A_R = \pi * \left(\frac{0{,}1\ m}{2}\right)^2 = 0{,}007854\ m^2$$

- Recirculation rate for data No. 1:

$$Q_R = \frac{600\ mL}{60\ sec}\left|\frac{1\ L}{1000\ mL}\right|\left|\frac{60\ sec}{1\ min}\right|\left|\frac{60\ min}{1\ h}\right| = 36{,}0\ L/h$$

- Average recirculation rate for Batch No. 1 in SFBBR-1 system:

$$\overline{Q_R} = \frac{36{,}0\frac{L}{h} + 36{,}0\frac{L}{h} + 36{,}0\frac{L}{h}}{3} = 36{,}0\ L/h$$

- HLR calculation for Batch 1 in SFBBR-1 system:

$$HLR = \frac{36{,}0\ \frac{L}{h}\left|\frac{m^3}{1000\ L}\right|}{0{,}007854\ m^2} = 4{,}6\ m/h$$

The recirculation liquid flow rate for the semi-batch operation performed in the SFBBR-1 system was calculated based on the individual recirculation rates corresponding to each collected data for each week. An overall average recirculation rate was obtained from the average value corresponding to each week by using equation 44. The overall average recirculation rate was used to estimate the HLR by using equations 20 and 21. Additionally, the HRT was calculated by using equation 22 and the already measured bioreactor liquid volume.

The calculations done for the semi-batch process are shown below.

- Overall average recirculation rate by using week average values:

$$\overline{Q_R} = \frac{97{,}8\frac{L}{h} + 98{,}6\frac{L}{h} + 98{,}0\frac{L}{h} + 96{,}6\frac{L}{h}}{4} = 97{,}8\ L/h$$

- HLR calculation:

$$Q_{in} = 3{,}0\frac{L}{d}\left|\frac{1\ d}{24\ h}\right| = 0{,}13\ L/h$$

$$HLR = \frac{0{,}13\,\frac{L}{h}\left|\frac{m^3}{1000\,L}\right| + 97{,}8\,\frac{L}{h}\left|\frac{m^3}{1000\,L}\right|}{0{,}007854\,m^2} = 12{,}5\,m/h$$

- HRT calculation:

$$HRT = \frac{9{,}5\,L}{3{,}0\,\frac{L}{d}} = 3{,}2\,d$$

The recirculation liquid flow rate and the HLR corresponding to the experimental activities performed in the SFBBR-2 system were estimated in a similar way for the batch case as described above.

The air flow rates for each experimental practice were estimated as described in the methodology section. The air flow rate corresponding to batches 1, 2 and 3 was measured after the batches were already finished. Thus, the specific value was not determined but rather an approximated value was estimated based on the bubble flow within the column at two valve positions. After observation, it was concluded that the air flow rate value for batches 1, 2 and 3 was approximately in between the two calculated average values corresponding to the two valve positions set for lower and higher flow rates as indicated in appendix B. The calculations are shown below.

- Air flow rate corresponding to valve set for lower flow:

$$\overline{Q_{Air_{low}}} = \frac{\frac{10}{9}\frac{mL}{sec} + \frac{20}{18}\frac{mL}{sec} + \frac{30}{28}\frac{mL}{sec}}{3} = 1{,}1\,mL/sec$$

- Air flow rate corresponding to valve set for higher flow:

$$\overline{Q_{Air_{high}}} = \frac{\frac{50}{11}\frac{mL}{sec} + \frac{50}{11}\frac{mL}{sec} + \frac{50}{11}\frac{mL}{sec}}{3} = 4{,}5\,mL/sec$$

- Air flow rate approximation:

$$\overline{Q_{Air}} = \frac{1{,}1\,\frac{mL}{sec}\left|\frac{1\,L}{1000\,mL}\right|\left|\frac{3600\,sec}{1\,h}\right| + 4{,}5\,\frac{mL}{sec}\left|\frac{1\,L}{1000\,mL}\right|\left|\frac{3600\,sec}{1\,h}\right|}{2} = 10{,}1\,L/h$$

The air flow rate corresponding to the other experimental activities were calculated in a similar way as described above but at their specific valve positions.

The results obtained for the recirculation liquid flow rate, HLR and air flow rate used in each the experimental activities are indicated in table 30.

Table 30. Liquid and air flow rates used during the experimental activities

Bioreactor system	Operation		Q_R (L/h)	HLR (m/h)	Air flow rate (L/h)
SFBBR-1	Batch No.1		36,0	4,6	≈ 10,1
	Batch No.2		78,0	9,9	
	Batch No.3		108,0	13,8	
	Batch No.4		38,4	4,9	1,5
	Batch No.5		79,2	10,1	
	Batch No.6		91,2	11,6	
	Semi-batch HRT ≈ 3,0 d		97,8	12,5	
SFBBR-2	Bioreactor starting	Week 1:	46,6	5,9	9,0
		Week 2 – 4:	21,5	2,7	
	Batch		22,5	2,9	

The different HLR values used during the different experimental activities ranged from 2,7 to 13,8 m/h. The experimental HLR range is very closed to the 2,4 to 12 m/h range given in table 11 for the Biocarbone® and Biofor® processes. Moreover, air flow rates varying in between 30 to 90 L/h are reported in other experimental works with similar configurations as the ones used (Dizge, et al., 2011) & (El-Shafai & Zahid, 2013). As seen in table 30, the air flow rate range found in the literature is so much larger compared to the ones used during the experimental work. Furthermore, high air flow rate values guarantee DO concentrations of at least 5 mg O_2/L in the upper zone of the bioreactor and the implementation of a DO control system is required in order to maintain the desire DO concentration in the bioreactor system.

4.4. EFFECTS OF LIQUID VELOCITY & OXYGEN LIMITATION

- **Effect of liquid velocity on biofilm mass transfer mechanisms:**

The effects of the different liquid velocities used during the experimental activities on the biofilm mass transfer mechanisms were analyzed with the help of equations 10 through 17.

The calculations done for batch No.1 performed in the SFBBR-1 system are described below. The sludge water properties such as density and viscosity were approximated to those corresponding to water at 20°C.

- Reynolds number calculation by using equation 13:

ρ_{SW} = 998,2 Kg/m^3 (The Engineering ToolBox, 2017)
μ_{SW} = 0,001 Pa · s (The Engineering ToolBox, 2017)

$$Re = \frac{4{,}6\frac{m}{h}\left|\frac{1\,h}{3600\,sec}\right| * 998{,}2\frac{Kg}{m^3} * 12{,}0\,mm\,\left|\frac{1\,m}{1000\,mm}\right|}{0{,}001\,Pa.sec} = 15{,}3$$

The calculated Reynold numbers given in table 30 and the porosity values of 0,63 and 0,71 corresponding to the SFBBR-1 and SFBBR-2 respectively are within the application limits of equation 11. The porosity value of 0,67 used in equation 17 corresponds to the average of the porosity values estimated for the SFBBR-1 and SFBBR-2. For the SFBBR-2 an average HLR value of 2,8 m/h between the 2,7 and 2,9 m/h values was used in the calculations.

- Schmidt number calculation by using equation 14:
  - Ammonium Schmidt number:

$D_{NH4\text{-}SW}$ = 1,86 * 10^{-9} m^2/s (Picioreanu, et al., 1997)

$$Sc_{NH_4^+} = \frac{0{,}001\,Pas.s}{998{,}2\frac{Kg}{m^3} * 1{,}86 * 10^{-9}\,\frac{m^2}{s}} = 538{,}6$$

  - Oxygen Schmidt number:

$D_{O2\text{-}SW}$ = 2,0 * 10^{-9} m^2/s (Picioreanu, et al., 1997)

$$Sc_{O_2} = \frac{0{,}001\,Pas.s}{998{,}2\frac{Kg}{m^3} * 2{,}0 * 10^{-9}\,\frac{m^2}{s}} = 500{,}9$$

- Stagnant liquid film thickness calculation by using equation 17:
  - Ammonium stagnant liquid film thickness:

$$\delta_{S_{NH_4^+}} = \frac{12{,}0\,mm\,*\,0{,}67}{1{,}09}\,15{,}3^{-\frac{1}{3}} * 538{,}6^{-\frac{1}{3}}\left|\frac{1000\,\mu m}{1\,mm}\right| = 365{,}2\ \mu m$$

  - oxygen stagnant liquid film thickness:

$$\delta_{s_{O_2}} = \frac{12{,}0\ mm\ *\ 0{,}67}{1{,}09}\, 15{,}3^{-\frac{1}{3}} * 500{,}9^{-\frac{1}{3}} \left|\frac{1000\ \mu m}{1\ mm}\right| = 374{,}1\ \mu m$$

- Mass transfer coefficient calculation by using equation 16:
  - Ammonium mass transfer coefficient:

$$k_{sw_{NH_4^+}} = \frac{1{,}86 * 10^{-9}\ \frac{m^2}{sec} \left|\frac{86400\ sec}{1\ d}\right|}{365{,}2\ \mu m\ \left|\frac{1\ m}{1000000\ \mu m}\right|} = 0{,}44\ m/d$$

  - Oxygen mass transfer coefficient:

$$k_{sw_{O_2}} = \frac{2{,}0 * 10^{-9}\ \frac{m^2}{sec} \left|\frac{86400\ sec}{1\ d}\right|}{374{,}1\ \mu m\ \left|\frac{1\ m}{1000000\ \mu m}\right|} = 0{,}46\ m/d$$

The results obtained for the ammonium and oxygen stagnant liquid films thickness and mass transfer coefficients corresponding to each of the experimental operations are given in table 31.

Table 31. Ammonium and oxygen stagnant liquid film thicknesses and mass transfer coefficients

$D_{NH4\text{-}SW}$ = 1,86 * 10^{-9} m^2/s; $D_{O2\text{-}SW}$ = 2,0 * 10^{-9} m^2/s
Sc_{NH4} = 538,6; Sc_{O2} = 500,9

Bioreactor system	Operation	HLR (m/h)	Re	δ_s (µm)		k_{SW} (m/d)	
				NH_4^+	O_2	NH_4^+	O_2
SFBBR-1	Batch No.1	4,6	15,3	365,2	374,1	0,44	0,46
	Batch No.2	9,9	33,0	282,5	289,4	0,57	0,60
	Batch No.3	13,8	45,8	253,5	259,7	0,63	0,67
	Batch No.4	4,9	16,3	357,8	366,5	0,45	0,47
	Batch No.5	10,1	33,6	281,1	288,0	0,57	0,60
	Batch No.6	11,6	38,6	268,2	274,7	0,60	0,63
	Semi-batch	12,5	41,5	261,9	268,3	0,61	0,64
SFBBR-2	Starting & batch	2,8	9,3	430,8	441,4	0,37	0,39

Table 31 shows the effect that the increase of the HLR has in the Reynolds number and the flow conditions within the bioreactor system. In general, the Reynolds number increment is proportional to the HLR increment and since all the calculated values are

smaller than 2300 then the flow conditions for all the experimental operations were within the laminar flow regime when compared to flows in pipes or ducts (The Engineering ToolBox, 2017). For instance, from batch No. 1 to batch No. 3 the HLR was increased 3 times from 4,6 to 13,8 m/h and by approximately the same factor the Reynolds number also increase from 15,3 to 45,8 respectively. Furthermore, the lower Schmidt number value for oxygen compared to the ammonium value can be explained by the greater ability of oxygen molecules to diffuse in the liquid medium under the same momentum transport conditions.

The graphical representation of the data given in table 31 for the stagnant liquid film thicknesses and the mass transfer coefficients are illustrated in figures 63 and 64 respectively at the different HLRs conditions.

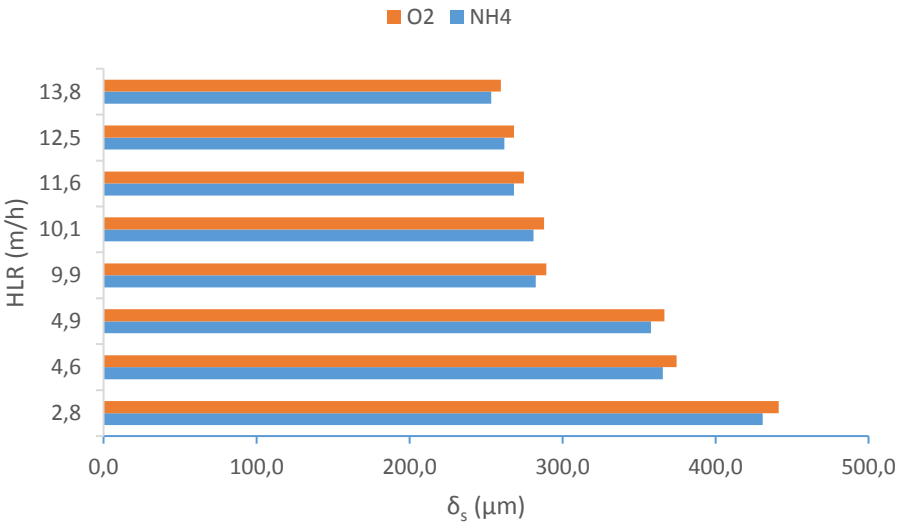

Figure 63. Stagnant liquid film thickness at different HLR

In figure 63 it can be seen how an increment of HLR in the system reduces the resistance to mass transfer or the stagnant film thickness corresponding to each of the substrates. For instance, an increase of almost 5 times in the HLR from 2,8 to 13,8 m/h can reduce the stagnant film thickness to almost half the value and thus facilitating the mas transfer transport of substrates from the bulk fluid to the biofilm surface. Moreover, for all the cases the stagnant film thicknesses corresponding to oxygen were a little higher than the ones corresponding to ammonium and the stagnant film thickness values calculated for oxygen are comparable to those shown in figure 24.

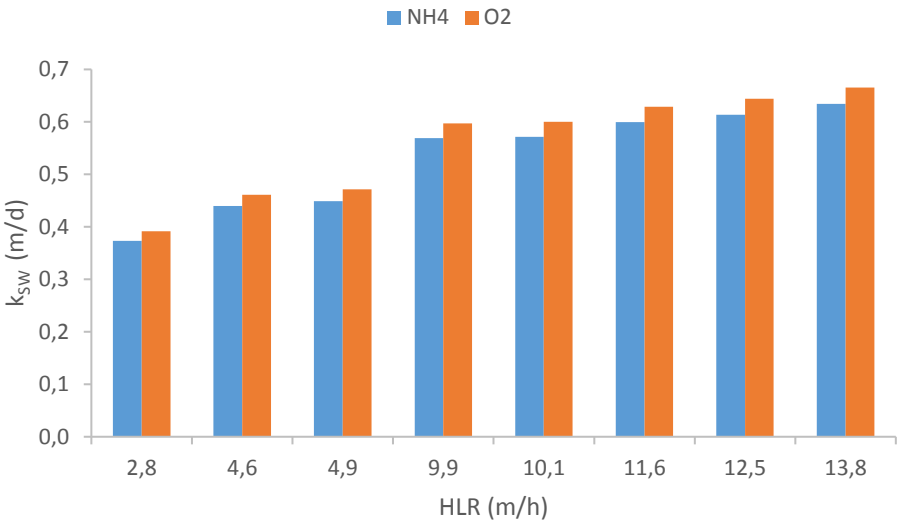

Figure 64. Mass transfer coefficient values at different HLRs

Figure 64 illustrates the final effect that flow velocities have on the transport mechanisms for the case of biofilms on spherical packed bed material. It can be seen that the same increase of almost 5 times the HLR from 2,8 to 13,8 m/h can increase almost twice the mass transfer coefficient values from 0,39 to 0,67 m/d and from 0,37 to 0,63 m/d for the oxygen and ammonium case respectively. For that reason ammonium oxidation is expected to occur at faster rates for those treatment processes ran at higher HLRs. Furthermore, the diffusivity values had a greater effect on the mass transfer coefficient than the calculated stagnant liquid film thickness values. Hence, for all the cases the calculated oxygen mass transfer coefficients were a little higher compare to the ammonium values.

- **Oxygen limitation in nitrification processes:**

The oxygen limitation in nitrification processes was analyzed by using equations 27 through 30. The oxygen saturation coefficient values of 0,3 and 1,1 mg O_2/L corresponding to AOB and NOB respectively given by Wiesmann (1994) at 20°C were used to estimate the oxygen concentrations required to reach specific growth rates equivalent to 90% their maximum specific growth rates. The calculations for the AOB case are described below.

$$c' = \frac{0{,}9 * 0{,}3\ mg\ O_2/L}{(1 - 0{,}9)} = 2{,}7\ mg\ O_2/L$$

The results for both AOB and NOB are given in table 32.

Table 32. Oxygen concentration limit values in Nitrification processes for specific growth rates equal to 90% the maximum specific growth rates

Bacteria	K_{O_2} (mg O_2/L)	c' (mg O_2/L)
AOB	0,3	2,7
NOB	1,1	9,9

The results show that in order to avoid oxygen limitations the concentrations of oxygen for AOB and NOB must be maintained at values equal or greater than 2,7 and 9,9 mg O_2/L respectively. In general, the oxygen concentration in nitrification processes is a limiting factor due to the high concentrations of oxygen required for the optimal growth of the microorganisms and the mass transfer limitations in biofilm processes where the oxygen concentration at the biofilm surface is lower than the bulk liquid concentration.

4.5. OPERATIONAL CONDITIONS FOR THE DIFFERENT EXPERIMENTAL PROCESSES

4.5.1. Batch No. 1 in SFBBR-1

This batch was operated for 10 days with a HLR of 4,6 m/h and air flow rate of approximately 10,1 L/h. A sludge water volume of approximately 24,0 L was treated and the operational conditions including pH, temperature, and the volume of the 0,7 M K_2CO_3 solution consumed were monitored in the collection tank during the sludge water treatment process.

The volume of the treated sludge water was estimated daily by taking into account the sludge water loss value for the SFBBR-1 given in table 29 and the volumes of sample taken and the added pH adjust solution. The calculations in between day 0 and day 1 are described below.

- Sludge water loss rate at HLR = 4,6 m/h:

$$Loss\ rate_{HLR-1} = \frac{150{,}0\,\frac{mL}{d} * 4{,}6\,\frac{m}{h}}{12{,}5\,\frac{m}{h}} = \ 55{,}2\ mL/d$$

- Day 1, treated sludge water estimation volume:

$$V_{day\,1} = 24{,}0\ L - 50{,}0\ mL \left|\frac{1\ L}{1000\ mL}\right| - 55{,}2\ \frac{mL}{d} * 1\ d \left|\frac{1\ L}{1000\ mL}\right| + 0 = 23{,}9\ L$$

The consumed potassium carbonate solution was estimated as the volume difference between the monitored days. The pH, T and volume values collected during the treatment process and the results are given in table 33. The average values were calculated by using equation 44.

Table 33. Operational conditions measured during Batch No. 1 in SFBBR-1 system

Day No.	pH	TK-T (°C)	Total Vol. (L)	Vol. Sample taken (mL)	Vol. K_2CO_3 (mL)	Vol. K_2CO_3 consumed (mL)
0	8,1	20,0	24,0	50,0	1000,0	0,0
1	8,3	22,0	23,9	70,0	1000,0	0,0
2	8,2	22,0	23,8	80,0	1000,0	0,0
3	7,8	22,0	23,6	80,0	1000,0	0,0
4	7,5	22,0	23,7	80,0	840,0	160,0
5	-	-	23,5	0,0	-	-
6	-	-	23,5	0,0	-	-
7	7,5	22,0	24,1	80,0	170,0	670,0
8	7,6	23,0	24,0	80,0	160,0	10,0
9	7,7	23,0	23,8	80,0	155,0	5,0
10	7,7	22,0	23,7	0,0	155,0	0,0
	Aver. =	22,0	Total =	600,0	Total =	845,0

As seen in table 33, during the treatment period the average temperature in the collection tank was approximately equal to 22,0° C. Around this temperature conditions, the specific growth rate of NOB generally represented by the genus *Nitrobacter* as indicted in equation 2 was expected to be higher than the AOB generally represented by the genus *Nitrosomonas* as indicated in equation 1. The specific growth rates at 22,0°C were determined based on the expressions given by equations 39 and 40 with values of 0,922 d^{-1} and 1,172 d^{-1} for *Nitrosomonas* and *Nitrobacter* respectively.

Furthermore, by day 10 the volume of the treated sludge water was approximately equal to 23,7 L which corresponded to a 300,0 mL reduction from the original volume of 24,0 L. The total sampling volume of the treated sludge water was equal to 600,0 mL and the pH was maintained at values within 7,5 to 8,3 which corresponded to the pH range where maximum nitrification rate can be expected as already illustrated in figure 36.

The graphical representation of the data given in table 33 is illustrated in figure 65

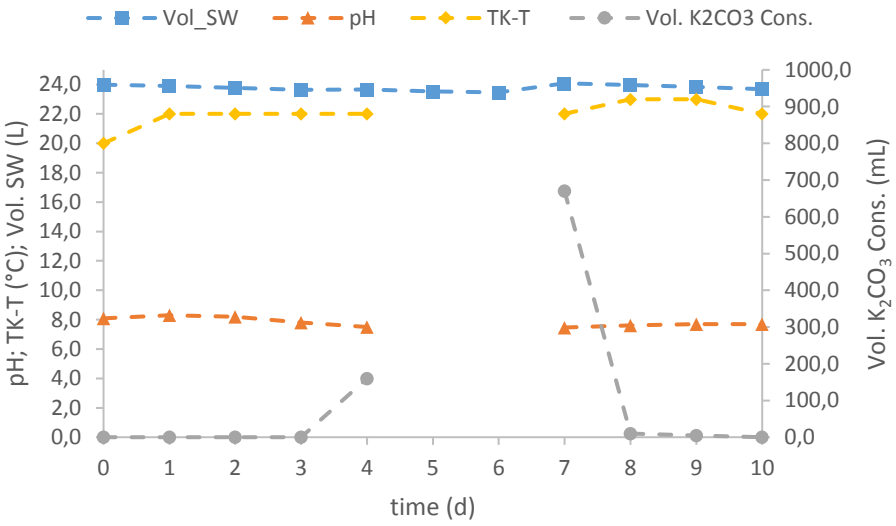

Figure 65. Operational conditions measured during Batch No. 1 in SFBBR-1 system

The consumption of the 0,7 M K_2CO_3 solution is better visualized in figure 65. It can be seen that the addition of the solution started on day 3 and ended by day 7 with a total volume consumption of 845,0 mL. Moreover, based on the process pH values and figure 37 the presence of bicarbonate ions were dominant among the different inorganic carbon species and the moles of hydrogen ions that reacted with the added carbonate ions were calculated by using equation 36. The calculations are described below.

- Added moles of carbonate ions:

$$n_{CO_3^{2-}} = 845{,}0\ mL \left| \frac{1\ L}{1000\ mL} \right| * \frac{0{,}7\ mol\ K_2CO_3}{L\ Sltn} \left| \frac{1\ mol\ CO_3^{2-}}{1\ mol\ K_2CO_3} \right| = 0{,}6\ mol\ CO_3^{2-}$$

- Reacted moles of hydrogen ions:

$$n_{H^+} = 0{,}6\ mol\ CO_3^{2-} \left| \frac{2\ mol\ H^+}{1\ mol\ CO_3^{2-}} \right| = 1{,}2\ mol\ H^+$$

Furthermore, the acid capacity of the treated sludge water was calculated based on its estimated specific alkalinity value of 68,9 mmol H^+/L as indicated below.

$$K_{SW} = 68{,}9\ \frac{mmol\ H^+}{L} \left| \frac{1\ mol}{1000\ mmol} \right| * 24{,}0\ L = 1{,}7\ mol\ H^+$$

Then, the total acid capacity of the system was calculated as:

$$K_{SW_{Tot.}} = 1{,}2\ mol\ H^+ + 1{,}7\ mol\ H^+ = 2{,}9\ mol\ H^+$$

The DO concentration and temperature values recorded at the top of the packed bed biofilm by the Portavo® 907 MULTI from Knick are given in appendix C.

A daily average DO and T values were calculated based on the daily recorded DO and T data. The sample standard deviation and standard error of the sample mean for the recorded data were calculated by using equations 45 and 46 respectively with the help of Microsoft® Excel® 2013. The calculated values are given in appendix C and the graphical representation of the calculated values are given in figure 66.

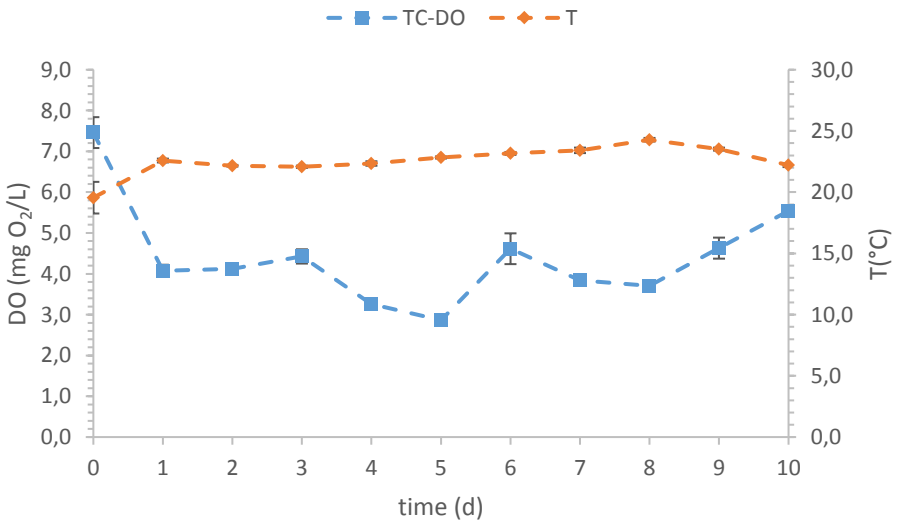

Figure 66. DO conc. & T values measured during Batch No. 1 in SFBBR-1 system

As seen in figure 66, the daily average DO concentration varied in between 2,86 to 7,46 mg O_2/L with an overall average value of 4,41 ± 0,37 mg O_2/L. In general, the DO concentration at the top of the column was higher than the theoretical value of 2,7 mg O_2/L value already described in table 32 and required for an AOB specific growth rate

equal to 90% of their maximum growth rate and the overall DO concentration average value was almost equal to the DO suggested value for biofilm processes of at least 5 mg/L already discussed in section 2.8.1.

The variability in the DO concentration values can be attributed to two observed situations. The first situation was related to an intermittent foaming formation at the top of the column during the treatment period which may have led to fluctuations in the DO values and potential oversaturation of oxygen in the sludge water at the top of the column. A picture of the foaming formed at some point of this process is illustrated in figure 67.

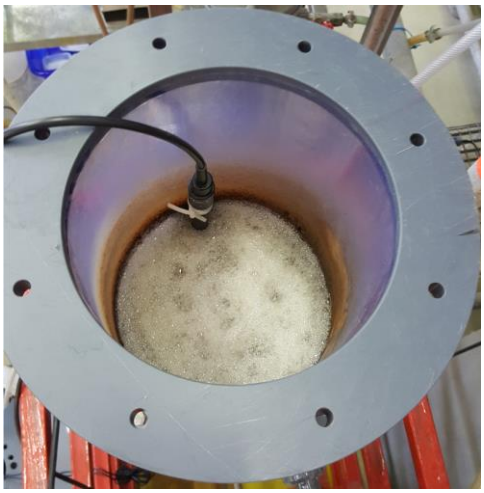

Figure 67. Foaming formation at the top of the column during Batch No. 1 in SFBBR-1 system

And, a second situation was observed in which some rising bubbles got stock at the tip of the DO probe and probably leading to misreadings in the DO concentration.

The temperatures at the top of the packed bed biofilm were relatively constant with values ranging in between 19,6 to 24,3°C and an average temperature value of 22,6 ± 0,4°C which was almost equal to the average collection tank temperature of 22,0°C.

4.5.2. Batch No. 2 in SFBBR-1

Batch No. 2 was also operated for a total of 10 days with a HLR of 9,9 m/h and air flow rate of approximately 10,1 L/h. The initial volume of sludge water treated was approximately equal to 20,0 L and the pH was adjusted by using the 0,7 M K_2CO_3 solution. The daily change in volume of the treated sludge water was calculated in the

same way as already described for Batch No.1 in the SFBBR-1 system. The calculated loss rate value was equal to 119,5 mL/d and a total volume of 400,0 mL were sampled from the collection tank.

The operational condition values monitored during the treatment period are given in appendix C. The graphical representation of the collected data is given in figure 68.

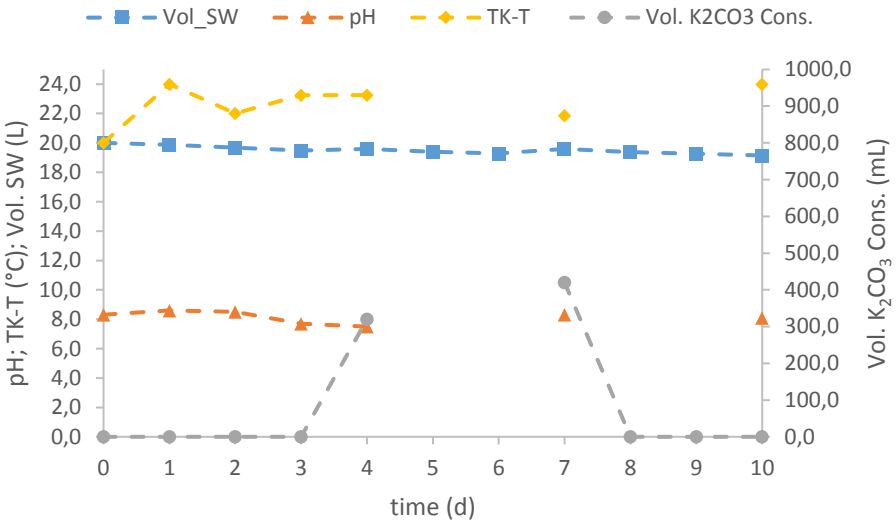

Figure 68. Operational conditions measured during Batch No. 2 in SFBBR-1 system

As illustrated in figure 68, the temperature in the collection tank was in between 20,0 and 24,0°C with an average value of 22,6°C. The daily volume of the treated sludge water was calculated to a final volume of approximately 19,1 L which represented a decrease of approximately 900,0 mL from the initial volume of 20,0 L.

The pH values ranged in between 7,5 to 8,6 during the treatment period with a total consumed volume of the 0,7 M K_2CO_3 solution equal to 740,0 mL. The moles of hydrogen ions that reacted with the added carbonate ions, the acid capacity of the treated sludge water and the total acid capacity of the system were calculated as already described in the batch No. 1 section with values equal to 1,1 mol H^+, 1,4 mol H^+ and 2,5 mol H^+ respectively.

For this batch the DO concentration was measured in the collection tank and at the top of the packed bed biofilm. The data analysis for the raw data recorded at the top of the packed bed biofilm was done in the same way as already described in batch No. 1. The calculated values and raw data are given in appendix C for batch No. 2. The graphical representation of the calculated values are given in figure 69.

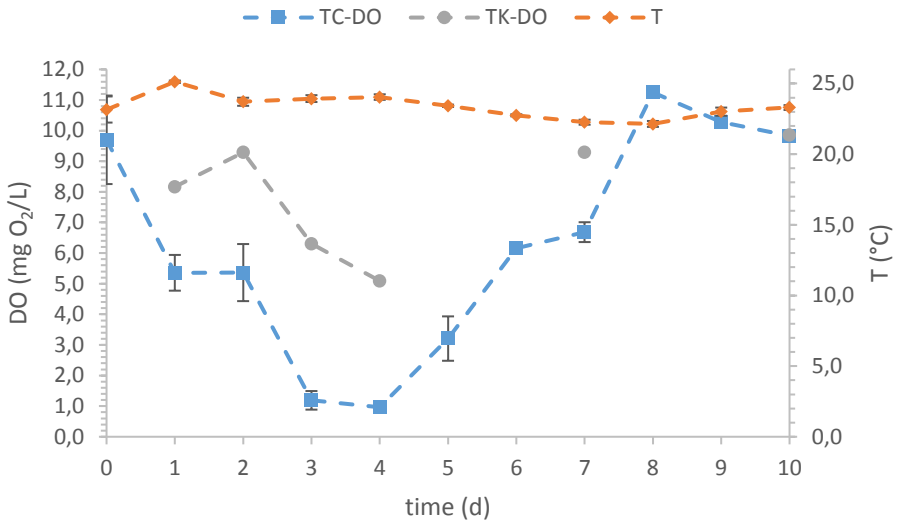

Figure 69. DO conc. & T values measured during Batch No. 2 in SFBBR-1 system

The average DO concentration values at the top of the packed bed biofilm fluctuated during the treatment process in between 0,96 to 11,25 mg O_2/L with an overall average value of 6,36 ± 1,09 mg O_2/L. The overall average value is higher than the suggested value of 5 mg/L for nitrification in biofilm processes. The lower DO values were registered for days 3 and 4 with average values of 1,19 ± 0,30 mg O_2/L and 0,96 ± 0,12 mg O_2/L respectively. These values are below the theoretical value of 2,7 mg O_2/L required for optimal growth of AOB. The oversaturated concentration of oxygen at the top of the column can be attributed to the already discussed intermittent foaming formation that occurred during the process which was more intense compare to batch No. 1 due to the higher HLR. Furthermore, the DO concentration in the collection tank varied in between 5,09 to 9,86 mg O_2/L with an average value of 8,00 mg O_2/L. The larger than 5 mg O_2/L DO values registered in the collection tank and the top of the packed bed biofilm help to reduce the oxygen limitations for AOB and NOB growth and thus guaranteeing an efficient ammonium and nitrite oxidation during the treatment process.

Finally, the temperatures at the top of the column were relatively constant with values ranging in between 22,1 to 25,1°C and an overall average temperature of 23,4 ± 0,3°C which was a little higher than the average collection tank temperature of 22,6°C. The slightly difference in temperature can be explained by energy conservation as stated by the first law of thermodynamics where some of the mechanical energy provided by the pump gets converted into thermal energy and thus increasing the temperature of the fluid.

4.5.3. Batch No. 3 in SFBBR-1

Batch No. 3 was operated for a total of 6 days at a HLR of 13,8 m/h and the approximated air flow rate of 10,1 L/h. The total volume of sludge water treated in this batch was equal to 20,0 L and the pH was adjusted by using the 0,7 M K_2CO_3 solution. The daily change in the volume of treated sludge water was calculated as indicated for batch No. 1 where the calculated loss rate value was equal to 165,5 mL/d and a total volume of 240,0 mL were sampled from the collection tank.

The operational condition values monitored during the treatment period are given in appendix C. The graphical representation of the collected data is given in figure 70.

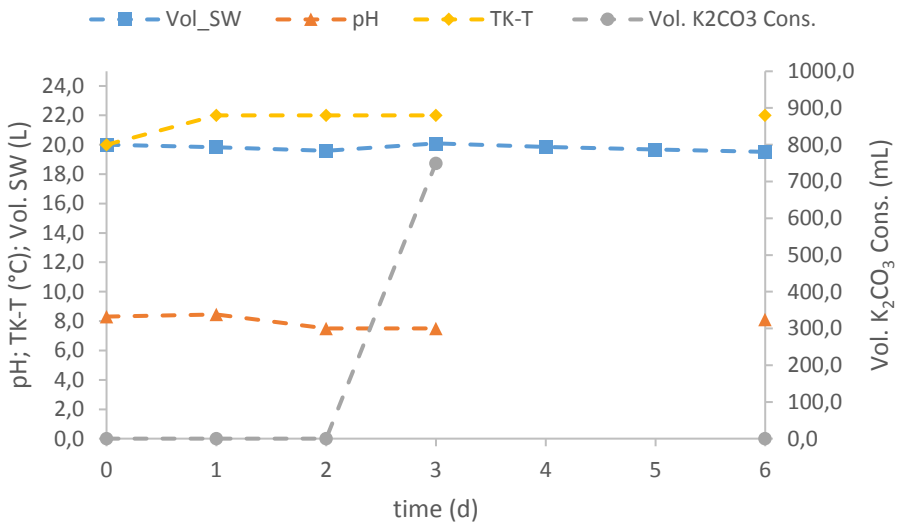

Figure 70. Operational conditions measured during Batch No. 3 in SFBBR-1 system

Figure 70 shows that the temperature in the collection tank varied in between 20,0 to 22,0 °C during the process with an average value of 21,6°C. The volume of the treated sludge water was calculated for day 6 as approximately 19,5 L which represented a decrease of about 500,0 mL from the initial volume of 20,0 L.

The pH values ranged in between 7,5 to 8,5 with a total consumed volume of the 0,7 M K_2CO_3 solution of 750,0 mL. The moles of hydrogen ions that reacted with the added carbonate ions, the acid capacity of the treated sludge water and the total acid capacity of the system were calculated as already described for the batch No. 1 case with values equal to 1,1 mol H^+, 1,4 mol H^+ and 2,5 mol H^+ respectively. These values corresponded to the same values calculated for the batch No. 2 process.

Furthermore, the DO concentration was measured and recorded at top of the packed bed biofilm. The data analysis for these data was done in the same way as already

described in batch No. 1. The calculated values and raw data are given in appendix C for batch No. 3. The graphical representation of the calculated values are illustrated in figure 71.

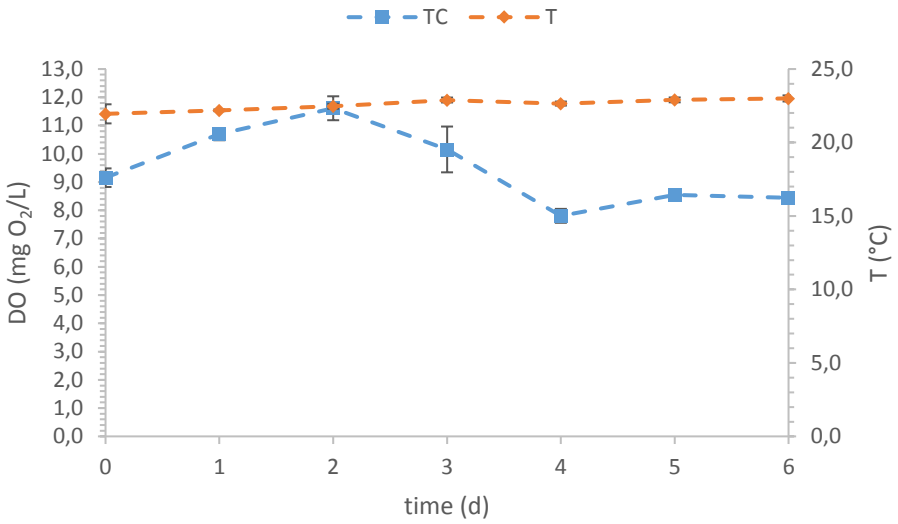

Figure 71. DO conc. & T values measured during Batch No. 3 in SFBBR-1 system

As observed in figure 71, during this treatment process the average DO concentrations at the top of the column reached a highest value of 11,61 mg O_2/L with a lowest point of 7,81 mg O_2/L for days 2 and 4 respectively. The overall average DO value was equal to 9,49 ± 0,52 which was slightly higher than the saturation value of 9,09 mg O_2/L at 20°C. The oversaturated recorded values were probably due to the relative high HLR and air flow rate used during this treatment process which resulted in strong foaming formation at the top of the column. Furthermore, the larger than 5 mg O_2/L DO values registered during the process at the top of the packed bed biofilm considerable reduced the oxygen limitations in the growth of the AOB and NOB within the biofilm, hence an efficient ammonium and nitrite oxidation was expected for this treatment process.

The temperatures at the top of the column were found to be in between 22,0 to 23,0°C with an average value of 22,6 ± 0,1°C. This value was slightly higher than the average value of 21,6°C registered during the treatment process in the collection tank.

4.5.4. Batch No. 4 in SFBBR-1

This batch was operated for a total of 14 days at HLR of 4,9 m/h and a constant air flow rate of 1,5 L/h. The initial volume of sludge water treated was approximately equal to 20,0 L and the pH was adjusted by using the 0,7 M K_2CO_3 solution. The daily change

in volume of the treated sludge water was calculated in the same way as already described for Batch No.1 in the SFBBR-1 system. The calculated loss rate value was equal to 58,9 mL/d and a total volume of 720,0 mL were sampled from the collection tank.

The operational condition values monitored during the treatment period are given in appendix C and their graphical representation is given in figure 72.

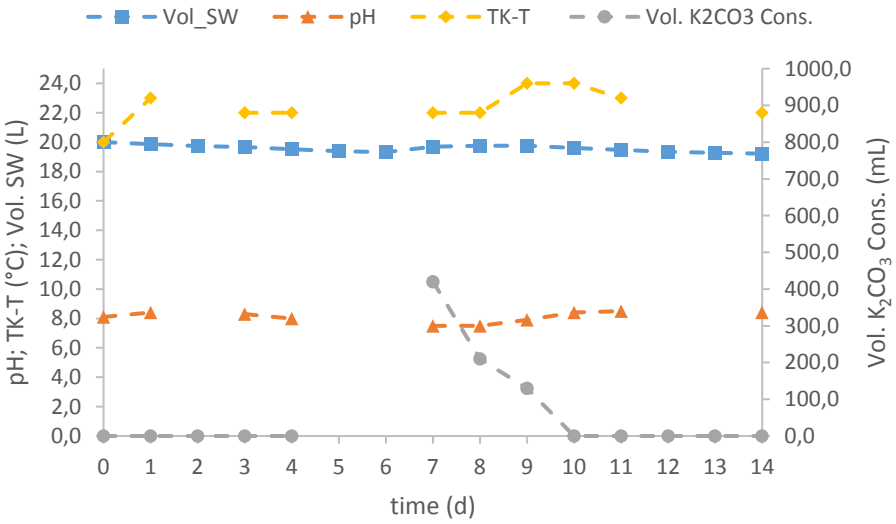

Figure 72. Operational conditions measured during Batch No. 4 in SFBBR-1 system

As illustrated in figure 72, the temperature in the collection tank varied in between 20,0 to 24,0°C with an average value of 22,4°C. The daily volume of the treated sludge water was calculated to a final volume of approximately 19,2 L by day 14 which represented a decrease of approximately 800,0 mL from the initial volume of 20,0 L.

The pH values ranged in between 7,5 to 8,5 during the treatment period with a total consumed volume of 760,0 mL corresponding to the 0,7 M K_2CO_3 solution. The moles of hydrogen ions that reacted with the added carbonate ions, the acid capacity of the treated sludge water and the total acid capacity of the system were calculated as already described in the batch No. 1 section with values equal to 1,1 mol H^+, 1,4 mol H^+ and 2,5 mol H^+ respectively.

The DO concentration was measured in the collection tank and at top of the packed bed biofilm. The data analysis for the raw data recorded at the top of the packed bed biofilm was done in the same way as already described in batch No. 1. The calculated values and raw data are given in appendix C for batch No. 4.

The graphical representation of the calculated values are given in figure 73.

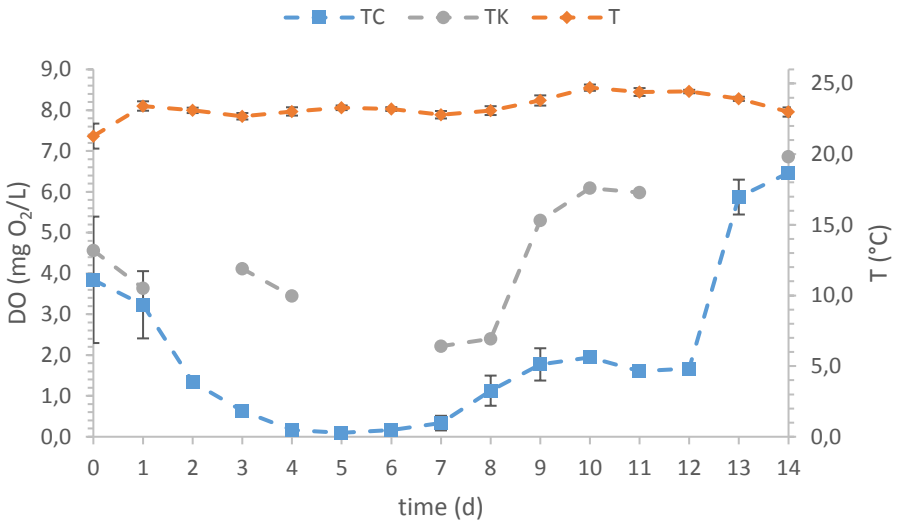

Figure 73. DO conc. & T values measured during Batch No. 4 in SFBBR-1 system

As seen in figure 73, the average DO concentration values measured at the top of the column varied from 1,0 to 4,0 mg O_2/L in between days 0 and 2. For days 3 through 7 the DO concentration was at the lowest points being smaller than 1,0 mg O_2/L. Then, the DO concentration increased in between days 8 to 12 with values in between 1,0 to 2,0 mg O_2/L and during the last two days of treatment the DO concentration was greater than 5,0 mg O_2/L. The overall DO concentration average value was equal to 2,02 ± 0,52 mg O_2/L, this value was smaller than the calculated theoretical value of 2,7 mg O_2/L required for optimal growth of AOB and was less than half the value corresponding to the suggested DO concentration value of 5 mg O_2/L. Furthermore, the DO concentration in the collection tank varied in between 2,22 to 6,86 mg O_2/L with an average value of 4,46 mg O_2/L.

Based on the measured values and considering the fact that in average the DO concentration of the system was smaller than 5 mg O_2/L. Then, oxygen limitations on AOB and NOB growth were expected during this process and thus affecting ammonium and nitrite oxidation and the overall efficiency of the treatment process.

The temperatures at the top of the column varied in between 21,3 to 24,7°C with an overall average temperature of 23,3 ± 0,2°C which was a little higher than the average collection tank temperature of 22,4°C.

The formation of foaming at the top of the column was not observed at the process conditions.

4.5.5. Batch No. 5 in SFBBR-1

This batch was operated for a total of 11 days at HLR of 10,1 m/h and a constant air flow rate of 1,5 L/h. The initial volume of sludge water treated was approximately equal to 20,0 L and the pH was adjusted by using the 0,7 M K_2CO_3 solution. The daily change in volume of the treated sludge water was calculated in the same way as already described for Batch No.1 in the SFBBR-1 system. The calculated loss rate value was equal to 121,4 mL/d and a total volume of 720,0 mL were sampled from the collection tank.

The operational condition values monitored during the treatment period are given in appendix C and their graphical representation is illustrated in figure 74.

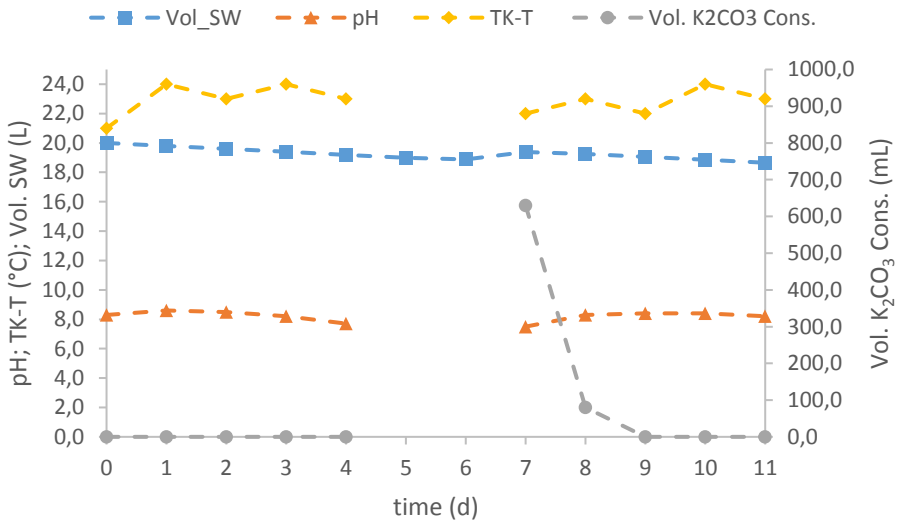

Figure 74. Operational conditions measured during Batch No. 5 in SFBBR-1 system

As illustrated in figure 74, the temperature in the collection tank varied in between 21,0 to 24,0°C with an average value of 22,9°C. The daily volume of the treated sludge water was calculated to a final volume of approximately 18,7 L corresponding to the last day which represented a decrease of approximately 1,3 L from the initial volume of 20,0 L.

The pH values ranged in between 7,5 to 8,6 during the treatment period with a total consumed volume of 710,0 mL corresponding to the 0,7 M K_2CO_3 solution. The moles of hydrogen ions that reacted with the added carbonate ions, the acid capacity of the treated sludge water and the total acid capacity of the system were calculated as already described in the batch No. 1 section with values equal to 1,0 mol H^+, 1,4 mol H^+ and 2,4 mol H^+ respectively.

The DO concentration was measured in the collection tank and at top of the packed bed biofilm. The data analysis for the raw data recorded at the top of the packed bed biofilm was done in the same way as already described in batch No. 1. The calculated values and raw data are given in appendix C for batch No. 5. The graphical representation of the calculated values are given in figure 75.

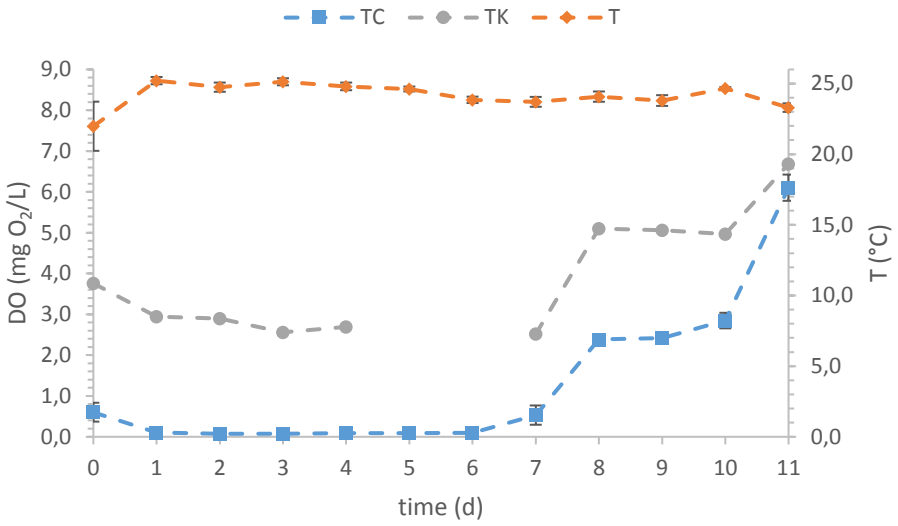

Figure 75. DO conc. & T values measured during Batch No. 5 in SFBBR-1 system

Figure 75 shows that the average DO concentration values measured at the top of the column were below 1,0 mg O_2/L in between days 0 to 7. For days 8 through 10 the DO concentration was in between 2,0 to 3,0 mg O_2/L and by day 11 the DO concentration had increased to 6,1 mg O_2/L.

The overall DO concentration average value at the top of the packed bed biofilm was equal to 1,29 ± 0,53 mg O_2/L and the DO concentration in the collection tank varied in between 2,52 to 6,68 mg O_2/L with an average value of 3,92 mg O_2/L. The average DO concentration values are lower than the calculated theoretical value of 2,7 mg O_2/L required for the optimal growth of AOB and are so much less than the suggested DO concentration value of 5 mg O_2/L. For that reason, the same oxygen limitation as previously described for the batch No. 4 case was expected for this treatment process.

The temperatures at the top of the column varied in between 22,0 to 25,2°C with an overall average temperature of 24,2 ± 0,3°C which was a little higher than the average collection tank temperature of 22,9°C.

The formation of foaming at the top of the column was not observed at the process conditions.

4.5.6. Batch No. 6 in SFBBR-1

This batch was operated for a total of 10 days at a HLR of 11,6 m/h and at a constant air flow rate of 1,5 L/h. The initial volume of sludge water treated was approximately equal to 20,0 L and the pH was adjusted by using the 0,7 M K_2CO_3 solution. The daily change in volume of the treated sludge water was calculated in the same way as already described for the Batch No.1 process. The calculated loss rate value was equal to 139,8 mL/d and a total volume of 640,0 mL were sampled from the collection tank.

The operational condition values monitored during the treatment period are given in appendix C and their graphical representation is shown in figure 76.

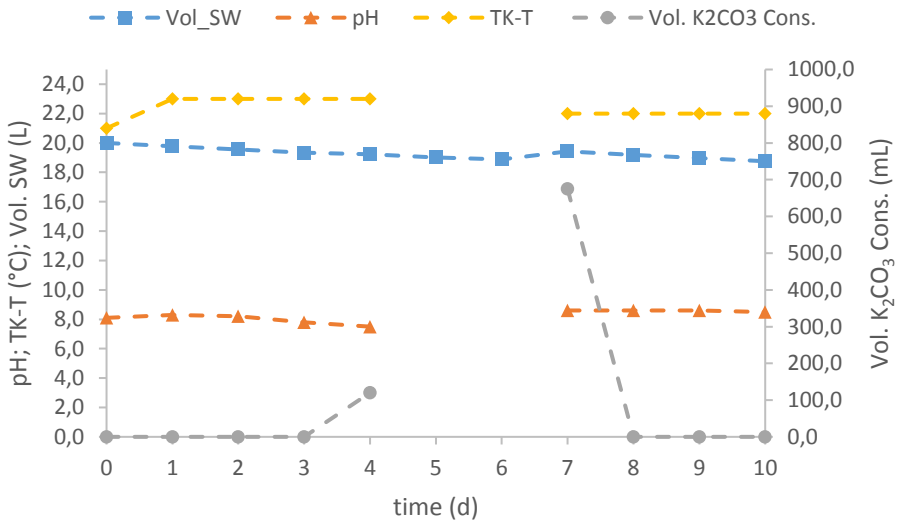

Figure 76. Operational conditions measured during Batch No. 6 in SFBBR-1 system

As illustrated in figure 76, the temperature in the collection tank varied in between 21,0 to 23,0°C with an average value of 22,3°C. The daily volume of the treated sludge water was calculated to a final volume of approximately 18,8 L which corresponded to day 10 and represented a decrease of approximately 1,2 L from the initial volume of 20,0 L.

The pH values ranged in between 7,5 to 8,6 during the treatment period with a total consumed volume of 795,0 mL of the 0,7 M K_2CO_3 solution. The moles of hydrogen ions that reacted with the added carbonate ions, the acid capacity of the treated sludge water and the total acid capacity of the system were calculated as already described for batch No. 1 with values equal to 1,1 mol H^+, 1,4 mol H^+ and 2,5 mol H^+ respectively.

The DO concentration was measured in the collection tank and at top of the packed bed biofilm. The data analysis for the raw data recorded at the top of the packed bed biofilm was done in the same way as already described in batch No. 1. The calculated values and raw data are given in appendix C for batch No. 6. The graphical representation of the calculated values are given in figure 77.

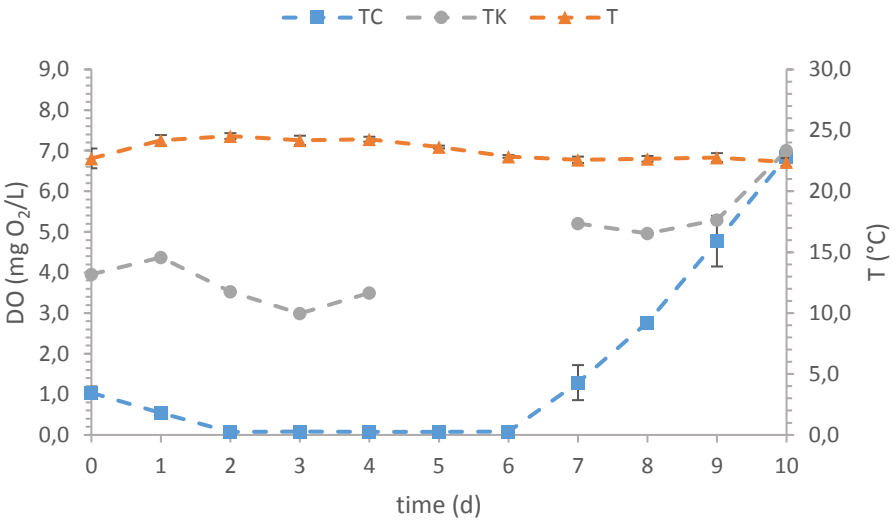

Figure 77. DO conc. & T values measured during Batch No. 6 in SFBBR-1 system

Figure 77 shows that the average DO concentration values measured at the top of the column were equal to 1,0 mg O_2/L for day 0 but in between days 1 to 6 the average value was lower than 1,0 mg O_2/L and in between days 7 to 10 the DO concentration increased from 1,3 to 6,9 mg O_2/L respectively.

The overall DO concentration average value at the top of the packed bed biofilm was equal to 1,60 ± 0,69 mg O_2/L and the DO concentration in the collection tank varied in between 3,0 to 7,0 mg O_2/L with an average value of 4,53 mg O_2/L. As already discussed in batches No. 4 and 5, the average low concentrations of oxygen in the system are indications of possible oxygen limitation in the growth of the AOB and leading to lower ammonium consumption rates.

The temperature at the top of the column varied in between 22,4 to 24,5°C with an overall average temperature of 23,3 ± 0,2°C which was a little higher than the average collection tank temperature of 22,3°C.

4.5.7. Semi-Batch operation in SFBBR-1

The daily change in volume of the treated sludge water was calculated as described in the batch No. 1 section. The loss rate value was estimated as 150,0 mL/d as indicated in table 29 and a total of 400,0 mL were sampled from the collection tank.

The operational condition values measured during this treatment process are given in appendix D and their graphical representation is illustrated in figure 78.

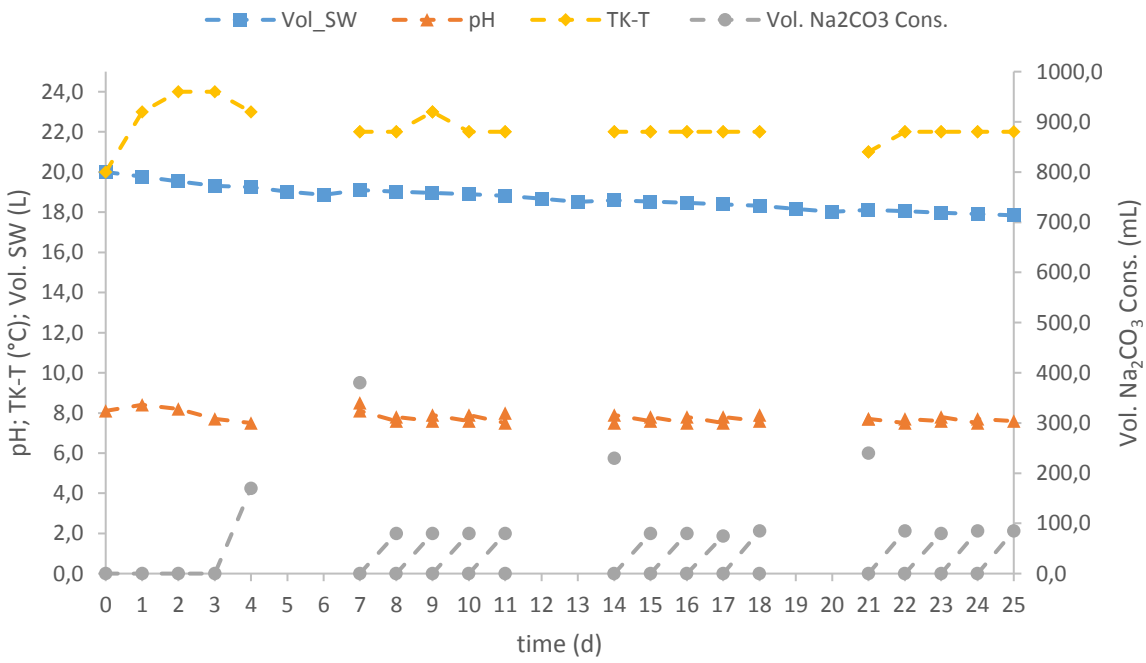

Figure 78. Operational conditions measured during the semi-batch process in SFBBR-1 system

As seen in figure 78, the temperature in the collection tank was maintained in between 20,0 to 24,0°C with an average temperature of 22,1°C and by day 25 the volume of the treated sludge water had decreased to a value of 17,8 L representing a total liquid loss of approximately 2,2 L from the initial volume of 20,0 L.

The pH was maintained during the process within 7,5 to 8,5 with a total consumption of the 0,9 M sodium carbonate solution of 1995,0 mL. The consumption of the pH adjust solution was almost equal during the daily sludge water renewal period with values ranging from 75,0 to 85,0 mL corresponding to an acid capacity range of 0,1 to 0,2 mol H^+. Furthermore, the 3,0 L of the sludge water contained approximately an alkalinity equal to 0,2 mol H^+ leading to a daily total acid capacity range of 0,3 to 0,4 mol H^+. Additionally, on the weekends, 9,0 L of the sludge water were renewed which represented a 3 day treatment. The consumptions of the pH adjust solution during the two weekends were 230,0 and 240,0 mL with a daily average consumption of 76,6

and 80,0 mL respectively, these values were found to be within the range observed during the daily treatment renewal. The acid capacity values were calculated as indicated in the batch No. 1 section but by using the 0,9 M concentration of the sodium carbonate solution.

The DO concentration and temperature values measured at the top of the packed bed biofilm and the DO concentration measured in the collection tank are illustrated in figure 79. The values are given in appendix D.

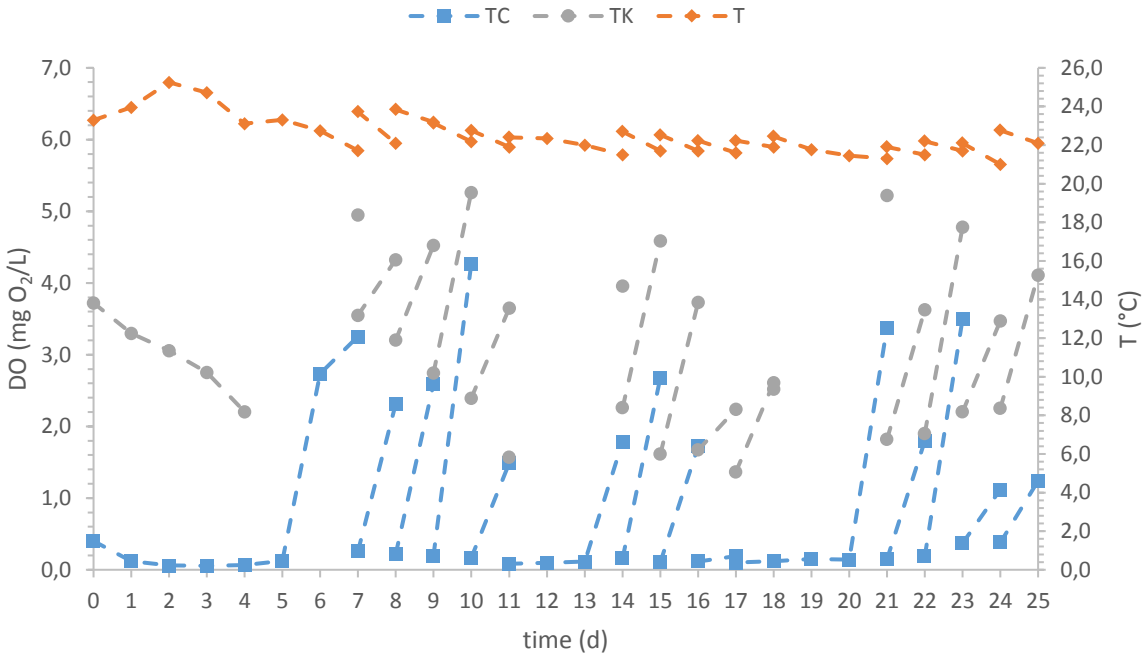

Figure 79. DO conc. & T values measured during the semi-batch process in SFBBR-1 system

As illustrated in figure 79, the DO concentration measured at the top of the column followed the same trend as already described for batches No. 4 through 6 with approximately the same constant air flow rate of 1,5 L/h. In general, during the daily treatment the concentration of DO in the top column decreased to values lower than 1,0 mg O_2/L and then increased to values greater than 1,0 mg O_2/L with a total average of 0,95 mg O_2/L. The same trend was observed for the DO concentration in the collection tank but at higher values. In general, during the daily treatment the DO concentration in the collection tank decreased to values ranging in between 1,4 to 3,2 mg O_2/L and had total average DO concentration value of 3,15 mg O_2/L. The total average DO concentration values were below the suggested DO concentration of 5 mg O_2/L possible leading to oxygen limitations in the biofilm system.

The temperature at the top of the column varied in between 21,0 to 25,3°C with an average value of 22,5°C and being slightly higher than the collection tank average temperature of 22,1°C.

4.5.8. Starting of bioreactor in SFBBR-2

The daily change in volume corresponding to the treated sludge water was calculated as described in the batch No. 1 section. Based on the value indicated in table 29, two values of the loss SW rate were calculated as 72,4 and 30,3 mL/d corresponding to the HLRs of 6,0 and 2,7 m/h respectively used during the starting of the bioreactor period and a total of 850,0 mL were sample from the collection tank.

The operational condition values measured during the starting of the bioreactor are given in appendix E. The graphical representation of the values is shown in figure 80.

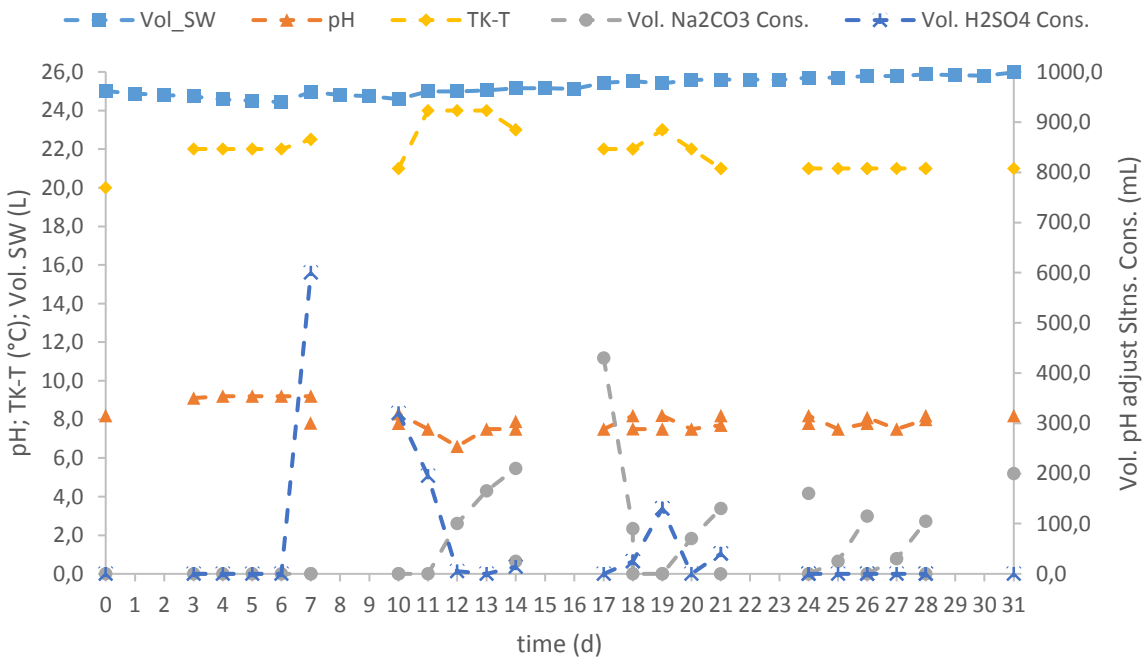

Figure 80. Operational conditions measured during starting of bioreactor in SFBBR-2 system

As illustrated in figure 80, during the starting of the bioreactor the temperature in the collection tank varied in between 20,0 to 24,0°C with an average value of 21,9°C. In contrast to the already discussed processes, the estimated volume of the treated sludge water corresponding to the last day of treatment was equal to 26,0 L which represented an increase of 1,0 L from the initial value of 25,0 L.

As already indicated in table 20, during the first 7 days the pH was not controlled allowing the system to behave on its own. As seen in figure 80, during these days the pH increased from 8,2 on day 0 to 9,2 on day 7. The increase in pH can be explained by the degradation of nitrogen bound organic material indicated in figure 2 resulting in ammonia production and the shift towards ammonia in the ammonium/ammonia equilibrium reaction described by equation 32 due to the sludge water alkalinity. At the pH conditions of 9,2 the presence of ammonia and ammonium are almost equal as illustrated in figure 1 at 20°C. On day 7, due to the inhibitory effects that high FA concentration can caused in nitrifying microorganisms the pH started to be adjusted by using the 1 N sulfuric acid solution. After day 7, the pH ranged in between 6,6 to 8,3 and was adjusted by using the acid and alkaline solutions as described in table 20.

Furthermore, during the last week where 5,0 L of SW were renewed the consumption of the sodium carbonate solution was almost constant with final consumption values of 140,0 and 135,0 mL corresponding to days 26 and 28 respectively. Thus, by taking into account the alkalinity value of 0,3 mol H^+ corresponding to the 5,0 L of renewed SW and the calculated 0,3 mol of hydrogen ions that reacted with the added carbonate then the total acid capacity during the last week was approximately equal to 0,6 mol H^+ for each of the last two renewal stages. Moreover, a total of 1855,0 and 1329,0 mL of the 0,9 M Na_2CO_3 and 1 N H_2SO_4 solutions were used during the starting of the bioreactor process respectively.

The DO concentration and temperature values measured at the top of the packed bed biofilm and the DO concentration measured in the collection tank are illustrated in figure 81. The values are given in appendix E.

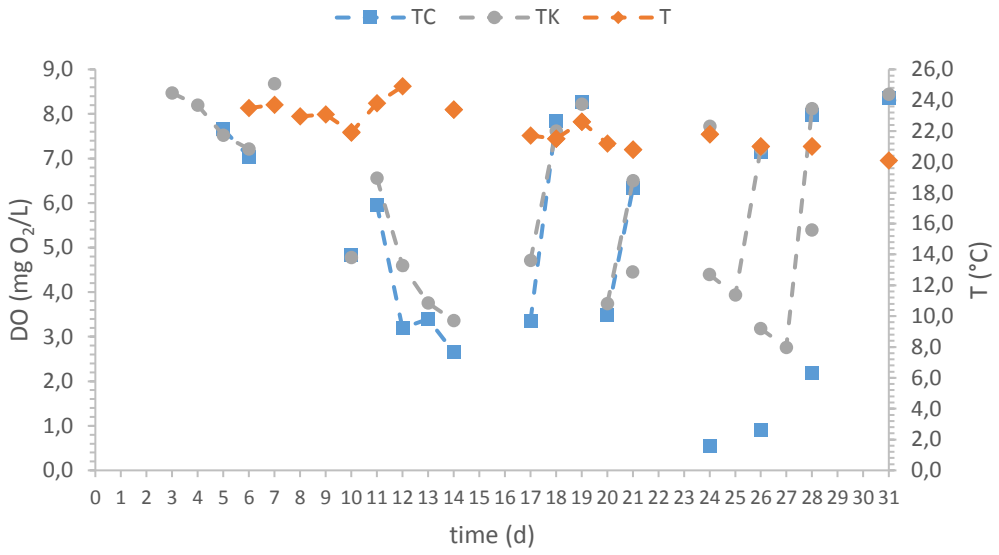

Figure 81. DO conc. & T values measured during starting of bioreactor in SFBBR-2 system

As shown in figure 81, the DO concentration was measured periodically during the process. On the first seven days, a decreased in the DO concentration was observed at the top of the column and in the collection tank. The decreased in the DO concentration can be attributed partially to biological activity and also by the increased of the ammonia concentration in the liquid phase which led to the decrease of the oxygen concentration. In general, in between days 7 to 24 the DO concentrations at the top of the column were very closed to the ones measured in the collection tank with values ranging in between 2,6 to 8,3 mg O_2/L. On the other hand, after day 24 a deviation was observed specially within the renewal stages. For instance, at day 24 after renewing the 5,0 L of sludge water the DO concentration at the top of the packed bed biofilm dropped to an approximately value of 0,5 mg O_2/L and to 4,4 mg O_2/L in the collection tank but at day 26 before the other renewal took place both DO concentrations had approximately the same values being around 7,0 mg O_2/L. The same trend was observed in between days 26 and 28 and in between days 24 to 31 the average DO concentration value at the top of the column and the collection tank were equal to 4,52 and 5,43 mg O_2/L respectively.

The temperature at the top of the column varied in between 20,0 to 25,0°C with an average value of 22,1°C which was very closed to the average value of 21,9°C calculated for the collection tank.

4.5.9. Batch operation in SFBBR-2

The daily treated sludge water volume change was estimated as indicated in the batch No. 1 section by using a calculated loss rate value of 33,2 mL/d and a total of 640,0 mL were sampled out from the collection tank.

The operational condition values measured during this treatment process are given in appendix E. The graphical representation of the values is illustrated in figure 82.

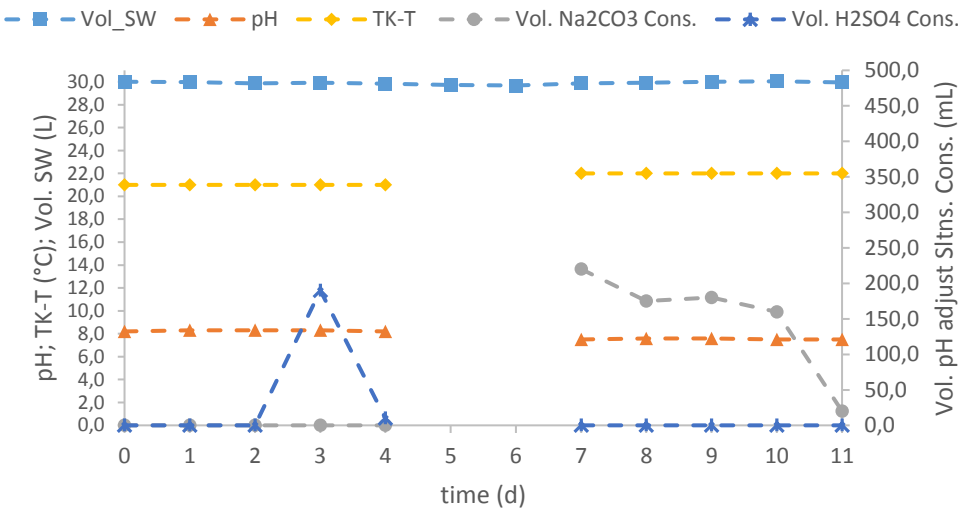

Figure 82. Operational conditions measured during batch operation in SFBBR-2 system

As shown in figure 82, the temperature in collection tank was relatively constant with an average value of 21,5 °C and in contrast to any of the performed processes, by the last day of treatment, the volume of the treated sludge water was approximately equal to the initial value of 30,0 L.

The pH varied in between 7,5 to 8,3 with a total consumption of 755,0 and 200,0 mL of the 0,9 M sodium carbonate and 1 N sulfuric acid solutions respectively. Moreover, the moles of hydrogen ions that reacted with the added carbonate ions, the acid capacity of the treated sludge water and the total acid capacity of the system were calculated as already described for batch No. 1 with values equal to 1,4 mol H^+, 2,1 mol H^+ and 3,5 mol H^+ respectively.

The DO concentration and temperature average values obtained from the recording data at the top of the column and the DO concentration measured in the collection

tank are illustrated in figure 83. The calculated values and raw data are given in appendix E.

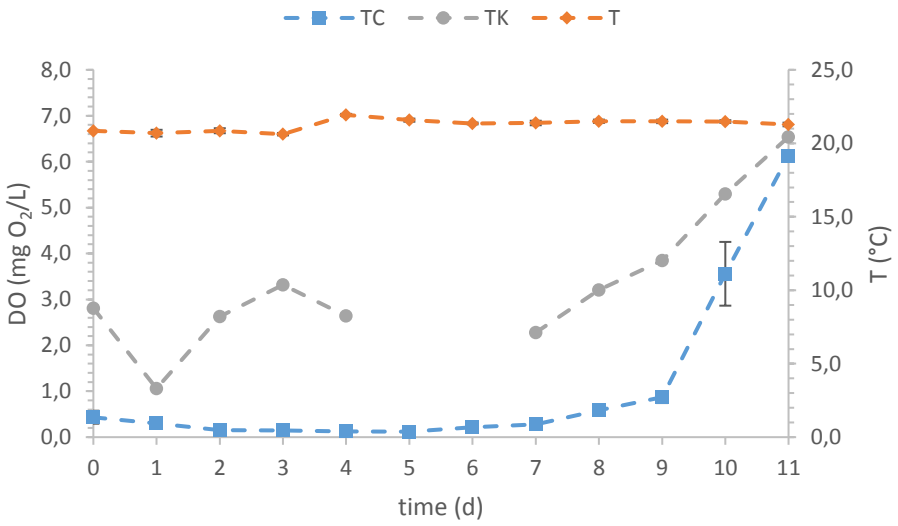

Figure 83. DO conc. & T values measured during batch operation in SFBBR-2 system

Figure 83 shows that in between days 0 to 9 at the top of the packed bed biofilm the average DO concentration was below 1,0 mg O_2/L and after day 9 the DO concentration started to increased up to an average value of 6,13 mg O_2/L corresponding to day 11. The overall average DO concentration value at the top of the packed bed biofilm was calculated as 1,08 ± 0,54 mg O_2/L. Moreover, in between days 0 to 9 the DO concentration measured in the collection tank varied in between 1,06 to 3,85 mg O_2/L and after day 9 it started to increase reaching a value of 6,54 mg O_2/L by day 11. The average DO concentration in the collection tank during the treatment period was equal to 3,36 mg O_2/L.

In general, at the top of the packed bed biofilm the DO concentrations were below the concentration of 2,7 mg O_2/L required for the AOB optimal growth and additionally the average concentration in the collection tank was below the suggested value of 5 mg O_2/L. Hence, oxygen limitations may have been present in the biofilm system.

The temperatures at the top of the column varied in between 20,6 to 21,9°C with an average temperature of 21,3 ± 0,1°C. In contrast to any of the other treatment processes the average temperature value of 21,5 °C corresponding to the collection tank was a little higher than the top column average value. This temperature difference can be related to the loss of heat from the bioreactor to the surroundings due to the colder ambient temperatures.

4.5.10. Operational conditions results summary

Some of the main operation conditions corresponding to each of the experimental practices are described in tables 34 and 35 for bioreactors 1 and 2 respectively.

Table 34. Operation conditions summary for each process in the SFBBR-1 system

Air flow rate (L/h)	Process	pH range	Aver. DO (mg O_2/L)		Aver. T (°C)		Total Acid capacity (mol H^+)
			TK	TC	TK	TC	
≈10,1	Batch No.1	7,5 - 8,3	-	4,41±0,37	22,0	22,6±0,4	2,9
	Batch No.2	7,5 - 8,6	8,00	6,36±1,09	22,6	23,4±0,3	2,5
	Batch No.3	7,5 - 8,5	-	9,49±0,52	21,6	22,6±0,1	2,5
1,5	Batch No.4	7,5 - 8,5	4,46	2,02±0,52	22,4	23,3±0,2	2,5
	Batch No.5	7,5 - 8,6	3,92	1,29±0,53	22,9	24,2±0,3	2,4
	Batch No.6	7,5 - 8,6	4,53	1,60±0,69	22,3	23,3±0,2	2,5
	Semi-batch	7,5 - 8,5	3,15	0,95	22,1	22,5	0,3-0,4

Table 35. Operation conditions summary for each process in the SFBBR-2 system

Air flow rate (L/h)	Process	pH range	Aver. DO (mg O_2/L)		Aver. T (°C)		Total Acid capacity (mol H^+)
			TK	TC	TK	TC	
9,0	Starting	6,6 - 9,2	5,43	4,52	21,9	22,1	-
	Batch	7,5 - 8,3	3,36	1,08±0,54	21,5	21,3	3,5

As indicated in tables 34 and 35, in general the pH values were maintained within ranges closed to the optimal reported pH value of 8,4 where maximum nitrification rate can be expected as illustrated in figure 36. Furthermore, it can be seen that all the processes ran in the SFBBR-1 system at the air flow rate of 1,5 L/h presented at the top of the packed bed biofilm DO concentration values lower than 2,7 mg O_2/L. As indicated in table 32 this concentration corresponds to the lowest oxygen concentration required for the AOB to growth at a specific growth rate equal to 90% the maximum growth rate. Additionally, the DO concentration measured in the collection tank for the same processes were less than the suggested DO concentration value of 5 mg O_2/L as discussed in section 2.8.1. On the other hand, for the processes ran in the same system with the flow rate of about 10,1 L/h the DO concentrations at the top the column and in the collection tank were for the most part greater than 5 mg

O_2/L. The larger concentration values may have contributed to reduce significantly the oxygen limitations in the biofilm system.

The total acid capacity of the system was relatively the same for those processes that treated the same amount of sludge water and in the case of the semi-batch process the daily acid capacity was relatively constant with values in between 0,3 to 0,4 mol H^+.

In general, for all the processes the temperatures in the collection tank were maintained at values around 22,0°C and for most of the processes the temperatures were slightly higher at the top of the packed bed biofilm. However, this temperature range is lower compared to the optimal nitrification temperature range of 30 to 37,5°C for a pH of 7,5 already described in section 2.8.3.

4.6. NITRIFICATION AND AMMONIUM CONSUMPTION RATES FOR THE DIFFERENT EXPERIMENTAL PROCESSES

4.6.1. Batch No. 1 in SFBBR-1

The concentrations of ammonium, nitrate and nitrite nitrogen were analyzed periodically during the process as described in the material and methods section.

The concentrations of ammonium and nitrate nitrogen were determined by using the relations obtained through their respective calibration curves given in appendix F and the nitrite-nitrogen concentration was determined by using the conversion factor.

The nitrogen species mass amount was determined based on the treated sludge water volume and the species concentration for the particular day. And, based on the calculated nitrogen species mass amount and the packed bed surface area a surface loading value (SLV) for the different nitrogen species was calculated during the process by using equation 18 for the batch case. Furthermore, in order to determine possible substrate inhibitions the concentrations of FA and FNA were estimated by using equations 34 and 35 respectively. In equation 34 the total ammonia was approximated to the respective ammonium-nitrogen concentration value.

The calculations performed for each nitrogen species corresponding to day 0 are described below. The raw data and all the calculated values are given in appendix G.

- Day 0: Ammonium-nitrogen calculation:

Absorbance= 0,3071
df = 3125
Packed bed SA = 1,0 m²

$$Calc.Conc._{NH_4^+\_N} = \frac{0{,}3071 - 0{,}0266}{0{,}9364} = 0{,}2996 \frac{mg\ NH_4^+\_N}{L}$$

$$Real, Conc._{NH_4^+\_N} = 0{,}2996\ \frac{mg\ NH_4^+\_N}{L} *\ 3125 =\ 936{,}20\ \frac{mg\ NH_4^+\_N}{L}$$

$$m_{NH_4^+\_N} =\ 936{,}20\ \frac{mg\ NH_4^+\_N}{L} * 24{,}0\ L = 22468{,}86\ mg\ NH_4^+\_N$$

$$B_{NH_4^+\_N} = \frac{22468{,}86\ mg\ NH_4^+\_N}{1{,}0\ m^2} =\ 22468{,}86\ \frac{mg\ NH_4^+\_N}{m^2}$$

- Day 0: Nitrate-nitrogen calculation:

Absorbance= 0,0432
df = 5
Packed bed SA = 1,0 m²

$$Calc.Conc._{NO_3^-\_N} = \frac{0{,}0432 - 0{,}0282}{0{,}0523} = 0{,}2868 \frac{mg\ NO_3^-\_N}{L}$$

$$Real, Conc._{NO_3^-\_N} = 0{,}2868\ \frac{mg\ NO_3^-\_N}{L} *\ 5 =\ 1{,}43\ \frac{mg\ NO_3^-\_N}{L}$$

$$m_{NO_3^-\_N} =\ 1{,}43\ \frac{mg\ NO_3^-\_N}{L} * 24{,}0\ L = 34{,}42\ mg\ NO_3^-\_N$$

$$B_{NO_3^-\_N} = \frac{34{,}42\ mg\ NO_3^-\_N}{1{,}0\ m^2} =\ 34{,}42\ \frac{mg\ NO_3^-\_N}{m^2}$$

- Day 0: Nitrite-nitrogen calculation:

Measured Conc. 1 = 1,6 mg NO_2/L
Measured Conc. 2 = 1,8 mg NO_2/L
df = 5
Conv. factor = 0,304
Packed bed SA = 1,0 m²

$$Conc._{NO_2^-} = \frac{1{,}6\ \frac{mg\ NO_2^-}{L} *\ 5 + 1{,}8\ \frac{mg\ NO_2^-}{L} *\ 5}{2} = 8{,}5\ \frac{mg\ NO_2^-}{L}$$

$$Conc._{NO_2^-\_N} = 8{,}5\ \frac{mg\ NO_2^-}{L} * \left| 0{,}304\ \frac{\frac{mg\ NO_2^-\_N}{L}}{\frac{mg\ NO_2^-}{L}} \right| = 2{,}6\ \frac{mg\ NO_2^-\_N}{L}$$

$$m_{NO_2^-\_N} = 2{,}6\ \frac{mg\ NO_2^-\_N}{L} * 24{,}0\ L = 62{,}0\ mg\ NO_2^-\_N$$

$$B_{NO_2^-\_N} = \frac{62{,}0\ mg\ NO_2^-\_N}{1{,}0\ m^2} = 62{,}0\ \frac{mg\ NO_2^-\_N}{m^2}$$

- Day 0: FA calculation:

$$FA = \frac{17}{14} * \frac{936{,}20\ \frac{mg\ NH_4^+\_N}{L} * 10^{8{,}1}}{e^{\left(\frac{6344}{273+20{,}0°C}\right)} + 10^{8{,}1}} = 53{,}9\ \frac{mg\ NH_3}{L}$$

- Day 0: FNA calculation:

$$FNA = \frac{46}{14} * \frac{2{,}6\ \frac{mg\ NO_2^-\_N}{L}}{e^{\left(\frac{-2300}{273+20{,}0°C}\right)} * 10^{8{,}1}} = 1{,}7 * 10^{-4}\ \frac{mg\ HNO_2}{L} \approx 0{,}0\ \frac{mg\ HNO_2}{L}$$

The results for the surface loading values corresponding to each of the nitrogen species obtained during the treatment period are given in figure 84.

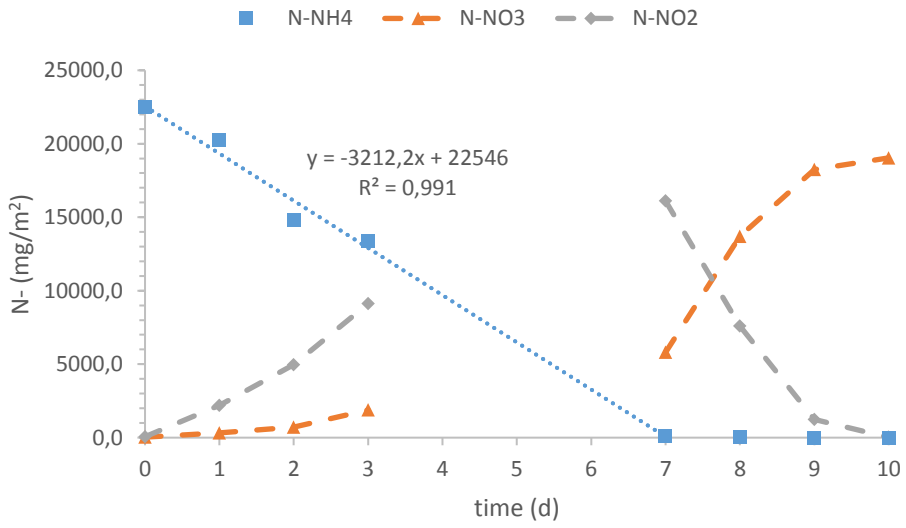

Figure 84. Nitrification and ACR during Batch No. 1 in SFBBR-1 system

The ammonium-nitrogen surface consumption rate (ACR) was estimated by applying a linear regression on the calculated ammonium-nitrogen surface loading values (SLV). The linear regression was performed by using Microsoft® Excel® 2013.

As seen in figure 84, ammonium oxidation took place approximately within the first 7,0 days of treatment and the ammonium data fits relatively well the linear model with a R-squared of 0,991. Hence, the approximated ACR for this process was estimated as 3212,2 mg NH_4^+-N/m^2·d at the working conditions summarized in tables 18 and 34.

As described in equation 1, the oxidation of ammonium leads to the generation of 2 moles of hydrogen ions and since the pH controller was set at 7,5 then by comparing figures 84 and 65 it can be seen that the consumption of the 0,7 M K_2CO_3 solution took place within the period where the oxidation of ammonium was taken place and basically ending on day 7 when the ammonium concentration was very low with a value of 4,88 mg NH_4^+-N/L.

Furthermore, by comparing figures 66 and 84 a decreased in the DO concentration was observed within the period where nitrification was taking place. For instance, the DO concentration decreased from 7,46 mg O_2/L on day 0 to 4,07 mg O_2/L on day 1 and in between days 1 to 9 the DO concentrations were below 5,0 mg O_2/L which corresponded to the same days where ammonium and nitrite were being consumed by the nitrifiers in the biofilm system.

The nitrification process during batch No. 1 seems to resemble more the schematic corresponding to a typical non-inhibited nitrification process presented in figure 33. However, as illustrated in figure 84 during the first days of treatment the nitrite generation was so much greater than the nitrate one. For instance, at day 3 the concentration of nitrate was equal to 79,59 mg NO_3^--N/L while the concentration of nitrite was estimated as 385,7 mg NO_2^--N/L corresponding to almost 40% of the initial ammonium nitrogen concentration of 936,20 mg NH_4^+-N/L. These results suggests that a partial accumulation of nitrite was taken place in the system while ammonium was being oxidized.

The results for the calculated concentrations of FA and FNA obtained during the treatment period are given in figure 85.

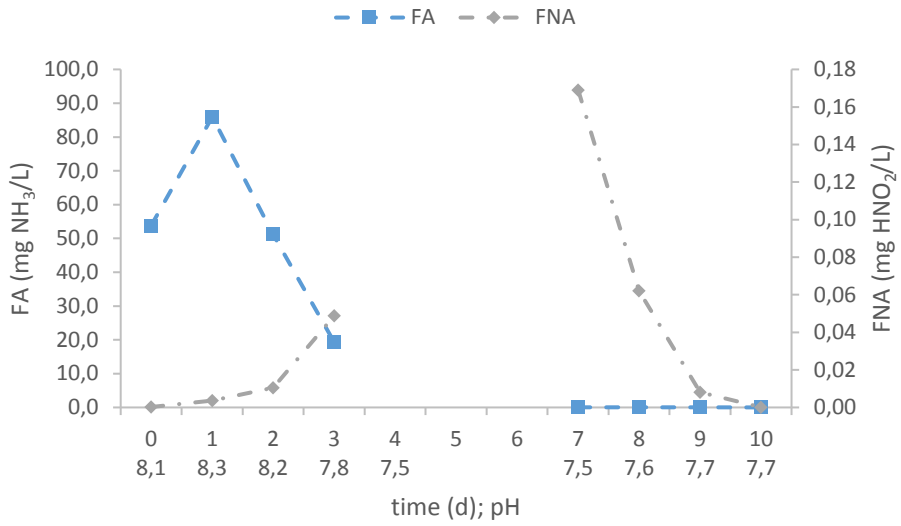

Figure 85. FA and FNA Conc. during Batch No. 1 in SFBBR-1 system

As already mentioned in section 2.8.1, the un-ionized forms of ammonium and nitrite are ammonia (NH_3) and nitrous acid (HNO_2) respectively and depending on their concentrations these species may lead to inhibitory effects in the nitrification process.

As seen in figure 85, during the process the FNA concentrations were below 0,18 mg HNO_2/L. This means that inhibitory effects on nitrifying microorganisms due to the presence of FNA were not considerable since all of the calculated FNA values were below the reported concentration of 0,2 mg HNO_2/L where inhibitory effects start to take place for NOB. Additionally, during the first 3 days of treatment the FA concentrations were approximately in between 19,3 to 86,0 mg NH_3/L, these values are greater than the reported limiting inhibitory concentrations of 10 mg NH_3/L and 0,1 mg NH_3/L for AOB and NOB respectively.

At the end of the process the amount of nitrate-nitrogen generated represented approximately 85,0% of the converted ammonium-nitrogen and a total ammonium consumption of 99,9%. The calculations for the nitrification and ammonium consumption percentages are described below. The ammonium-nitrogen concentration for the last two days of treatment corresponded to the average concentration value between these two days.

$$Conv.NH_4^+\_N = 22468{,}86\ mg\ NH_4^+\_N - 4{,}79\ mg\ NH_4^+\_N = 22464{,}07 mg\ NH_4^+\_N$$

$$Gener.NO_3^-\_N = 19038{,}43\ mg\ NO_3^-\_N - 34{,}42\ mg\ NO_3^-\_N = 19004{,}01\ mg\ NO_3^-\_N$$

$$Nitrification\ \% = \frac{19004{,}01\ mg\ NO_3^-\_N}{22464{,}07 mg\ NH_4^+\_N} * 100\% = 84{,}6\ \%$$

$$AC\ (\%) = \frac{22464{,}07 mg\ NH_4^+\_N}{22468{,}86\ mg\ \ NH_4^+\_N} * 100 = 99{,}9\ \%$$

Finally, based on the nitrification percentage, the ammonium-nitrogen converted value and equation 1, the moles of hydrogen ion generated during the process were estimated. The calculations are described below.

Conv. factor = 0,776

$$n_{NH_4^+\_N} = 19004{,}01\ mg\ NH_4^+\_N \left|\frac{1\ mmol\ N}{14\ mg\ N}\right| \left|\frac{1\ mol}{1000\ mmol}\right| = 1{,}35\ mol\ NH_4^+\_N$$

$$n_{H^+} = 1{,}4\ mol\ NH_4^+\_N \left|\frac{2\ mol\ H^+}{1\ mol\ NH_4^+\_N}\right| = 2{,}71\ mol\ H^+$$

The estimated value of 2,71 mol H^+ generated during the nitrification process was relatively closed to the acid capacity of the system with a value of 2,9 mol H^+ as indicated in table 34. The relatively higher acid capacity of the system was due to the response time of the pH controller which ended in a slightly over dosing of the 0,7 M K_2CO_3 solution and it explains the observed increase in pH from the set value of 7.5 to a value of 7,7 by the end of the treatment process.

4.6.2. Batch No. 2 in SFBBR-1

The nitrogen species concentrations, surface loading values (SLV) and the ammonium-nitrogen surface consumption rate (ACR) were calculated in the same way as previously described in the batch No. 1 section.

The raw data and all the calculated values are given in appendix G.

The results for the surface loading values corresponding to each of the nitrogen species obtained during the treatment period are given in figure 86.

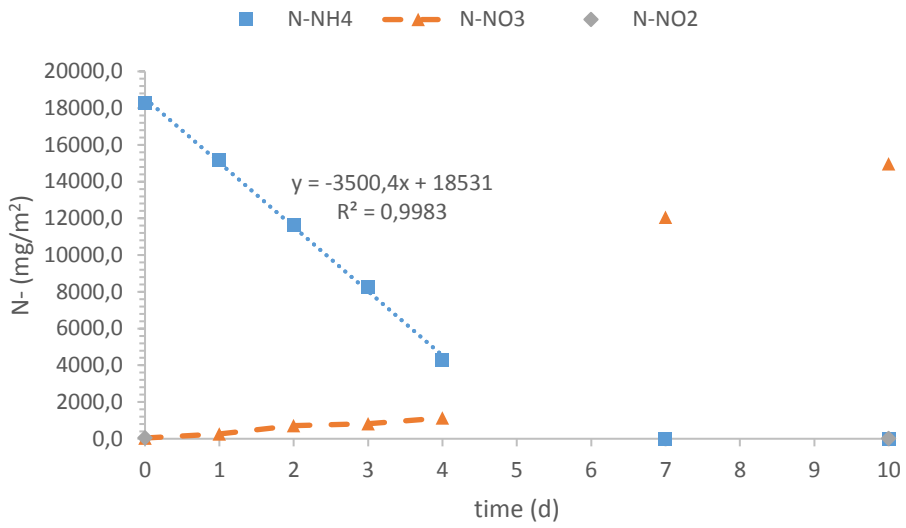

Figure 86. Nitrification and ACR during Batch No. 2 in SFBBR-1 system

As seen in figure 86, by extrapolation of the linear model ammonium oxidation took place approximately within the first 5,2 days of treatment and the ammonium data fits relatively well the linear model with a R-squared of 0,9983. For that reason, the approximated ACR for this process was estimated as 3500,4 mg NH_4^+-N/m^2·d at the working conditions summarized in tables 18 and 34.

As in the case of batch No. 1, by looking at figures 68 and 86 it can be seen that the consumption of the 0,7 M K_2CO_3 solution took place within the same period where the oxidation of ammonium took place and ended on day 7 where the ammonium concentration was already at the lowest point with an average value of 0,20 mg NH_4^+-N/L.

Furthermore, by comparing figures 69 and 86 it can be seen that a decrease in the DO concentration was observed within the period where ammonium oxidation was taking place. As described in equations 1 and 2, the oxidation of ammonium consumes 3 times more oxygen than the oxidation of nitrite, this fact explains the gradual increase in the DO concentrations after most of the ammonium present in the sludge water was consumed by the microorganisms.

Due to the fact that the nitrite concentration was only measured at the beginning and final days of the process, a comparison with figures 33 and 34 was not possible. However, as already discussed in Batch No. 1 the oxidation of nitrite was limited during

the first days of treatment and nitrate generation started to considerable increase only after a low ammonium concentration value was reached.

The results for the calculated concentrations of FA and FNA obtained during the treatment period are given in figure 87.

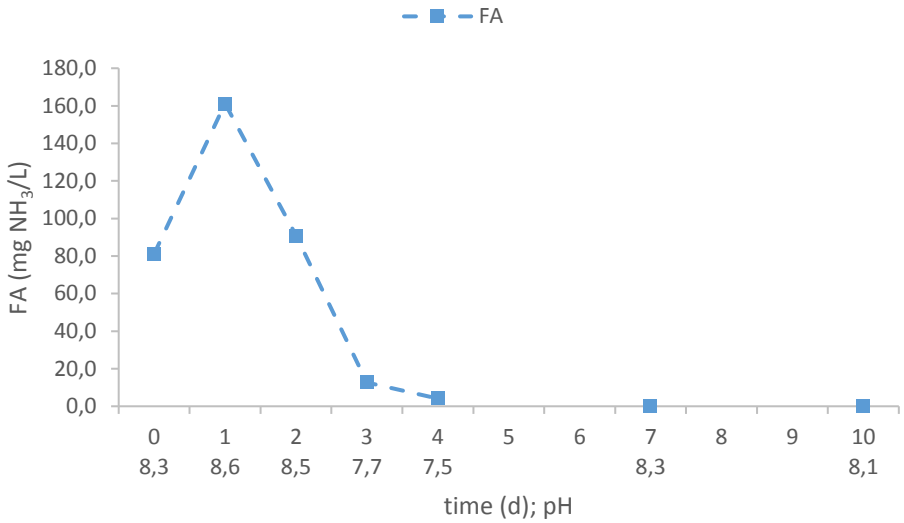

Figure 87. FA and FNA Conc. during Batch No. 2 in SFBBR-1 system

For this process the FNA concentration profile was not obtained considering that the nitrite concentration in the system was only monitored at the first and last days of the treatment.

Figure 87 shows that in between days 0 to 4 the FA concentration ranged in between 4,1 to 161,2 mg NH_3/L. These values are way above the limiting inhibitory concentration value of 0,1 mg NH_3/L for NOB and during the first three days the FA concentrations were higher than the limiting inhibitory concentration value of 10 mg NH_3/L for AOB.

The nitrification and total ammonium consumption percentages and the H^+ moles generated during the nitrification process were calculated in the same way as already described in Batch No. 1 with values of 81,6%, 99,9% and 2,13 mol H^+ respectively. The same situation as batch No. 1 was observed, in which the generated H^+ moles were lower than the acid capacity of the system with a value of 2,5 mol H^+ as indicated in table 34. This explains the increased in pH from 7,5 to a final value of 8,1 by the end of the process.

The ammonium-nitrogen concentration for days 7 and 10 corresponded to the average concentration value between these two days.

4.6.3. Batch No. 3 in SFBBR-1

The nitrogen species concentrations, surface loading values (SLV) and the ammonium-nitrogen surface consumption rate (ACR) were calculated in the same way as previously described in the batch No. 1 section.

The raw data and all the calculated values are given in appendix G.

The results for the surface loading values corresponding to each of the nitrogen species obtained during the treatment period are given in figure 88.

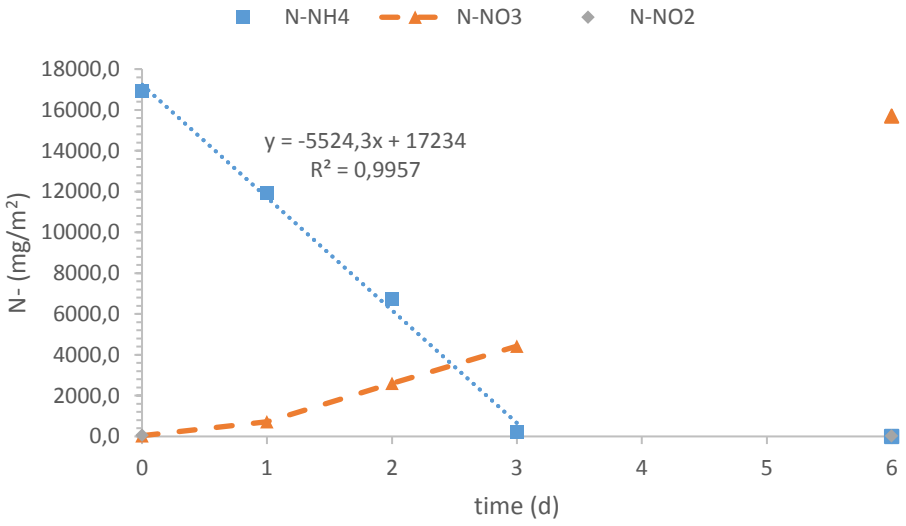

Figure 88. Nitrification and ACR during Batch No. 3 in SFBBR-1 system

As seen in figure 88, ammonium oxidation took place approximately within the first 3,0 days of treatment and the ammonium data fits relatively well the linear model with a R-squared of 0,9957. Thus, the approximated ACR for this process was estimated as 5524,3 mg NH_4^+-N/m^2·d at the working conditions summarized in tables 18 and 34.

The comparison between figures 70 and 88 shows that the 0,7 M K_2CO_3 solution was consumed in between days 2 and 3 which corresponded to the period in which ammonium oxidation took place with a concentration of 10,87 mg NH_4^+-N/L for day 3.

Furthermore, when comparing figures 71 and 88 it can be seen that the DO concentration trend observed in batches No. 1 and 2 consisting of a decreased in DO concentration during the ammonium oxidation and then the gradual increase in DO concentration after oxidation of ammonium was not observed in batch No. 3, but rather

over saturated DO concentrations were registered during the treatment process as already discussed in the operational conditions section for to this treatment process.

The concentration of nitrite was measured at the first and last days of treatment. Thus, a comparison with figures 33 and 34 was not possible. However, as seen in figure 88 the same partial nitrite accumulation most likely took place during the process considering that by day 3 when the ammonium was almost depleted only about 26,3% of the consumed ammonium was converted to nitrate despite the greater growth rate of the NOB at the temperature conditions.

The results for the calculated concentrations of FA and FNA obtained during the treatment period are given in figure 89. The values were calculated as described in batch No. 1.

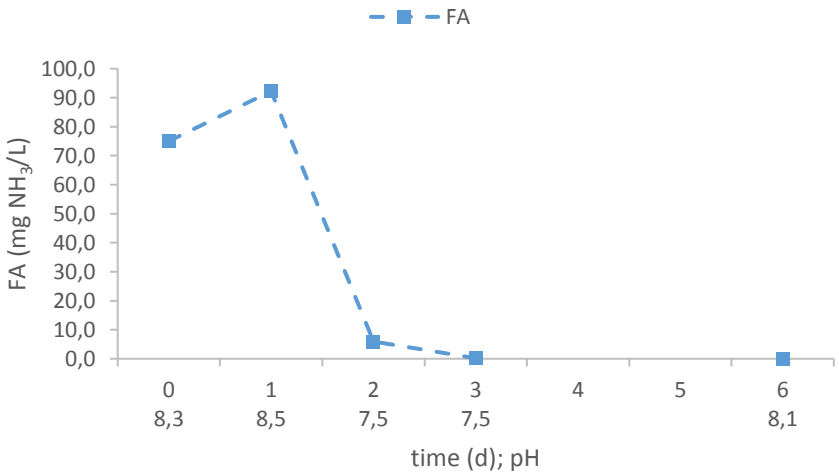

Figure 89. FA and FNA Conc. during Batch No. 3 in SFBBR-1 system

For this process the FNA concentration profile was not obtained considering that the nitrite concentration in the system was only monitored at the first and last days of the treatment period.

As seen in figure 88 and as it was the case for batches No. 1 and 2, on day 1 even though the concentration of ammonium was decreasing due to the increased in the pH, the FA concentration increased in the system to a value of 92,3 mg NH_3/L but as the pH value and the ammonium concentration were decreasing so did the FA concentration until reaching a value of 0,0 mg NH_3/L by the last day of treatment.

Furthermore, a possible FA inhibition took place within the first 3 days of treatment being more pronounced in between days 0 to 1 where the FA reached its maximum value. In general, the calculated FA values ranging in between 0,0 to 92,3 mg NH_3/L

are found to be within the FA reported limiting inhibitory concentrations of 10 mg NH_3/L and 0,1 mg NH_3/L for AOB and NOB respectively.

The nitrification and total ammonium consumption percentages and the H^+ moles generated during the nitrification process were calculated in the same way as already described in Batch No. 1 with values of 92,6%, 99,9% and 2,24 mol H^+ respectively. The same situation as the previous batches was observed, in which the generated H^+ moles were lower than the acid capacity of the system with a value of 2,5 mol H^+ as indicated in table 34. This explains the increased in pH from 7,5 to a final value of 8,1 by the end of the treatment process.

4.6.4. Batch No. 4 in SFBBR-1

The nitrogen species concentrations, surface loading values (SLV) and the ammonium-nitrogen surface consumption rate (ACR) were calculated in the same way as previously described in the batch No. 1 section.

The raw data and all the calculated values are given in appendix G.

The results for the surface loading values corresponding to each of the nitrogen species obtained during the treatment period are given in figure 90.

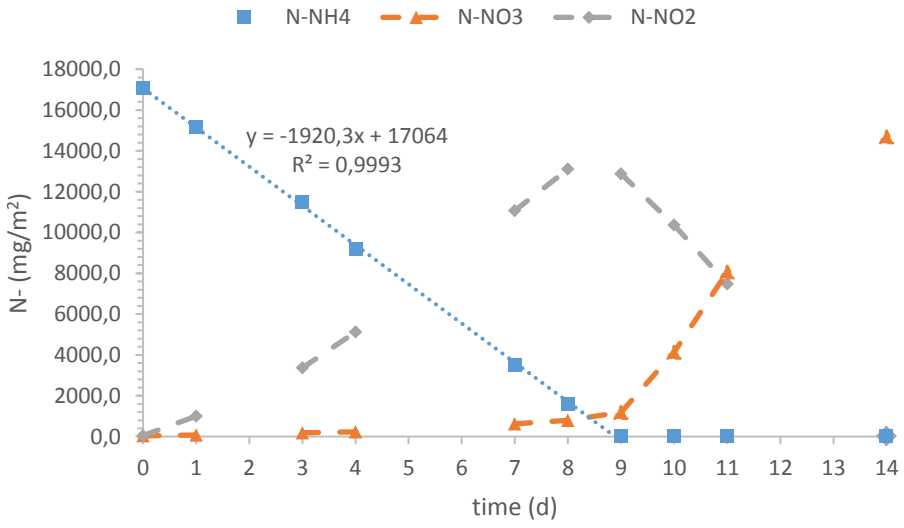

Figure 90. Nitrification and ACR during Batch No. 4 in SFBBR-1 system

As seen in figure 90, ammonium oxidation took place approximately within the first 9,0 days of treatment at which the ammonium concentration was already at 1,04 mg NH_4^+-N/L. Furthermore, the ammonium data fits relatively well the linear model with a R-squared of 0,9993, thus the approximated ACR for this process was estimated as 1920,3 mg NH_4^+-N/m^2·d at the working conditions summarized in tables 18 and 34.

The comparison between figures 72 and 90 shows that the consumption of the 0,7 M K_2CO_3 solution matches the ammonium oxidation period during the treatment process. Additionally, the comparison between figures 73 and 90 shows a sharp decreased in the DO concentration at the top of the packed bed biofilm for most of the ammonium oxidation period. During this period the DO concentration at the top of the packed bed biofilm decreased from 3,84 mg O_2/L for day 0 to values smaller than 1,0 mg O_2/L for days 3 through 7 and after day 7 for the most part the gradual increase in the DO concentration was observed. The same trend was registered for the DO concentration at the collection tank but at higher values as indicated in the operational condition section for Batch No. 4.

Moreover, figure 90 shows that the nitrification process seems to resemble more the schematic corresponding to a typical non-inhibited nitrification process presented in figure 33. However, as was the case for batch No. 1 it seem that a partial accumulation of nitrite was taking place. For instance, in between days 0 to 9 the nitrate concentration was very low, and only reached a concentration value of 60,04 mg NO_3^--N/L for day 9 while the concentration of nitrite was measured as 651,7 mg NO_2^--N/L for the same day. After day 9, nitrite oxidation started to be important and by day 14 the nitrate concentration was measured as 764,58 mg NO_3^--N/L.

The results for the calculated concentrations of FA and FNA obtained during the treatment period are given in figure 91. The values were calculated as described in batch No. 1

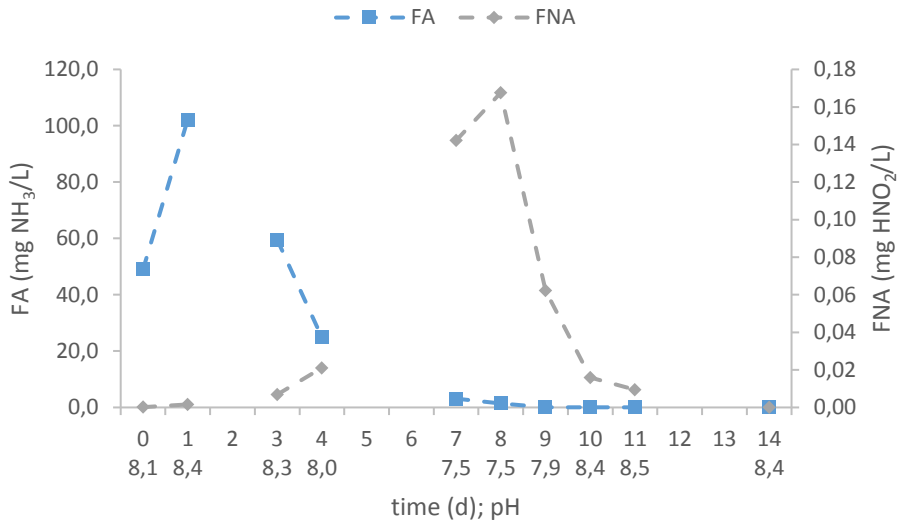

Figure 91. FA and FNA Conc. during Batch No. 4 in SFBBR-1 system

As seen in figure 91, due to the relatively higher pH value of 8,4 the FA concentration reached a value of 102,1 mg NH_3/L at day 1. After day 1, the FA decreased to values of 0,1 and 0,0 mg NH_3/L for days 9 and 10 respectively. In general, the calculated FA values ranging in between 0,0 to 102,1 mg NH_3/L were found to be within the FA reported limiting inhibitory concentrations of 10 mg NH_3/L and 0,1 mg NH_3/L for AOB and NOB respectively. Moreover, during the process the FNA concentrations were below 0,18 mg HNO_2/L. This means that the inhibitory effects on the NOB due to high FNA concentrations were minimum considering that all of the calculated FNA values were below the reported concentration of 0,2 mg HNO_2/L where inhibitory effects start to take place.

The nitrification and total ammonium consumption percentages and the H^+ moles generated during the nitrification process were calculated in the same way as already described in Batch No. 1 with values of 85,9%, 99,9% and 2,09 mol H^+ respectively. The same situation as the previous batches was observed, in which the generated H^+ moles were lower than the acid capacity of the system with a value of 2,5 mol H^+ as indicated in table 34. This explains the increased in pH from 7,5 to a final value of 8,4 by the end of the treatment process.

4.6.5. Batch No. 5 in SFBBR-1

The nitrogen species concentrations, surface loading values (SLV) and the ammonium-nitrogen surface consumption rate (ACR) were calculated in the same way as previously described in the batch No. 1 section.

The raw data and all the calculated values are given in appendix G.

The results for the surface loading values corresponding to each of the nitrogen species obtained during the treatment period are given in figure 92.

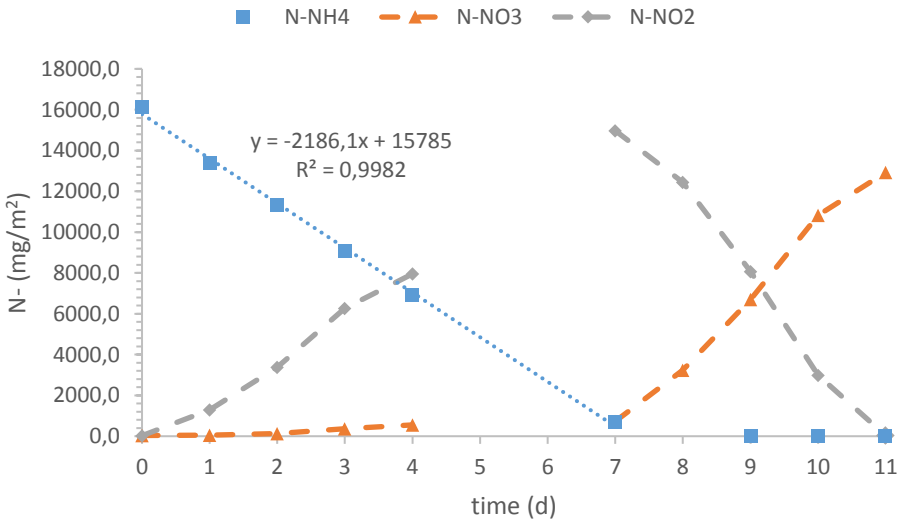

Figure 92. Nitrification and ACR during Batch No. 5 in SFBBR-1 system

As seen in figure 92, based on the linear extrapolation, ammonium oxidation took place approximately within the first 7,3 days of treatment and the ammonium data fits relatively well the linear model with a R-squared of 0,9982, thus the approximated ACR for this process was estimated as 2186,1 mg NH_4^+-N/m^2·d at the working conditions summarized in tables 18 and 34.

The comparison between figures 74 and 92 shows that the consumption of the 0,7 M K_2CO_3 solution took place within the period of ammonium oxidation and ended at day 8. Furthermore, after comparing figures 75 and 92 it can be seeing that during the whole ammonium oxidation period the DO concentration at the top the packed bed biofilm was below 1,0 mg O_2/L and after day 7 the gradual increase in the DO concentration was observed until reaching a value of 6,1 mg O_2/L at the end of the process.

As was the case for batch No. 4, figure 92 resembles figure 33 which corresponds to the schematic for a typical non-inhibited nitrification process. However, and as previously discussed the same partial accumulation of nitrite is observed and its oxidation starts to considerably take place after the ammonium has been almost consumed which corresponded to a high nitrite concentration point. For instance, at day 4 the concentration of nitrate was only 28,61 mg NO_3^--N/L and at the same day the nitrite concentration had already reach an approximate value of 414,2 mg NO_2^--N/L which corresponded to almost 50% of the initial ammonium-nitrogen concentration of 808,28 mg NH_4^+-N/L. After day 7, nitrate generation started to be significant until reaching a concentration value of 692,88 mg NO_3^--N/L at day 11.

The results for the calculated concentrations of FA and FNA obtained during the treatment period are given in figure 93. The values were calculated as described in batch No. 1

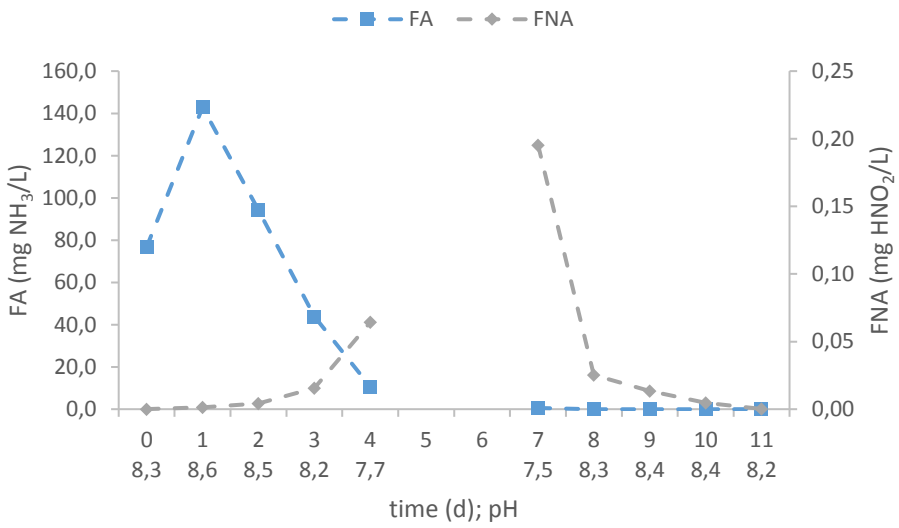

Figure 93. FA and FNA Conc. during Batch No. 5 in SFBBR-1 system

As seen in figure 93, at day 1 the FA concentration reached a value of 142,9 mg NH_3/L, the reason of this was the relatively high pH and ammonium concentration values of 8,6 and 676,79 mg NH_4^+-N/L respectively. After day 1 the FA concentration decreased with the decreased of ammonium until reaching a value of 0,0 mg NH_3/L by day 8. In general, the calculated FA values ranging in between 0,0 to 142,9 mg NH_3/L were found to be within the FA reported limiting inhibitory concentrations of 10 mg NH_3/L and 0,1 mg NH_3/L for AOB and NOB respectively. Additionally, during the process the FNA concentration values were in between the range of 0,0 to 0,20 mg HNO_2/L and

they were below the reported concentration of 0,2 mg HNO_2/L where inhibitory effects start to take place for NOB.

The nitrification and total ammonium consumption percentages and the H^+ moles generated during the nitrification process were calculated in the same way as already described in Batch No. 1 with values of 79,8%, 99,9% and 1,84 mol H^+ respectively. The same situation as the previous batches was observed, in which the generated H^+ moles were lower than the acid capacity of the system with a value of 2,4 mol H^+ as indicated in table 34. This explains the increased in pH from 7,5 to a final value of 8,2 by the end of the treatment process.

4.6.6. Batch No. 6 in SFBBR-1

The nitrogen species concentrations, surface loading values (SLV) and the ammonium-nitrogen surface consumption rate (ACR) were calculated in the same way as previously described in the batch No. 1 section.

The raw data and all the calculated values are given in appendix G.

The results for the surface loading values corresponding to each of the nitrogen species obtained during the treatment period are given in figure 94.

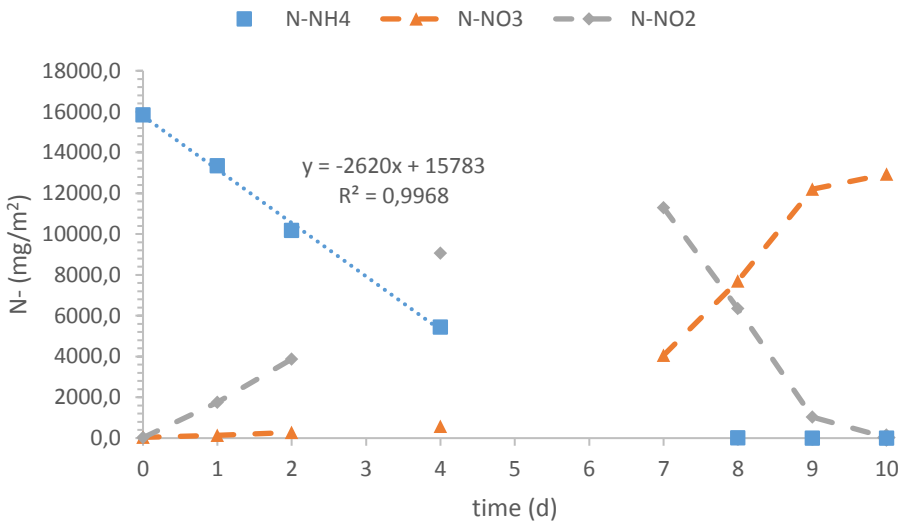

Figure 94. Nitrification and ACR during Batch No. 6 in SFBBR-1 system

As seen in figure 94, based on the linear extrapolation ammonium oxidation took place approximately within the first 6,0 days of treatment and the ammonium data fits relatively well the linear model with a R-squared of 0,9968, thus the approximated

ACR for this process was estimated as 2620,0 mg NH_4^+-N/m^2·d at the working conditions summarized in tables 18 and 34.

The comparison between figures 76 and 94 shows that the consumption of the 0,7 M K_2CO_3 solution took place within the period of ammonium oxidation. Furthermore, after comparing figures 77 and 94 it can be seeing that during the whole ammonium oxidation period the DO concentration at the top the packed bed biofilm was below 1,0 mg O_2/L and after day 6 a gradual increase in the DO concentration was observed until reaching a value of almost 7,0 mg O_2/L at the end of the process.

Figure 94 resembles figure 33 which corresponds to the schematic for a typical non-inhibited nitrification process. However, the same apparent nitrite accumulation observed in the previous processes also took place during this treatment process where the oxidation of nitrite started to be important after almost all of the ammonium was consumed. For instance, at day 4 the concentration of nitrate was only 29,63 mg NO_3^--N/L and at the same day the nitrite concentration had already reached an approximated value of 471,2 mg NO_2^--N/L which corresponded to almost 60% of the initial ammonium-nitrogen concentration of 791,60 mg NH_4^+-N/L. After day 6, nitrate generation started to be significant until reaching a concentration value of 689,77 mg NO_3^--N/L at day 10.

The results for the calculated concentrations of FA and FNA obtained during the treatment period are given in figure 95. The values were calculated as described in the batch No. 1 section.

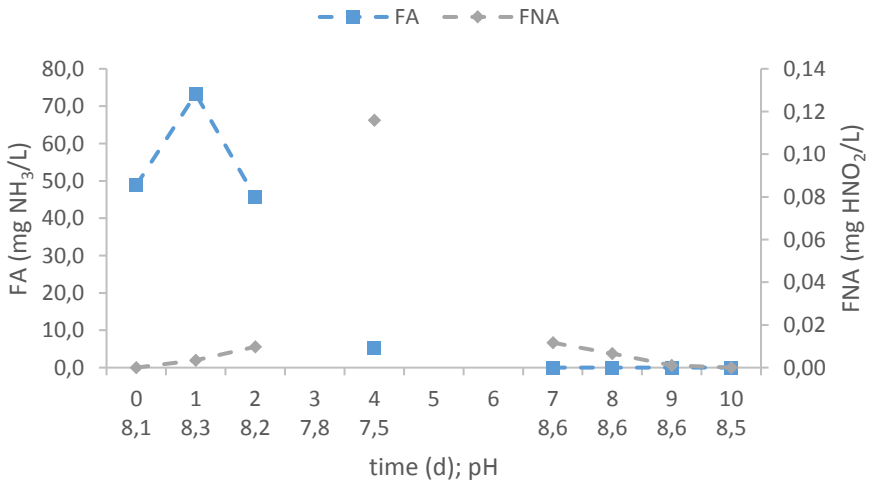

Figure 95. FA and FNA Conc. during Batch No. 6 in SFBBR-1 system

As seen in figure 95, the maximum FA concentration value was reached at day 1 with a value of 73,3 mg NH_3/L and it varied during the process within values ranging in between 0,0 to 73,3 mg NH_3/L. In general, during the first 3 days of treatment the FA concentration values were within the FA reported limiting inhibitory concentrations of 10 mg NH_3/L and 0,1 mg NH_3/L for AOB and NOB respectively. Moreover, the maximum FNA concentration value was estimated as 0,12 mg HNO_2/L. This means that in general, the FNA concentration values were below the reported concentration of 0,2 mg HNO_2/L where inhibitory effects start to take place for NOB.

The nitrification and total ammonium consumption percentages and the H^+ moles generated during the nitrification process were calculated in the same way as already described in Batch No. 1 with values of 81,5%, 99,9% and 1,84 mol H^+ respectively. The same situation as the previous batches was observed, in which the generated H^+ moles were lower than the acid capacity of the system with a value of 2,5 mol H^+ as indicated in table 34. This explains the increased in pH from 7,5 to a final value of 8,5 by the end of the treatment process.

4.6.7. Semi-Batch operation in SFBBR-1

The nitrogen species concentrations, surface loading values (SLV) and the ammonium-nitrogen surface consumption rate (ACR) were calculated in a similar way as previously described in the batch No. 1 section. However, during the semi-batch period the calculations were performed before and after the renewal of the sludge water and they were based on the mass balance corresponding to each treatment day.

The calculations performed for ammonium at day 8 are described below. The concentrations of the nitrogen species corresponding to the added SW were measured twice a week, based on these values weekly average concentrations for each of the nitrogen species were obtained and used during the calculations for the days within the corresponding week. The liquid volumes in the system were assumed to be constant during the same day and for the weekends the SW renewed volume of 9,0 L was used instead of 3,0 L. The ACR calculated for each of the two weekends was divided by 3 in order to get an average value for each day within that treatment period.

The raw data and the calculated values are given in appendix K.

- Day 8: Ammonium-nitrogen calculation:

Day 7: added SW Conc. = 821,34 mg NH_4^+-N/L

Day 11: added SW Conc. = 818,35 mg NH_4^+-N/L

Day 7: Treated SW Conc. after renewal = 129,26 mg NH_4^+-N/L

Day 8: Treated SW Conc. before renewal = 3,82 mg NH_4^+-N/L

Day 7: Vol. treated SW in the system = 19,1 L

Day 8: Vol. SW renewed = 3,0 L

Day 8: Vol. treated SW in the system = 19,0 L

Packed bed SA = 1,0 m^2

$$Aver.Add.SW_{Conc.day\ 8-10} = \frac{821{,}34\,\frac{mg\ NH_4^+\_N}{L} + 818{,}35\,\frac{mg\ NH_4^+\_N}{L}}{2} = 819{,}84\,\frac{mg\ NH_4^+\_N}{L}$$

$$m_{NH_4^+\_N,renewed\_SW,day\ 8} = 819{,}84\ \frac{mg\ NH_4^+\_N}{L} * 3{,}0\ L = 2459{,}53\ mg\ NH_4^+\_N$$

$$m_{NH_4^+\_N,treated\_SW,remained,day\ 8} = 3{,}82\ \frac{mg\ NH_4^+\_N}{L} *\ \ (19{,}0\ L - 3{,}0\ L) = 61{,}27\ mg\ NH_4^+\_N$$

$$m_{NH_4^+\_N,treated\_SW,day\ 8,after} = 2459{,}53\ mg\ NH_4^+\_N + 61{,}27\ mg\ NH_4^+\_N = 2520{,}79\ \ mg\ NH_4^+\_N$$

$$Conc._{,treated\_SW,day\ 8,after} = \frac{2520{,}79\ \ mg\ NH_4^+\_N}{19{,}0\ L} = 132{,}46\ \frac{mg\ NH_4^+\_N}{L}$$

$$B_{NH_4^+\_N,treated\_SW,day\ 8,after} = \frac{2520{,}79\ \ mg\ NH_4^+\_N}{1{,}0\ m^2} =\ \ 2520{,}79\ \frac{mg\ NH_4^+\_N}{m^2}$$

$$m_{NH_4^+\_N,treated\_SW,day\ 7,after} =\ \ 129{,}26\ \frac{mg\ NH_4^+\_N}{L} *\ 19{,}1\ L = 2468{,}88\ mg\ NH_4^+\_N$$

$$B_{NH_4^+\_N,treated\_SW,day\ 7,after} = \frac{2468{,}88\ \ mg\ NH_4^+\_N}{1{,}0\ m^2} =\ \ 2468{,}88\,\frac{mg\ NH_4^+\_N}{m^2}$$

$$m_{NH_4^+\_N,treated\_SW,day\ 8,before} =\ \ 3{,}82\ \ \frac{mg\ NH_4^+\_N}{L} *\ \ 19{,}0\ L = 72{,}73\ mg\ NH_4^+\_N$$

$$B_{NH_4^+\_N,treated\_SW,day\ 8,before} = \frac{72{,}73\ \ mg\ NH_4^+\_N}{1{,}0\ m^2} =\ \ 72{,}73\ \frac{mg\ NH_4^+\_N}{m^2}$$

$$\Delta B_{NH_4^+\_N,treated\_SW,day\ 7-8} = 72{,}73\,\frac{mg\ NH_4^+\_N}{m^2} - 2468{,}88\,\frac{mg\ NH_4^+\_N}{m^2} = -2396{,}14\,\frac{mg\ NH_4^+\_N}{m^2}$$

$$ACR_{day\ 7-8} = \frac{2396{,}14\,\frac{mg\ NH_4^+\_N}{m^2}}{1\ d} = 2396{,}14\ \frac{mg\ NH_4^+\_N}{m^2.d}$$

$$AC\ (\%) = \frac{(2468{,}88\ mg\ NH_4^+\_N\ - 72{,}73\ mg\ NH_4^+\_N)}{2468{,}88\ mg\ NH_4^+\_N} * 100 = 97{,}1\ \%$$

The volume of 3,0 L of sludge water used during the semi-batch treatment was calculated based on the ACR observed during the batch period as illustrated in figure 96. For the calculation an average sludge water concentration value was used which was calculated based on the initial concentrations values corresponding to batches 1 through 6 and including the initial value of this treatment process as described in table 36.

The calculations are shown below.

Table 36. SW initial concentrations corresponding to different processes

Process	SW initial Conc. (mg NH_4^+-N/L)
Batch No. 1	936,20
Batch No. 2	915,07
Batch No. 3	845,33
Batch No. 4	852,84
Batch No. 5	808,28
Batch No. 6	791,60
Semi-batch initial Conc.	812,15
Aver.	851,64

$$Vol._{SW} = \frac{2975{,}9\ \frac{mg\ NH_4^+\_N}{m^2} * 1\ m^2}{851{,}64\ \frac{mg\ NH_4^+\_N}{L}} = 3{,}5\ L$$

The calculated sludge water volume of 3,5 L was an approximation, thus a sludge water volume of 3,0 L was chosen to be used during the semi-batch period.

The results for the surface loading values corresponding to each of the nitrogen species obtained during the treatment period are given in figure 96.

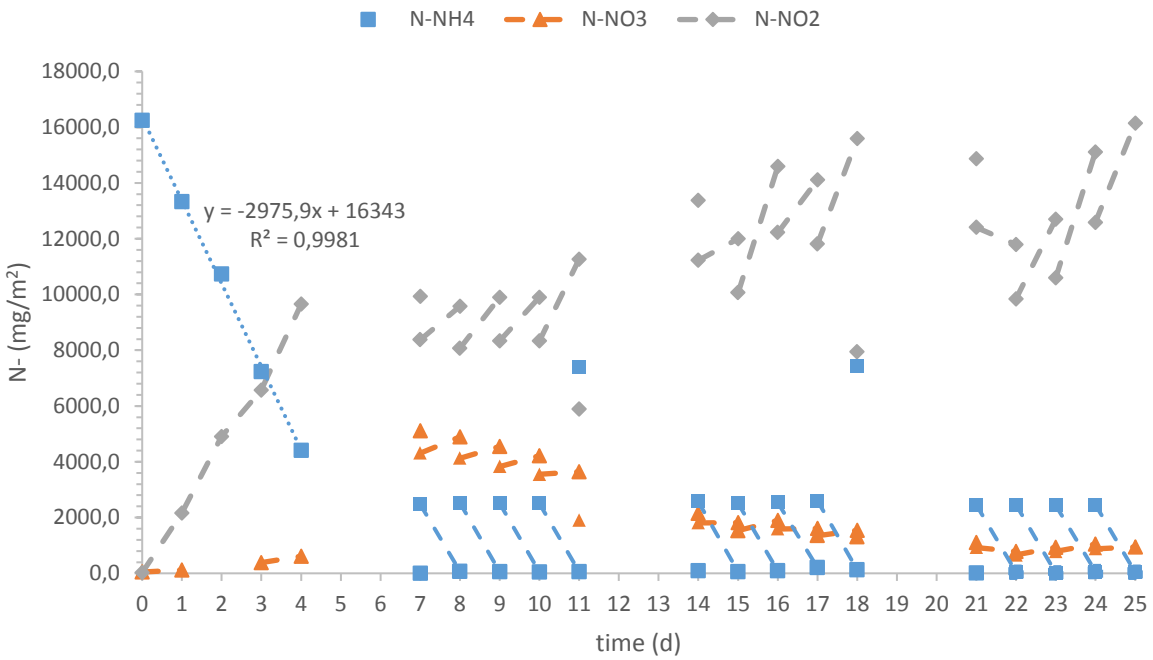

Figure 96. Nitrification during the semi-batch process in SFBBR-1 system

As seen in figure 96, based on the linear extrapolation during the batch period the ammonium oxidation took place approximately within the first 5,5 days of treatment and the ammonium data fits relatively well the linear model with a R-squared of 0,9981. Thus, the approximated ACR for this period was estimated as 2975,9 mg NH_4^+-N/m^2·d at the working conditions summarized in tables 19 and 34.

After comparing figures 78 and 96 it was seen that the consumption of the 0,9 M Na_2CO_3 solution took place all along the treatment process and was in agreement with the ammonium oxidation periods as discussed in the operational conditions section.

Furthermore, after comparing figures 79 and 96 it was seeing that within the first 5 days of the batch treatment the DO concentrations at the top of the packed bed biofilm were below 1,0 mg O_2/L which also corresponded to the ammonium oxidation period. Additionally, in general during the semi-batch stages after the sludge water was renewed the DO concentrations dropped to values below 1,0 mg O_2/L and then gradually increased by the next day to values greater than 1,0 mg O_2/L before the new renewal took place.

Moreover, the same partial nitrite accumulation observed in all other batch processes also occurred during the batch period. For instance, at day 4 the nitrite concentration was estimated as 501,6 mg NO_2^--N/L which corresponded to almost 60% of the initial ammonium concentration of 812,15 mg NH_4^+-N/L but the nitrate concentration was

only equal to 31,68 mg NO_3^--N/L. At day 7, before the renewal took place the nitrate concentration had increased to an approximate value of 267,88 mg NO_3^--N/L but a gradual decrease on the nitrate concentration was observed as the semi-batch process continued until reaching a concentration of 53,15 mg NO_3^--N/L by the last day of treatment. However, as indicated in figure 96 by the last week of treatment the nitrate concentrations were relatively constant with values ranging in between 36,21 to 58,70 mg NO_3^--N/L. On the other hand, as the semi-batch process continued a gradual nitrite accumulation took place since the nitrite concentration increased more than twice the value from 438,4 mg NO_2^--N/L at day 7 up to 904,4 mg NO_2^--N/L by day 25.

The results for the calculated concentrations of FA and FNA obtained during the treatment period are given in figure 97. The values were calculated as described in the batch No. 1 section and by using the nitrogen species concentrations calculated during the semi-bath period treatment.

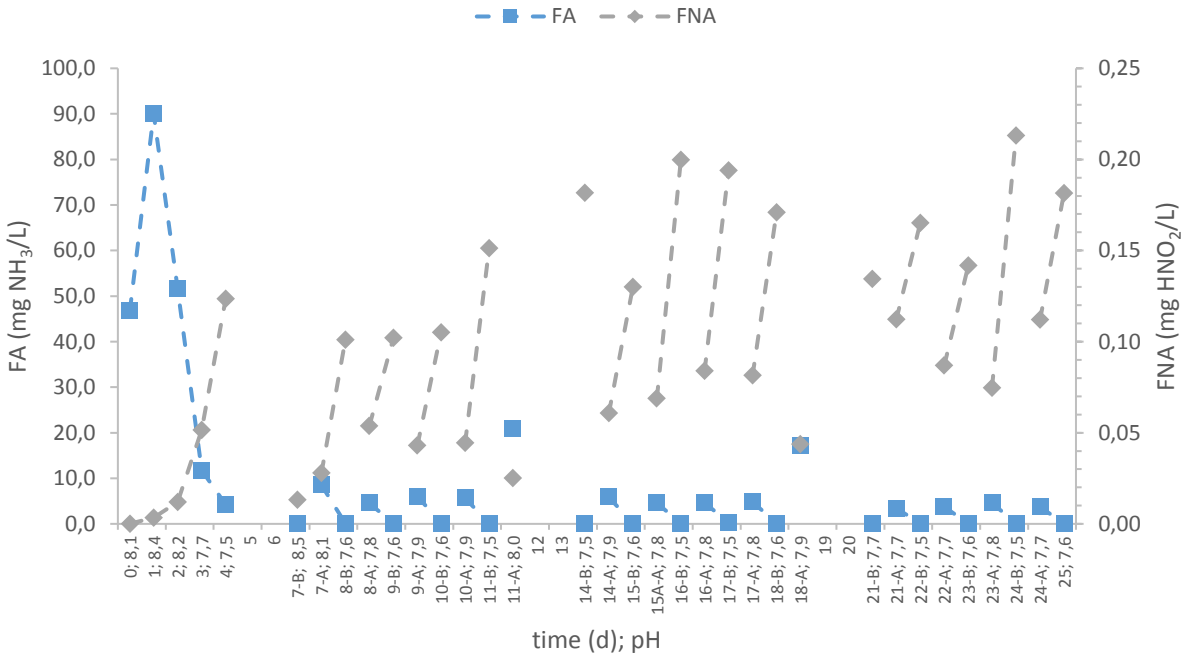

Figure 97. FA and FNA Conc. during the semi-batch process in SFBBR-1 system

As seen in figures 97 and 96, as the nitrite concentration increased so did the FNA concentration. During the treatment period the FNA ranged in between 0,0 to 0,21 mg HNO_2/L and for the most part the FNA concentrations were below the reported concentration of 0,2 mg HNO_2/L where inhibitory effects start to take place for NOB. Additionally, the calculated FA concentration ranged in between 0,0 to 90,0 mg NH_3/L

and reaching the highest value at day 1 as also observed in the other batch processes. In general, FA concentration values greater than 10 mg NH_3/L were only observed during the batch period and for the most part during the semi-batch period they were below 10 mg NH_3/L. As mentioned before, the reported FA limiting inhibitory concentrations are 10 mg NH_3/L for AOB and 0,1 mg NH_3/L for NOB. This means that during the batch period both types of microorganisms were possibly affected by FA concentrations but during the semi-batch period the NOB were probably greatly affected.

The results obtained for the ACR during the semi-batch process are illustrated in figure 98.

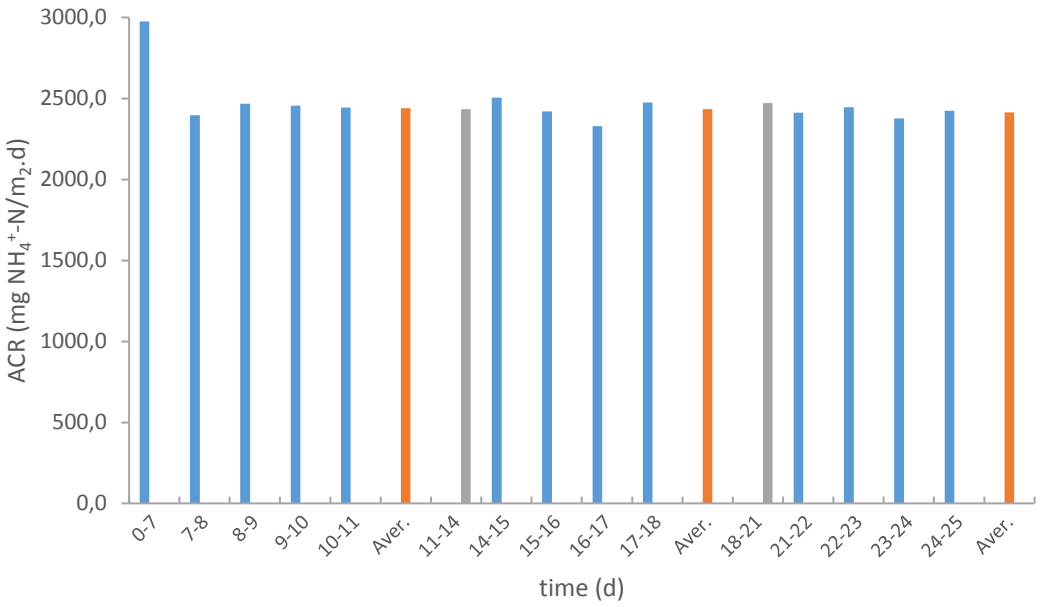

Figure 98. ACR during the semi-batch process in SFBBR-1 system

As seen in figure 98, The ACR values during the semi-batch period were relatively constant with average values of 2440,6, 2434,3, 2432,9, 2470,7 and 2414,5 mg NH_4^+-N/m^2.d for days in between 7 – 11, 11 – 14, 14 – 18, 18 – 21 and 21 – 25 respectively and with an overall average value of 2432,6 mg NH_4^+-N/m^2.d. Additionally based on equation 19, an ammonium volume consumption rate was obtained by using the packed bed surface area and the volume of the biofilm reactor containing the filter media as indicated in table 28. The calculation is shown below.

$$ACR_{Vol.} = \frac{2432{,}6\ \frac{mg\ NH_4^+\_N}{m^2.d} * 1{,}0\ m^2 \left|\frac{1\ g}{1000\ mg}\right| \left|\frac{1\ Kg}{1000\ g}\right|}{6{,}0\ L \left|\frac{1\ m^3}{1000\ L}\right|} = 0{,}40\ \frac{Kg\ NH_4^+\_N}{m^3.d}$$

In general during the semi-batch treatment process the ACR values were below 2500,0 mg NH_4^+-N/m^2.d with an overall average value of 2432,6 mg NH_4^+-N/m^2.d which was lower than the ACR of 2975,9 mg NH_4^+-N/m^2.d estimated during the batch stage. A possible reason related to the lower efficiency of the semi-batch process compared to the batch one included the constant alteration of the system by the daily addition and removal of the liquid medium which led to partial stress of the microorganisms within the biofilm system, hence reducing the efficiency in ammonium consumption. Another possible reason can be related to the initial substrate or ammonium concentrations used for the batch and during the semi-batch treatment periods. For instance, the initial ammonium concentrations used during the semi-batch period varied approximately in between 130,0 to 140,0 mg NH_4^+-N/L and 390,0 to 400,0 mg NH_4^+-N/L for the week days and weekends respectively which were lower compared to the initial concentration of 812,15 mg NH_4^+-N/L used for the batch period. Thus, by looking at the Monod model in figure 32 which illustrates the effect that the substrate concentration has on the specific growth of the microorganisms, it can be seen that the greater growth of AOB obtained during the batch process due to the higher initial substrate concentration led to a larger ACR.

The results obtained for the ammonium consumption percentage during the treatment are illustrated in figure 99.

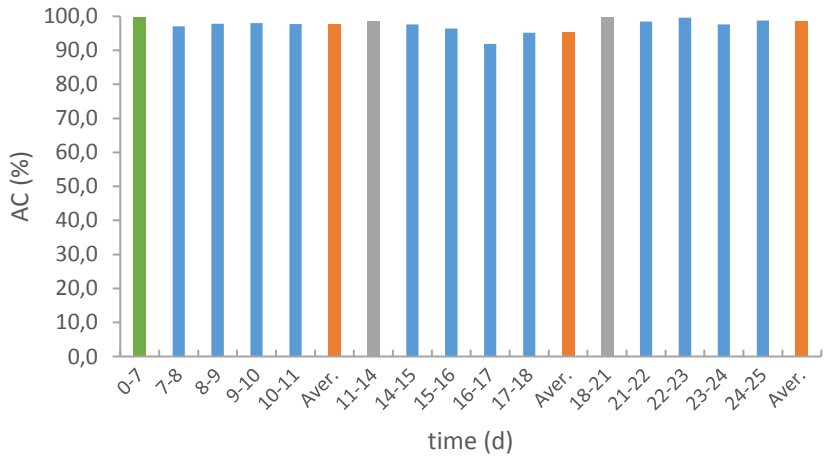

Figure 99. AC percentage during the semi-batch process in SFBBR-1 system

As seen in figure 99, overall the consumption of ammonium was greater than 90% during the whole semi-batch process and it was almost equal to 100% for the batch period and ranged approximately in between 91,9 to 99,9% during the semi-batch treatment. Thus, at the working conditions the AOB in the biofilm system was stable

and led to almost complete consumption of the ammonium found in the fed sludge water. Additionally, the nitrification percentage was estimated during the semi-batch process as indicated in figure 100.

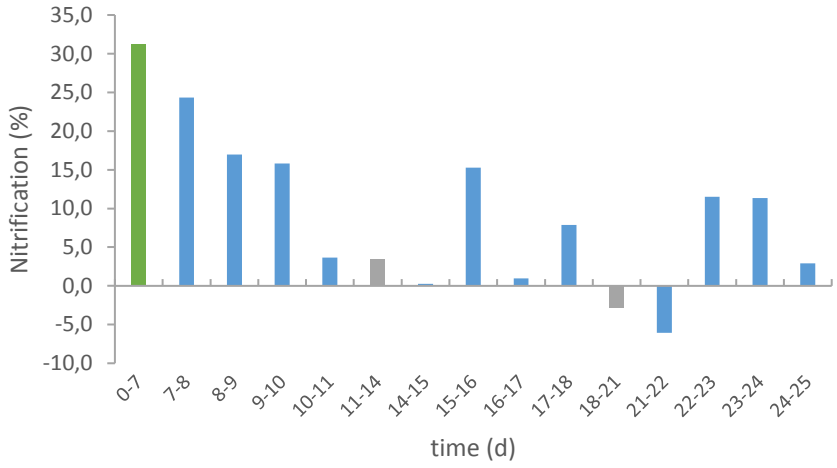

Figure 100. Nitrification percentage during the semi-batch process in SFBBR-1 system

As seen in figure 100, in contrast to ammonium consumption, complete nitrification was very low during the treatment period. The maximum conversion from ammonium to nitrate was observed during the batch period where about 30% of the consumed ammonium was converted into nitrate. Then, in between days 7 to 11 a gradual decreased in the generation of nitrate was observed to a value of 3,7% for days 10 to 11 and it maintained relatively constant in between days 11 to 14 with a value of 3,4%. After day 14, complete nitrification was partially observed ranging in between -6,0 to 15,3%. The negative and low nitrification percentage values indicated that some other biological processes besides nitrification such as denitrification, denitritation and/or deammonification were possible taking place in the biofilm system. This was due to the characteristics of the biofilm system and the operation conditions during the treatment period which included low DO concentrations and relatively high nitrite concentrations in combination with the fed ammonium and organic carbon concentrations.

4.6.8. Starting of bioreactor in SFBBR-2

The calculations were performed as previously described in the batch No. 1 section and during the renewal stages they were done in a similar way as described in the semi-batch section. The packed bed surface area used during the calculations was approximately equal to 2,0 m^2.

The raw data and the calculated values are given in appendix L.

The results for the surface loading values corresponding to each of the nitrogen species obtained during the treatment period are given in figure 101.

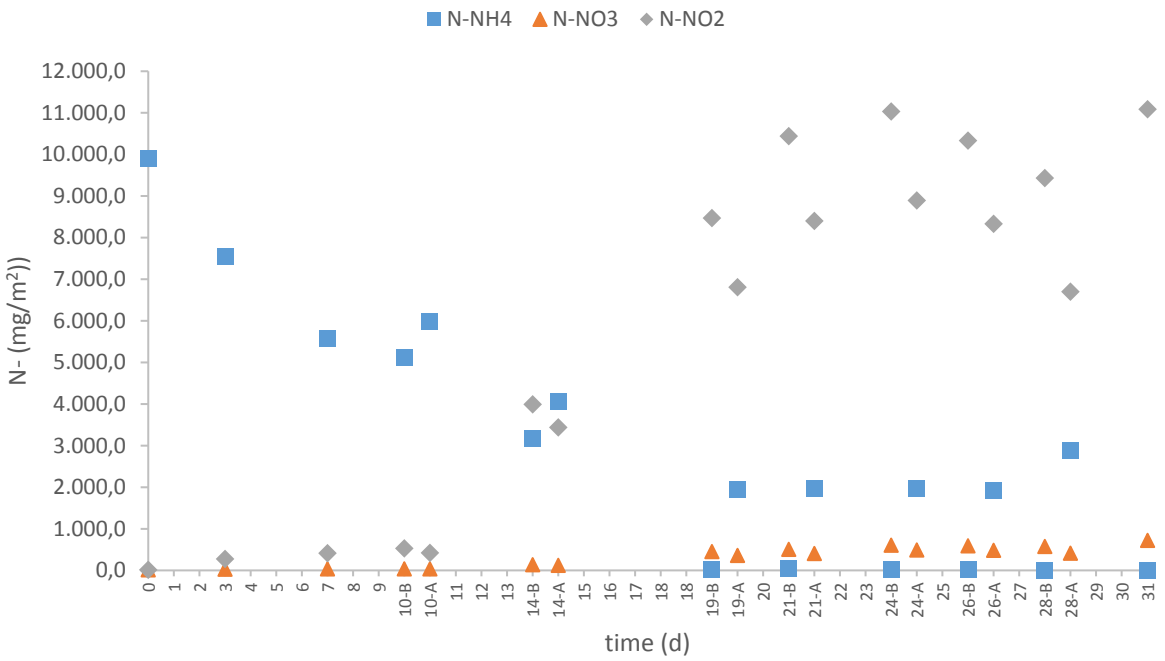

Figure 101. Nitrification and ACR during the starting of bioreactor in SFBBR-2 system

As seen in figure 101, during the first 7 days which corresponded to the period in which the pH was not controlled, the ammonium concentration dropped from a value of 842,38 mg NH_4^+-N/L for day 0 to a concentration of 473,94 mg NH_4^+-N/L for day 7. This decrease in ammonium concentration corresponded to almost 60% of the initial value and was due mainly to the high pH values of about 9,2 as indicated in figure 80 and resulting in high FA concentrations of about 288,1 and 247,0 mg NH_3/L calculated for days 3 and 7 respectively and as indicated in figure 102. Additionally, during the same period the nitrite and nitrate concentrations were very low reaching values of 35,3 mg NO_2^--N/L and 2,87 mg NO_3^--N/L by day 7 respectively. Even though, formation and development of the biofilm on the carrier material was only taking place within the first seven days, the low nitrite and nitrate concentrations were an indication that the conditions in the system were not appropriate for an acceptable formation and development of a biofilm system. Furthermore, after the operation conditions in the system were changed, a transition zone in between days 10 to 19 was observed. In this transition zone, the ammonium concentration started to decrease possible mainly

due to biological activity until reaching a concentration value of 1,56 mg NH_4^{+}-N/L at day 19. After day 19, a relatively stable ammonium oxidation zone was observed in which an average ACR of about 962,77 mg NH_4^{+}-N/m^2·d took place in between days 19 to 31. Moreover, by day 31 the concentration of nitrite in the system reached a value of 906,9 mg NO_2^{-}-N/L while the nitrate concentration varied only approximately in between 30,0 to 60,0 mg NO_3^{-}-N/L within days 19 to 31. The low nitrate concentrations obtained during the starting of the bioreactor indicated the larger sensitivity of the NOB compared to the AOB which were able to adopt faster at the working conditions within the system.

The results for the calculated concentrations of FA and FNA obtained during the starting of the bioreactor are given in figure 102. The values were calculated as described in the batch No. 1 section and by using the nitrogen species concentrations calculated for this process.

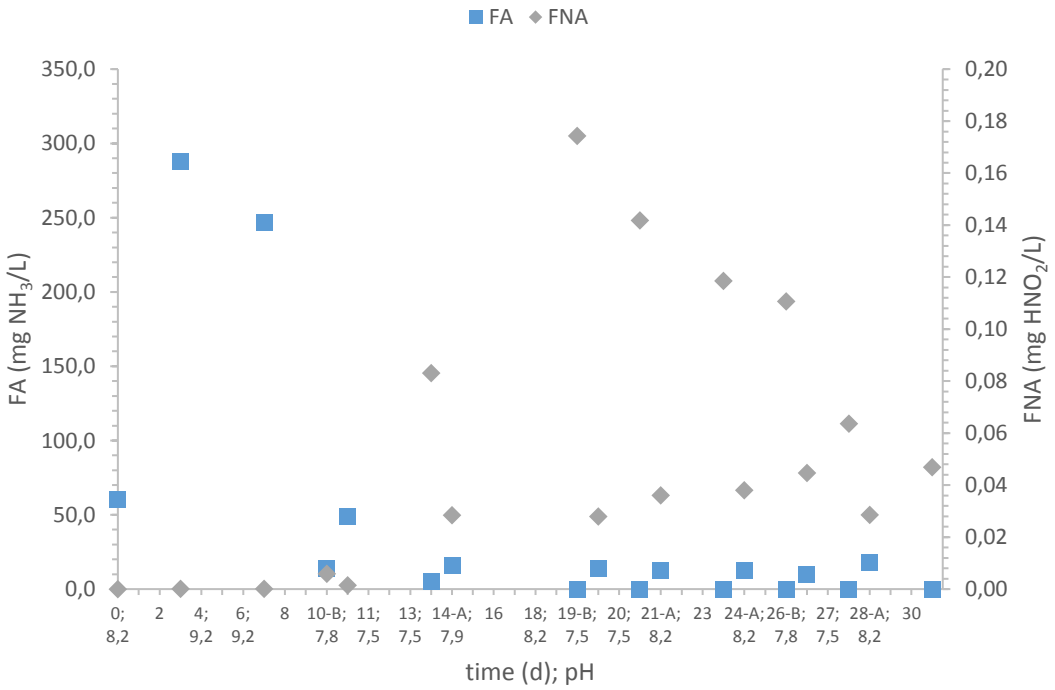

Figure 102. FA and FNA Conc. during the starting of bioreactor in SFBBR-2 system

As seen in figure 102, the FA concentration values were larger during the first 7 days of the process with concentrations varying approximately in between 60,3 to 288,1 mg NH_3/L and after day 7 the FA concentration values ranged in between 0,0 to 49,2 mg NH_3/L. Based on the reported FA limiting inhibitory concentrations of 10 mg NH_3/L for AOB and 0,1 mg NH_3/L for NOB. The FA concentration values indicated that for the majority of the process, the FA concentrations in the system probably affected

considerably the NOB and in a less extent the AOB which were probably more affected during the first 7 days of the process. On the other hand, the FNA concentration values were below the reported concentration of 0,2 mg HNO_2/L where inhibitory effects start to take place for NOB.

The results obtained for the ACR during the starting of the bioreactor process are illustrated in figure 103.

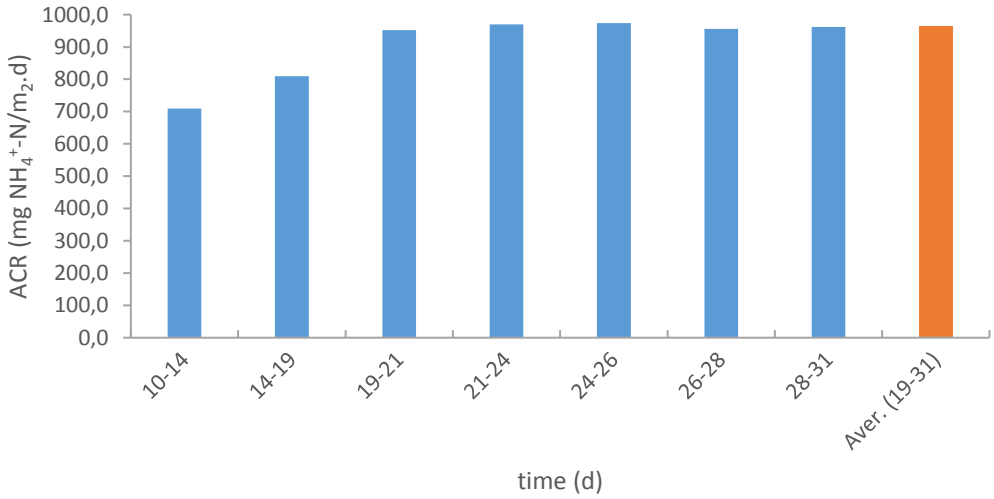

Figure 103. ACR during the starting of bioreactor in SFBBR-2 system

Figure 103, shows how the ACR increased gradually from 709,18 mg NH_4^+-N/m^2.d to 809,79 mg NH_4^+-N/m^2.d corresponding to days 10 – 14 and 14 – 19 respectively until reaching relatively constant values with an average ACR of 962,77 mg NH_4^+-N/m^2.d in between days 19 to 31 and with an average ammonium consumed percentage of 99,1% for the same period.

4.6.9. Batch operation in SFBBR-2

The nitrogen species concentrations, surface loading values (SLV) and the ammonium-nitrogen surface consumption rate (ACR) were calculated in the same way as previously described in the batch No. 1 section. The packed bed surface area used during the calculations was approximately equal to 2,0 m^2.

The raw data and all the calculated values are given in appendix L.

The results for the surface loading values corresponding to each of the nitrogen species obtained during the treatment period are given in figure 104.

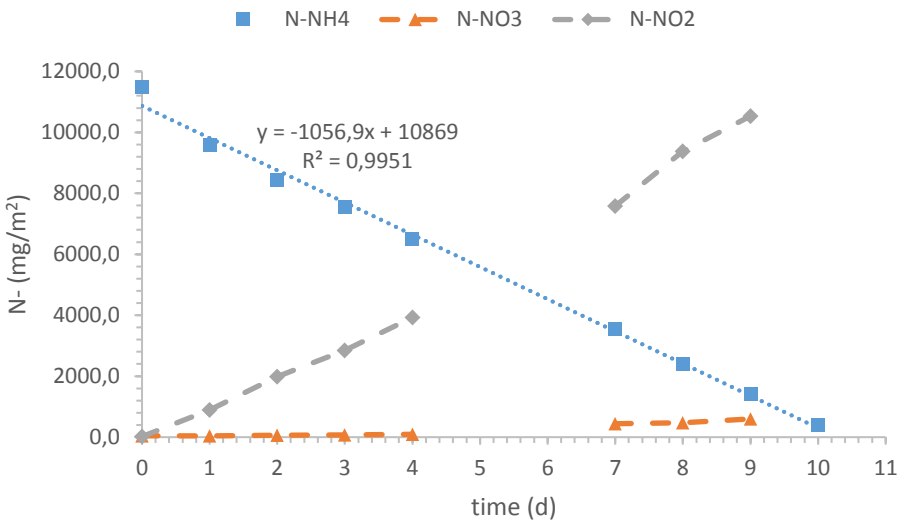

Figure 104. Nitrification and ACR during the batch process in SFBBR-2 system

As seen in figure 104, ammonium oxidation took place approximately within the first 10,4 days of treatment and the ammonium data fits relatively well the linear model with a R-squared of 0,9951. Thus, the approximated ACR for this process was estimated as 1056,9 mg NH_4^{+}-N/m^2·d at the working conditions summarized in tables 21 and 35.

The comparison between figures 82 and 104 shows that the consumption of the 0,9 M Na_2CO_3 solution took place within the period of ammonium oxidation. Furthermore, after comparing figures 83 and 104 it can be seeing that in between days 0 to 9 the DO concentration at the top the packed bed biofilm was below 1,0 mg O_2/L and after day 9 a sharp increase in the DO concentration was observed and quickly reaching a DO concentration value of around 6,0 mg O_2/L by day 11.

The comparison of the process with figures 33 and 34 was not possible since it was performed until ammonium consumption was almost completed. However, the same nitrite accumulation already discussed in the previous processes also took place but in a more severe way. For instance, at day 9 the concentration of nitrite was estimated as 746,3 mg NO_2^{-}-N/L which corresponded to about 90% of the initial ammonium concentration of 813,97 mg NH_4^{+}-N/L and at the same day the measured nitrate concentration was only equal to 42,33 mg NO_3^{-}-N/L. This results indicated that the nitrite oxidizing microorganisms were not yet well developed in the biofilm system due to possible inhibitions and the need for more time require to adjust at the working conditions.

The results for the calculated concentrations of FA and FNA obtained during the treatment period are given in figure 105. The values were calculated as described in the batch No. 1 section.

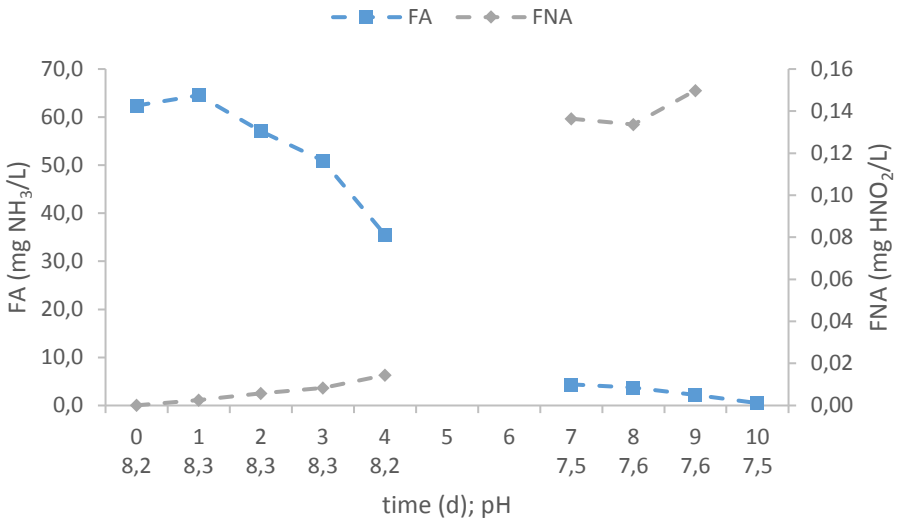

Figure 105. FA and FNA Conc. during the batch process in SFBBR-2 system

As seen in figure 105, at day 1 the same increase in the pH and FA observed in the SFBBR-1 batch processes also took place in this process reaching a FA concentration value of 64,5 mg NH_3/L. The FA concentration varied during the measured treatment period between 0,5 to 64,5 mg NH_3/L being higher during the first 4 days of treatment. In general, the calculated FA concentration values were within the FA reported limiting inhibitory concentrations of 10 mg NH_3/L and 0,1 mg NH_3/L for AOB and NOB respectively. Additionally, the maximum FNA concentration value was estimated as 0,15 mg HNO_2/L. This means that in general the FNA concentration values were below the reported concentration of 0,2 mg HNO_2/L where inhibitory effects start to take place for NOB.

The nitrification and total ammonium consumption percentages and the generated moles of H^+ were calculated up to day 9 with values of 5,5%, 88,0% and 3,06 mol H^+ respectively. The generated moles of H^+ were calculated based on the consumed ammonium up to day 9.

4.6.10. Nitrification and ammonium consumption rate results summary

The summary of the ACR results obtained during the different processes performed in the SFBBR-1 and SFBBR-2 systems are described in tables 37 and 38 respectively.

Table 37. ACR results for the different processes performed in the SFBBR-1 system

Processes	Air flow rate (L/h)	HLR (m/h)	ACR (mg NH_4^+-N/m^2·d)		time for AO (d)	FA (mg NH_3/L)	FNA (mg HNO_2/L)
Batch No.1	≈10,1	4,6	3212,2		7,0	0,0 – 86,0	0,0 – 0,17
Batch No.2	≈10,1	9,9	3500,4		5,2	0,0 – 161,2	–
Batch No.3	≈10,1	13,8	5524,3		3,0	0,0 – 92,3	–
Batch No.4	1,5	4,9	1920,3		9,0	0,0 – 102,1	0,0 – 0,17
Batch No.5	1,5	10,1	2186,1		7,3	0,0 – 142,9	0,0 – 0,20
Batch No.6	1,5	11,6	2620,0		6,0	0,0 – 73,3	0,0 – 0,12
Semi-batch	1,5	12,5	B	2975,9	5,5	0,0 – 90,0	0,0 – 0,21
			S-b	2432,6	1,0		

B: Batch period; S-b: Semi-batch period

Table 38. ACR results for the different processes performed in the SFBBR-2 system

Processes	Air flow rate (L/h)	HLR (m/h)	ACR (mg NH_4^+-N/m^2·d)	time for AO (d)	FA (mg NH_3/L)	FNA (mg HNO_2/L)
Starting	9,0	2,7	962,8	-	60,3 – 288,1[a] 0,0 – 49,2[b]	0,0 – 0,17
Batch	9,0	2,9	1056,9	10,4	0,5 – 64,5	0,0 – 0,15

a. From day 0 to day 7
b. After day 7

Table 37 shows that batches number 1 and 4 and batches number 2 and 5 were operated at very similar HLRs conditions of about 5,0 and 10,0 m/h respectively. However, the air flow rate for batches number 1 and 2 with an approximated value of 10,1 L/h was 6,7 times higher than the value of 1,5 L/h corresponding to batches number 4 and 5. The low air flow rate at which batches number 4 and 5 were operated led to low average DO concentration values as indicated in table 34 and consequently resulted in lower ACR values. For the HLR case of about 5,0 m/h, the 6,7 times increase in the air flow rate led to a 67,3% increase in the ACR from a value of 1920,3 to 3212,2 mg NH_4^+-N/m^2.d corresponding to batches number 4 and 1 respectively.

And, for the HLR of about 10,0 m/h the 6,7 times increase in the air flow rate led to a 60,1% increase in the ACR from a value of 2186,1 mg NH_4^+-N/m^2.d to 3500,4 mg NH_4^+-N/m^2.d for batches number 5 and 2 respectively. In general, the 6,7 times increase in the air flow rate at the same HLR conditions led to an average of 64,0% increase in the ACR value.

Furthermore, at the same air flow rate conditions the ACR increase with the increase in the HLR. For instance, at the air flow rate of 1,5 L/h the 2,1 times increase in the HLR from 4,9 to 10,1 m/h led to almost 14,0% increase in the ACR from a value of 1920,3 to 2186,1 mg NH_4^+-N/m^2.d for batches 4 and 5 respectively. Additionally, at the same air flow rate the 2,5 times increase in the HLR from 4,9 to 12,5 m/h led to a 55,0% increase in the ACR from a value of 1920,3 to 2975,9 mg NH_4^+-N/m^2.d which corresponded to batch No. 4 and the batch stage in the semi-batch process respectively. The same increase in the ACR was observed at the air flow rate of approximately 10,1 L/h where the 3,0 times increase of the HLR from 4,6 to 13,8 m/h resulted in a 72,0% increase in the ACR value from 3212,2 to 5524,3 mg NH_4^+-N/m^2.d for batches 1 and 3 respectively.

The results indicated that the increase in the HLR conditions had a major impact in the ACR values than the increase in the air flow rates. For instance, the 3,0 times increase in the HLR led to a 72,0% increase in the ACR value which was greater than the average 64,0% increase in the ACR obtained by increasing the air flow rate 6,7 times. The increase in the air flow rate mainly provided the system with a larger oxygen supply and probably to a lesser extent it help to increase the mixing and hence reducing the resistances to mass transfer. On the other hand and as already indicated in table 31, the increase in the HLR led to a decrease in the stagnant liquid film thickness for each of the substrates and consequently increasing the mass transfer coefficients and helping to overcome the mass transfer limitations which are characteristic of biofilm systems.

The ACR values obtained in the SFBBR-1 system during the different treatment processes at the different operation conditions were compared to the values reported in the literature for other biofilm reactor technologies. The TAN removal rates reported for trickling filters range in between 100 to 900 mg/m^2.d (Ebeling, 2006) and as seen in table 37 the ACRs values obtained during each of the treatment processes and despite the low air flow rates used during some of the processes were far greater than

the range reported for trickling filters at the given conditions. Furthermore, the nitrification rate for the Biocarbone® process is reported as 0,45 Kg/m^3·d and as indicated in section 4.6.7 for the semi-batch process the ammonium volume consumption rate was estimated as 0,40 Kg NH_4^+-N/m^3·d which is very closed to the value reported for the one of the most known SFBBR technologies.

In general, the ACR values obtained in the SFBBR-2 system were lower than the ones corresponding to the SFBBR-1 system. The possible reasons were mainly related to the lower HLR conditions of about 3,0 m/h used during the staring of the bioreactor and the batch process and the still ongoing formation and development of the biofilm system on the carrier materiel. However at the same HLR and air flow rate conditions, an increase of almost 10,0% in the ACR took place from the ammonium oxidation stable period during the starting of the bioreactor to the batch process with ACR values of 962,8 and 1056,9 mg NH_4^+-N/m^2.d respectively.

Moreover, as seen in tables 37 and 38 FA inhibition possible took place within the biofilm system which affected considerable the NOB, considering that for these microorganism FA inhibition has been reported to take place at concentrations greater than 0,1 mg NH_3/L as already mentioned in section 2.8.1. On the other hand, AOB can tolerate greater FA concentrations where inhibitions has been reported to take place at concentrations greater than 10 mg NH_3/L. Additionally, the FNA concentration values were in general below 0,2 mg HNO_2/L, this indicated that FNA inhibition for the NOB was low considering that the FNA inhibition for NOB has been reported to take place at values greater than 0,2 mg HNO_2/L as already indicated section 2.8.1.

The FA inhibition probably contributed to the low generation of nitrate and the partial accumulation of nitrite observed in the majority of the treatment processes while ammonium oxidation was taking place. However, the results indicated that the low generation of nitrate was more likely linked to the operation conditions of the system than the inhibitory effects caused by the substrates or other toxic agents present in the liquid medium. Thus, the low DO concentrations observed during the different processes and especially for batches number 4 through 6 and during the semi-batch process indicated a limited availability of oxygen within the biofilm system. This low availability of oxygen probably led to a competition for the substrate within the biofilm system between the two types of microorganisms and since the NOB are characterized for being more sensitive to inhibitory effects and requiring higher oxygen

concentrations for optimal growth as indicated in table 32, then the AOB took over and were dominant while their substrates were at high concentrations. Then, after depletion of ammonium took place, the conditions for NOB growth were better considering the high nitrite concentrations due to its partial accumulation and the larger availability of oxygen due to the decreased on its competition and consequently leading to their faster growth and larger generation of nitrate.

Additionally, one of the main advantages related to the partial accumulation of nitrite is related to the possibility of using the bioreactor system as a primary stage to other nitrogen removal biological processes such as nitritation/denitritation and deammonification as indicated in figure 9.

The summary of the results in the nitrification percentages obtained for batches No.1 through 6 performed in the SFBBR-1 system are described in table 39.

Table 39. Nitrification percentages results for the different processes performed in SFBBR-1 system

Processes		AC (%)	Nitrification (%)	Total Acid capacity (mol H^+)	Generated (mol H^+)
Batch No. 1		99,9	84,6	2,9	2,71[a]
Batch No. 2		99,9	81,6	2,5	2,13[a]
Batch No. 3		99,9	92,6	2,5	2,24[a]
Batch No. 4		99,9	85,9	2,5	2,09[a]
Batch No. 5		99,9	79,8	2,4	1,84[a]
Batch No. 6		99,9	81,5	2,5	1,84[a]
Semi-batch	B	99,9	31,2	2,4	2,32[b]
	S-b	91,9 – 99,9	-6,0 – 24,3	0,4 1,1	0,33 – 0,36[c] 1,05 – 1,06[d]

B: Batch period; S-b: Semi-batch period
a. Based on complete nitrification
b. Based on consumed ammonium
c. Based on consumed ammonium for one day interval
d. Based on consumed ammonium for three day interval

The nitrification percentage values obtained for batches number 1 through 6 were around the nitrification percentage range of 80 to 90% reported for similar processes such as the Biostyr® process indicated in table 11. The difference between the ammonium consumptions and the nitrification percentages and the negative nitrification values obtained during the semi-batch process were indications of other nitrogen related mechanisms taking place within the biofilm system mainly due to the

different metabolic zones which are characteristic of a biofilm system as already illustrated in figure 20. Finally, in general, the generated moles of H^+ were always lower but relatively close to the total acid capacity of the system corresponding to each of the treatment processes.

5. CONCLUSIONS

- The density of the plastic carrier material with nominal dimensions of 12,0 mm * 12,0 mm and an approximate SSA value of 660 m^2/m^3 used in each of the bioreactors was estimated as 0,7 g/mL.
- The porosity and the packed bed surface area for the SFBBR-1 were estimated as 63,0% and 1,0 m^2 respectively with a biofilter depth of 0,77 m.
- The porosity and the packed bed surface area for the SFBBR-2 were estimated as 71,0% and 2,0 m^2 respectively with a biofilter depth of 1,8 m.
- The alkalinity and the COD for the collected sludge water were determined as 68,9 mmol H^+/L and 385,0 mg O_2/L respectively.
- The bioreactors were operated at estimated HLRs ranging in between 2,8 m/h to 13,8 m/h and at three air flow rates with values of 1,5 L/h, 9,0 L/h and approximately 10,1 L/h.
- The liquid flow conditions for each of the experimental practices where within the laminar regime with Reynolds numbers varying in between 9,3 to 45,8 corresponding to HLRs values ranging in between 2,8 m/h to 13,8 m/h.
- The stagnant liquid film thicknesses at the liquid flow conditions were estimated to range in between 253,5 µm to 430,8 µm and 259,7 µm to 441,4 µm for ammonium and oxygen respectively at HLRs ranging in between 2,8 m/h to 13,8 m/h where the liquid stagnant film thicknesses increase with the decrease in the HLR conditions.
- The liquid mass transfer coefficients at the liquid flow conditions were estimated to range in between 0,37 m/d to 0,63 m/d and 0,39 m/d to 0,67 m/d for ammonium and oxygen respectively at HLRs varying in between 2,8 m/h to 13,8 m/h where the mass transfer coefficients increase with the increase in the HLR conditions.
- The ammonium-nitrogen concentration of the collected sludge water ranged in between 791,60 mg NH_4^+-N/L to 936,20 mg NH_4^+-N/L with an average value of 833,19 mg NH_4^+-N/L.

- The ammonium consumption rates in the SFBBR-1 operated in batch mode with an air flow rate of approximately 10,1 L/h were equal to 3212,2 mg NH_4^+-N/m^2·d, 3500,4 mg NH_4^+-N/m^2·d and 5524,3 mg NH_4^+-N/m^2·d at HLRs of 4,6 m/h, 9,9 m/h and 13,8 m/h respectively.
- The ammonium consumption rates in the SFBBR-1 operated in batch mode with an air flow rate of 1,5 L/h were equal to 1920,3 mg NH_4^+-N/m^2·d, 2186,1 mg NH_4^+-N/m^2·d and 2620,0 mg NH_4^+-N/m^2·d at HLRs of 4,9 m/h, 10,1 m/h and 11,6 m/h respectively.
- The ammonium consumption rates in the SFBBR-1 operated in semi-batch mode with an air flow rate of 1,5 L/h were equal to 2975,9 mg NH_4^+-N/m^2·d and 2432,6 mg NH_4^+-N/m^2·d during the batch and semi-batch stages respectively at a HLR of 12,5 m/h.
- The percentage of ammonium consumed during all of the batch processes performed in the SFBBR-1 system were equal to 99,9% and for the semi-batch process ranged in between 91,9% to 99,9%.
- The percentage of complete nitrification obtained for the batch processes performed in the SFBBR-1 ranged in between 79,8% to 92,6%, being higher for the process operating at a HLR of 13,8 m/h and an approximated air flow rate of 10,1 m/h.
- The ammonium consumption rates in the SFBBR-2 obtained for the starting of the bioreactor during the ammonium oxidation stabilization period and the batch process were equal to 962,8 mg NH_4^+-N/m^2·d and 1056,9 mg NH_4^+-N/m^2·d respectively with an air flow rate of 9,0 L/h and a HLR of about 3,0 m/h.
- The increase in the HLR conditions impacted more the ACR values than the increase in the air flow rates. A 3,0 times increase in the HLR led to a 72,0% increase in the ACR while a 6,7 times increase in the air flow rate value led to an average of 64,0% increase in the ACR.
- High FA concentrations may had considerably affected NOB and contributed to the partial nitrite accumulation observed during all of the treatment processes, considering that the FA concentrations were higher than their reported FA inhibitory concentration of 0,1 mg NH_3/L at some stages during each of the treatment processes.

6. REFERENCES

Andreoli, C. V., Sperling, M. V. & Fernandes, F., 2007. Biological Wastewater Treatment Series. In: *Volume 6, Sludge Treatment and Disposal.* London, UK: IWA Publishing.

Anthonisen, A., Loehr, R., Prakasam, T. & Srinath, E., 1976. *Inhibition of Nitrification by Ammonia and Nitrous Acid; Journal (Water Pollution Control Federation); Vol. 48, No. 5 (May, 1976), pp. 835-852; Water Environment Federation.* [Online]
Available at: http://www.jstor.org/stable/25038971
[Accessed 02 11 2017].

AQUAFIX, 2016. *Ammonia-Oxidizing Bacteria (AOB) and Nitrite-Oxidizing Bacteria (NOB).* [Online]
Available at: https://teamaquafix.com/ammonia-removal-restoring-nitrification/
[Accessed 12 10 2017].

Balteau, 2012. *Rotating biocontactor (RBC).* [Online]
Available at: http://www.balteau.be/0159/en/Rotating-biocontactor-RBC
[Accessed 31 10 2017].

Capodaglio, A. G., Hlavínek, P. & Raboni, M., 2015. *Revista Ambient & Agua On-line version ISSN 1980-993X; Physico-chemical technologies for nitrogen removal from wastewaters: a review.* [Online]
Available at: http://www.scielo.br/scielo.php?script=sci_arttext&pid=S1980-993X2015000300481
[Accessed 07 10 2017].

Capodaglio, A. G., Hlavinek, P. & Raboni, M., 2016. *Advances in wastewater nitrogen removal by biological processes: state of the art review.* [Online]
Available at: http://www.scielo.br/scielo.php?script=sci_arttext&pid=S1980-993X2016000200250
[Accessed 15 10 2017].

Constantine, T. A., 2006. *NORTH AMERICAN EXPERIENCE WITH CENTRATE TREATMENT TECHNOLOGIES FOR AMMONIA AND NITROGEN REMOVAL.* [Online]
Available at: https://www.environmental-expert.com/articles/north-american-experience-with-centrate-treatment-technologies-for-amonia-and-nitrogen-removal-13105
[Accessed 11 10 2017].

Costerton, W. J. & Lappin-Scott, H. M., 2003. *Microbial Biofilms; Chapter 2 Dynamics of Bacterial Biofilm Formation.* [Online]
Available at:
https://books.google.de/books?id=opTs2ufPizMC&pg=PA55&lpg=PA55&dq=Sloughing+in+biofilms&source=bl&ots=36neGxPkPM&sig=rxGPb_WC1AQefWv9BQyqXESnVYE&hl=en&sa=X&ved=0ahUKEwj9rsCukJ3XAhXQI-wKHeo0C-kQ6AEISzAH#v=onepage&q&f=false
[Accessed 10 10 2017].

Daigger, G. T., Grady, L., Love, N. G. & Filipe, C. D., 2011. Chapter 16 Biofilm Modeling. In: *Biological Wastewater Treatment.* USA: CRC Press & IWA Publishing.

Daigger, G. T., Grady, L., Love, N. G. & Filipe, C. D., 2011. Chapter 17 Biofilm Reactors. In: *Biological Wastewater Treatment.* USA: CRC Press & IWA Publishing.

Daigger, G. T., Grady, L., Love, N. G. & Filipe, C. D., 2011. Chapter 18 Biofilm Reactors. In: *Biological Wastewater Treatment.* USA: CRC Press & IWA Publishing.

Dizge, N., Tansel, B. & Sizirici, B., 2011. *Process intensification with a hybrid system: A tubular packed bed bioreactor with immobilized activated sludge culture coupled with membrane filtration.* [Online]
Available at:
https://www.researchgate.net/publication/251539141_Process_intensification_with_a_hybrid_system_A_tubular_packed_bed_bioreactor_with_immobilized_activated_sludge_culture_coupled_with_membrane_filtration
[Accessed 15 11 2017].

Dombrowski, E. M. & In Su Choi, U. W., 2007. Chapter 10 Biological Nutrient Removal. In: *Fundamentals of Biological Wastewater Treatment.* Germany: WILEY.

Dombrowski, E. M. & In Su Choi, U. W., 2007. Chapter 3 Microbial Metabolism. In: *Fundamentals of Biological Wastewater Treatment.* Germany: WILEY.

Dombrowski, E. M. & In Su Choi, U. W., 2007. Chapter 6 Aerobic Wastewater Treatment in Activated Sludge Systems. In: *Fundamentals of Biological Wastewater Treatment.* Germany: WILEY.

Dombrowski, E. M. & In Su Choi, U. W., 2007. Chapter 7 Aerobic Treatment with Biofilm Systems. In: *Fundamentals of Biological Wastewater Treatment.* Germany: WILEY.

Ebeling, J. M., 2006. *Biofiltration-Nitrification Design Overview.* [Online]
Available at:

https://cals.arizona.edu/azaqua/ista/ISTA7/RecircWorkshop/Workshop%20PP%20%20&%20Misc%20Papers%20Adobe%202006/7%20Biofiltration/Nitrification-Biofiltration/Biofiltration-Nitrification%20Design%20Overview.pdf
[Accessed 08 10 2017].

El-Shafai, S. A. & Zahid, W. M., 2013. *Performance of aerated submerged biofilm reactor packed with local scoria for carbon and nitrogen removal from municipal wastewater.* [Online]
Available at: http://www.sciencedirect.com/science/article/pii/S0960852413009462?via%3Dihub
[Accessed 15 11 2017].

emis, 2015. *Biological nutrient removal.* [Online]
Available at: https://emis.vito.be/en/techniekfiche/biological-nutrient-removal
[Accessed 12 10 2017].

EPA, 1985. *Sidestreams in Advanced Wastewater Treatment Plants: Problems and Remedies.* [Online]
Available at:
https://nepis.epa.gov/Exe/ZyNET.exe?ZyActionL=Register&User=anonymous&Password=anonymous&Client=EPA&Init=1
[Accessed 09 10 2017].

EPA, 1987. *Sidestreams in Wastewater Treatment Plants; Journal (Water Pollution Control Federation) Vol. 59, No. 1, pp. 54-59.* [Online]
Available at: http://www.jstor.org/stable/25043169?seq=1#page_scan_tab_contents
[Accessed 09 10 2017].

EPA, 2007. *Wastewater Technology Fact Sheet Side Stream Nutrient Removal.* [Online]
Available at:
https://nepis.epa.gov/Exe/ZyNET.exe?ZyActionL=Register&User=anonymous&Password=anonymous&Client=EPA&Init=1
[Accessed 12 10 2017].

European Commision, 2017. *Environment - Water.* [Online]
Available at: http://ec.europa.eu/environment/water/index_en.htm
[Accessed 09 10 2017].

European Commission, 2016. *Sewage Sludge.* [Online]
Available at: http://ec.europa.eu/environment/waste/sludge/
[Accessed 08 10 2017].

Fux, C., 2003. *Biological nitrogen elimination of ammonium-rich sludge digester liquids.* [Online]
Available at: https://www.research-collection.ethz.ch/handle/20.500.11850/147532
[Accessed 11 10 2017].

Greenion, 2014. *TRICKLING FILTER.* [Online]
Available at: http://igreenion.com/trickling-filter.html
[Accessed 31 10 2017].

Gustavsson, D., 2010. *Biological sludge liquor treatment at municipal wastewater treatment plants – a review.* [Online]
Available at: http://www.tidskriftenvatten.se/wp-content/uploads/2017/04/48_article_4264.pdf
[Accessed 12 10 2017].

HACH, 2017. *COD cuvette test 150-1000 mg/L O2.* [Online]
Available at: https://uk.hach.com/cod-cuvette-test-150-1000-mg-l-o-sub-2-sub/product?id=26370268939
[Accessed 05 11 2017].

Henze, M., van Loosdrecht, M. C., Ekama, G. A. & Brdjanovic, D., 2008. Chapter 17 Modelling Biofilms. In: *Biological Wastewater Treatment; Principles, Modelling and Design.* UK: IWA Publishing.

Henze, M., van Loosdrecht, M. C., Ekama, G. A. & Brdjanovic, D., 2008. Chapter 18 Biofilm Reactors. In: *Biological Wastewater Treatment; Principles, Modelling and Design.* UK: IWA Publishing.

ISWA, 1998. *Sludge Treatment and Disposal, Management Approaches and Experiences. Environmental Issues Series No. 7.* [Online]
Available at: https://www.eea.europa.eu/publications/GH-10-97-106-EN-C/file
[Accessed 08 10 2017].

Jardin, N., Thöle, D. & Wett, B., 2006. *Treatment of Sludge Return Liquors: Experiences from the Operation of Full-Scale Plants.* [Online]
Available at:
https://www.researchgate.net/publication/233488224_Treatment_of_Sludge_Return_Liquors_Experiences_from_the_Operation_of_Full-Scale_Plants
[Accessed 11 10 2017].

Jenkins, D. & Wanner, J., 2014. *Activated Sludge - 100 Years and Counting; IWA Publishing.* [Online]
Available at:
https://books.google.de/books?id=J7cDBAAAQBAJ&pg=PA235&dq=deammonification&hl=en&sa=X&ved=0ahUKEwib2LzbvoHXAhWsJ8AKHRooDjEQ6AEITDAI#v=onepage&q=deammonification&f=false
[Accessed 15 10 2017].

Kempen, R. v., Mulder, J., Uijterlinde, C. & Loosdrecht, M., 2001. *Overview: full scale experience of the SHARON® process for treatment of rejection water of digested sludge dewatering.* [Online]
Available at:
http://m2ttech.com/pdfs/Paper%20003%20IWA%20WST%202001%20VOL%2044%20pages%20145-152.pdf
[Accessed 19 10 2017].

Knick, 2017. *Portavo 907 Multi.* [Online]
Available at: https://www.knick-international.com/en/products/portables/portavo/portavo-907-multi/index.html#
[Accessed 5 10 2017].

Knowles, G., Downing, A. & Barrett, M., 1965. *Determination of Kinetic Constants for Nitrifying Bacteria in Mixed Culture, with the Aid of an Electronic Computer.* [Online]
Available at: http://mic.microbiologyresearch.org/content/journal/micro/10.1099/00221287-38-2-263;jsessionid=ANH7DngxsZoDXCl5b-UKE9up.x-sgm-live-03
[Accessed 05 11 2017].

Langenkamp, H. & Marmo, L., 2000. *Workshop on Problems Around Sludge, Proceedings, Session 3, Technology and innovative options related to sludge management.* [Online]
Available at: http://ec.europa.eu/environment/archives/waste/sludge/pdf/workshoppart4.pdf
[Accessed 08 10 2017].

Lee, Y. K., 2016. Microalgae Cultivation Fundamentals. In: F. Bux & Y. Chisti, eds. *Algae Biotechnology - Products and Processes; Green Energy and Technology.* Switzerland: Springer.

LENNTECH, 2017. *Thickening.* [Online]
Available at: https://www.lenntech.com/library/sludge/thickening/sludgethickening.htm
[Accessed 08 10 2017].

Lens, P., Pol, L. H., Wilderer, P. & Asano, T., 2002. *Water Recycling and Resource Recovery in Industry; Analysis, Technologies and Implementations.* UK: IWA Publishing.

Lewandowski, Z. & Beyenal, H., 2014. Chapter 1: Introduction to biofilms and to biofilm research. In: *Fundamentals of BIOFILM RESEARCH; 2nd Ed..* USA: CRC Press.

Logan, B. E., 2012. Chapter 9 Biofilms. In: *Environmental Transport Processes; 2nd Ed..* USA: John Wiley & Sons.

Magdum, S. S. & Kalyanraman , V., 2017. *Existing biological nitrogen removal processes and current scope of advancement.* [Online]
Available at: https://papers.ssrn.com/sol3/papers.cfm?abstract_id=2994656
[Accessed 14 10 2017].

Maine Lagoon Systems, 2003. *NITRITES AND THEIR IMPACT ON EFFLUENT CHLORINATION.* [Online]
Available at: http://www.lagoonsonline.com/technote4.htm
[Accessed 08 10 2017].

Marsalek, J., Sztruhar, D., Guilianelli, M. & Urbonas, B., 2005. UPGRADING SEWAGE TREATMENT PLANTS FOR HIGHER PERFORMANCE BY OPTIMISING REJECT WATER TREATMENT. In: *Enhancing Urban Environment by Environmental Upgrading and Restoration.* NY: KLUWER ACADEMIC.

Metcalf & Eddy, Inc., 2003. Chapter 14 Treatment, Reuse, and Disposal of Solids and Biosolids. In: *Wastewater Engineering - Treatment and Reuse, 4th Ed..* USA: McGraw-Hill.

Metcalf & Eddy, Inc., 2003. Chapter 2 Constituents in Wastewater. In: *Wastewater Engineering - Treatment and Reuse, 4th Ed..* 4th ed. USA: McGraw-Hill.

Metcalf & Eddy, Inc., 2003. Chapter 7 Fundamentals of Biological Treatment. In: *Wastewater Engineering - Treatment and Reuse, 4th Ed..* USA: McGraw-Hill.

Metcalf & Eddy, Inc., 2003. Chapter 8 Suspended Growth Biological Treatment Process. In: *Wastewater Engineering - Treatment and Reuse; 4th Ed..* USA: McGraw-Hill.

Metcalf & Eddy, Inc., 2003. Chapter 9 Attached Growth and Combined Biological Treatment Processes. In: *Wastewater Engineering - Treatment and Reuse, 4th Ed..* USA: McGraw-Hill.

MILTON ROY, 2007. *MOTOR-DRIVEN DOSING PUMPS - MECHANICALLY ACTUATED; Series G Dosing pumps; Series G A.* [Online]
Available at: http://www.miltonroy-europe.com/series-g-a,literature-13.html
[Accessed 5 10 2017].

Muffler, K. & Ulber, R., 2014. Application of Biofilm Bioreactors in White Biotechnology. In: *Productive Biofilms; Advances in Biochemical Engineering/Biotechnology 146; Series Editor: T. Scheper.* Germany: Springer.

Orhon, D. & Artan, N., 1994. Chapter 6 Biological Oxidation of Nitrogen. In: *Modelling of Activated Sludge Systems.* USA: TECHNOMIC.

Pedersen, O., Colmer, T. D. & Sand-Jensen, K., 2013. *Underwater Photosynthesis of Submerged Plants – Recent Advances and Methods.* [Online]
Available at: https://www.researchgate.net/publication/237018256
[Accessed 02 11 2017].

Pedros, P., Hayden, O. & Tyler, C., 2006. *INVESTIGATION OF NITRIFICATION AND NITROGEN REMOVAL FROM CENTRATE IN A SUBMERGED ATTACHED GROWTH BIOREACTOR.* [Online]
Available at: https://www.environmental-expert.com/Files/5306/articles/8470/002.pdf
[Accessed 10 10 2017].

Picioreanu, C., Loosdrecht, M. C. M. v. & Heijnen, J., 1997. *Modelling the effect of oxygen concentration on nitrite accumulation in a biofilm airlift suspension reactor.* [Online]
Available at:
https://www.academia.edu/679159/Modelling_the_effect_of_oxygen_concentration_on_nitrite_accumulation_in_a_biofilm_airlift_suspension_reactor?auto=download
[Accessed 20 10 2017].

Pugh, L. & AECOM, 2010. *Sustainable Approaches for Sidestream Nutrient Removal and Recovery.* [Online]
Available at:
ftp://ft.dphe.state.co.us/wqc/wqcc/31_85NutrientsRMH_2012/ResponsivePrehearing/MWRDex24.pdf
[Accessed 11 10 2017].

RVT, 2015. *Ammonia recovery Removal from liquids and gases.* [Online]
Available at: http://rvtpe.com/wp-content/uploads/2013/04/RVT_Ammonia_Recovery_150423.pdf
[Accessed 15 10 2017].

Sanchez, A. R. et al., 2014. *The Effect of Influent Characteristics and Operational Conditions over the Performance and Microbial Community Structure of Partial Nitritation Reactors.* [Online]
Available at:
https://www.researchgate.net/publication/269947861_The_Effect_of_Influent_Characteristics_and_Operational_Conditions_over_the_Performance_and_Microbial_Community_Structure_of_Partial_Nitritation_Reactors
[Accessed 12 10 2017].

Schmidt, I. et al., 2003. *New concepts of microbial treatment processes for the nitrogen removal in wastewater.* [Online]
Available at: http://onlinelibrary.wiley.com/doi/10.1016/S0168-6445(03)00039-1/pdf
[Accessed 12 10 2017].

Sedlak, R., 1991. *Phosphorus and nitrogen removal from municipal wastewater: principles and practice.* 2nd ed. NY - USA: LEWIS PUBLISHERS.

SIGMA-ALDRICH, 2017. *catalog/product.* [Online]
Available at: https://www.sigmaaldrich.com/germany.html
[Accessed 05 07 2017].

StatsDirect, 2000. [Online]
Available at: https://www.statsdirect.com/help/Default.htm#basic_descriptive_statistics/univariate_summary.htm
[Accessed 10 11 2017].

Stoodley, P., Sauer, K., Davies, D. & Costerton, J., 2002. *BIOFILMS AS COMPLEX DIFFERENTIATED COMMUNITIES.* [Online]
Available at: http://www.annualreviews.org/doi/full/10.1146/annurev.micro.56.012302.160705?url_ver=Z39.88-2003&rfr_id=ori%3Arid%3Acrossref.org&rfr_dat=cr_pub%3Dpubmed&
[Accessed 20 10 2017].

stowa, 2012. *Explorative research on innovative nitrogen recovery.* [Online]
Available at: http://www.stowa.nl/Upload/publicaties/STOWA%202012%2051_LR.pdf
[Accessed 19 10 2017].

Sudarno, 2011. *Nitrification in Fixed Bed Reactors Treating Saline Wastewater; Chapter 2 Literature Review; Karlsruhe; KIT Scientific Publishing.* [Online]
Available at: https://www.ksp.kit.edu/download/1000023321
[Accessed 20 10 2017].

TASK , 2017. *NH3 stripping tower absorber, Ammonia removal wastewater - NH3 stripping towers (stripper-absorber combination).* [Online]

Available at: http://task.be/en/content/nh3-stripping-tower-absorber
[Accessed 19 10 2017].

The Engineering ToolBox, 2017. *Reynolds Number.* [Online]
Available at: https://www.engineeringtoolbox.com/reynolds-number-d_237.html
[Accessed 20 10 2017].

The Engineering ToolBox, 2017. *Water - Density and Specific Weight.* [Online]
Available at: https://www.engineeringtoolbox.com/water-density-specific-weight-d_595.html
[Accessed 15 10 2017].

The Engineering ToolBox, 2017. *Water - Dynamic and Kinematic Viscosity.* [Online]
Available at: https://www.engineeringtoolbox.com/water-dynamic-kinematic-viscosity-d_596.html
[Accessed 15 10 2017].

Thorndahl, U., 1994. Nitrogen Removal by Treatment of Reject Water. In: *Nutrient Removal from Wastewaters.* UK: TECHNOMIC.

USA-EPA, 2009. *National Service Center for Environmental Publications (NSCEP): Nutrient Control Design Manual State of Technology Review Report.* [Online]
Available at: https://www.epa.gov/nscep
[Accessed 07 10 2017].

USA-EPA, 2009. *National Service Center for Environmental Publications (NSCEP): Nutrient Control Design Manual State of Technology Review Report.* [Online]
Available at: https://www.epa.gov/nscep
[Accessed 14 10 2017].

Wang, G., Zhou, L., Wang, C. & Yang, F., 2017. *A pilot-scale study on the start-up of partial nitrification-anammox process for anaerobic sludge digester liquor treatment.* [Online]
Available at: http://www.sciencedirect.com/science/article/pii/S0960852417302547
[Accessed 10 10 2017].

Wang, L. K., Pereira, N. C. & Hung, Y.-T., 2009. Chapter 13 Biological Nitrification and Denitrification Processes. In: *Biological Treatment Processes; Handbook of Environmental Engineering; Volume 8.* USA: Human Press.

Ward, B. B., 2013. *Nitrification.* [Online]
Available at: https://www.princeton.edu/nitrogen/publications/pdfs/Ward_2015_Nitrification.pdf
[Accessed 12 10 2017].

WEF, 2008. *Operation of Municipal Wastewater Treatment Plants; Volume I: Management and Support Systems; Manual of Practice No. 11.* 6th ed. USA: McGraw-Hill.

WEF, 2010. Chapter 1 Introduction . In: *Biofilm Reactors WEF Manual of Practice No. 35.* USA: WEF Press; McGraw-Hill.

WEF, 2010. Chapter 5 Moving-Bed Biofilm Reactors. In: *Biofilm Reactors WEF Manual of Practice No. 35.* USA: WEF Press; McGraw-Hill.

Wett, B., Rostek, R., Rauch, W. & Ingerle, K., 1998. *pH-CONTROLLED REJECT WATER TREATMENT.* [Online]
Available at: http://araconsult.at/download/literature/ph_control_wett.pdf
[Accessed 11 10 2017].

Wolfram, 1999. *Rule of Three.* [Online]
Available at: http://mathworld.wolfram.com/RuleofThree.html
[Accessed 15 10 2017].

WRIG, 2007. *wheatleyriver.* [Online]
Available at: http://www.wheatleyriver.ca/current-projects/wrig-pilot-nitrate-study/nitrates-and-their-effect-on-water-quality-a-quick-study/
[Accessed 07 10 2017].

7. APPENDICES

APPENDIX A: Alkalinity titration

Conc. Acid Sltn. = 0,1 M HCL

Vol. SW sample = 100,0 mL

No.	Vol. HCL_{aq} (mL)	pH
1	0,0	8,1
2	1,0	8,0
3	2,0	7,9
4	3,0	7,8
5	4,0	7,7
6	5,0	7,6
7	6,0	7,5
8	7,0	7,5
9	8,0	7,4
10	9,0	7,3
11	10,0	7,3
12	11,0	7,2
13	12,0	7,2
14	13,0	7,1
15	14,0	7,1
16	15,0	7,1
17	16,0	7,0
18	17,0	7,0
19	18,0	7,0
20	19,0	6,9
21	20,0	6,9
22	21,0	6,9
23	22,0	6,9
24	23,0	6,8
25	24,0	6,8

No.	Vol. HCL_{aq} (mL)	pH
26	25,0	6,8
27	26,0	6,8
28	28,0	6,7
29	30,0	6,6
30	32,0	6,6
31	34,0	6,5
32	36,0	6,5
33	38,0	6,4
34	40,0	6,4
35	42,0	6,3
36	44,0	6,3
37	46,0	6,2
38	48,0	6,1
39	50,0	6,1
40	52,0	6,0
41	54,0	5,9
42	56,0	5,9
43	58,0	5,8
44	60,0	5,7
45	62,0	5,6
46	64,0	5,4
47	66,0	5,2
48	68,0	4,7
49	68,9	4,3

APPENDIX B: Liquid and air flow rates raw data

Batch operations in SFBBR-1 System

Liquid recirculation flow rate

	No.	Measured Vol. (mL)	t (s)
Batch No. 1	1	600,0	60
	2	600,0	60
	3	600,0	60
Batch No. 2	1	650,0	30
	2	650,0	30
	3	650,0	30
Batch No. 3	1	600,0	20
	2	600,0	20
	3	600,0	20
Batch No. 4	1	640,0	60
	2	640,0	60
	3	640,0	60
Batch No. 5	1	660,0	30
	2	660,0	30
	3	660,0	30
Batch No. 6	1	760,0	30
	2	760,0	30
	3	760,0	30

Air flow rate for Batches No. 1, 2 and 3

	No.	Measured Vol. (mL)	t (s)
Control valve set for lower flow	1	10,0	9
	2	20,0	18
	3	30,0	28
Control valve set for higher flow	1	50,0	11
	2	50,0	11
	3	50,0	11

Air flow rate for Batches No. 4, 5 and 6

	No.	Measured Vol. (mL)	t (s)
Control valve set for lowest flow	1	20,0	49
	2	20,0	48
	3	20,0	49
	4	20,0	49
	5	20,0	48

Semi-batch operation in SFBBR-1 System

Liquid recirculation flow rate

	No.	Measured Vol. (mL)	t (s)
Week 1	1	815	30
	2	815	30
	3	815	30
Week 2	1	820	30
	2	825	30
	3	820	30
Week 3	1	820	30
	2	810	30
	3	820	30
Week 4	No.	Measured Vol.	t (s)

Air flow rate

	No.	Measured Vol. (mL)	t (s)
Control valve set for lowest flow	1	10,0	24
	2	10,0	24
	3	10,0	24
	4	10,0	24
	5	10,0	24
	6	10,0	24
	7	10,0	24
	8	10,0	24

		(mL)	
	1	805	30
	2	805	30
	3	805	30

Starting of Bioreactor in SFBBR-2 System

Liquid recirculation flow rate

	No.	Measured Vol. (mL)	t (s)
Week 1	1	775	60
	2	775	60
	3	780	60
Week 2	No.	Measured Vol. (mL)	t (s)
	1	275	60
	2	280	60
	3	275	60
Week 3	No.	Measured Vol. (mL)	t (s)
	1	395	60
	2	390	60
	3	395	60
Week 4	No.	Measured Vol. (mL)	t (s)
	1	400	60
	2	405	60
	3	405	60

Air flow rate

	No.	Measured Vol. (mL)	t (s)
Control valve set for low flow	1	10,0	4
	2	10,0	4
	3	10,0	4
	4	10,0	4

Batch operation in SFBBR-2 System

Liquid recirculation flow rate

	No.	Measured Vol. (mL)	t (s)
No. 1	1	300	60
	2	300	60
	3	300	60
No. 2	No.	Measured Vol. (mL)	t (s)
	1	395	60
	2	400	60
	3	400	60
No. 3	No.	Measured Vol. (mL)	t (s)
	1	400	60
	2	400	60
	3	400	60
No. 4	No.	Measured Vol. (mL)	t (s)
	1	400	60
	2	400	60
	3	400	60

Air flow rate

	No.	Measured Vol. (mL)	t (s)
Control valve set for low flow	1	10,0	4
	2	10,0	4
	3	10,0	4
	4	10,0	4

APPENDIX C: Operational conditions for batches No. 1 through 6 in SFBBR-1

- **Batch No. 1 in SFBBR-1:**
  - DO concentration and T values at the top of the packed bed biofilm

day	TC-DO (mg O_2/L)	DO-SEM (mg O_2/L)	TC-T (°C)	T- SEM (°C)
0	7,46	0,38	19,6	1,3
1	4,08	0,15	22,6	0,2
2	4,13	0,14	22,2	0,1
3	4,43	0,18	22,1	0,1
4	3,26	0,10	22,3	0,2
5	2,86	0,07	22,8	0,1
6	4,61	0,38	23,2	0,1
7	3,84	0,10	23,4	0,2
8	3,71	0,05	24,3	0,1
9	4,63	0,26	23,5	0,1
10	5,54	0,03	22,2	0,2
Avera. =	4,41	Avera. =	22,6	
SD =	1,24	SD =	1,2	
SEM =	0,37	SEM =	0,4	

  - Batch No. 1 in SFBBR-1: DO & T recorded at top of the packed bed biofilm by Portavo® 907 MULTI from Knick

Day No.	Data No.	time (h:min)	DO (mg O_2/L)	T (°C)	Day No.	Data No.	time (h:min)	DO (mg O_2/L)	T (°C)
0	1	16:09	6,63	16,1	4	41	00:09	3,51	22,4
	2	18:09	7,51	19,1		42	02:09	3,88	22,2
	3	20:09	8,45	21,1		43	04:09	3,53	21,9
	4	22:09	7,25	21,9		44	06:09	3,35	21,7
1	5	00:09	4,23	22,2		45	08:09	3,29	21,6
	6	02:09	5,05	22,2		46	10:09	3,41	21,9
	7	04:09	4,36	22,2		47	12:09	3,27	21,9
	8	06:09	3,77	22,1		48	14:09	3,28	22,1
	9	08:09	3,90	22,0		49	16:09	2,94	22,6
	10	10:09	4,25	22,0		50	18:09	2,63	23,0
	11	12:09	4,30	22,5		51	20:09	3,10	23,4
	12	14:09	3,46	22,9		52	22:09	2,90	23,4
	13	16:09	3,41	23	5	53	00:09	3,33	23,3
	14	18:09	4,51	23,4		54	02:09	3,05	22,9
	15	20:09	4,29	23,4		55	04:09	3,13	22,8
	16	22:09	3,39	23,1		56	06:09	2,86	22,6
2	17	00:09	3,95	22,6		57	08:09	3,06	22,4
	18	02:09	3,53	22,4		58	10:09	2,88	22,5
	19	04:09	3,62	22,1		59	12:09	2,68	22,6
	20	06:09	3,57	21,8		60	14:09	2,65	22,8
	21	08:09	3,96	21,9		61	16:09	2,62	22,8
	22	10:09	3,98	22,0		62	18:09	2,63	22,9
	23	12:09	4,29	21,9		63	20:09	2,73	23,1
	24	14:09	4,46	22,1		64	22:09	2,74	23,3
	25	16:09	3,93	22,3	6	65	00:09	2,47	23,3
	26	18:09	4,87	22,3		66	02:09	2,70	23,1
	27	20:09	5	22,3		67	04:09	2,87	22,9
	28	22:09	4,34	22,2		68	06:09	3,93	22,9
3	29	00:09	5,26	22,1		69	08:09	4,68	22,6
	30	02:09	5,17	22,0		70	10:09	5,32	22,7
	31	04:09	4,62	21,9		71	12:09	5,94	22,9
	32	06:09	5,13	21,7		72	14:09	6,02	23,1
	33	08:09	4,27	21,7		73	16:09	5,87	23,3

	34	10:09	4,79	21,7		74	18:09	5,49	23,5
	35	12:09	4,83	21,9		75	20:09	5,22	23,8
	36	14:09	3,74	22,1		76	22:09	4,86	23,9
	37	16:09	3,96	22,2					
	38	18:09	3,73	22,5					
	39	20:09	3,81	22,5					
	40	22:09	3,80	22,6					

Day No.	Data No.	time (h:min)	DO (mg O_2/L)	T (°C)	Day No.	Data No.	time (h:min)	DO (mg O_2/L)	T (°C)
7	77	00:09	4,60	23,6	10	113	00:09	5,69	23,1
	78	02:09	4,35	23,4		114	02:09	5,64	22,6
	79	04:09	4,04	23,0		115	04:09	5,60	22,2
	80	06:09	3,99	22,6		116	06:09	5,59	21,9
	81	08:09	3,85	22,5		117	08:09	5,53	21,8
	82	10:09	3,71	22,5		118	10:09	5,52	21,7
	83	12:09	3,59	22,9		119	12:09	5,47	21,9
	84	14:09	3,60	23,3		120	14:09	5,44	22,1
	85	16:09	3,64	23,7		121	16:09	5,40	22,5
	86	18:09	3,54	24,2					
	87	20:09	3,58	24,6					
	88	22:09	3,58	24,7					
8	89	00:09	3,63	24,5					
	90	02:09	3,53	24,4					
	91	04:09	3,64	24,1					
	92	06:09	3,47	23,9					
	93	08:09	3,47	23,6					
	94	10:09	3,76	23,5					
	95	12:09	3,94	23,8					
	96	14:09	3,76	24,3					
	97	16:09	3,93	24,6					
	98	18:09	3,72	24,9					
	99	20:09	3,75	25,0					
	100	22:09	3,89	24,8					
9	101	00:09	3,99	24,4					
	102	02:09	3,83	24,1					
	103	04:09	3,75	23,8					
	104	06:09	3,68	23,3					
	105	08:09	4,04	23,1					
	106	10:09	4,20	23,0					
	107	12:09	4,27	23,1					
	108	14:09	4,64	23,3					
	109	16:09	5,65	23,4					
	110	18:09	5,90	23,6					
	111	20:09	5,84	23,6					
	112	22:09	5,76	23,5					

- **Batch No. 2 in SFBBR-1:**
  - Operational conditions

Day No.	pH	TK-T (°C)	Total Vol. (L)	Vol. Sample taken (mL)	Vol. K_2CO_3 (mL)	Vol. K_2CO_3 consumed (mL)	TK-DO (mg O_2/L)
0	8,3	20,0	20,0	0,0	1000,0	0,0	-
1	8,6	24,0	19,9	80,0	1000,0	0,0	8,17
2	8,5	22,0	19,7	80,0	1000,0	0,0	9,29
3	7,7	23,3	19,5	80,0	1000,0	0,0	6,30
4	7,5	23,3	19,6	80,0	680,0	320,0	5,09
5	-	-	19,4	0,0	-	-	-
6	-	-	19,3	0,0	-	-	-

7	8,3	21,9	19,6	80,0	260,0	420,0	9,30
8	-	-	19,4	0,0	260,0	0,0	-
9	-	-	19,3	0,0	260,0	0,0	-
10	8,1	24,0	19,1	0,0	260,0	0,0	9,86
	Aver. =	22,6	Total =	400,0	Total =	740,0	Aver.= 8,00

- DO concentration and T values at the top of the packed bed biofilm

day	TC-DO (mg O_2/L)	DO-SEM (mg O_2/L)	TC-T (°C)	T- SEM (°C)
0	9,70	1,45	23,2	0,9
1	5,36	0,58	25,1	0,1
2	5,36	0,93	23,7	0,3
3	1,19	0,30	23,9	0,2
4	0,96	0,12	24,0	0,2
5	3,21	0,73	23,4	0,1
6	6,15	0,11	22,8	0,1
7	6,68	0,32	22,3	0,2
8	11,25	0,14	22,1	0,2
9	10,28	0,09	23,0	0,3
10	9,83	0,05	23,3	0,2
Avera. =	6,36	Avera. =	23,4	
SD =	3,61	SD =	0,9	
SEM =	1,09	SEM =	0,3	

- Batch No. 2 in SFBBR-1: DO & T recorded at the top of the packed bed biofilm by Portavo® 907 MULTI from Knick

Day No.	Data No.	time (h:min)	DO (mg O_2/L)	T (°C)	Day No.	Data No.	time (h:min)	DO (mg O_2/L)	T (°C)
0	1	15:21	7,24	19,8	4	42	01:21	1,07	24,7
	2	17:21	11,55	22,6		43	03:21	0,469	24,4
	3	19:21	12,92	24,0		44	05:21	0,700	23,9
	4	21:21	11,44	24,6		45	07:21	0,825	23,4
	5	23:21	5,35	24,8		46	09:21	0,678	22,9
1	6	01:21	6,18	25,0		47	11:21	0,660	23,1
	7	03:21	3,46	24,9		48	13:21	0,549	23,5
	8	05:21	5,25	24,9		49	15:21	1,78	24,0
	9	07:21	3,91	24,9		50	17:21	1,48	24,5
	10	09:21	4,65	24,9		51	19:21	1,40	24,8
	11	11:21	5,18	24,9		52	21:21	1,03	24,8
	12	13:21	4,05	25,0		53	23:21	0,918	24,5
	13	15:21	4,76	25,3	5	54	01:21	1,43	24,1
	14	17:21	3,26	25,5		55	03:21	1,01	23,6
	15	19:21	8,52	25,7		56	05:21	0,995	23,4
	16	21:21	10,0	25,5		57	07:21	1,11	23,1
	17	23:21	5,05	25,0		58	09:21	1,30	23,1
2	18	01:21	9,44	24,5		59	11:21	1,08	23,1
	19	03:21	5,69	24,0		60	13:21	1,45	23,3
	20	05:21	7,90	23,3		61	15:21	5,24	23,4
	21	07:21	10,59	22,6		62	17:21	5,89	23,5
	22	09:21	5,83	22,4		63	19:21	6,79	23,6
	23	11:21	8,73	22,5		64	21:21	6,21	23,6
	24	13:21	2,19	22,9		65	23:21	5,98	23,3
	25	15:21	2,25	23,4	6	66	01:21	5,99	23,0
	26	17:21	5,05	24,1		67	03:21	6,52	22,7
	27	19:21	3,59	24,8		68	05:21	6,15	22,5
	28	21:21	1,04	25,1		69	07:21	6,63	22,4
	29	23:21	2,05	24,9		70	09:21	6,16	22,5
3	30	01:21	1,03	24,4		71	11:21	6,50	22,6
	31	03:21	2,89	24,0		72	13:21	5,63	22,8

	32	05:21	1,46	23,4		73	15:21	5,65	22,9
	33	07:21	3,73	22,8		74	17:21	6,20	23,1
	34	09:21	0,694	22,8		75	19:21	5,71	23,1
	35	11:21	0,624	23,4		76	21:21	5,99	22,9
	36	13:21	1,14	23,5		77	23:21	6,72	22,5
	37	15:21	0,636	23,5					
	38	17:21	0,684	24,2					
	39	19:21	0,487	25,0					
	40	21:21	0,457	25,2					
	41	23:21	0,438	25,0					

Day No.	Data No.	time (h:min)	DO (mg O_2/L)	T (°C)	Day No.	Data No.	time (h:min)	DO (mg O_2/L)	T (°C)
7	78	01:21	6,18	22,1	9	111	19:21	9,91	24,3
	79	03:21	6,14	21,9		112	21:21	9,88	24,3
	80	05:21	6,19	21,7		113	23:21	9,91	24,1
	81	07:21	5,84	21,5	10	114	01:21	9,89	23,8
	82	09:21	6,83	21,5		115	03:21	9,91	23,5
	83	11:21	-	-		116	05:21	9,94	23,1
	84	13:21	7,24	22,1		117	07:21	10,02	22,6
	85	15:21	6,29	22,6		118	09:21	9,92	22,8
	86	17:21	5,82	22,6		119	11:21	9,62	23,1
	87	19:21	6,45	22,9		120	13:21	9,60	23,5
	88	21:21	6,90	23,1		121	15:21	9,76	24,0
	89	23:21	9,64	22,9					
8	90	01:21	11,63	22,4					
	91	03:21	11,91	21,9					
	92	05:21	11,84	21,6					
	93	07:21	11,73	21,3					
	94	09:21	11,57	21,3					
	95	11:21	11,41	21,5					
	96	13:21	11,20	21,7					
	97	15:21	11,02	22,0					
	98	17:21	10,85	22,5					
	99	19:21	10,66	23,1					
	100	21:21	10,61	23,3					
	101	23:21	10,54	23,1					
9	102	01:21	10,56	22,8					
	103	03:21	10,58	22,5					
	104	05:21	10,58	22,1					
	105	07:21	10,62	21,6					
	106	09:21	10,53	21,8					
	107	11:21	10,39	22,2					
	108	13:21	10,25	22,9					
	109	15:21	10,12	23,5					
	110	17:21	10,03	24,0					

- **Batch No. 3 in SFBBR-1:**
  - Operational conditions

Day No.	pH	TK-T (°C)	Total Vol. (L)	Vol. Sample taken (mL)	Vol. K_2CO_3 (mL)	Vol. K_2CO_3 consumed (mL)
0	8,3	20,0	20,0	0,0	1000,0	0,0
1	8,5	22,0	19,8	80,0	1000,0	0,0
2	7,5	22,0	19,6	80,0	950,0	0,0
3	7,5	22,0	20,1	80,0	200,0	750,0
4	-	-	19,8	0,0	-	0,0
5	-	-	19,7	0,0	-	0,0
6	8,1	22,0	19,5	0,0	200,0	0,0
	Aver. =	21,6	Total =	240,0	Total =	750,0

- DO concentration and T values at the top of the packed bed biofilm

day	TC-DO (mg O_2/L)	DO-SEM (mg O_2/L)	TC-T (°C)	T- SEM (°C)
0	9,16	0,33	22,0	0,7
1	10,70	0,22	22,2	0,1
2	11,61	0,42	22,5	0,2
3	10,15	0,81	22,9	0,2
4	7,81	0,25	22,7	0,1
5	8,55	0,02	22,9	0,2
6	8,44	0,01	23,0	0,2
Avera. =	9,49	Avera. =	22,6	
SD =	1,37	SD =	0,4	
SEM =	0,52	SEM =	0,1	

- Batch No. 3 in SFBBR-1: DO & T recorded at the top of the packed bed biofilm by Portavo® 907 MULTI from Knick

Day No.	Data No.	time (h:min)	DO (mg O_2/L)	T (°C)	Day No.	Data No.	time (h:min)	DO (mg O_2/L)	T (°C)
0	1	17:07	8,29	23,2	4	41	01:07	6,52	22,8
	2	19:07	9,80	20,2		42	03:07	6,67	22,4
	3	21:07	9,50	21,8		43	05:07	6,91	22,2
	4	23:07	9,03	22,6		44	07:07	7,19	22,1
1	5	01:07	10,11	22,5		45	09:07	7,51	22,0
	6	03:07	10,15	22,4		46	11:07	7,44	22,3
	7	05:07	9,51	22,4		47	13:07	8,24	22,4
	8	07:07	9,85	21,9		48	15:07	8,67	22,8
	9	09:07	10,23	22,1		49	17:07	8,66	23,1
	10	11:07	10,49	22,1		50	19:07	8,61	23,3
	11	13:07	11,26	22,1		51	21:07	8,63	23,3
	12	15:07	11,14	22,1		52	23:07	8,61	23,1
	13	17:07	10,87	21,9	5	53	01:07	8,62	22,9
	14	19:07	11,51	22,1		54	03:07	8,65	22,6
	15	21:07	11,26	22,4		55	05:07	8,62	22,4
	16	23:07	11,97	22,3		56	07:07	8,63	22,1
2	17	01:07	12,00	22,1		57	09:07	8,61	22,2
	18	03:07	12,22	22,1		58	11:07	8,59	22,4
	19	05:07	12,77	21,9		59	13:07	8,55	22,8
	20	07:07	14,28	21,7		60	15:07	8,51	23,1
	21	09:07	11,20	21,8		61	17:07	8,49	23,5
	22	11:07	8,28	22,0		62	19:07	8,46	23,6
	23	13:07	10,35	22,6		63	21:07	8,45	23,6
	24	15:07	12,79	22,8		64	23:07	8,42	23,6
	25	17:07	11,01	23,1	6	65	01:07	8,47	23,4
	26	19:07	11,52	23,3		66	03:07	8,42	23,3
	27	21:07	11,57	23,1		67	05:07	8,42	23,3
	28	23:07	11,35	23,1		68	07:07	8,44	22,6
3	29	01:07	12,60	23,0		69	09:07	8,47	22,4
	30	03:07	11,74	22,6					
	31	05:07	12,45	22,3					
	32	07:07	12,21	22,1					
	33	09:07	13,10	22,1					
	34	11:07	12,87	22,5					
	35	13:07	11,27	23,1					

	36	15:07	9,07	23,6					
	37	17:07	7,30	23,9					
	38	19:07	6,61	23,4					
	39	21:07	6,29	23,1					
	40	23:07	6,34	23					

- **Batch No. 4 in SFBBR-1:**
  - Operational conditions

Day No.	pH	TK-T (°C)	Total Vol. (L)	Vol. Sample taken (mL)	Vol. K_2CO_3 (mL)	Vol. K_2CO_3 consumed (mL)	TK-DO (mg O_2/L)
0	8,1	20,0	20,0	80,0	1000,0	0,0	4,56
1	8,4	23,0	19,9	80,0	1000,0	0,0	3,64
2	-	-	19,7	0,0	1000,0	-	-
3	8,3	22,0	19,7	80,0	1000,0	0,0	4,12
4	8,0	22,0	19,5	80,0	1000,0	0,0	3,45
5	-	-	19,4	0,0	-	-	-
6	-	-	19,3	0,0	-	-	-
7	7,5	22,0	19,7	80,0	580,0	420,0	2,22
8	7,5	22,0	19,8	80,0	370,0	210,0	2,40
9	7,9	24,0	19,8	80,0	240,0	130,0	5,30
10	8,4	24,0	19,6	80,0	240,0	0,0	6,09
11	8,5	23,0	19,5	80,0	240,0	0,0	5,98
12	-	-	19,3	0,0	-	-	-
13	-	-	19,3	0,0	-	-	-
14	8,4	22,0	19,2	0,0	240,0	0,0	6,86
	Aver. =	22,4	Total =	720,0	Total =	760,0	Aver.= 4,46

  - DO concentration and T values at the top of the packed bed biofilm

day	TC-DO (mg O_2/L)	DO-SEM (mg O_2/L)	TC-T (°C)	T- SEM (°C)
0	3,84	1,55	21,3	0,9
1	3,23	0,82	23,4	0,3
2	1,34	0,10	23,1	0,2
3	0,63	0,09	22,7	0,2
4	0,17	0,03	23,0	0,3
5	0,10	0,01	23,3	0,2
6	0,17	0,06	23,2	0,1
7	0,33	0,18	22,8	0,3
8	1,13	0,37	23,1	0,3
9	1,77	0,40	23,8	0,4
10	1,95	0,14	24,7	0,2
11	1,61	0,03	24,4	0,3
12	1,67	0,03	24,4	0,1
13	5,87	0,43	23,9	0,1
14	6,47	0,02	23,0	0,3
Avera. =	2,02	Avera. =	23,3	
SD =	2,01	SD =	0,8	
SEM =	0,52	SEM =	0,2	

- Batch No. 4 in SFBBR-1: DO & T recorded at the top of the packed bed biofilm by Portavo® 907 MULTI from Knick

Day No.	Data No.	time (h:min)	DO (mg O_2/L)	T (°C)	Day No.	Data No.	time (h:min)	DO (mg O_2/L)	T (°C)
0	1	14:31	0,419	18,1	4	42	00:31	0,369	23,6
	2	16:31	0,564	20,7		43	02:31	0,118	23,1
	3	18:31	6,97	22,0		44	04:31	0,177	22,5
	4	20:31	3,48	22,6		45	06:31	0,290	21,7
	5	22:31	7,79	23,0		46	08:31	0,302	21,5
1	6	00:31	7,11	23,0		47	10:31	0,243	21,9
	7	02:31	4,63	22,8		48	12:31	0,108	22,4
	8	04:31	7,92	22,5		49	14:31	0,106	23,1
	9	06:31	1,80	22,1		50	16:31	0,077	23,8
	10	08:31	1,31	22,0		51	18:31	0,078	24,3
	11	10:31	1,93	22,4		52	20:31	0,073	24,3
	12	12:31	-	-		53	22:31	0,074	24,1
	13	14:31	2,11	23,8	5	54	00:31	0,073	23,8
	14	16:31	0,975	24,5		55	02:31	0,078	23,4
	15	18:31	1,49	24,9		56	04:31	0,152	23,0
	16	20:31	0,895	25,0		57	06:31	0,143	22,6
	17	22:31	0,715	24,9		58	08:31	0,110	22,5
2	18	00:31	1,21	24,6		59	10:31	0,082	22,6
	19	02:31	1,76	24,1		60	12:31	0,094	22,8
	20	04:31	1,82	23,6		61	14:31	0,078	23,3
	21	06:31	0,773	22,8		62	16:31	0,076	23,6
	22	08:31	1,02	22,5		63	18:31	0,094	23,8
	23	10:31	1,08	22,6		64	20:31	0,101	24,0
	24	12:31	1,60	22,8		65	22:31	0,080	24,0
	25	14:31	1,04	22,9	6	66	00:31	0,080	23,6
	26	16:31	1,25	23,0		67	02:31	0,073	23,3
	27	18:31	1,24	22,8		68	04:31	0,085	22,9
	28	20:31	1,73	22,6		69	06:31	0,075	22,6
	29	22:31	1,60	22,9		70	08:31	0,171	22,5
3	30	00:31	1,13	22,8		71	10:31	0,094	22,6
	31	02:31	0,676	22,6		72	12:31	0,247	23,0
	32	04:31	0,844	22,4		73	14:31	0,116	23,3
	33	06:31	0,787	21,7		74	16:31	0,769	23,5
	34	08:31	0,739	21,6		75	18:31	0,107	23,6
	35	10:31	0,511	21,9		76	20:31	0,082	23,8
	36	12:31	0,452	22,2		77	22:31	0,117	23,6
	37	14:31	0,179	22,6					
	38	16:31	1,14	23,1					
	39	18:31	0,420	23,5					
	40	20:31	0,399	23,8					
	41	22:31	0,314	24,0					

Day No.	Data No.	time (h:min)	DO (mg O_2/L)	T (°C)	Day No.	Data No.	time (h:min)	DO (mg O_2/L)	T (°C)
7	78	00:31	0,083	23,4	10	122	16:31	1,58	24,9
	79	02:31	0,083	22,9		123	18:31	1,55	25,4
	80	04:31	0,081	22,5		124	20:31	1,51	25,7
	81	06:31	0,086	21,7		125	22:31	1,52	25,8
	82	08:31	0,084	21,5	11	126	00:31	1,53	25,5
	83	10:31	0,086	21,7		127	02:31	1,58	25,0
	84	12:31	-	-		128	04:31	1,63	24,4
	85	14:31	0,097	22,6		129	06:31	1,71	23,6
	86	16:31	2,19	23,3		130	08:31	1,73	23,1
	87	18:31	0,188	23,8		131	10:31	1,74	23,1
	88	20:31	0,102	24,0		132	12:31	1,66	23,5
	89	22:31	0,101	24,0		133	14:31	1,62	23,9
8	90	00:31	1,49	23,6		134	16:31	1,60	24,4

	91	02:31	3,00	23,3		135	18:31	1,53	25,0
	92	04:31	0,215	22,6		136	20:31	1,49	25,6
	93	06:31	1,06	21,9		137	22:31	1,48	25,7
	94	08:31	0,104	21,6		138	00:31	1,53	25,3
	95	10:31	-	-		139	02:31	1,57	24,7
	96	12:31	0,537	22,2		140	04:31	1,62	24,3
	97	14:31	0,081	22,9		141	06:31	1,67	23,9
	98	16:31	3,28	23,5		142	08:31	1,68	23,8
	99	18:31	2,35	24,1	12	143	10:31	1,68	24,0
	100	20:31	0,209	24,6		144	12:31	1,65	24,3
	101	22:31	0,09	24,8		145	14:31	1,66	24,4
	102	00:31	0,086	24,4		146	16:31	1,67	24,6
	103	02:31	0,081	23,9		147	18:31	1,70	24,7
	104	04:31	0,103	23,3		148	20:31	1,77	24,7
	105	06:31	1,06	22,4		149	22:31	1,87	24,5
9	106	08:31	1,71	22,0		150	00:31	2,20	24,1
	107	10:31	1,76	22,1		151	02:31	3,44	23,8
	108	12:31	1,75	23,0		152	04:31	5,65	23,5
	109	14:31	1,72	23,9		153	06:31	6,57	23,4
	110	16:31	1,78	24,6		154	08:31	6,76	23,4
	111	18:31	3,89	25,1	13	155	10:31	6,79	23,4
	112	20:31	3,75	25,5		156	12:31	6,69	23,6
	113	22:31	3,58	25,4		157	14:31	6,64	23,8
	114	00:31	2,35	25,3		158	16:31	6,53	24,1
	115	02:31	1,95	25,0		159	18:31	6,47	24,4
	116	04:31	3,05	24,7		160	20:31	6,37	24,8
10	117	06:31	2,46	23,9		161	22:31	6,35	24,7
	118	08:31	2,08	23,6		162	00:31	6,41	24,1
	119	10:31	1,96	23,8		163	02:31	6,41	23,6
	120	12:31	1,70	24,0		164	04:31	6,45	23,3
	121	14:31	1,64	24,4	14	165	06:31	6,52	22,4
						166	08:31	6,53	22,1
						167	10:31	6,47	22,4

- **Batch No. 5 in SFBBR-1:**
  - Operational conditions

Day No.	pH	TK-T (°C)	Total Vol. (L)	Vol. Sample taken (mL)	Vol. K_2CO_3 (mL)	Vol. K_2CO_3 consumed (mL)	TK-DO (mg O_2/L)
0	8,3	21,0	20,0	80,0	1000,0	0,0	3,76
1	8,6	24,0	19,8	80,0	1000,0	0,0	2,94
2	8,5	23,0	19,6	80,0	1000,0	0,0	2,90
3	8,2	24,0	19,4	80,0	1000,0	0,0	2,56
4	7,7	23,0	19,2	80,0	1000,0	0,0	2,69
5	-	-	19,0	0,0	-	-	-
6	-	-	18,9	0,0	-	-	-
7	7,5	22,0	19,4	80,0	370,0	630,0	2,52
8	8,3	23,0	19,3	80,0	290,0	80,0	5,10
9	8,4	22,0	19,1	80,0	290,0	0,0	5,06
10	8,4	24,0	18,9	80,0	290,0	0,0	4,97
11	8,2	23,0	18,7	0,0	290,0	0,0	6,68
	Aver. =	22,9	Total =	720,0	Total =	710	Aver.= 3,92

  - DO concentration and T values at the top of the packed bed biofilm

day	TC-DO (mg O_2/L)	DO-SEM (mg O_2/L)	TC-T (°C)	T- SEM (°C)
0	0,603	0,23	22,0	1,7
1	0,101	0,01	25,2	0,3

2	0,076	0,01	24,7	0,3
3	0,075	0,00	25,1	0,2
4	0,092	0,00	24,8	0,3
5	0,091	0,00	24,6	0,2
6	0,099	0,00	23,9	0,2
7	0,532	0,24	23,7	0,3
8	2,38	0,03	24,1	0,4
9	2,42	0,04	23,8	0,4
10	2,85	0,19	24,7	0,1
11	6,10	0,32	23,3	0,3
Avera. =	1,29	Avera. =	24,2	
SD =	1,85	SD =	0,9	
SEM =	0,53	SEM =	0,3	

- Batch No. 5 in SFBBR-1: DO & T recorded at the top of the packed bed biofilm by Portavo® 907 MULTI from Knick

Day No.	Data No.	time (h:min)	DO (mg O_2/L)	T (°C)	Day No.	Data No.	time (h:min)	DO (mg O_2/L)	T (°C)
0	1	14:02	1,50	15,9	4	42	00:02	0,080	25,7
	2	16:02	0,577	20,5		43	02:02	0,084	25,2
	3	18:02	0,393	23,3		44	04:02	0,087	24,7
	4	20:02	0,304	24,8		45	06:02	0,089	23,9
	5	22:02	0,240	25,4		46	08:02	0,092	23,4
1	6	00:02	0,187	25,4		47	10:02	0,096	23,4
	7	02:02	0,147	25,2		48	12:02	-	-
	8	04:02	0,12	24,8		49	14:02	0,115	24,5
	9	06:02	0,102	24,3		50	16:02	0,101	25,1
	10	08:02	0,090	23,9		51	18:02	0,094	25,5
	11	10:02	0,081	24,0		52	20:02	0,090	25,7
	12	12:02	-	-		53	22:02	0,089	25,7
	13	14:02	0,112	25,4	5	54	00:02	0,086	25,2
	14	16:02	0,082	25,8		55	02:02	0,085	24,8
	15	18:02	0,068	26,2		56	04:02	0,085	24,3
	16	20:02	0,063	26,2		57	06:02	0,087	23,9
	17	22:02	0,064	26,1		58	08:02	0,090	23,6
2	18	00:02	0,069	25,7		59	10:02	0,092	23,9
	19	02:02	0,070	25,0		60	12:02	0,093	24,3
	20	04:02	0,073	24,4		61	14:02	0,094	24,7
	21	06:02	0,075	23,5		62	16:02	0,094	25,0
	22	08:02	0,073	23,0		63	18:02	0,096	25,2
	23	10:02	0,073	23,3		64	20:02	0,096	25,3
	24	12:02	-	-		65	22:02	0,094	25,2
	25	14:02	0,130	24,6	6	66	00:02	0,093	24,5
	26	16:02	0,079	25,2		67	02:02	0,093	23,9
	27	18:02	0,065	25,7		68	04:02	0,094	23,4
	28	20:02	0,061	25,9		69	06:02	0,095	23,0
	29	22:02	0,064	25,9		70	08:02	0,097	22,7
3	30	00:02	0,067	25,7		71	10:02	0,100	22,9
	31	02:02	0,071	25,3		72	12:02	0,101	23,4
	32	04:02	0,072	24,9		73	14:02	0,104	23,8
	33	06:02	0,073	24,3		74	16:02	0,105	24,2
	34	08:02	0,075	23,9		75	18:02	0,104	24,6
	35	10:02	0,076	23,8		76	20:02	0,104	24,9
	36	12:02	-	-		77	22:02	0,101	24,9
	37	14:02	0,092	25,0					
	38	16:02	0,077	25,5					
	39	18:02	0,072	25,9					
	40	20:02	0,072	26,1					
	41	22:02	0,076	26,0					

Day No.	Data No.	time (h:min)	DO (mg O_2/L)	T (°C)
7	78	00:02	0,098	24,4
	79	02:02	0,097	23,6
	80	04:02	0,100	23,1
	81	06:02	0,104	22,4
	82	08:02	0,108	22,1
	83	10:02	0,113	22,2
	84	12:02	0,210	22,9
	85	14:02	0,124	23,6
	86	16:02	0,131	24,4
	87	18:02	0,845	24,9
	88	20:02	2,18	25,4
	89	22:02	2,27	25,5
8	90	00:02	2,29	25,1
	91	02:02	2,38	24,5
	92	04:02	2,42	23,9
	93	06:02	2,47	23,1
	94	08:02	2,52	22,5
	95	10:02	2,51	22,6
	96	12:02	-	-
	97	14:02	-	-
	98	16:02	-	-
	99	18:02	2,29	25,0
	100	20:02	2,28	25,0
	101	22:02	2,29	25,00
9	102	00:02	2,31	24,7
	103	02:02	2,32	24,3
	104	04:02	2,37	23,8
	105	06:02	2,44	23,0
	106	08:02	2,50	22,4
	107	10:02	-	-
	108	12:02	-	-
	109	14:02	-	-
	110	16:02	2,59	24,6
10	111	17:01	2,54	24,4
	112	19:01	2,63	24,6
	113	21:01	2,83	24,8
	114	23:01	3,39	24,8
11	115	01:01	4,61	24,4
	116	03:01	5,87	23,9
	117	05:01	6,44	23,3
	118	07:01	6,70	22,6
	119	09:01	6,62	22,5
	120	11:01	-	-
	121	13:01	-	-
	122	15:01	-	-
	123	16:20	6,38	23,1

- **Batch No. 6 in SFBBR-1:**
  - Operational conditions

Day No.	pH	TK-T (°C)	Total Vol. (L)	Vol. Sample taken (mL)	Vol. K_2CO_3 (mL)	Vol. K_2CO_3 consumed (mL)	TK-DO (mg O_2/L)
0	8,1	21,0	20,0	80,0	1000,0	0,0	3,95
1	8,3	23,0	19,8	80,0	1000,0	0,0	4,37
2	8,2	23,0	19,6	80,0	1000,0	0,0	3,53
3	7,8	23,0	19,3	80,0	1000,0	0,0	2,99
4	7,5	23,0	19,2	80,0	880,0	120,0	3,50
5	-	-	19,0	0,0	-	-	-
6	-	-	18,9	0,0	-	-	-

7	8,6	22,0	19,4	80,0	205,0	675,0	5,21
8	8,6	22,0	19,2	80,0	205,0	0,0	4,96
9	8,6	22,0	19,0	80,0	205,0	0,0	5,29
10	8,5	22,0	18,8	0,0	205,0	0,0	7,00
	Aver. =	22,3	Total =	640,0	Total =	795,0	Aver.= 4,53

- DO concentration and T values at the top of the packed bed biofilm

day	TC-DO (mg O_2/L)	DO-SEM (mg O_2/L)	TC-T (°C)	T- SEM (°C)
0	1,04	0,15	22,7	0,8
1	0,539	0,13	24,2	0,4
2	0,074	0,01	24,5	0,2
3	0,084	0,00	24,2	0,4
4	0,077	0,00	24,3	0,2
5	0,078	0,00	23,6	0,1
6	0,080	0,00	22,9	0,1
7	1,29	0,43	22,6	0,3
8	2,77	0,03	22,7	0,2
9	4,77	0,62	22,8	0,4
10	6,85	0,04	22,4	0,3
Avera. =	1,60	Avera. =	23,3	
SD =	2,28	SD =	0,8	
SEM =	0,69	SEM =	0,2	

- Batch No. 6 in SFBBR-1: DO & T recorded at the top of the packed bed biofilm by Portavo® 907 MULTI from Knick

Day No.	Data No.	time (h:min)	DO (mg O_2/L)	T (°C)	Day No.	Data No.	time (h:min)	DO (mg O_2/L)	T (°C)
0	1	15:31	1,37	19,8	4	42	00:35	0,072	24,7
	2	17:31	1,26	22,1		43	02:35	0,073	24,4
	3	19:31	1,23	23,4		44	04:35	0,072	24,0
	4	21:31	0,731	24,1		45	06:35	0,071	23,5
	5	23:31	0,607	24,1		46	08:35	0,071	23,4
1	6	01:31	0,601	23,9		47	10:35	-	-
	7	03:31	0,953	23,5		48	12:35	-	-
	8	05:31	1,04	23,0		49	14:35	-	-
	9	07:31	0,876	22,5		50	16:35	-	-
	10	09:31	0,781	22,8		51	18:35	0,097	24,7
	11	11:31	-	-		52	20:35	0,080	24,8
	12	13:31	-	-		53	22:35	0,077	24,7
	13	14:35	-	-	5	54	00:35	0,074	24,2
	14	16:35	0,272	25,1		55	02:35	0,074	23,9
	15	18:35	0,136	25,6		56	04:35	0,074	23,5
	16	20:35	0,107	25,8		57	06:35	0,074	23,1
	17	22:35	0,087	25,4		58	08:35	0,075	23,0
2	18	00:35	0,074	25,0		59	10:35	0,077	23,3
	19	02:35	0,060	24,5		60	12:35	0,078	23,5
	20	04:35	0,056	23,9		61	14:35	0,079	23,6
	21	06:35	0,05	23,4		62	16:35	0,080	23,8
	22	08:35	0,045	23,3		63	18:35	0,081	24,1
	23	10:35	-	-		64	20:35	0,082	24,1
	24	12:35	-	-		65	22:35	0,082	23,5
	25	14:35	0,122	24,5	6	66	00:35	0,081	23,0
	26	16:35	0,089	24,9		67	02:35	0,080	22,6
	27	18:35	0,080	25,3		68	04:35	0,081	22,3
	28	20:35	0,080	25,4		69	06:35	0,082	22,4
	29	22:35	0,081	25,1		70	08:35	0,084	22,4
3	30	00:35	0,084	24,5		71	10:35	0,085	22,6

	31	02:35	0,087	23,9		72	12:35	0,086	22,9
	32	04:35	0,092	23,3		73	14:35	0,087	23,1
	33	06:35	0,098	22,6		74	16:35	0,088	23,1
	34	08:35	0,098	22,5		75	18:35	0,079	23,4
	35	10:35	-	-		76	20:35	0,069	23,4
	36	12:35	-	-		77	22:35	0,059	23,1
	37	14:35	-	-					
	38	16:35	0,077	25,3					
	39	18:35	0,072	25,4					
	40	20:35	0,072	25,2					
	41	22:35	0,072	24,9					

Day No.	Data No.	time (h:min)	DO (mg O_2/L)	T (°C)	Day No.	Data No.	time (h:min)	DO (mg O_2/L)	T (°C)
7	78	00:35	0,051	22,6	9	104	04:35	2,92	21,7
	79	02:35	0,047	22,2		105	06:35	3,05	21,3
	80	04:35	0,042	21,8		106	08:35	3,17	21,2
	81	06:35	0,040	21,4		107	10:35	-	-
	82	08:35	0,040	21,5		108	12:35	-	-
	83	10:35	0,041	21,9		109	14:35	5,59	22,8
	84	12:35	-	-		110	16:35	6,84	23,5
	85	14:35	2,88	22,9		111	18:35	6,81	24,0
	86	16:35	2,80	23,4		112	20:35	6,90	24,3
	87	18:35	2,76	23,6		113	22:35	6,87	23,9
	88	20:35	2,73	23,7	10	114	00:35	6,91	23,4
	89	22:35	2,74	23,4		115	02:35	6,93	22,9
8	90	00:35	2,79	22,9		116	04:35	6,92	22,2
	91	02:35	2,83	22,4		117	06:35	6,75	21,8
	92	04:35	2,90	21,9		118	08:35	6,74	21,7
	93	06:35	2,92	21,5					
	94	08:35	2,93	21,6					
	95	10:35	2,86	22,1					
	96	12:35	2,78	22,4					
	97	14:35	2,71	22,8					
	98	16:35	2,67	23,4					
	99	18:35	2,61	23,8					
	100	20:35	2,61	23,8					
	101	22:35	2,67	23,40					
9	102	00:35	2,74	22,8					
	103	02:35	2,82	22,2					

APPENDIX D: Operational conditions for semi-batch process in SFBBR-1

- Operational conditions

Day No.	pH	TK-T (°C)	Total Vol. (L)	Vol. Sample taken (mL)	Vol. Na_2CO_3 (mL)	Vol. Na_2CO_3 consumed (mL)
0	8,1	20,0	20,0	80,0	1000,0	0,0
1	8,4	23,0	19,8	80,0	1000,0	0,0
2	8,2	24,0	19,5	80,0	1000,0	0,0
3	7,7	24,0	19,3	80,0	1000,0	0,0
4	7,5	23,0	19,3	80,0	830,0	170,0
5	-	-	19,0	0,0	-	-
6	-	-	18,9	0,0	-	-
7-B	8,5	22,0	19,1	0,0	450,0	380,0
7-A	8,1	22,0	19,1	0,0	450,0	0,0
8-B	7,6	22,0	19,0	0,0	370,0	80,0
8-A	7,8	22,0	19,0	0,0	370,0	0,0
9-B	7,6	23,0	19,0	0,0	290,0	80,0
9-A	7,9	23,0	19,0	0,0	290,0	0,0
10-B	7,6	22,0	18,9	0,0	210,0	80,0
10-A	7,9	22,0	18,9	0,0	210,0	0,0
11-B	7,5	22,0	18,8	0,0	130,0	80,0
11-A	8,0	22,0	18,8	0,0	1000,0	0,0
12	-	-	18,7	0,0	-	-
13	-	-	18,5	0,0	-	-
14-B	7,5	22,0	18,6	0,0	770,0	230,0
14-A	7,9	22,0	18,6	0,0	770,0	0,0
15-B	7,6	22,0	18,5	0,0	690,0	80,0
15-A	7,8	22,0	18,5	0,0	690,0	0,0
16-B	7,5	22,0	18,5	0,0	610,0	80,0
16-A	7,8	22,0	18,5	0,0	610,0	0,0
17-B	7,5	22,0	18,4	0,0	535,0	75,0
17-A	7,8	22,0	18,4	0,0	535,0	0,0
18-B	7,6	22,0	18,3	0,0	450,0	85,0
18-A	7,9	22,0	18,3	0,0	450,0	0,0
19	-	-	18,2	0,0	-	-
20	-	-	18,0	0,0	-	-
21-B	7,7	21,0	18,1	0,0	210,0	240,0
21-A	7,7	21,0	18,1	0,0	210,0	0,0
22-B	7,5	22,0	18,0	0,0	125,0	85,0
22-A	7,7	22,0	18,0	0,0	200,0	0,0
23-B	7,6	22,0	18,0	0,0	120,0	80,0
23-A	7,8	22,0	18,0	0,0	1000,0	0,0
24-B	7,5	22,0	17,9	0,0	915,0	85,0
24-A	7,7	22,0	17,9	0,0	915,0	0,0
25	7,6	22,0	17,8	0,0	830,0	85,0
0	Aver. =	22,1	Total =	400,0	Total =	1995,0

- DO concentration and T values at the top of the packed bed biofilm and DO concentration in the collection tank

Day No.	TC-DO (mg O_2/L)	TK-DO (mg O_2/L)	TC-T (°C)
0	0,402	3,72	23,3
1	0,120	3,30	24,0
2	0,059	3,06	25,3
3	0,055	2,75	24,7
4	0,065	2,21	23,1
5	0,125	-	23,3
6	2,74	-	22,8

7-B	3,25	4,95	21,7
7-A	0,254	3,55	23,7
8-B	2,31	4,33	22,1
8-A	0,215	3,20	23,8
9-B	2,59	4,52	23,2
9-A	0,190	2,74	23,1
10-B	4,26	5,26	22,2
10-A	0,165	2,39	22,8
11-B	1,49	3,65	21,9
11-A	0,084	1,57	22,4
12	0,098	-	22,4
13	0,115	-	22,0
14-B	1,79	3,96	21,5
14-A	0,158	2,26	22,7
15-B	2,68	4,59	21,7
15-A	0,106	1,62	22,5
16-B	1,72	3,73	21,7
16-A	0,117	1,67	22,2
17-B	0,189	2,24	21,6
17-A	0,102	1,37	22,2
18-B	0,120	2,61	21,9
18-A	0,119	2,52	22,5
19	0,150	-	21,8
20	0,143	-	21,5
21-B	3,38	5,22	21,3
21-A	0,145	1,82	21,9
22-B	1,80	3,63	21,5
22-A	0,188	1,90	22,2
23-B	3,50	4,78	21,7
23-A	0,370	2,20	22,1
24-B	1,12	3,47	21,0
24-A	0,379	2,25	22,8
25	1,24	4,11	22,1
Avera. =	0,95	3,15	22,5

APPENDIX E: Operational conditions for starting and batch in SFBBR-2

- **Starting of bioreactor in SFBBR-2:**
  - Operational conditions

Day No.	pH	TK-T (°C)	Total Vol. (L)	Vol. Sample taken (mL)	Vol. Na_2CO_3 consume (mL)	Vol. H_2SO_4 consumed (mL)
0	8,2	20,0	25,0	50,0	0,0	0,0
1	-		24,9	0,0	-	-
2	-		24,8	0,0	-	-
3	9,1	22,0	24,7	80,0	0,0	0,0
4	9,2	22,0	24,6	0,0	0,0	0,0
5	9,2	22,0	24,5	0,0	0,0	0,0
6	9,2	22,0	24,4	0,0	0,0	0,0
7	9,2	22,5	25,0	80,0	0,0	600,0
7	7,8	22,5	25,0	0,0	0,0	-
8	-	-	24,8	0,0	-	-
9	-	-	24,7	0,0	-	-
10-B	7,8	21,0	24,6	80,0	0,0	-
10-A	8,3	21,0	24,6	0,0	0,0	320,0
11	7,5	24,0	25,0	80,0	0,0	195,0
12	6,6	24,0	25,0	80,0	100,0	5,0
13	7,5	24,0	25,0	80,0	165,0	0,0
14-B	7,5	23,0	25,2	80,0	210,0	-
14-A	7,9	23,0	25,2	0,0	25,0	14,0
15	-	-	25,1	0,0	-	-
16	-	-	25,1	0,0	-	-
17	7,5	22,0	25,4	80,0	430,0	0,0
18	8,2	22,0	25,5	0,0	90,0	25,0
18	7,5	22,0	25,5		0,0	-
19-B	7,5	23,0	25,4	80,0	0,0	-
19-A	8,2	23,0	25,4		0,0	130,0
20	7,5	22,0	25,6	0,0	70,0	0,0
21-B	7,7	21,0	25,6	80,0	130,0	-
21-A	8,2	21,0	25,6	0,0	0,0	40,0
22	-	-	25,6	0,0	-	-
23	-	-	25,6	0,0	-	-
24-B	7,8	21,0	25,7	0,0	160,0	0,0
24-A	8,2	21,0	25,7	0,0	0,0	0,0
25	7,5	21,0	25,7	0,0	25,0	0,0
26-B	7,8	21,0	25,8	0,0	115,0	0,0
26-A	8,1	21,0	25,8	0,0	0,0	0,0
27	7,5	21,0	25,8	0,0	30,0	0,0
28-B	8,0	21,0	25,9	0,0	105,0	0,0
28-A	8,2	21,0	25,9	0,0	0,0	0,0
29	-	-	25,8	0,0	-	-
30	-	-	25,8	0,0	-	-
31	8,2	21,0	26,0	0,0	200,0	0,0
	Aver. =	21,9	Total =	850,0	1855,0	1329,0

  - DO concentration and T values at the top of the packed bed biofilm and DO concentration in the collection tank

Day No.	TC-DO (mg O_2/L)	TK-DO (mg O_2/L)	TC-T (°C)
0	-	-	-
1	-	-	-
2	-	-	-
3	-	8,47	-

4	-	8,20	-
5	7,66	7,52	-
6	7,04	7,21	23,5
7	-	-	23,7
7	-	8,68	-
8	-	-	23,0
9	-	-	23,1
10-B	4,84	4,78	21,9
10-A	-	-	21,9
11	5,96	6,56	23,8
12	3,19	4,60	24,9
13	3,40	3,76	-
14-B	2,65	3,36	23,4
14-A	-	-	23,4
15	-	-	-
16	-	-	-
17	3,37	4,71	21,7
18	7,85	7,62	21,5
18	-	-	21,5
19-B	8,27	8,22	22,6
19-A			22,6
20	3,49	3,74	21,2
21-B	6,34	6,50	20,8
21-A	-	4,45	20,8
22	-	-	-
23	-	-	-
24-B	-	7,72	21,8
24-A	0,540	4,39	21,8
25	-	3,94	-
26-B	7,14	7,22	21,0
26-A	0,900	3,18	21,0
27	-	2,76	-
28-B	7,98	8,12	21,0
28-A	2,18	5,39	21,0
29	-	-	-
30	-	-	-
31	8,35	8,44	20,1
Avera. =	days 24 -31: 4,52	days 24 -31: 5,43	22,1

- **Batch in SFBBR-2:**
  - Operational conditions

Day No.	pH	TK-T (°C)	Total Vol. (L)	Vol. Sample taken (mL)	Vol. Na_2CO_3 consumed (mL)	Vol. H_2SO_4 consumed (mL)	TK-DO (mg O_2/L)
0	8,2	21,0	30,0	0,0	0,0	0,0	2,81
1	8,3	21,0	30,0	80,0	0,0	0,0	1,06
2	8,3	21,0	29,9	80,0	0,0	0,0	2,63
3	8,3	21,0	29,9	80,0	0,0	190,0	3,32
4	8,2	21,0	29,8	80,0	0,0	10,0	2,64
5	-	-	29,7	-	-	-	
6	-	-	29,7	-	-	-	
7	7,5	22,0	29,9	80,0	220,0	0,0	2,28
8	7,6	22,0	29,9	80,0	175,0	0,0	3,21
9	7,6	22,0	30,0	80,0	180,0	0,0	3,85
10	7,5	22,0	30,0	80,0	160,0	0,0	5,30
11	7,5	22,0	30,0	0,0	20,0	0,0	6,54
	Aver. =	21,5	Total =	640,0	755,0	200,0	Aver.= 3,36

- DO concentration and T values at the top of the packed bed biofilm

day	TC-DO (mg O_2/L)	DO-SEM (mg O_2/L)	TC-T (°C)	T- SEM (°C)
0	0,435	0,14	20,9	0,1
1	0,301	0,06	20,7	0,2
2	0,151	0,00	20,9	0,2
3	0,147	0,00	20,6	0,1
4	0,122	0,00	21,9	0,1
5	0,120	0,00	21,6	0,1
6	0,213	0,01	21,4	0,1
7	0,280	0,01	21,4	0,2
8	0,586	0,10	21,5	0,1
9	0,87	0,13	21,5	0,1
10	3,56	0,69	21,5	0,1
11	6,13	0,09	21,3	0,1
Avera. =	1,08	Avera. =	21,3	
SD =	1,86	SD =	0,4	
SEM =	0,54	SEM =	0,1	

- DO & T recorded at the top of the packed bed biofilm by Portavo® 907 MULTI

Day No.	Data No.	time (h:min)	DO (mg O_2/L)	T (°C)	Day No.	Data No.	time (h:min)	DO (mg O_2/L)	T (°C)
0	1	16:48	0,856	20,8	6	46	00:48	0,145	21,6
	2	18:48	0,311	21,0		47	02:48	0,183	21,4
	3	20:48	0,325	20,9		48	04:48	0,198	21,1
	4	22:48	0,248	20,7		49	06:48	0,216	21,1
1	5	00:48	0,329	20,5		50	08:48	0,210	21,1
	6	02:48	0,508	20,3		51	10:48	0,208	21,1
	7	04:48	0,234	20,1		52	12:48	0,220	21,2
	8	06:48	0,529	19,8		53	14:48	0,226	21,4
	9	08:48	0,569	20,0		54	16:48	0,234	21,5
	10	16:48	0,148	21,5		55	18:48	0,248	21,6
	11	18:48	0,132	21,5		56	20:48	0,233	21,6
	12	20:48	0,129	21,3		57	22:48	0,233	21,5
	13	22:48	0,127	21,2	7	58	00:48	0,250	21,2
2	14	00:48	0,136	20,9		59	02:48	0,248	21,1
	15	02:48	0,158	20,7		60	04:48	0,236	20,9
	16	04:48	0,153	20,4		61	06:48	0,244	20,7
	17	06:48	0,155	20,2		62	08:48	0,246	20,8
	18	08:48	0,156	20,2		63	10:48	0,276	21,1
	19	16:48	0,157	21,5		64	12:48	-	-
	20	18:48	0,153	21,4		65	14:48	0,329	21,9
	21	20:48	0,148	21,3		66	16:48	0,304	22,1
	22	22:48	0,147	21,1		67	18:48	0,312	22,0
3	23	00:48	0,148	21,0		68	20:48	0,327	21,7
	24	02:48	0,147	20,8		69	22:48	0,311	21,7
	25	04:48	0,149	20,6	8	70	00:48	0,317	21,5
	26	06:48	0,144	20,3		71	02:48	0,323	21,5
	27	08:48	0,146	20,4		72	04:48	0,329	21,1
4	28	12:48	0,155	21,5		73	06:48	0,354	21,0
	29	14:48	0,122	21,9		74	08:48	0,366	21,0
	30	16:48	0,118	22,1		75	16:48	0,609	22,0
	31	18:48	0,115	22,1		76	18:48	0,844	21,9
	32	20:48	0,112	22,1		77	20:48	0,803	21,8
	33	22:48	0,112	21,9		78	22:48	1,33	21,7
5	34	00:48	0,111	21,7	9	79	00:48	1,38	21,6
	35	02:48	0,114	21,5		80	02:48	1,40	21,5
	36	04:48	0,116	21,4		81	04:48	1,47	21,1
	37	06:48	0,114	21,2		82	06:48	0,982	20,9
	38	08:48	0,116	21,1		83	08:48	0,962	21,0
	39	10:48	0,120	21,1		84	10:48	0,861	21,1

	40	12:48	0,123	21,3		85	14:48	0,367	21,7
	41	14:48	0,119	21,6		86	16:48	0,408	21,9
	42	16:48	0,120	21,9		87	18:48	0,391	21,9
	43	18:48	0,123	22,1		88	20:48	0,880	21,9
	44	20:48	0,127	22,1		89	22:48	0,470	21,8
	45	22:48	0,133	21,9					

Day No.	Data No.	time (h:min)	DO (mg O_2/L)	T (°C)
10	90	00:48	0,534	21,7
	91	02:48	0,676	21,6
	92	04:48	1,01	21,3
	93	06:48	1,72	21,0
	94	08:48	2,71	21,1
	95	10:48	3,59	21,1
	96	14:48	5,35	21,6
	97	16:48	5,93	21,8
	98	18:48	5,66	21,7
	99	20:48	6,00	21,7
	100	22:48	5,96	21,7
11	101	00:48	5,85	21,6
	102	02:48	6,00	21,5
	103	04:48	6,18	21,3
	104	06:48	6,30	21,0
	105	08:48	6,33	21,0

APPENDIX F: Ammonium and nitrate calibration curves

- **Ammonium-nitrogen calibration curve:**

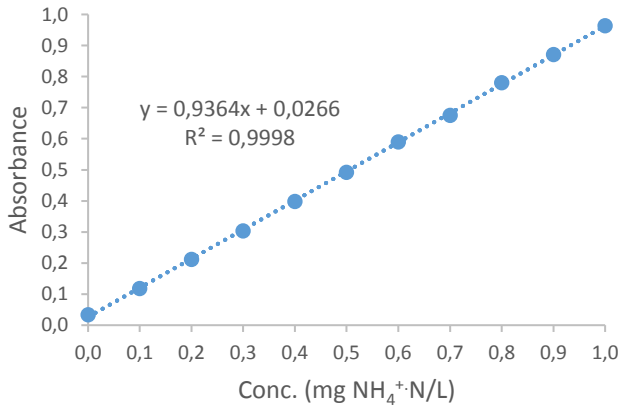

No.	Cal. curved Std. Sltns Conc. (mg NH_4^+-N/L)	Absorbance Reference (Distilled water)
Blank	0,0	0,0342
1	0,1	0,1189
2	0,2	0,2124
3	0,3	0,3043
4	0,4	0,3984
5	0,5	0,4923
6	0,6	0,5903
7	0,7	0,6760
8	0,8	0,7808
9	0,9	0,8712
10	1,0	0,9644

- **Nitrate-nitrogen calibration curve:**

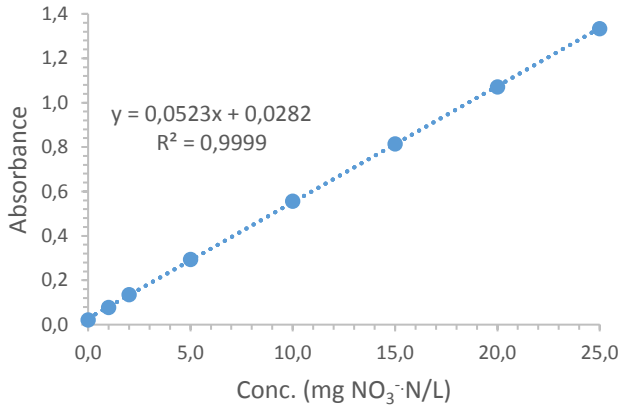

No.	Cal. curved Std. Sltns Conc. (mg NO_3^--N/L)	Absorbance Reference (Distilled water)
Blank	0,0	0,0210
1	1,0	0,0778
2	2,0	0,1358
3	5,0	0,2936
4	10,0	0,5570
5	15,0	0,8150
6	20,0	1,0718
7	25,0	1,3333

APPENDIX G: Nitrification during batches No. 1 through 6 in SFBBR-1

- **Batch No. 1 in SFBBR-1:**
  - Calculated data:

Nitrogen species concentrations and mass values							
Day No.	Total Vol. (L)	Ammonium-N		Nitrite-N		Nitrate-N	
		(mg NH_4^+-N/L)	(mg NH_4^+-N)	(mg NO_2^--N/L)	(mg NO_2^--N)	(mg NO_3^--N/L)	(mg NO_3^--N)
0	24,0	936,20	22468,86	2,6	62,0	1,43	34,42
1	23,9	846,33	20222,82	92,0	2197,4	13,67	326,67
2	23,8	622,73	14802,09	209,0	4967,9	29,88	710,14
3	23,6	565,33	13361,28	385,7	9115,8	79,59	1881,04
4	23,7	-	-	-	-	-	-
5	23,5	-	-	-	-	-	-
6	23,5	-	-	-	-	-	-
7	24,1	4,88	117,47	668,8	16107,2	240,92	5802,21
8	24,0	0,99	23,77	317,3	7602,1	571,46	13691,46
9	23,8	0,20	4,82	51,7	1231,5	765,54	18241,52
10	23,7	0,20	4,79	0,8	18,0	803,54	19038,43

Nitrogen species Surface loading values			
Day No.	Ammonium-N (mg NH_4^+-N/m^2)	Nitrite-N (mg NO_2^--N/m^2)	Nitrate-N (mg NO_3^--N/m^2)
0	22468,86	62,0	34,42
1	20222,82	2197,4	326,67
2	14802,09	4967,9	710,14
3	13361,28	9115,8	1881,04
4	-	-	-
5	-	-	-
6	-	-	-
7	117,47	16107,2	5802,21
8	23,77	7602,1	13691,46
9	4,82	1231,5	18241,52
10	4,79	18,0	19038,43

FA and FNA concentrations				
Day No.	pH	TK-T (°C)	FA (mg NH_3/L)	FNA (mg HNO_2/L)
0	8,1	20,0	53,9	0,0
1	8,3	22,0	86,0	0,0
2	8,2	22,0	51,1	0,01
3	7,8	22,0	19,3	0,05
4	7,5	22,0	-	-
5	-	-	-	-
6	-	-	-	-
7	7,5	22,0	0,1	0,17
8	7,6	23,0	0,0	0,06
9	7,7	23,0	0,0	0,01
10	7,7	22,0	0,0	0,0

  - Ammonium raw data:

Day No.	Absorbance	Calculated Conc. (mg NH_4^+-N/L)	dilution factor	Real Conc. (mg NH_4^+-N/L)
0	0,3071	0,30	3125	936,20
1	0,2802	0,27	3125	846,33
2	0,2132	0,20	3125	622,73
3	0,196	0,18	3125	565,33
4	-	-	-	-
5	-	-	-	-

6	-	-	-	-
7	0,9401	0,98	5	4,88
8	0,2124	0,20	5	0,99
9	0,0541	0,03	5	0,15
10	0,0748	0,05	5	0,26

- Nitrate raw data:

Day No.	Absorbance	Calculated Conc. (mg NO_3^--N/L)	dilution factor	Real Conc. (mg NO_3^--N/L)
0	0,0432	0,29	5	1,43
1	0,0568	0,55	25	13,67
2	0,0407	0,24	125	29,88
3	0,0615	0,64	125	79,59
4	-	-	-	-
5	-	-	-	-
6	-	-	-	-
7	0,1290	1,93	125	240,92
8	0,2673	4,57	125	571,46
9	0,3485	6,12	125	765,54
10	0,3644	6,43	125	803,54

- Nitrite raw data:

Day No.	Measured Nitrite (mg NO_2^-/L)	dilution factor	Calculated Nitrite (mg NO_2^-/L)	Calculated Nitrite-N (mg NO_2^--N/L)
0	1,6	5	8,0	2,4
	1,8	5	9,0	2,7
		Aver.	8,5	2,6
1	12,3	25	307,5	93,5
	11,9	25	297,5	90,4
		Aver.	302,5	92,0
2	5,5	125	687,5	209,0
3	10,3	125	1287,5	391,4
	10,0	125	1250,0	380,0
		Aver.	1268,8	385,7
7	17,8	125	2225,0	676,4
	17,4	125	2175,0	661,2
		Aver.	2200,0	668,8
8	8,3	125	1037,5	315,4
	8,4	125	1050,0	319,2
		Aver.	1043,8	317,3
9	6,9	25	172,5	52,4
	6,7	25	167,5	50,9
		Aver.	170,0	51,7
10	0,5	5	2,5	0,8

- **Batch No. 2 in SFBBR-1:**
  - Calculated data:

Nitrogen species concentrations and mass values							
Day No.	Total Vol. (L)	Ammonium-N		Nitrite-N		Nitrate-N	
		(mg NH_4^+-N/L)	(mg NH_4^+-N)	(mg NO_2^--N/L)	(mg NO_2^--N)	(mg NO_3^--N/L)	(mg NO_3^--N)
0	20,0	915,07	18301,47	2,7	54,7	1,98	39,58
1	19,9	763,23	15173,34	-	-	13,43	267,04
2	19,7	592,76	11666,10	-	-	36,09	710,28
3	19,5	423,43	8249,00	-	-	41,83	814,83
4	19,6	217,42	4261,74	-	-	57,84	1133,76
5	19,4	-	-	-	-	-	-

6	19,3	-	-	-	-	-	-
7	19,6	0,20	3,97	-	-	616,16	12066,33
8	19,4	-	-	-	-	-	-
9	19,3	-	-	-	-	-	-
10	19,1	0,20	3,88	0,8	14,5	782,03	14971,59

Nitrogen species Surface loading values			
Day No.	Ammonium-N (mg NH_4^+-N/m^2)	Nitrite-N (mg NO_2^--N/m^2)	Nitrate-N (mg NO_3^--N/m^2)
0	18301,47	54,7	39,58
1	15173,34	-	267,04
2	11666,10	-	710,28
3	8249,00	-	814,83
4	4261,74	-	1133,76
5	-	-	-
6	-	-	-
7	3,97	-	12066,33
8	-	-	-
9	-	-	-
10	3,88	14,5	14971,59

FA and FNA concentrations				
Day No.	pH	TK-T (°C)	FA (mg NH_3/L)	FNA (mg HNO_2/L)
0	8,3	20,0	81,2	0,0
1	8,6	24,0	161,2	-
2	8,5	22,0	91,0	-
3	7,7	23,3	12,6	-
4	7,5	23,3	4,1	-
5	-	-	-	-
6	-	-	-	-
7	8,3	21,9	0,0	-
8	-	-	-	-
9	-	-	-	-
10	8,1	24,0	0,0	0,0

- Ammonium raw data:

Day No.	Absorbance	Calculated Conc. (mg NH_4^+-N/L)	dilution factor	Real Conc. (mg NH_4^+-N/L)
0	0,3008	0,29	3125	915,07
1	0,2553	0,24	3125	763,23
2	0,9147	0,95	625	592,76
3	0,6610	0,68	625	423,43
4	1,6553	1,74	125	217,42
5	-	-	-	-
6	-	-	-	-
7	0,0624	0,04	5	0,19
8	-	-	-	-
9	-	-	-	-
10	0,0668	0,04	5	0,21

- Nitrate raw data:

Day No.	Absorbance	Calculated Conc. (mg NO_3^--N/L)	dilution factor	Real Conc. (mg NO_3^--N/L)
0	0,0489	0,40	5	1,98
1	0,0563	0,54	25	13,43
2	0,0433	0,29	125	36,09
3	0,0457	0,33	125	41,83
4	0,0524	0,46	125	57,84
5	-	-	-	-

6	-	-	-	-
7	0,2860	4,93	125	616,16
8	-	-	-	-
9	-	-	-	-
10	0,3554	6,26	125	782,03

- Nitrite raw data:

Day No.	Measured Nitrite (mg NO_2^-/L)	dilution factor	Calculated Nitrite (mg NO_2^-/L)	Calculated Nitrite-N (mg NO_2^--N/L)
0	1,8	5	9,0	2,7
10	≤ 0,5	5	2,5	0,8

- **Batch No. 3 in SFBBR-1:**
  - Calculated data:

Nitrogen species concentrations and mass values							
Day No.	Total Vol. (L)	Ammonium-N		Nitrite-N		Nitrate-N	
		(mg NH_4^+-N/L)	(mg NH_4^+-N)	(mg NO_2^--N/L)	(mg NO_2^--N)	(mg NO_3^--N/L)	(mg NO_3^--N)
0	20,0	845,33	16906,50	2,7	54,7	1,83	36,52
1	19,8	601,04	11921,29	-	-	36,52	724,36
2	19,6	344,20	6742,60	-	-	133,13	2607,80
3	20,1	10,87	218,44	-	-	220,12	4423,06
4	19,8	-	-	-	-	-	-
5	19,7	-	-	-	-	-	-
6	19,5	0,22	4,25	0,8	14,8	804,02	15691,88

Nitrogen species Surface loading values			
Day No.	Ammonium-N (mg NH_4^+-N/m^2)	Nitrite-N (mg NO_2^--N/m^2)	Nitrate-N (mg NO_3^--N/m^2)
0	16906,50	54,7	36,52
1	11921,29	-	724,36
2	6742,60	-	2607,80
3	218,44	-	4423,06
4	-	-	-
5	-	-	-
6	4,25	14,8	15691,88

FA and FNA concentrations				
Day No.	pH	TK-T (°C)	FA (mg NH_3/L)	FNA (mg HNO_2/L)
0	8,3	20,0	75,0	0,0
1	8,5	22,0	92,3	-
2	7,5	22,0	6,0	-
3	7,5	22,0	0,2	-
4	-	-	-	-
5	-	-	-	-
6	8,1	22,0	0,0	0,0

- Ammonium raw data:

Day No.	Absorbance	Calculated Conc. (mg NH_4^+-N/L)	dilution factor	Real Conc. (mg NH_4^+-N/L)
0	0,2799	0,27	3125	845,33
1	0,9271	0,96	625	601,04
2	0,5423	0,55	625	344,20
3	0,4338	0,43	25	10,87

4	-	-	-	-
5	-	-	-	-
6	0,0674	0,04	5	0,22

- Nitrate raw data:

Day No.	Absorbance	Calculated Conc. (mg NO_3^--N/L)	dilution factor	Real Conc. (mg NO_3^--N/L)
0	0,0473	0,37	5	1,83
1	0,1046	1,46	25	36,52
2	0,0839	1,07	125	133,13
3	0,1203	1,76	125	220,12
4	-	-	-	-
5	-	-	-	-
6	0,3646	6,43	125	804,02

- Nitrite raw data:

Day No.	Measured Nitrite (mg NO_2^-/L)	dilution factor	Calculated Nitrite (mg NO_2^-/L)	Calculated Nitrite-N (mg NO_2^--N/L)
0	1,8	5	9,0	2,7
6	≤ 0,5	5	2,5	0,8

- **Batch No. 4 in SFBBR-1:**
  - Calculated data:

Nitrogen species concentrations and mass values							
Day No.	Total Vol. (L)	Ammonium-N		Nitrite-N		Nitrate-N	
		(mg NH_4^+-N/L)	(mg NH_4^+-N)	(mg NO_2^--N/L)	(mg NO_2^--N)	(mg NO_3^--N/L)	(mg NO_3^--N)
0	20,0	852,84	17056,81	2,4	48,6	1,79	35,76
1	19,9	764,56	15185,11	50,2	996,2	3,63	72,15
2	19,7	-	-	-	-	-	-
3	19,7	585,02	11503,51	171,0	3362,4	9,66	189,87
4	19,5	469,62	9169,10	262,2	5119,3	11,85	231,46
5	19,4	-	-	-	-	-	-
6	19,3	-	-	-	-	-	-
7	19,7	177,14	3487,56	562,4	11072,6	31,79	625,84
8	19,8	79,80	1576,79	663,1	13102,3	40,39	798,11
9	19,8	1,04	20,54	651,7	12871,3	60,04	1185,78
10	19,6	0,26	5,07	528,2	10358,8	211,28	4143,54
11	19,5	0,22	4,22	383,8	7473,6	414,67	8074,82
12	19,3	-	-	-	-	-	-
13	19,3	-	-	-	-	-	-
14	19,2	0,22	4,25	1,4	26,3	764,58	14692,23

Nitrogen species Surface loading values			
Day No.	Ammonium-N (mg NH_4^+-N/m^2)	Nitrite-N (mg NO_2^--N/m^2)	Nitrate-N (mg NO_3^--N/m^2)
0	17056,81	48,6	35,76
1	15185,11	996,2	72,15
2	-	-	-
3	11503,51	3362,4	189,87
4	9169,10	5119,3	231,46
5	-	-	-
6	-	-	-
7	3487,56	11072,6	625,84
8	1576,79	13102,3	798,11
9	20,54	12871,3	1185,78
10	5,07	10358,8	4143,54
11	4,22	7473,6	8074,82

12	-	-	-
13	-	-	-
14	4,25	26,3	14692,23

FA and FNA concentrations				
Day No.	pH	TK-T (°C)	FA (mg NH_3/L)	FNA (mg HNO_2/L)
0	8,1	20,0	49,1	0,00
1	8,4	23,0	102,1	0,00
2	-	-	-	-
3	8,3	22,0	59,4	0,01
4	8,0	22,0	25,0	0,02
5	-	-	-	-
6	-	-	-	-
7	7,5	22,0	3,1	0,14
8	7,5	22,0	1,4	0,17
9	7,9	24,0	0,1	0,06
10	8,4	24,0	0,0	0,02
11	8,5	23,0	0,0	0,01
12	-	-	-	-
13	-	-	-	-
14	8,4	22,0	0,0	0,00

- Ammonium raw data:

Day No.	Absorbance	Calculated Conc. (mg NH_4^+-N/L)	dilution factor	Real Conc. (mg NH_4^+-N/L)
0	0,8252	0,85	1000	852,84
1	0,2557	0,24	3125	764,56
2	-	-	-	-
3	0,9031	0,94	625	585,02
4	0,7302	0,75	625	469,62
5	-	-	-	-
6	-	-	-	-
7	0,2920	0,28	625	177,14
8	0,6244	0,64	125	79,80
9	0,2214	0,21	5	1,04
10	0,0750	0,05	5	0,26
11	0,0672	0,04	5	0,22
12	-	-	-	-
13	-	-	-	-
14	0,0680	0,04	5	0,22

- Nitrate raw data:

Day No.	Absorbance	Calculated Conc. (mg NO_3^--N/L)	dilution factor	Real Conc. (mg NO_3^--N/L)
0	0,0469	0,36	5	1,79
1	0,0662	0,73	5	3,63
2	-	-	-	-
3	0,0484	0,39	25	9,66
4	0,0530	0,47	25	11,85
5	-	-	-	-
6	-	-	-	-
7	0,0947	1,27	25	31,79
8	0,1127	1,62	25	40,39
9	0,1538	2,40	25	60,04
10	0,1166	1,69	125	211,28
11	0,2017	3,32	125	414,67
12	-	-	-	-
13	-	-	-	-
14	0,3481	6,12	125	764,58

- Nitrite raw data:

Day No.	Measured Nitrite (mg NO_2^-/L)	dilution factor	Calculated Nitrite (mg NO_2^-/L)	Calculated Nitrite-N (mg NO_2^--N/L)
0	1,6	5	8,0	2,4
1	6,6	25	165,0	50,2
2	-	-	-	-
3	4,5	125	562,5	171,0
4	6,9	125	862,5	262,2
5	-	-	-	-
6	-	-	-	-
7	14,8	125	1850,0	562,4
8	17,5	125	2181,3	663,1
9	17,2	125	2143,8	651,7
10	13,9	125	1737,5	528,2
11	10,1	125	1262,5	383,8
12	-	-	-	-
13	-	-	-	-
14	0,9	5	4,5	1,4

- **Batch No. 5 in SFBBR-1:**
  - Calculated data:

Nitrogen species concentrations and mass values							
Day No.	Total Vol. (L)	Ammonium-N		Nitrite-N		Nitrate-N	
		(mg NH_4^+-N/L)	(mg NH_4^+-N)	(mg NO_2^--N/L)	(mg NO_2^--N)	(mg NO_3^--N/L)	(mg NO_3^--N)
0	20,0	808,28	16165,63	1,4	27,4	1,79	35,76
1	19,8	676,79	13399,59	65,4	1294,0	3,01	59,62
2	19,6	577,34	11314,35	172,5	3380,9	6,73	131,90
3	19,4	468,08	9078,86	323,0	6264,9	19,09	370,30
4	19,2	359,96	6909,16	414,2	7950,4	28,61	549,23
5	19,0	-	-	-	-	-	-
6	18,9	-	-	-	-	-	-
7	19,4	34,91	676,52	772,7	14974,5	37,81	732,78
8	19,3	0,16	3,17	646,0	12441,3	167,73	3230,39
9	19,1	0,16	3,13	423,7	8074,7	351,58	6700,22
10	18,9	0,16	3,10	158,1	2980,8	574,09	10825,19
11	18,7	0,16	3,07	1,7	31,2	692,88	12925,51

Nitrogen species Surface loading values			
Day No.	Ammonium-N (mg NH_4^+-N/m^2)	Nitrite-N (mg NO_2^--N/m^2)	Nitrate-N (mg NO_3^--N/m^2)
0	16165,63	27,4	35,76
1	13399,59	1294,0	59,62
2	11314,35	3380,9	131,90
3	9078,86	6264,9	370,30
4	6909,16	7950,4	549,23
5	-	-	-
6	-	-	-
7	676,52	14974,5	732,78
8	3,17	12441,3	3230,39
9	3,13	8074,7	6700,22
10	3,10	2980,8	10825,19
11	3,07	31,2	12925,51

FA and FNA concentrations				
Day No.	pH	TK-T (°C)	FA (mg NH_3/L)	FNA (mg HNO_2/L)
0	8,3	21,0	76,8	0,00
1	8,6	24,0	142,9	0,00
2	8,5	23,0	94,4	0,00
3	8,2	24,0	44,0	0,02
4	7,7	23,0	10,5	0,06
5	-	-	-	-
6	-	-	-	-
7	7,5	22,0	0,6	0,20
8	8,3	23,0	0,0	0,03
9	8,4	22,0	0,0	0,01
10	8,4	24,0	0,0	0,00
11	8,2	23,0	0,0	0,00

- Ammonium raw data:

Day No.	Absorbance	Calculated Conc. (mg NH_4^+-N/L)	dilution factor	Real Conc. (mg NH_4^+-N/L)
0	0,2688	0,26	3125	808,28
1	0,2294	0,22	3125	676,79
2	0,1996	0,18	3125	577,34
3	0,7279	0,75	625	468,08
4	0,5659	0,58	625	359,96
5	-	-	-	-
6	-	-	-	-
7	0,2881	0,28	125	34,91
8	0,0548	0,030	5	0,15
9	0,0628	0,039	5	0,19
10	0,0517	0,027	5	0,13
11	0,0603	0,036	5	0,18

- Nitrate raw data:

Day No.	Absorbance	Calculated Conc. (mg NO_3^--N/L)	dilution factor	Real Conc. (mg NO_3^--N/L)
0	0,0469	0,36	5	1,79
1	0,0597	0,60	5	3,01
2	0,0986	1,35	5	6,73
3	0,2279	3,82	5	19,09
4	0,3275	5,72	5	28,61
5	-	-	-	-
6	-	-	-	-
7	0,1073	1,51	25	37,81
8	0,3791	6,71	25	167,73
9	0,1753	2,81	125	351,58
10	0,2684	4,59	125	574,09
11	0,3181	5,54	125	692,88

- Nitrite raw data:

Day No.	Measured Nitrite (mg NO_2^-/L)	dilution factor	Calculated Nitrite (mg NO_2^-/L)	Calculated Nitrite-N (mg NO_2^--N/L)
0	0,9	5	4,5	1,4
1	8,6	25	215,0	65,4
2	22,7	25	567,5	172,5
3	8,5	125	1062,5	323,0
4	10,9	125	1362,5	414,2
5	-	-	-	-
6	-	-	-	-
7	20,3	125	2541,7	772,7
8	17,0	125	2125,0	646,0
9	11,2	125	1393,8	423,7

10	20,8	25	520,0	158,1
11	1,1	5	5,5	1,7

- **Batch No. 6 in SFBBR-1:**
  - Calculated data:

Nitrogen species concentrations and mass values							
Day No.	Total Vol. (L)	Ammonium-N		Nitrite-N		Nitrate-N	
		(mg NH_4^+-N/L)	(mg NH_4^+-N)	(mg NO_2^--N/L)	(mg NO_2^--N)	(mg NO_3^--N/L)	(mg NO_3^--N)
0	20,0	791,60	15831,91	1,1	21,3	1,91	38,24
1	19,8	674,79	13347,54	88,9	1758,9	7,07	139,75
2	19,6	519,94	10170,33	197,6	3865,1	14,39	281,44
3	19,3	-	-	-	-	-	-
4	19,2	282,93	5443,87	471,2	9066,3	29,63	570,05
5	19,0	-	-	-	-	-	-
6	18,9	-	-	-	-	-	-
7	19,4	0,23	4,48	581,4	11288,8	209,32	4064,31
8	19,2	0,20	3,76	330,6	6346,5	400,81	7694,34
9	19,0	0,15	2,80	54,0	1024,0	643,16	12205,38
10	18,8	0,15	2,77	1,4	25,7	689,77	12938,23

Nitrogen species Surface loading values			
Day No.	Ammonium-N (mg NH_4^+-N/m^2)	Nitrite-N (mg NO_2^--N/m^2)	Nitrate-N (mg NO_3^--N/m^2)
0	15831,91	21,3	38,24
1	13347,54	1758,9	139,75
2	10170,33	3865,1	281,44
3	-	-	-
4	5443,87	9066,3	570,05
5	-	-	-
6	-	-	-
7	4,48	11288,8	4064,31
8	3,76	6346,5	7694,34
9	2,80	1024,0	12205,38
10	2,77	25,7	12938,23

FA and FNA concentrations				
Day No.	pH	TK-T (°C)	FA (mg NH_3/L)	FNA (mg HNO_2/L)
0	8,1	21,0	48,9	0,00
1	8,3	23,0	73,3	0,00
2	8,2	23,0	45,7	0,01
3	7,8	23,0	-	-
4	7,5	23,0	5,3	0,12
5	-	-	-	-
6	-	-	-	-
7	8,6	22,0	0,0	0,01
8	8,6	22,0	0,0	0,01
9	8,6	22,0	0,0	0,00
10	8,5	22,0	0,0	0,00

  - Ammonium raw data:

Day No.	Absorbance	Calculated Conc. (mg NH_4^+-N/L)	dilution factor	Real Conc. (mg NH_4^+-N/L)
0	0,2638	0,25	3125	791,60
1	0,2288	0,22	3125	674,79
2	0,1824	0,17	3125	519,94
3	-	-	-	-

4	0,4505	0,45	625	282,93
5	-	-	-	-
6	-	-	-	-
7	0,0698	0,05	5	0,23
8	0,0633	0,04	5	0,20
9	0,0521	0,03	5	0,14
10	0,0564	0,03	5	0,16

- Nitrate raw data:

Day No.	Absorbance	Calculated Conc. (mg NO_3^--N/L)	dilution factor	Real Conc. (mg NO_3^--N/L)
0	0,0482	0,38	5	1,91
1	0,1021	1,41	5	7,07
2	0,1787	2,88	5	14,39
3	-	-	-	-
4	0,3381	5,93	5	29,63
5	-	-	-	-
6	-	-	-	-
7	0,4661	8,37	25	209,32
8	0,1959	3,21	125	400,81
9	0,2973	5,15	125	643,16
10	0,3168	5,52	125	689,77

- Nitrite raw data:

Day No.	Measured Nitrite (mg NO_2^-/L)	dilution factor	Calculated Nitrite (mg NO_2^-/L)	Calculated Nitrite-N (mg NO_2^--N/L)
0	0,7	5	3,5	1,1
1	11,7	25	292,5	88,9
2	5,2	125	650,0	197,6
3	-	-	-	-
4	12,4	125	1550,0	471,2
5	-	-	-	-
6	-	-	-	-
7	15,3	125	1912,5	581,4
8	8,7	125	1087,5	330,6
9	7,1	25	177,5	54,0
10	0,9	5	4,5	1,4

APPENDIX K: Nitrification during semi-batch process in SFBBR-1

- Calculated data:

Nitrogen species concentrations and mass values							
Day No.	Total Vol. (L)	Ammonium-N		Nitrite-N		Nitrate-N	
		(mg NH_4^+-N/L)	(mg NH_4^+-N)	(mg NO_2^--N/L)	(mg NO_2^--N)	(mg NO_3^--N/L)	(mg NO_3^--N)
0	20,0	812,15	16243,06	1,2	24,3	2,28	45,51
1	19,8	674,07	13326,38	109,4	2163,6	6,07	120,02
2	19,5	549,55	10738,24	250,8	4900,6	-	-
3	19,3	374,84	7238,16	340,5	6574,7	19,67	379,92
4	19,3	228,96	4407,52	501,6	9655,8	31,68	609,89
5	19,0	-	-	-	-	-	-
6	18,9	-	-	-	-	-	-
7-B	19,1	0,30	5,77	519,8	9928,9	267,88	5116,46
7-A	19,1	129,26	2468,88	438,4	8372,9	225,88	4314,32
8-B	19,0	3,82	72,73	503,1	9574,4	257,36	4897,59
8-A	19,0	132,46	2520,79	424,0	8068,8	216,87	4127,02
9-B	19,0	2,86	54,16	521,9	9894,6	239,77	4546,05
9-A	19,0	132,13	2505,12	439,5	8332,8	201,91	3828,26
10-B	18,9	2,63	49,67	523,9	9896,3	223,23	4216,84
10-A	18,9	132,41	2501,30	440,9	8328,4	187,86	3548,67
11-B	18,8	3,04	57,26	598,9	11270,9	193,31	3638,05
11-A	18,8	392,93	7395,00	313,1	5893,0	101,11	1902,93
12	18,7	-	-	-	-	-	-
13	18,5	-	-	-	-	-	-
14-B	18,6	4,95	92,05	719,0	13372,7	115,68	2151,63
14-A	18,6	137,95	2565,88	603,2	11219,8	97,27	1809,18
15-B	18,5	3,28	60,69	647,5	11998,5	97,99	1815,80
15-A	18,5	135,48	2510,39	542,9	10060,0	82,32	1525,46
16-B	18,5	4,87	89,97	790,4	14590,8	102,68	1895,41
16-A	18,5	137,32	2534,88	662,2	12223,6	86,19	1591,03
17-B	18,4	11,16	205,11	767,6	14112,3	87,76	1613,52
17-A	18,4	141,53	2602,02	642,6	11813,5	73,59	1352,93
18-B	18,3	6,88	125,97	851,2	15594,0	84,51	1548,27
18-A	18,3	405,16	7422,48	433,7	7945,2	71,43	1308,67
19	18,2	-	-	-	-	-	-
20	18,0	-	-	-	-	-	-
21-B	18,1	0,57	10,33	820,8	14864,7	60,99	1104,61
21-A	18,1	135,31	2450,52	685,1	12406,3	51,12	925,70
22-B	18,0	2,09	37,71	653,6	11794,2	43,21	779,76
22-A	18,0	136,10	2455,89	545,1	9837,2	36,21	653,37
23-B	18,0	0,59	10,65	706,8	12704,7	52,01	934,84
23-A	18,0	135,37	2433,32	589,0	10588,1	43,51	782,06
24-B	17,9	3,17	56,75	843,6	15108,9	58,70	1051,31
24-A	17,9	137,03	2454,23	702,5	12581,6	49,00	877,62
25	17,8	1,72	30,76	904,4	16139,0	53,15	948,55

Nitrogen species Surface loading values			
Day No.	Ammonium-N (mg NH_4^+-N/m^2)	Nitrite-N (mg NO_2^--N/m^2)	Nitrate-N (mg NO_3^--N/m^2)
0	16243,06	24,3	45,51
1	13326,38	2163,6	120,02
2	10738,24	4900,6	
3	7238,16	6574,7	379,92
4	4407,52	9655,8	609,89
5	-	-	-
6	-	-	-
7-B	5,77	9928,9	5116,46
7-A	2468,88	8372,9	4314,32
8-B	72,73	9574,4	4897,59
8-A	2520,79	8068,8	4127,02

9-B	54,16	9894,6	4546,05
9-A	2505,12	8332,8	3828,26
10-B	49,67	9896,3	4216,84
10-A	2501,30	8328,4	3548,67
11-B	57,26	11270,9	3638,05
11-A	7395,00	5893,0	1902,93
12	-	-	-
13	-	-	-
14-B	92,05	13372,7	2151,63
14-A	2565,88	11219,8	1809,18
15-B	60,69	11998,5	1815,80
15-A	2510,39	10060,0	1525,46
16-B	89,97	14590,8	1895,41
16-A	2534,88	12223,6	1591,03
17-B	205,11	14112,3	1613,52
17-A	2602,02	11813,5	1352,93
18-B	125,97	15594,0	1548,27
18-A	7422,48	7945,2	1308,67
19	-	-	-
20	-	-	-
21-B	10,33	14864,7	1104,61
21-A	2450,52	12406,3	925,70
22-B	37,71	11794,2	779,76
22-A	2455,89	9837,2	653,37
23-B	10,65	12704,7	934,84
23-A	2433,32	10588,1	782,06
24-B	56,75	15108,9	1051,31
24-A	2454,23	12581,6	877,62
25	30,76	16139,0	948,55

Ammonium-N mass balance

Day No.	Renewed NH_4^+-N (mg)	Taken Out NH_4^+-N (mg)	Remains NH_4^+-N (mg)	After Renewal NH_4^+-N (mg)	Before Renewal NH_4^+-N (mg)	AC (mg NH_4^+-N)	AC (%)	ACR (mg NH_4^+-N/m^2.d)
7	2464,01	0,91	4,87	2468,88	5,77	-	-	-
8	2459,53	11,47	61,27	2520,79	72,73	2396,14	97,1	2396,14
9	2459,53	8,57	45,59	2505,12	54,16	2466,63	97,9	2466,63
10	2459,53	7,89	41,78	2501,30	49,67	2455,45	98,0	2455,45
11	7365,12	27,38	29,88	7395,00	57,26	2444,04	97,7	2444,04
					Aver.	2440,57	97,7	2440,57
12-13	-	-	-	-	-	-		-
14	2488,68	14,85	77,20	2565,88	92,05	7302,95	98,8	7302,95
					Aver.	2434,32		2434,32
15	2459,53	9,83	50,87	2510,39	60,69	2505,19	97,6	2505,19
16	2459,53	14,62	75,35	2534,88	89,97	2420,42	96,4	2420,42
17	2430,37	33,47	171,64	2602,02	205,11	2329,76	91,9	2329,76
18	7358,39	61,89	64,09	7422,48	125,97	2476,04	95,2	2476,04
					Aver.	2432,85	95,3	2432,85
19-20	-	-	-	-	-	-		-
21	2441,91	1,71	8,62	2450,52	10,33	7412,15	99,9	7412,15
					Aver.	2470,72		2470,72
22	2424,44	6,27	31,44	2455,89	37,71	2412,81	98,5	2412,81
23	2424,44	1,78	8,88	2433,32	10,65	2445,23	99,6	2445,23
24	2406,98	9,51	47,24	2454,23	56,75	2376,57	97,7	2376,57
25	-	-	-	-	30,76	2423,47	98,7	2423,47
					Aver.	2414,52	98,6	2414,52
				Overall Aver.		2432,63	97,5	2432,63

Nitrate-N mass balance

Day No.	Renewed NO_3^--N (mg)	Taken out NO_3^--N (mg)	Remains NO_3^--N (mg)	After Renewal NO_3^--N (mg)	Before Renewal NO_3^--N (mg)

7	1,49	803,63	4312,83	4314,32	5116,46
8	1,52	772,08	4125,50	4127,02	4897,59
9	1,52	719,31	3826,74	3828,26	4546,05
10	1,52	669,69	3547,15	3548,67	4216,84
11	4,65	1739,77	1898,28	1902,93	3638,05
12	-	-	-	-	-
13	-	-	-	-	-
14	4,59	347,04	1804,59	1809,18	2151,63
15	3,64	293,98	1521,82	1525,46	1815,80
16	3,64	308,03	1587,38	1591,03	1895,41
17	2,70	263,29	1350,23	1352,93	1613,52
18	13,94	253,54	1294,73	1308,67	1548,27
19	-	-	-	-	-
20	-	-	-	-	-
21	4,07	182,98	921,62	925,70	1104,61
22	3,24	129,64	650,13	653,37	779,76
23	3,24	156,02	778,81	782,06	934,84
24	2,41	176,10	875,21	877,62	1051,31
25	-	-	-	-	948,55

Nitrite-N mass balance					
Day No.	Renewed NO_2^--N (mg)	Taken out NO_2^--N (mg)	Remains NO_2^--N (mg)	After Renewal NO_2^--N (mg)	Before Renewal NO_2^--N (mg)
7	3,5	1559,5	8369,4	8372,9	9928,9
8	3,8	1509,4	8065,0	8068,8	9574,4
9	3,8	1565,6	8329,0	8332,8	9894,6
10	3,8	1571,7	8324,7	8328,4	9896,3
11	12,0	5389,9	5881,0	5893,0	11270,9
12	-	-	-	-	-
13	-	-	-	-	-
14	4,0	2156,9	11215,8	11219,8	13372,7
15	4,0	1942,6	10056,0	10060,0	11998,5
16	4,0	2371,2	12219,6	12223,6	14590,8
17	4,0	2302,8	11809,5	11813,5	14112,3
18	12,0	7660,8	7933,2	7945,2	15594,0
19	-	-	-	-	-
20	-	-	-	-	-
21	4,0	2462,4	12402,3	12406,3	14864,7
22	3,8	1960,8	9833,4	9837,2	11794,2
23	3,8	2120,4	10584,3	10588,1	12704,7
24	3,5	2530,8	12578,1	12581,6	15108,9
25	-	-	-	-	16139,0

FA and FNA concentrations				
Day No.	pH	TK-T (°C)	FA (mg NH_3/L)	FNA (mg HNO_2/L)
0	8,1	20,0	46,7	0,00
1	8,4	23,0	90,0	0,00
2	8,2	24,0	51,6	0,01
3	7,7	24,0	11,8	0,05
4	7,5	23,0	4,3	0,12
5	-	-	-	
6	-	-	-	
7-B	8,5	22,0	0,0	0,01
7-A	8,1	22,0	8,5	0,03
8-B	7,6	22,0	0,1	0,10
8-A	7,8	22,0	4,5	0,05
9-B	7,6	23,0	0,1	0,10
9-A	7,9	23,0	6,0	0,04
10-B	7,6	22,0	0,1	0,11
10-A	7,9	22,0	5,6	0,04
11-B	7,5	22,0	0,1	0,15

11-A	8,0	22,0	20,9	0,03
12	-	-	-	
13	-	-	-	
14-B	7,5	22,0	0,1	0,18
14-A	7,9	22,0	5,9	0,06
15-B	7,6	22,0	0,1	0,13
15-A	7,8	22,0	4,6	0,07
16-B	7,5	22,0	0,1	0,20
16-A	7,8	22,0	4,7	0,08
17-B	7,5	22,0	0,2	0,19
17-A	7,8	22,0	4,8	0,08
18-B	7,6	22,0	0,1	0,17
18-A	7,9	22,0	17,3	0,04
19	-	-	-	
20	-	-	-	
21-B	7,7	21,0	0,0	0,13
21-A	7,7	21,0	3,4	0,11
22-B	7,5	22,0	0,0	0,17
22-A	7,7	22,0	3,7	0,09
23-B	7,6	22,0	0,0	0,14
23-A	7,8	22,0	4,6	0,07
24-B	7,5	22,0	0,1	0,21
24-A	7,7	22,0	3,7	0,11
25	7,6	22,0	0,0	0,18

- Ammonium raw data:

Day No.	Absorbance	Calculated Conc. (mg NH_4^+-N/L)	dilution factor	Real Conc. (mg NH_4^+-N/L)
0	0,7871	0,81	1000	812,15
1	0,6578	0,67	1000	674,07
2	0,5412	0,55	1000	549,55
3	0,3776	0,37	1000	374,84
4	0,2410	0,23	1000	228,96
5	-	-	-	-
6	-	-	-	-
7	0,0549	0,03	10	0,30
Renewed SW	0,7957	0,82	1000	821,34
8-B	0,3845	0,38	10	3,82
9-B	0,2941	0,29	10	2,86
10-B	0,2728	0,26	10	2,63
11-B	0,3115	0,30	10	3,04
Renewed SW	0,7929	0,82	1000	818,35
12	-	-	-	-
13	-	-	-	-
14-B	0,4900	0,49	10	4,95
Renewed SW	0,8034	0,83	1000	829,56
15-B	0,3333	0,33	10	3,28
16-B	0,4830	0,49	10	4,87
17-B	1,0713	1,12	10	11,16
Renewed SW	0,7852	0,81	1000	810,12
18-B	0,6705	0,69	10	6,88
Renewed SW	0,7922	0,82	1000	817,60
19	-	-	-	-
20	-	-	-	-
21-B	0,0800	0,057	10	0,57
Renewed SW	0,7888	0,81	1000	813,97
22-B	0,2223	0,21	10	2,09
23-B	0,0821	0,059	10	0,59
24-B	0,3233	0,32	10	3,17
Renewed SW	0,7779	0,80	1000	802,33
25-B	0,1880	0,17	10	1,72

- Nitrate raw data:

Day No.	Absorbance	Calculated Conc. (mg NO_3^--N/L)	dilution factor	Real Conc. (mg NO_3^--N/L)
0	0,0520	0,46	5	2,28
1	0,0917	1,21	5	6,07
2	-	-	-	-
3	0,1311	1,97	10	19,67
4	0,1939	3,17	10	31,68
5	-	-	-	-
6	-	-	-	-
7	0,1683	2,68	100	267,88
Renewed SW	0,0308	0,050	10	0,50
8-B	0,1628	2,57	100	257,36
9-B	0,1536	2,40	100	239,77
10-B	0,1450	2,23	100	223,23
11-B	0,1293	1,93	100	193,31
Renewed SW	0,0309	0,052	10	0,52
12	-	-	-	-
13	-	-	-	-
14-B	0,0887	1,16	100	115,68
Renewed SW	0,0362	0,15	10	1,53
15-B	0,0795	0,98	100	97,99
16-B	0,0819	1,03	100	102,68
17-B	0,0741	0,88	100	87,76
Renewed SW	0,0329	0,090	10	0,90
18-B	0,0724	0,85	100	84,51
Renewed SW	0,0363	0,15	10	1,55
19	-	-	-	-
20	-	-	-	-
21-B	0,0601	0,61	100	60,99
Renewed SW	0,0353	0,14	10	1,36
22-B	0,0508	0,43	100	43,21
23-B	0,0554	0,52	100	52,01
24-B	0,0589	0,59	100	58,70
Renewed SW	0,0324	0,080	10	0,80
25-B	0,0560	0,53	100	53,15

- Nitrite raw data:

Day No.	Measured Nitrite (mg NO_2^-/L)	dilution factor	Calculated Nitrite (mg NO_2^-/L)	Calculated Nitrite-N (mg NO_2^--N/L)
0	0,8	5	4,0	1,2
1	3,6	100	360,0	109,4
2	8,3	100	825,0	250,8
3	11,2	100	1120,0	340,5
4	16,5	100	1650,0	501,6
5	-	-	-	-
6	-	-	-	-
7	17,1	100	1710,0	519,8
Renewed SW	0,7	1	0,7	0,2
	0,7	10	7,0	2,1
			Aver.	1,2
8-B	16,6	100	1655,0	503,1
9-B	17,2	100	1716,7	521,9
10-B	17,2	100	1723,3	523,9
11-B	19,7	100	1970,0	598,9
Renewed SW	0,8	1	0,8	0,2
	0,8	10	8,0	2,4
			Aver.	1,3
12	-	-	-	-
13	-	-	-	-
14-B	23,7	100	2365,0	719,0
Renewed SW	0,8	1	0,8	0,2
	0,8	10	8,0	2,4
			Aver.	1,3

15-B	21,3	100	2130,0	647,5
16-B	5,2	500	2600,0	790,4
17-B	5,1	500	2525,0	767,6
Renewed SW	0,8	1	0,8	0,2
	0,8	10	8,0	2,4
			Aver.	1,3
18-B	5,6	500	2800,0	851,2
Renewed SW	0,8	1	0,8	0,2
	0,8	10	8,0	2,4
			Aver.	1,3
19	-	-	-	-
20	-	-	-	-
21-B	5,4	500	2700,0	820,8
Renewed SW	0,8	1	0,8	0,2
	0,8	10	8,0	2,4
			Aver.	1,3
22-B	4,3	500	2150,0	653,6
23-B	4,7	500	2325,0	706,8
24-B	5,6	500	2775,0	843,6
Renewed SW	0,7	1	0,7	0,2
	0,7	10	7,0	2,1
			Aver.	1,2
25-B	6,0	500	2975,0	904,4

APPENDIX L: Nitrification during the starting and batch processes in SFBBR-2

- **Starting of bioreactor in SFBBR-2:**
  - Calculated data:

Nitrogen species concentrations and mass values							
Day No.	Total Vol. (L)	Ammonium-N		Nitrite-N		Nitrate-N	
		(mg NH_4^+-N/L)	(mg NH_4^+-N)	(mg NO_2^--N/L)	(mg NO_2^--N)	(mg NO_3^--N/L)	(mg NO_3^--N)
0	25,0	842,38	21059,38	1,2	29,3	0,76	19,12
1	24,9	-	-	-	-	-	-
2	24,8	-	-	-	-	-	-
3	24,7	649,08	16053,68	23,4	578,9	2,18	53,91
4	24,6	-	-	-	-	-	-
5	24,5	-	-	-	-	-	-
6	24,4	-	-	-	-	-	-
7	25,0	473,94	11831,26	35,3	880,3	2,87	71,60
8	24,8	-	-	-	-	-	-
9	24,7	-	-	-	-	-	-
10-B	24,6	442,65	10883,24	45,6	1121,1	3,19	78,51
10-A	24,6	517,80	12730,74	36,6	899,8	3,01	73,92
11	25,0	-	-	-	-	-	-
12	25,0	-	-	-	-	-	-
13	25,0	-	-	-	-	-	-
14-B	25,2	266,45	6702,19	337,4	8488,0	11,38	286,17
14-A	25,2	343,65	8644,31	290,7	7311,0	9,86	248,09
15	25,1	-	-	-	-	-	-
16	25,1	-	-	-	-	-	-
17	25,4	-	-	-	-	-	-
18	25,5	-	-	-	-	-	-
18	25,5	-	-	-	-	-	-
19-B	25,4	1,56	39,62	708,32	18000,1	37,46	951,87
19-A	25,4	162,56	4131,04	569,2	14465,2	30,19	767,12
20	25,6	-	-	-	-	-	-
21-B	25,6	3,26	83,53	866,4	22181,3	42,05	1076,45
21-A	25,6	162,45	4158,95	697,5	17856,0	33,94	868,80
22	25,6	-	-	-	-	-	-
23	25,6	-	-	-	-	-	-
24-B	25,7	1,42	36,52	912	23448,1	50,27	1292,42
24-A	25,7	162,47	4177,22	734,9	18894,8	40,79	1048,72
25	25,7	-	-	-	-	-	-
26-B	25,8	1,56	40,16	851,2	21952,4	48,83	1259,42
26-A	25,8	158,32	4082,99	686,4	17703,1	39,54	1019,74
27	25,8						
28-B	25,9	0,70	18,01	775,2	20050,0	47,38	1225,46
28-A	25,9	237,58	6144,78	550,8	14246,0	34,09	881,73
29	25,8	-	-	-	-	-	-
30	25,8	-	-	-	-	-	-
31	26,0	0,46	11,87	906,9	23556,0	59,04	1533,57

Nitrogen species Surface loading values			
Day No.	Ammonium-N (mg NH_4^+-N/m^2)	Nitrite-N (mg NO_2^--N/m^2)	Nitrate-N (mg NO_3^--N/m^2)
0	9909,51	13,8	9,00
1	-	-	-
2	-	-	-
3	7554,07	272,4	25,37
4	-	-	-
5	-	-	-
6	-	-	-
7	5567,21	414,2	33,69
8	-	-	-

9	-	-	-
10-B	5121,12	527,6	36,94
10-A	5990,46	423,4	34,78
11	-	-	-
12	-	-	-
13	-	-	-
14-B	3153,72	3994,0	134,66
14-A	4067,59	3440,2	116,74
15	-	-	-
16	-	-	-
17	-	-	-
18	-	-	-
18	-	-	-
19-B	18,64	8470,0	447,90
19-A	1943,86	6806,6	360,97
20	-	-	-
21-B	39,30	10437,4	506,52
21-A	1957,00	8402,1	408,81
22	-	-	-
23	-	-	-
24-B	17,18	11033,5	608,15
24-A	1965,59	8891,0	493,48
25	-	-	-
26-B	18,90	10329,7	592,62
26-A	1921,25	8330,2	479,84
27	-	-	-
28-B	8,47	9434,5	576,64
28-A	2891,43	6703,5	414,90
29	-	-	-
30	-	-	-
31	5,59	11084,3	721,62

Ammonium-N mass balance

Day No.	Renewed NH_4^+-N (mg)	Taken Out NH_4^+-N (mg)	Remains NH_4^+-N (mg)	After Renewal NH_4^+-N (mg)	Before Renewal NH_4^+-N (mg)	AC (mg NH_4^+-N)	AC (%)	ACR (mg NH_4^+-N/m^2.d)
10	4060,76	2213,26	8669,97	12730,74	10883,24	-		
14	2874,68	932,56	5769,63	8644,31	6702,19	6028,54	47,4	709,18
19	4099,21	7,80	31,83	4131,04	39,62	8604,69	99,5	809,79
21	4091,73	16,31	67,21	4158,95	83,53	4047,51	98,0	952,28
24	4147,80	7,10	29,42	4177,22	36,52	4122,43	99,1	969,91
26	4050,62	7,79	32,37	4082,99	40,16	4137,06	99,0	973,35
28	6131,99	5,22	12,79	6144,78	18,01	4064,98	99,6	956,39
31	-	-	-	-	11,87	6132,91	99,8	961,95
					Aver. (days 19 – 31)		99,1	962,77

Nitrate-N mass balance

Day No.	Renewed NO_3^--N (mg)	Taken out NO_3^--N (mg)	Remains NO_3^--N (mg)	After Renewal NO_3^--N (mg)	Before Renewal NO_3^--N (mg)
10	11,38	15,97	62,54	73,92	78,51
14	1,74	39,82	246,35	248,09	286,17
19	2,53	187,28	764,58	767,12	951,87
21	2,58	210,23	866,22	868,80	1076,45
24	7,65	251,34	1041,08	1048,72	1292,42
26	4,49	244,17	1015,25	1019,74	1259,42
28	11,62	355,35	870,11	881,73	1225,46
31	-	-	-	-	1533,57

Nitrite-N mass balance					
Day No.	Renewed NO_2^--N (mg)	Taken out NO_2^--N (mg)	Remains NO_2^--N (mg)	After Renewal NO_2^--N (mg)	Before Renewal NO_2^--N (mg)
10	6,7	228,0	893,1	899,8	1121,1
14	4,1	1181,0	7306,9	7311,0	8488,0
19	6,7	3541,6	14458,5	14465,2	18000,1
21	6,7	4332,0	17849,3	17856,0	22181,3
24	6,7	4560,0	18888,1	18894,8	23448,1
26	6,7	4256,0	17696,4	17703,1	21952,4
28	10,0	5814,0	14236,0	14246,0	20050,0
31	-	-	-	-	23556,0

FA and FNA concentrations				
Day No.	pH	TK-T (°C)	FA (mg NH_3/L)	FNA (mg HNO_2/L)
0	8,2	20,0	60,3	0,00
1	-	-	-	-
2	-	-	-	-
3	9,1	22,0	288,1	0,00
4	9,2	22,0	-	-
5	9,2	22,0	-	-
6	9,2	22,0	-	-
7	9,2	22,5	247,0	0,00
8	-	-	-	-
9	-	-	-	-
10-B	7,8	21,0	14,0	0,01
10-A	8,3	21,0	49,2	0,00
11	7,5	24,0	-	-
12	6,6	24,0	-	-
13	7,5	24,0	-	-
14-B	7,5	23,0	5,0	0,08
14-A	7,9	23,0	15,7	0,03
15	-	-	-	-
16	-	-	-	-
17	7,5	22,0	-	-
18	8,2	22,0	-	-
18	7,5	22,0	-	-
19-B	7,5	23,0	0,0	0,17
19-A	8,2	23,0	14,3	0,03
20	7,5	22,0	-	-
21-B	7,7	21,0	0,1	0,14
21-A	8,2	21,0	12,5	0,04
22	-	-	-	-
23	-	-	-	-
24-B	7,8	21,0	0,0	0,12
24-A	8,2	21,0	12,5	0,04
25	7,5	21,0	-	-
26-B	7,8	21,0	0,0	0,11
26-A	8,1	21,0	9,8	0,04
27	7,5	21,0	-	-
28-B	8,0	21,0	0,0	0,06
28-A	8,2	21,0	18,2	0,03
29	-	-	-	-
30	-	-	-	-
31	8,2	21,0	0,0	0,05

- Ammonium raw data:

Day No.	Absorbance	Calculated Conc. (mg NH_4^+-N/L)	dilution factor	Real Conc. (mg NH_4^+-N/L)
0	0,8154	0,84	1000	842,38
1	-	-	-	-
2	-	-	-	-
3	0,6344	0,65	1000	649,08
4	-	-	-	-
5	-	-	-	-
6	-	-	-	-
7	0,4704	0,47	1000	473,94
8	-	-	-	-
9	-	-	-	-
10	0,4411	0,44	1000	442,65
Renewed SW	0,7871	0,81	1000	812,15
11	-	-	-	-
12	-	-	-	-
13	-	-	-	-
14	0,2761	0,27	1000	266,45
Renewed SW	0,7957	0,82	1000	821,34
15	-	-	-	-
16	-	-	-	-
17	-	-	-	-
18	-	-	-	-
19	0,1726	0,16	10	1,56
Renewed SW	0,7943	0,82	1000	819,8
20	-	-	-	-
21	0,3321	0,33	10	3,26
Renewed SW	0,7929	0,82	1000	818,35
22	-	-	-	-
23	-	-	-	-
24	0,1596	0,14	10	1,42
Renewed SW	0,8034	0,83	1000	829,56
25	-	-	-	-
26	0,1724	0,16	10	1,56
Renewed SW	0,7852	0,81	1000	810,12
27	-	-	-	-
28	0,09180	0,07	10	0,70
Renewed SW	0,7922	0,82	1000	817,60
29	-	-	-	-
30	-	-	-	-
31	0,06940	0,046	10	0,46

- Nitrate raw data:

Day No.	Absorbance	Calculated Conc. (mg NO_3^--N/L)	dilution factor	Real Conc. (mg NO_3^--N/L)
0	0,0322	0,08	10	0,76
1	-	-	-	-
2	-	-	-	-
3	0,0396	0,22	10	2,18
4	-	-	-	-
5	-	-	-	-
6	-	-	-	-
7	0,0432	0,29	10	2,87
8	-	-	-	-
9	-	-	-	-
10	0,0449	0,32	10	3,19
Renewed SW	0,0520	0,46	5	2,28
11	-	-	-	-
12	-	-	-	-
13	-	-	-	-
14	0,0877	1,14	10	11,38

Renewed SW	0,0308	0,05	10	0,50
15	-	-	-	-
16	-	-	-	-
17	-	-	-	-
18	-	-	-	-
19	0,2241	3,75	10	37,46
Renewed SW	0,0309	0,05	10	0,51
20	-	-	-	-
21	0,2481	4,20	10	42,05
Renewed SW	0,0309	0,05	10	0,52
22	-	-	-	-
23	-	-	-	-
24	0,2911	5,03	10	50,27
Renewed SW	0,0362	0,15	10	1,53
25	-	-	-	-
26	0,2836	4,88	10	48,83
Renewed SW	0,0329	0,09	10	0,90
27	-	-	-	-
28	0,2760	4,74	10	47,38
Renewed SW	0,0363	0,15	10	1,55
29	-	-	-	-
30	-	-	-	-
31	0,3370	5,90	10	59,04

- Nitrite raw data:

Day No.	Measured Nitrite (mg NO_2^-/L)	dilution factor	Calculated Nitrite (mg NO_2^-/L)	Calculated Nitrite-N (mg NO_2^--N/L)
0	0,7	1	0,7	0,2
	0,7	10	7,0	2,1
			Aver.	1,2
1	-	-	-	-
2	-	-	-	-
3	7,7	10	77,0	23,4
4	-	-	-	-
5	-	-	-	-
6	-	-	-	-
7	11,6	10	116,0	35,3
8	-	-	-	-
9	-	-	-	-
10	15,0	10	150,0	45,6
Renewed SW	0,8	1	0,8	0,2
	0,8	10	8,0	2,4
			Aver.	1,3
11	-	-	-	-
12	-	-	-	-
13	-	-	-	-
14	11,1	100	1110	337,4
Renewed SW	0,7	1	0,7	0,2
	0,7	10	7,0	2,1
			Aver.	1,2
15	-	-	-	-
16	-	-	-	-
17	-	-	-	-
18	-	-	-	-
19	23,3	100	2330	708,3
Renewed SW	0,8	1	0,8	0,2
	0,8	10	8,0	2,4
			Aver.	1,3
20	-	-	-	-
21	5,7	500	2850	866,4
Renewed SW	0,8	1	0,8	0,2
	0,8	10	8,0	2,4
			Aver.	1,3

22	-	-	-	-
23	-	-	-	-
24	6,0	500	3000	912,0
Renewed SW	0,8	1	0,8	0,2
	0,8	10	8,0	2,4
			Aver.	1,3
25	-	-	-	-
26	5,6	500	2800	851,2
Renewed SW	-	-	-	-
	-	-	-	-
	-	-	-	-
27	-	-	-	-
28	5,1	500	2550	775,2
Renewed SW	0,8	1	0,8	0,2
	0,8	10	8,0	2,4
			Aver.	1,3
29	-	-	-	-
30	-	-	-	-
31	6,0	500	2983,3	906,9

- **Batch in SFBBR-2:**
  - Calculated data:

Nitrogen species concentrations and mass values							
Day No.	Total Vol. (L)	Ammonium-N		Nitrite-N		Nitrate-N	
		(mg NH_4^+-N/L)	(mg NH_4^+-N)	(mg NO_2^--N/L)	(mg NO_2^--N)	(mg NO_3^--N/L)	(mg NO_3^--N)
0	30,0	813,97	24419,05	1,3	40,1	3,15	94,65
1	30,0	679,41	20359,78	63,1	1890,3	3,33	99,70
2	29,9	600,49	17926,87	141,4	4220,1	4,17	124,44
3	29,9	536,63	16061,60	202,2	6050,8	5,22	156,23
4	29,8	463,05	13811,55	279,7	8342,1	6,42	191,63
5	29,7	-	-	-	-	-	-
6	29,7	-	-	-	-	-	-
7	29,9	252,67	7546,71	539,6	16116,7	31,38	937,15
8	29,9	169,80	5082,04	665,8	19926,0	33,73	1009,48
9	30,0	99,79	2993,25	746,3	22387,0	42,33	1269,83
10	30,0	28,26	848,94	-	-	-	-

Nitrogen species Surface loading values			
Day No.	Ammonium-N (mg NH_4^+-N/m^2)	Nitrite-N (mg NO_2^--N/m^2)	Nitrate-N (mg NO_3^--N/m^2)
0	11490,41	18,9	44,54
1	9580,32	889,5	46,91
2	8435,51	1985,8	58,55
3	7557,80	2847,2	73,52
4	6499,04	3925,4	90,17
5	-	-	-
6	-	-	-
7	3551,11	7583,7	440,98
8	2391,36	9376,2	475,01
9	1408,48	10534,2	597,52
10	399,47	-	-

FA and FNA concentrations				
Day No.	pH	TK-T (°C)	FA (mg NH_3/L)	FNA (mg HNO_2/L)
0	8,2	21,0	62,4	0,00
1	8,3	21,0	64,5	0,00
2	8,3	21,0	57,0	0,01
3	8,3	21,0	51,0	0,01

4	8,2	21,0	35,5	0,01
5	-	-	-	-
6	-	-	-	-
7	7,5	22,0	4,4	0,14
8	7,6	22,0	3,7	0,13
9	7,6	22,0	2,2	0,15
10	7,5	22,0	0,5	0,00

- Ammonium raw data:

Day No.	Absorbance	Calculated Conc. (mg NH_4^+-N/L)	dilution factor	Real Conc. (mg NH_4^+-N/L)
0	0,7888	0,81	1000	813,97
1	0,6628	0,68	1000	679,41
2	0,5889	0,60	1000	600,49
3	0,5291	0,54	1000	536,63
4	0,4602	0,46	1000	463,05
5	-	-	-	-
6	-	-	-	-
7	0,2632	0,25	1000	252,67
8	0,3446	0,34	500	169,80
9	0,9610	1,00	100	99,79
10	0,2912	0,28	100	28,26

- Nitrate raw data:

Day No.	Absorbance	Calculated Conc. (mg NO_3^--N/L)	dilution factor	Real Conc. (mg NO_3^--N/L)
0	0,0447	0,32	10	3,15
1	0,0456	0,33	10	3,33
2	0,0500	0,42	10	4,17
3	0,0555	0,52	10	5,22
4	0,0618	0,64	10	6,42
5	-	-	-	-
6	-	-	-	-
7	0,1923	3,14	10	31,38
8	0,2046	3,37	10	33,73
9	0,2496	4,23	10	42,33

- Nitrite raw data:

Day No.	Measured Nitrite (mg NO_2^-/L)	dilution factor	Calculated Nitrite (mg NO_2^-/L)	Calculated Nitrite-N (mg NO_2^--N/L)
0	0,8	1	0,8	0,2
	0,8	10	8,0	2,4
			Aver.	1,3
1	20,8	10	207,5	63,1
2	4,7	100	465,0	141,4
3	6,7	100	665,0	202,2
4	9,2	100	920,0	279,7
5	-	-	-	-
6	-	-	-	-
7	17,75	100	1775,0	539,6
8	21,9	100	2190,0	665,8
9	24,55	100	2455,0	746,3